ISSN 1007-9327 (print)
ISSN 2219-2840 (online)

World Journal of *Gastroenterology*

World J Gastroenterol 2022 April 28; 28(16): 1608-1724

Published by Baishideng Publishing Group Inc

World Journal of Gastroenterology

Contents

Weekly Volume 28 Number 16 April 28, 2022

THERAPEUTIC AND DIAGNOSTIC GUIDELINES

REVIEW

ORIGINAL ARTICLE

Basic Study

Retrospective Cohort Study

Retrospective Study

SYSTEMATIC REVIEWS

LETTER TO THE EDITOR

World Journal of Gastroenterology

Weekly Volume 28 Number 16 April 28, 2022

Contents

ABOUT COVER

Editorial Board Member of *World Journal of Gastroenterology*, Mauro Bortolotti, MD, Gastroenterologist, Internist, Former Director of 1st level and contract Professor at the Department of Internal Medicine and Gastroenterology of the S.Orsola-Malpighi Polyclinic, University of Bologna, via Massarenti 9, Bologna 40138, Italy. bormau@tin.it

AIMS AND SCOPE

The primary aim of *World Journal of Gastroenterology* (*WJG*, *World J Gastroenterol*) is to provide scholars and readers from various fields of gastroenterology and hepatology with a platform to publish high-quality basic and clinical research articles and communicate their research findings online. *WJG* mainly publishes articles reporting research results and findings obtained in the field of gastroenterology and hepatology and covering a wide range of topics including gastroenterology, hepatology, gastrointestinal endoscopy, gastrointestinal surgery, gastrointestinal oncology, and pediatric gastroenterology.

INDEXING/ABSTRACTING

The *WJG* is now indexed in Current Contents®/Clinical Medicine, Science Citation Index Expanded (also known as SciSearch®), Journal Citation Reports®, Index Medicus, MEDLINE, PubMed, PubMed Central, and Scopus. The 2021 edition of Journal Citation Report® cites the 2020 impact factor (IF) for *WJG* as 5.742; Journal Citation Indicator: 0.79; IF without journal self cites: 5.590; 5-year IF: 5.044; Ranking: 28 among 92 journals in gastroenterology and hepatology; and Quartile category: Q2. The *WJG*'s CiteScore for 2020 is 6.9 and Scopus CiteScore rank 2020: Gastroenterology is 19/136.

RESPONSIBLE EDITORS FOR THIS ISSUE

Production Editor: *Hua-Ge Yu*; **Production Department Director:** *Xu Guo*; **Editorial Office Director:** *Ze-Mao Gong*.

NAME OF JOURNAL

World Journal of Gastroenterology

ISSN

ISSN 1007-9327 (print) ISSN 2219-2840 (online)

LAUNCH DATE

October 1, 1995

FREQUENCY

Weekly

EDITORS-IN-CHIEF

Andrzej S Tarnawski

EDITORIAL BOARD MEMBERS

http://www.wjgnet.com/1007-9327/editorialboard.htm

PUBLICATION DATE

April 28, 2022

COPYRIGHT

© 2022 Baishideng Publishing Group Inc

INSTRUCTIONS TO AUTHORS

https://www.wjgnet.com/bpg/gerinfo/204

GUIDELINES FOR ETHICS DOCUMENTS

https://www.wjgnet.com/bpg/GerInfo/287

GUIDELINES FOR NON-NATIVE SPEAKERS OF ENGLISH

https://www.wjgnet.com/bpg/gerinfo/240

PUBLICATION ETHICS

https://www.wjgnet.com/bpg/GerInfo/288

PUBLICATION MISCONDUCT

https://www.wjgnet.com/bpg/gerinfo/208

ARTICLE PROCESSING CHARGE

https://www.wjgnet.com/bpg/gerinfo/242

STEPS FOR SUBMITTING MANUSCRIPTS

https://www.wjgnet.com/bpg/GerInfo/239

ONLINE SUBMISSION

https://www.f6publishing.com

© 2022 Baishideng Publishing Group Inc. All rights reserved. 7041 Koll Center Parkway, Suite 160, Pleasanton, CA 94566, USA

E-mail: bpgoffice@wjgnet.com https://www.wjgnet.com

World Journal of Gastroenterology

Submit a Manuscript: https://www.f6publishing.com

World J Gastroenterol 2022 April 28; 28(16): 1608-1624

DOI: 10.3748/wjg.v28.i16.1608

ISSN 1007-9327 (print) ISSN 2219-2840 (online)

THERAPEUTIC AND DIAGNOSTIC GUIDELINES

Guidelines to diagnose and treat peri-levator high-5 anal fistulas: Supralevator, suprasphincteric, extrasphincteric, high outersphincteric, and high intrarectal fistulas

Pankaj Garg, Vipul D Yagnik, Sushil Dawka, Baljit Kaur, Geetha R Menon

Specialty type: Gastroenterology and hepatology

Provenance and peer review: Invited article; Externally peer reviewed.

Peer-review model: Single blind

Peer-review report's scientific quality classification
Grade A (Excellent): 0
Grade B (Very good): B
Grade C (Good): C, C, C, C, C
Grade D (Fair): 0
Grade E (Poor): 0

P-Reviewer: Elfeki H, Egypt; Zheng LH, China; Ozkan OF, Turkey; Tamburini AM, Italy

Received: August 25, 2021
Peer-review started: August 25, 2021
First decision: September 29, 2021
Revised: October 6, 2021
Accepted: March 16, 2022
Article in press: March 16, 2022
Published online: April 28, 2022

Pankaj Garg, Department of Colorectal Surgery, Garg Fistula Research Institute,Panchkula 134113, Haryana, India

Pankaj Garg, Department of Colorectal Surgery, Indus International Hospital,Mohali 140201, Punjab, India

Vipul D Yagnik, Department of Surgical Gastroenterology, Nishtha Surgical Hospital and Research Center, Patan 384265, Gujarat, India

Sushil Dawka, Department of Surgery, SSR Medical College, Belle Rive 744101,Mauritius

Baljit Kaur, Department of Radiology, SSRD Magnetic Resonance Imaging Institute, Chandigarh 160011, India

Geetha R Menon, Department of Statistics, Indian Council of Medical Research,New Delhi 110029, India

Corresponding author: Pankaj Garg, MD, MS, Chief Surgeon, Department of Colorectal Surgery, Garg Fistula Research Institute, 1042/15, Panchkula 134113, Haryana, India.
drgargpankaj@yahoo.com

Abstract

Supralevator, suprasphincteric, extrasphincteric, and high intrarectal fistulas (high fistulas in muscle layers of the rectal wall) are well-known high anal fistulas which are considered the most complex and extremely challenging fistulas to manage. Magnetic resonance imaging has brought more clarity to the patho-physiology of these fistulas. Along with these fistulas, a new type of complex fistula in high outersphincteric space, a fistula at the roof of ischiorectal fossa inside the levator ani muscle (RIFIL), has been described. The diagnosis, management, and prognosis of RIFIL fistulas is reported to be even worse than supralevator and suprasphincteric fistulas. There is a lot of confusion regarding the anatomy, diagnosis, and management of these five types of fistulas. The main reason for this is the paucity of literature about these fistulas. The common feature of all these fistulas is their complete involvement of the external anal sphincter. Therefore, fistulotomy, the simplest and most commonly performed procedure, is practically ruled out in these fistulas and a sphincter-saving procedure needs to be performed. Recent advances have provided new insights into the anatomy,

radiological modalities, diagnosis, and management of these five types of high fistulas. These have been discussed and guidelines formulated for the diagnosis and treatment of these fistulas for the first time in this paper.

Key Words: Anal fistula; Supralevator; Suprasphincteric; Extrasphincteric; Magnetic resonance imaging

©The Author(s) 2022. Published by Baishideng Publishing Group Inc. All rights reserved.

Core Tip: These are the first published guidelines to manage the five types of peri-levator anal fistulas that involve almost the complete external anal sphincter and have, therefore, been grouped together as high-5 fistulas. These are supralevator, suprasphincteric, extrasphincteric, and high intrarectal and fistulas at the roof of ischiorectal fossa inside the levator ani muscle. The diagnosis and management of these five fistulas is quite challenging. Magnetic resonance imaging is the best modality to accurately delineate these fistulas. Once diagnosed, care should be exercised to avoid sphincter-cutting procedures (fistulotomy) in these fistulas, as the risk of incontinence would be very high. Sphincter-sparing procedures should be done. However, there is little literature available on satisfactory management of these fistulas.

Citation: Garg P, Yagnik VD, Dawka S, Kaur B, Menon GR. Guidelines to diagnose and treat peri-levator high-5 anal fistulas: Supralevator, suprasphincteric, extrasphincteric, high outersphincteric, and high intrarectal fistulas. *World J Gastroenterol* 2022; 28(16): 1608-1624
URL: https://www.wjgnet.com/1007-9327/full/v28/i16/1608.htm
DOI: https://dx.doi.org/10.3748/wjg.v28.i16.1608

INTRODUCTION

Anal fistulas are feared by patients and surgeons alike[1]. The prime reasons for this are difficulty in understanding the pathophysiology, risk of debilitating incontinence, and high recurrence rates, especially in complex fistulas[2-5]. Amongst the category of complex fistulas, the three well-known notorious fistulas are supralevator, suprasphincteric and extrasphincteric fistulas[6,7]. Another less known fistula is the high intra-rectal fistula which occurs by cephalad extension of the fistula between the internal anal sphincter (IAS) and conjoint longitudinal muscle (CLM). This fistula was first described by Parks *et al*[8] in 1976. Recently, another fistula, fistula at the roof of ischiorectal fossa inside the levator ani muscle (RIFIL) has also joined the category of these high fistulas[9]. RIFIL fistulas are also highly complex and involve the complete external anal sphincter (EAS). The common feature of these five fistulas is that they are quite high as these reach up to the levator muscle and involve almost the complete EAS (Figure 1). Hence, these five fistulas have been grouped together as high-5 fistulas and are discussed in detail below.

The high-five anal fistulas include: (1) Supralevator (Figures 2 and 3); (2) Suprasphincteric (Figures 4-6); (3) Extrasphincteric (Figure 7); (4) High intra-rectal (Figures 3,8 and 9)[8]; and (5) RIFIL (Figures 10-12)[9]. These fistulas are considered most dreaded because understanding their anatomy and pathophysiology, proper diagnosis, and successful safe treatment are quite challenging. All these five fistulas involve almost the complete EAS[10,11] (Figures 2-12). As the EAS plays a major role in continence, muscle-dividing procedures like fistulotomy or cutting setons are strictly contraindicated in these fistulas. In fact, fistulotomy with primary sphincter reconstruction or fistulectomy with primary sphincter reconstruction are also best avoided in these patients[1,12-14]. Therefore, the choice of procedures becomes limited. Of these, the extrasphincteric is the only type which is trans-levator, whereas the other four fistulas (supralevator, sphincteric, high intrarectal, and RIFIL) are peri-levator fistulas which do not traverse through the levator muscle.

This article will address the major concerns of these fistulas, including the challenges in managing and diagnosing the high-5 fistulas, as well as methods to formulate management guidelines..

CHALLENGES IN MANAGING THESE FISTULAS

Confusion about pathophysiology of High-5 fistulas

There is a lot of confusion amongst surgeons about the exact anatomy, pathways of spread, and extent of these fistulas[2]. Not uncommonly, a high transsphincteric fistula is labelled as an extrasphincteric fistula and a suprasphincteric fistula is reported as a high transsphincteric fistula[2].

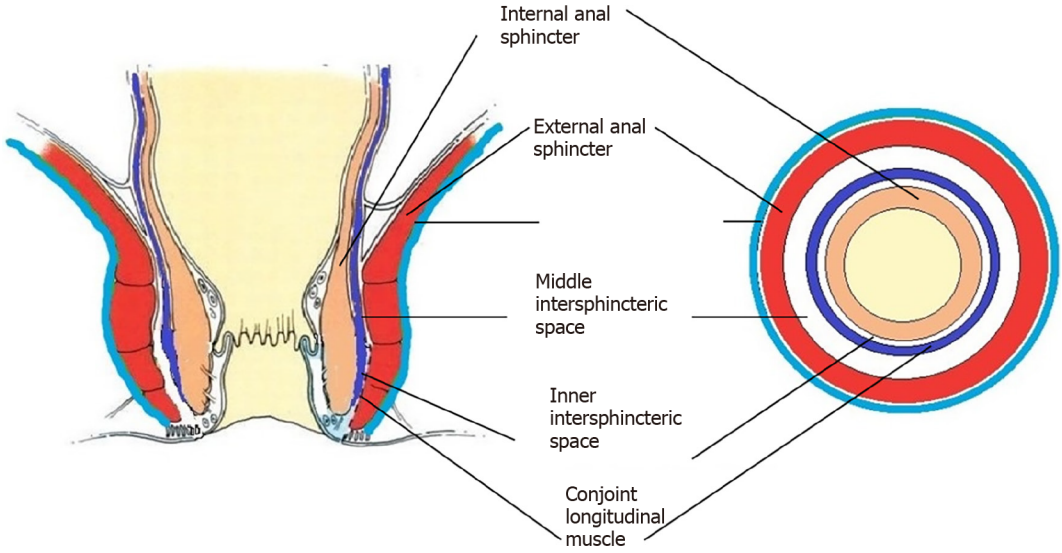

DOI: 10.3748/wjg.v28.i16.1608 **Copyright** ©The Author(s) 2022.

Figure 1 Normal anatomy.

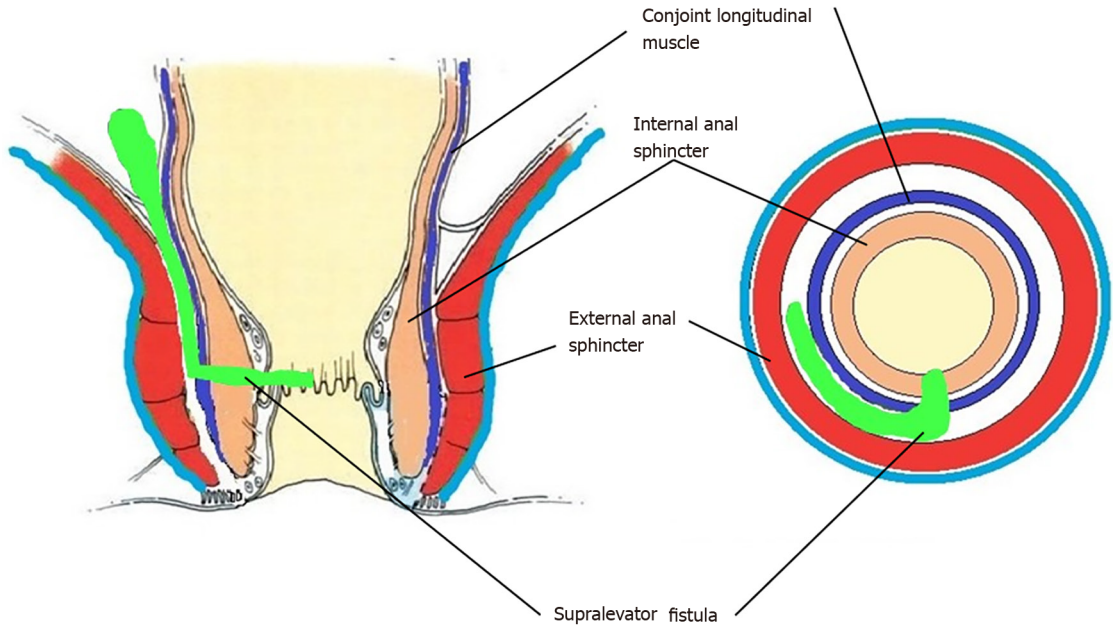

DOI: 10.3748/wjg.v28.i16.1608 **Copyright** ©The Author(s) 2022.

Figure 2 Supralevator fistula.

In order to understand the pathways of extension of these fistulas, it is important to understand the anatomy of the anal canal. There are three muscle layers in the sphincter-complex in the anorectum which are downward extensions of the muscle layers of the gut. There are potential spaces between these muscle layers in which the fistula and pus can spread[9] (Figures 1, 2, 4, 7, 8 and 10).

The three muscle layers in the sphincter-complex[9] are (1) Inner circular muscle layer of gut continues downwards in the anal sphincter complex as IAS; (2) Outer longitudinal muscle layer of gut continues downwards in the anal sphincter complex as CLM; and (3) Puborectalis component of levator ani muscle continues downwards in the anal sphincter complex as EAS (Figure 1). Conventionally, it was assumed that inside the sphincter-complex, there is only one space where the fistula extends and this space between the IAS and EAS was labelled as the 'intersphincteric space'. However, with the availability of higher resolution magnetic resonance imaging (MRI) and increasing experience, it has been demonstrated that there are three potential spaces associated with in these muscle layers through which the fistula can extend[9].

The three potential spaces in the anal sphincter-complex are (1) Inner intersphincteric space (inner space): Between IAS and CLM; (2) Middle intersphincteric space (middle space): Between CLM and EAS

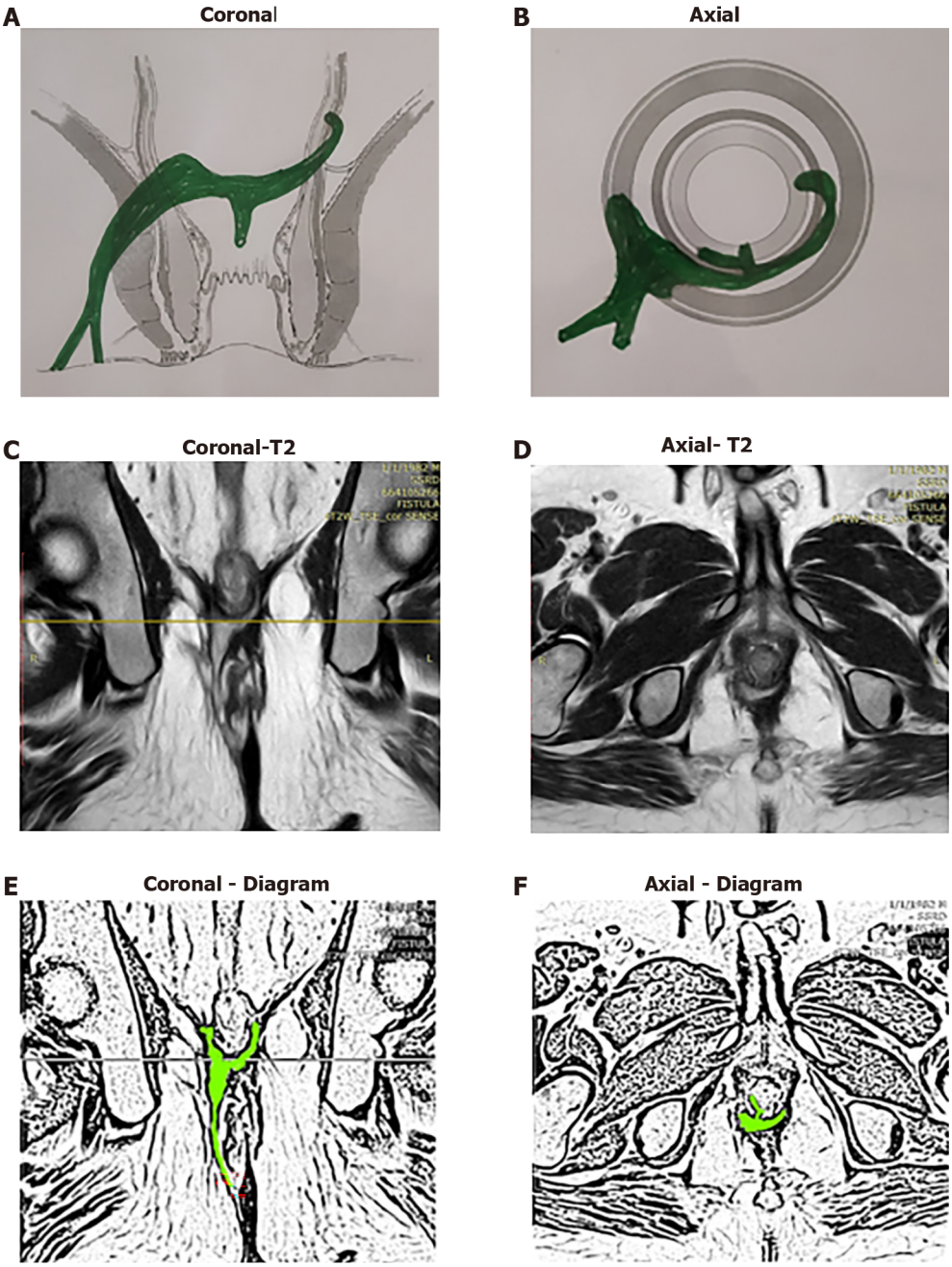

DOI: 10.3748/wjg.v28.i16.1608 **Copyright** ©The Author(s) 2022.

Figure 3 A 39-year-old male patient with a high transsphincteric fistula with supralevator extension at 3 o'clock. There is a high intrarectal tract from 6 to 7 o'clock. The internal opening is at 6 o'clock position. A: Coronal section (schematic diagram); B: Axial section (schematic diagram); C: T2-weighted magnetic resonance imaging (MRI) Coronal section showing supralevator tract; D: T2-weighted MRI Axial section; E: Sketch of MRI Coronal section highlighting fistula tract (light green color); F: Sketch of MRI Axial section highlighting fistula tract (light green color).

(conventional intersphincteric space); and (3) Outer-sphincteric space (outer space): Between the lateral muscle fibers of EAS and its covering fascia[9] (Figure 1).

The anal fistula, usually initiating at crypt glands at the level of the dentate line, can extend superiorly (cephalad) in any of these three spaces.

The fistulas traversing superiorly in (1) Inner intersphincteric space (inner space) between IAS and CLM inside the rectal wall to become a high intrarectal fistula as these fistulas are present between the muscle layers of the rectal wall[8]. At times, these are erroneously labelled as submucous fistula[8] (Figures 8 and 9); (2) Middle intersphincteric space (middle space) between CLM and EAS become a supralevator fistula (if it continues into the supralevator space) (Figures 2 and 3) or a suprasphincteric fistula (if pus extending superiorly in the middle space reaches up to the top of the EAS and then traverses through the junction between the EAS and puborectalis to enter the ischiorectal fossa[15]) (Figures 4-6); and (3) Outer-sphincteric space (outer space) between the EAS and its lateral fascia becomes a RIFIL fistula[9] (Figures 10-12).

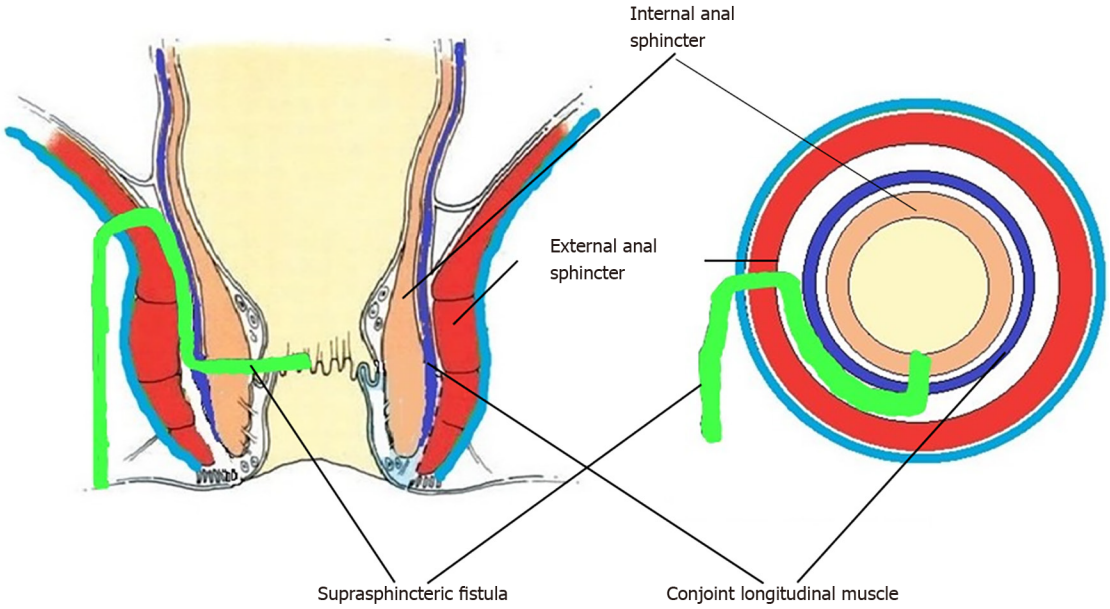

DOI: 10.3748/wjg.v28.i16.1608 **Copyright** ©The Author(s) 2022.

Figure 4 Suprasphincteric fistula.

Thus, the definition of these five fistulas is: (1) Supralevator (Figures 2 and 3): These fistulas traverse in the middle intersphincteric space to enter the supralevator space. The fistula may open into the rectum through an additional high rectal opening in the supralevator space (Figures 3 and 6); (2) Suprasphincteric (Figures 4-6): These fistulas extend superiorly in the middle intersphincteric space to reach up to the top of the EAS and then traverses through the junction between the EAS and puborectalis to enter the ischiorectal fossa; (3) Extrasphincteric (Figure 7): These fistulas traverse through the ischiorectal fossa and enter the supralevator space penetrating the levator muscle. They generally do not traverse through the sphincter-complex (EAS and IAS), which is why they are labelled as 'extra-sphincteric' fistulas; (4) High intra-rectal (Figures 8 and 9): These fistulas traverse cephalad between IAS and CLM in the rectal wall and is thus present between the muscle layers of the rectal wall; and (5) RIFIL (Figures 10-12): These fistulas traverse the EAS but do not enter the ischiorectal fossa. They extend cephalad between the EAS and its lateral fascia to continue on the undersurface of puborectalis and levator ani muscle[9].

Incidence: In recently published large cohorts, the prevalence of these high-5 fistulas has been highlighted[9,16]. The incidence of these fistulas in a cohort of 419 consecutively operated patients over a 2-year period were RIFIL–10% (42/419), supralevator-9.5% (40/419), suprasphincteric-5.5% (23/419) and extrasphincteric-0%[9,16].

Difficulty in diagnosis

As these fistulas are deep and high, they are extremely difficult to diagnose on clinical examination. It usually requires advanced imaging modalities, MRI, or transrectal ultrasound (TRUS), to diagnose these fistulas[17-21]. Both MRI and 3D-TRUS are very effective in delineating various parameters of these fistulas, including the internal opening, primary tracts, and secondary extensions[17-20,22], though MRI has a slight edge over TRUS. It is really impressive that in the pre-MRI era, doyens in the field like Parks *et al*[8] could describe these deep fistulas with a reasonably high level of accuracy.

MRI helps to clearly differentiate between supralevator, suprasphincteric, high intrarectal, and RIFIL fistulas[23]. Rather it would not be wrong to say that MRI is mandatory to properly diagnose these fistulas. Therefore, whenever a fistula has recurred several times, or a tract or side branch of the main fistula is seen extending superiorly during surgery, an MRI should be done to rule out these fistulas[23].

Status of extrasphincteric fistulas

Increasing experience with MRI in fistulas has highlighted that extrasphincteric fistulas do not occur or are extremely rare[24]. It stands to reason that it is almost impossible for a fistula in the ischiorectal fossa to penetrate through the strong levator plate when it can extend with ease in the surrounding fat of the ischiorectal fossa[24]. The only likely possibility for an extrasphincteric fistula to occur is iatrogenic when an artery forceps in a high transsphincteric fistula is pushed through the levator muscle. Even this seems improbable as it would require a lot of force by the operating surgeon. Moreover, due to increased awareness amongst surgeons of iatrogenic injuries, better understanding of regional anatomy, and easy availability of advanced radiological modalities, these iatrogenic blunders seem exceedingly

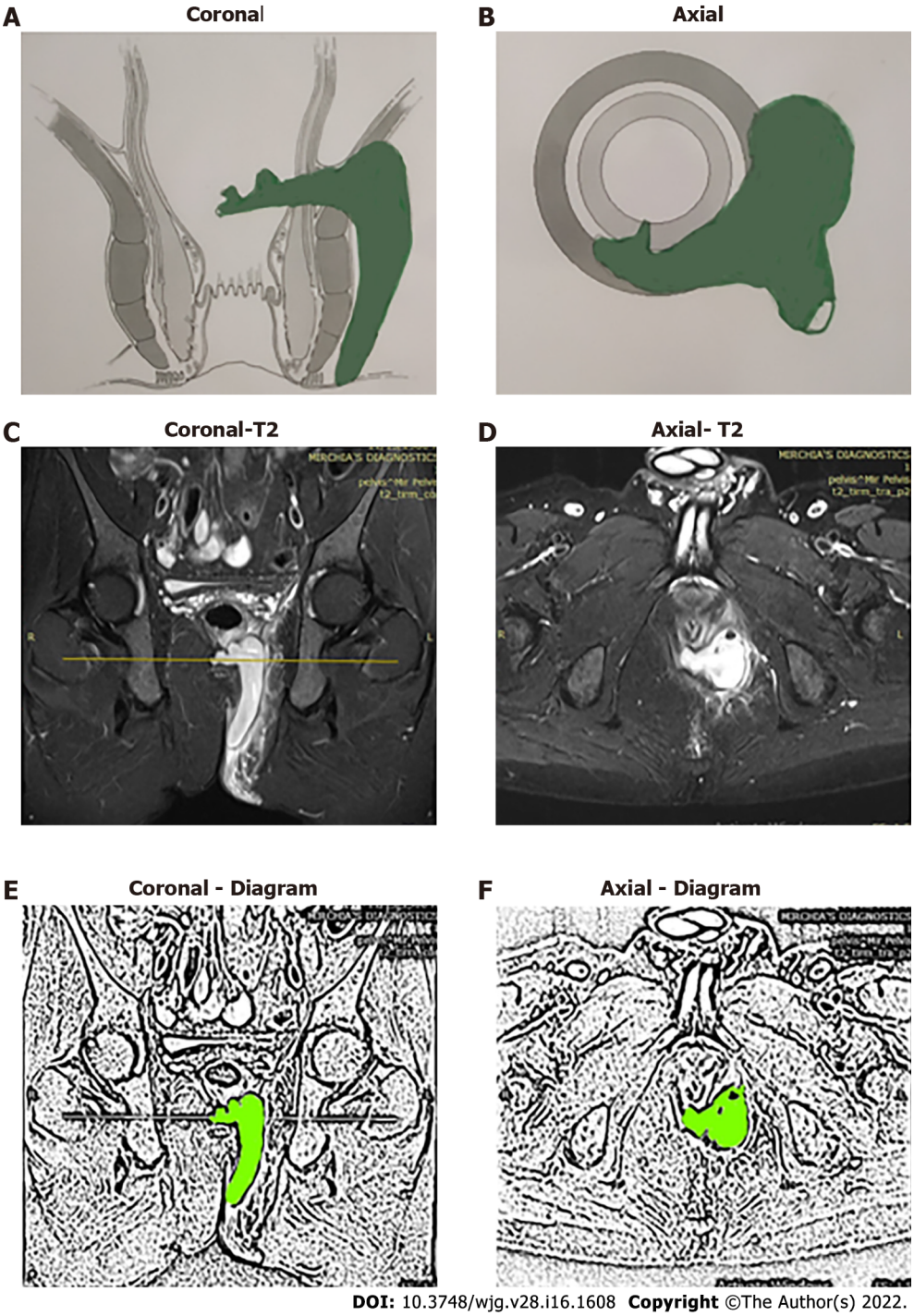

DOI: 10.3748/wjg.v28.i16.1608 **Copyright** ©The Author(s) 2022.

Figure 5 A 40-year-old male patient with a suprasphincteric fistula and abscess on left side. The internal opening is at 6:30 o'clock position. A: Coronal section (schematic diagram); B: Axial section (schematic diagram); C: Short Tau Inversion Recovery (STIR) magnetic resonance imaging (MRI) Coronal section showing suprasphincteric tract and abscess; D: STIR MRI Axial section; E: Sketch of MRI Coronal section highlighting suprasphincteric fistula tract and abscess (light green color); F: Sketch of MRI Axial section highlighting fistula tract and abscess (light green color).

unlikely. Due to this, extrasphincteric fistulas are not seen (or are extremely rare) these days[24]. It is quite possible that the fistulas diagnosed as extrasphincteric fistulas in the pre-MRI era were perhaps supralevator or RIFIL fistulas. Understandably, in the absence of MRI, it is extremely difficult to differentiate between an extrasphincteric fistula and other deep fistulas. So, a diagnosis of extrasphincteric fistula should be made only after due deliberation and detailed analysis of MRI[24].

Complete involvement of EAS

The main challenge in these five fistulas is that they involve almost the complete EAS (Figures 2, 4, 7, 8 and 10). The EAS plays a major role in maintaining continence and risk of damage to the EAS is very high in these fistulas. Because this risk of incontinence is so high, these fistulas are extra concerning[4,5,

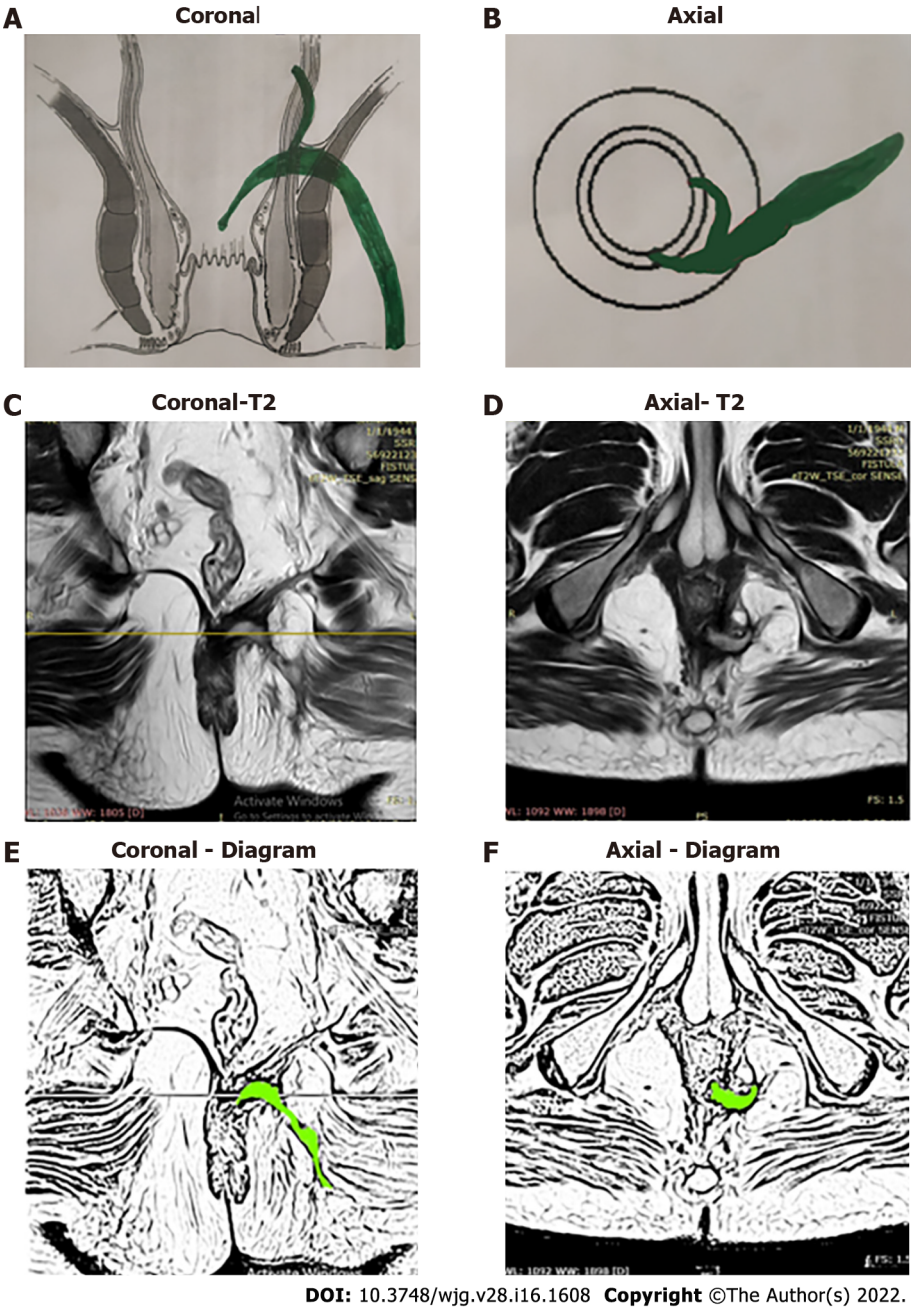

DOI: 10.3748/wjg.v28.i16.1608 **Copyright** ©The Author(s) 2022.

Figure 6 A 47-year-old male patient with a suprasphincteric fistula on left side and supralevator tract and high rectal opening at 3 o'clock. The internal opening is at 6 o'clock position. A: Coronal section (schematic diagram); B: Axial section (schematic diagram); C: T2-weighted magnetic resonance imaging (MRI) Coronal section showing suprasphincteric tract; D: T2-weighted MRI Axial section; E: Sketch of MRI Coronal section highlighting supralevator fistula tract (light green color); F: Sketch of MRI Axial section highlighting fistula tract (light green color).

25]. The most commonly performed procedure, fistulotomy, is contraindicated in these fistulas[25]. There is little published data and there are no standard guidelines to manage these fistulas. Therefore, the fear of managing these fistulas amongst surgeons in easy to understand.

Presence of ASRO (additional supralevator rectal opening)

One of the features that make these fistulas more challenging is the presence of an ASRO along with a primary internal opening at the dentate line[6]. In a large cohort, ASRO was present in 2.8% (23/836) anal fistulas, but in supralevator fistulas, the incidence was 16.6% (23/138)[6]. At times, the presence of ASRO is detected accidentally during surgery (intraoperatively) when a colored solution injected into the external opening comes out through the primary internal opening at the dentate line as well as through the ASRO[6]. In many cases, a granulation polyp or a papilla can be seen at the site of the ASRO. However, ASRO can be diagnosed preoperatively with the help of MRI in almost every case[6]. MRI is an excellent tool to diagnose ASRO with a high level of accuracy[6].

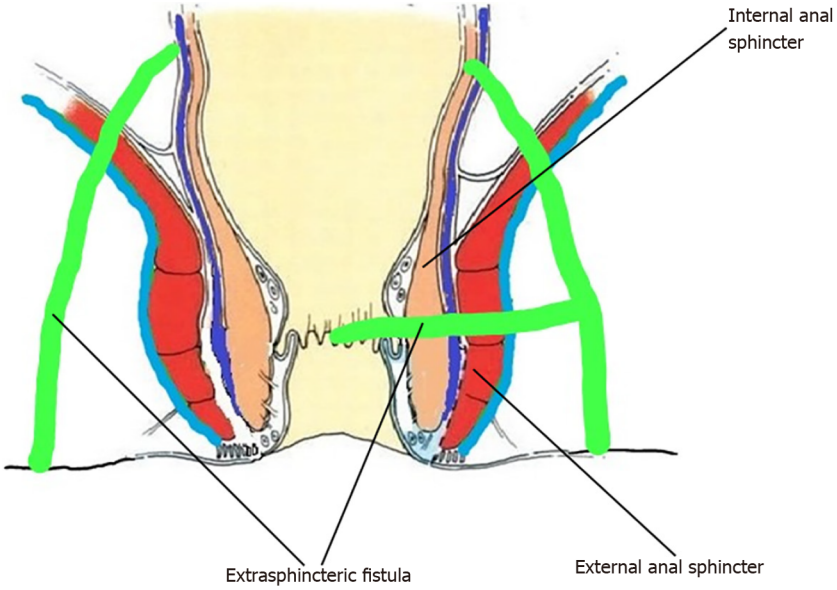

DOI: 10.3748/wjg.v28.i16.1608 **Copyright** ©The Author(s) 2022.

Figure 7 Extrasphincteric fistula.

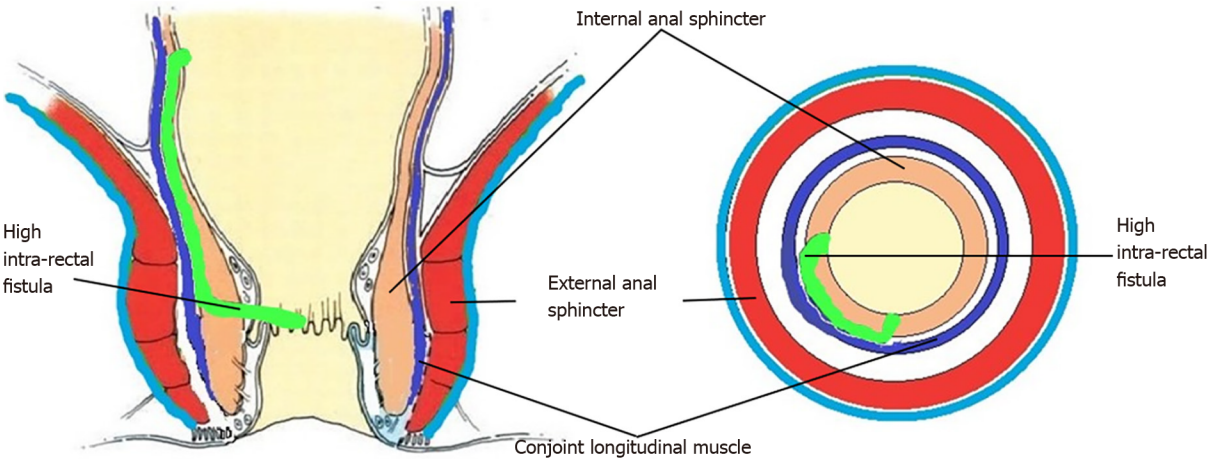

DOI: 10.3748/wjg.v28.i16.1608 **Copyright** ©The Author(s) 2022.

Figure 8 High Intrarectal fistula.

The management of ASRO seems challenging. Closure of an opening high up in the rectum which, at times, is even difficult to reach through the transanal route is not easy. However, there is a sliver of relief in these otherwise complex fistulas. A recent study has demonstrated that even if nothing is done to ASRO, there is no impact on ultimate fistula healing[6].

There is an explanation for this surprising finding. Anal fistulas usually initiate in crypt glands located at the dentate line. The fistula then can extend in different directions from here. Some fistulas or abscesses extend superiorly and enter the supralevator space[6]. In a small subset (16%) of these supralevator abscesses, the pressure generated by the supralevator abscess is so high that the abscess ruptures into the rectum, thus creating an ASRO. In such situations, the flow of infection (and bacteria) in ASRO is from the supralevator space into the rectum[6]. This continues in the same manner because, unlike in the anal canal where intraluminal pressure rises during defecation, pressure in the mid-rectum is quite low (as the rectum is primarily a storage organ). Therefore, the bacteria usually enter the fistula tract from the primary internal opening at the dentate line, bacterial multiplication leads to suppuration, and then the pus egresses through the external opening and the ASRO (if present)[6]. Hence, ultimate healing of the fistula depends primarily on successful closure of the primary internal opening at the dentate line. Once the primary internal opening at the dentate line heals, the fistula heals irrespective of whether the ASRO is closed or open[6]. Therefore, it is a reassuring fact that ASRO left untreated does not affect the ultimate fistula outcome[6].

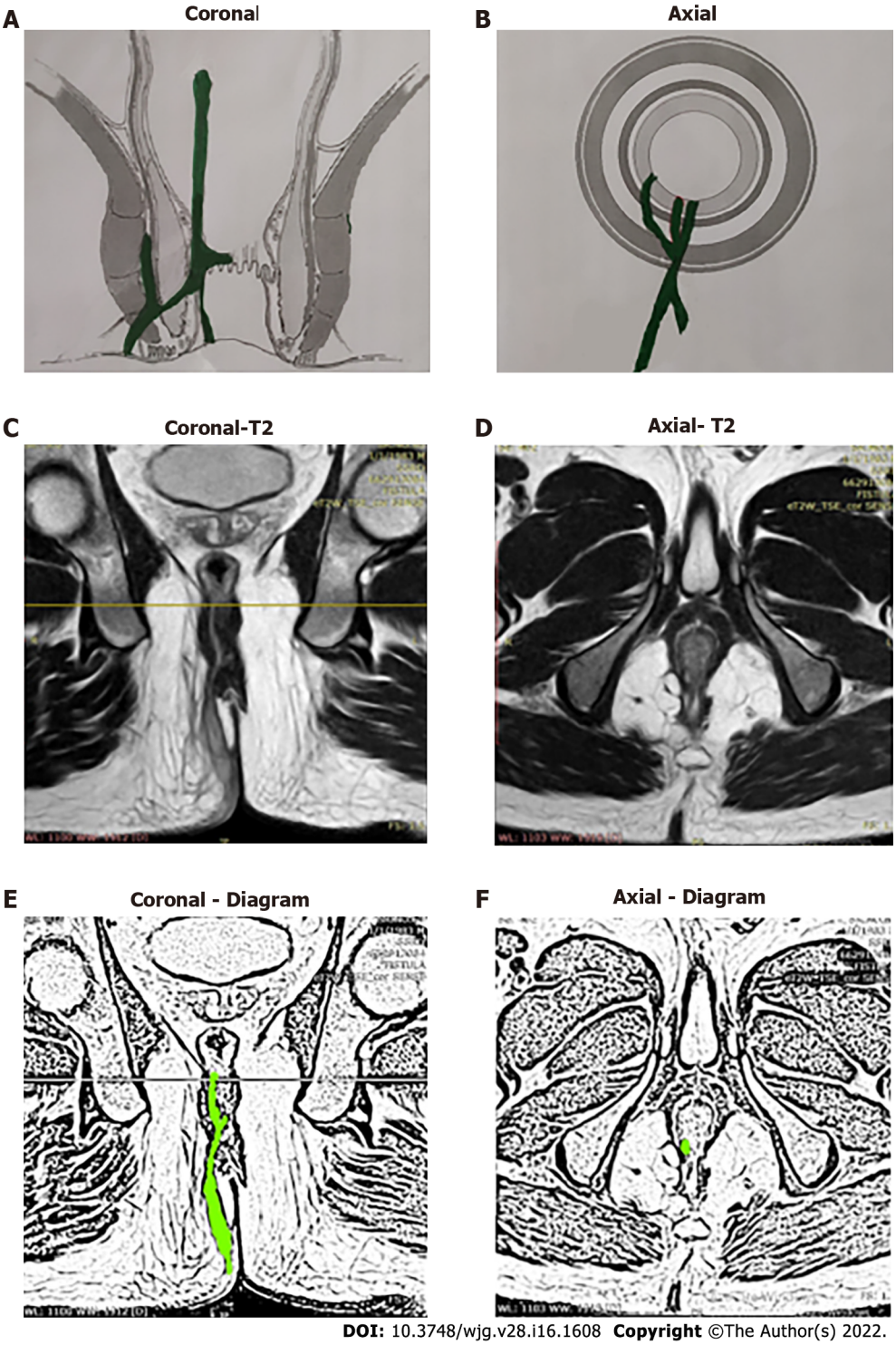

DOI: 10.3748/wjg.v28.i16.1608 **Copyright** ©The Author(s) 2022.

Figure 9 A 36-year-old male patient with a high intrarectal fistula at 7 o'clock. A: Coronal section (schematic diagram); B: Axial section (schematic diagram); C: T2-weighted magnetic resonance imaging (MRI) Coronal section showing high intrarectal fistula tract; D: T2-weighted MRI Axial section; E: Sketch of MRI Coronal section highlighting high intrarectal fistula tract (light green color); F: Sketch of MRI Axial section highlighting fistula tract (light green color).

Detection of underlying secondary pathology

The high-5 fistulas are more complex and refractory to treatment as compared to other fistulas. The incidence of associated complicating pathology like Crohn's disease and tuberculosis is higher in these fistulas[24,26,27]. Therefore, it is important that these diseases should be ruled out whenever any of these high fistulas are diagnosed or suspected.

In regions where Crohn's disease is common, a colonoscopy should be done in all cases of high fistulas[28]. On the other hand, in regions where tuberculosis is common, polymerase chain-reaction (PCR) should be done in samples from the fistula (pus or fistula tract wall or tract lining)[24,29]. In a large series published from a TB-endemic region (India), tuberculosis was detected in 10% (133/1336) of

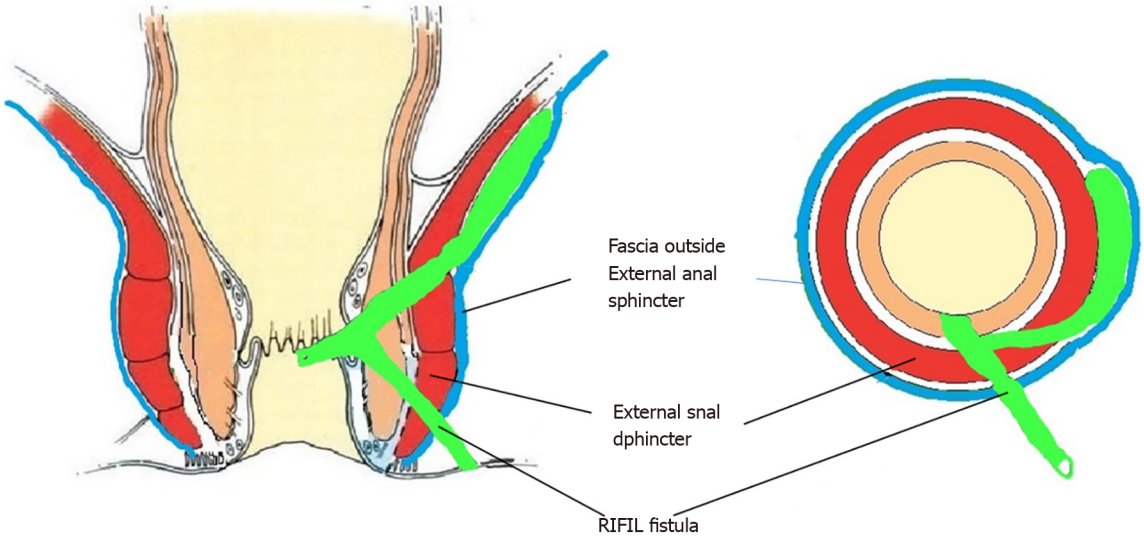

DOI: 10.3748/wjg.v28.i16.1608 **Copyright** ©The Author(s) 2022.

Figure 10 Roof of ischiorectal fossa inside the levator ani muscle fistula. RIFIL: Roof of ischiorectal fossa inside the levator ani muscle.

tested samples (fistula tract lining or pus)[29]. The detection rate of tuberculosis was 12.5% (129/1034) by PCR, 1.5% (3/197) by histopathology, and 0.9% (1/105) by GeneXpert tests[29]. Therefore, PCR is significantly more sensitive than histopathology or GeneXpert to detect tuberculosis[29]. However, in spite of high sensitivity, it is not uncommon that tuberculosis is missed and goes undetected in the first sample. Therefore, in regions where tuberculosis is endemic, it is recommended that repeated samples should be sent for testing, especially in more complex refractory fistulas[29].

METHODS USED TO FORMULATE MANAGEMENT GUIDELINES

A search was performed on MEDLINE, PubMed, EMBASE, and the Cochrane Database of Collected Reviews from January 1975 to September 2021. Keyword combinations using MeSH terms included supralevator, suprasphincteric, extrasphincteric, intrarectal, abscess, fistula, fistula-in-ano, anal, rectal, perianal, perineal, seton, fistula plug, fibrin glue, advancement flap, tuberculosis, Crohn's disease, ligation of intersphincteric tract, ligation of intersphincteric fistula tract (LIFT), fistulectomy with primary sphincter reconstruction (FPR), fistulectomy with primary sphincter repair, transanal opening of the intersphincteric space (TROPIS) and stem cells.

Various guidelines, such as GRADE[30,31], RIGHT[32] AGREE[33] were evaluated, but considering the rarity of the disease condition (Hi-5 fistulas) in the study, the Levels of Evidence for Therapeutic Studies developed by Centre for Evidence-Based Medicine, http://www.cebm.net. (Oxford, United Kingdom) (Table 1) and Grade Practice Recommendations recommended by American Society of Plastic Surgeons (Table 2) were utilized[34]. Each diagnostic and therapeutic intervention was assigned a 'level of evidence' from 1A to 5 (1A being the strongest evidence and 5 being the weakest) (Table 1) and then a 'grade of recommendation' was awarded ranging from 'A' to 'D' ('A' being a strong recommendation and 'D' being a weak option) (Table 2).

Authors (PG, VDY) reviewed all English language articles and tabulated all the evidence available and allotted the level of evidence. After that, the grade of recommendation was decided with consensus of all the authors.

MANAGEMENT GUIDELINES

Diagnostic evaluation of Hi-5 fistulas

MRI or TRUS are preferred modalities to evaluate Hi-5 fistulas. MRI is better than TRUS to evaluate high secondary extensions. Level of Evidence-2B. Grade of recommendation-B.

MRI and TRUS are the diagnostic modalities of choice to evaluate complex anal fistulas[17,19-21]. MRI and 3D-TRUS have comparable efficacy in outlining the internal opening and primary tracts; however, MRI is significantly more effective than 3D-TRUS in detecting deep secondary extensions[35]. The sensitivity of 3D-TRUS to detect deep secondary extensions was 73.9% while MRI had sensitivity of 97% (P = 0.041)[35]. Therefore, MRI is the preferred modality to diagnose high fistulas especially the high-5 fistulas[10,36].

Table 1 Levels of evidence for therapeutic studies[49]

Level		Type of evidence
1	A	Systematic review (with homogeneity) of RCTs
	B	Individual RCT (with narrow confidence intervals)
	C	All or none study
2	A	Systematic review (with homogeneity) of cohort studies
	B	Individual Cohort study (including low quality RCT, *e.g.*, < 80% follow-up)
	C	"Outcomes" research; Ecological studies
3	A	Systematic review (with homogeneity) of case-control studies
	B	Individual Case-control study
4		Case series (and poor-quality cohort and case-control study
5		Expert opinion without explicit critical appraisal or based on physiology bench research or "first principles"

Citation: CEBM. OCEBM levels of evidence. [cited 11 January 2022]. Available from: https://www.cebm.ox.ac.uk/resources/levels-of-evidence/ocebm-levels-of-evidence. Copyright© 2022 University of Oxford.
RCTs: Randomized controlled trials.

Table 2 Grade practice recommendations[1]

Grade	Level of Recommendation	Qualifying evidence	Implications for clinicians
A	Strong recommendation	Level I evidence or consistent findings from several studies of levels II, III, or IV	These recommendations should be followed unless an alternative approach with clear and compelling rationale is present
B	Recommendation	Consistent evidence of levels II, III, or IV	These recommendations should be followed but clinicians should understand that there is scope of improvement and these may be slightly modified as *per* patient preferences
C	Option	Levels II, III, or IV evidence, but findings are inconsistent	These guidelines are broad guidelines and clinicians should be flexible in their decision-making regarding appropriate practice keeping patient preferences in mind
D	Option	Level V evidence: Little or no substantial evidence	These recommendations may be referred but clinicians should consider all other available options while making decisions

[1]Based on the American Society of Plastic Surgeons[34].

Surgical procedure

Due to the challenging factors discussed above, the management of high-5 fistulas is quite difficult and far from satisfactory. Apart from the associated complex parameters, the additional problem is minimal experience or published data on the management of these fistulas. Due to this, the quality of data is of a low evidence level.

As discussed earlier, due to complete involvement of EAS, the most commonly performed procedure, fistulotomy, is contraindicated in these fistulas[25] unless it is coupled with primary sphincter repair. The newer sphincter-sparing procedures, like video-assisted anal fistula treatment[24], fistula laser closure[24], over-the scope clip (OTSC)[37-39], anal fistula plug (AFP)[40], stem cells[28] *etc,* have dismal success rates in complex fistulas. In fact, there are hardly any studies that have analyzed the success rates of these newer procedures in high-5 fistulas. Therefore, the sphincter-preserving procedures, such as LIFT, FPR, advancement flaps, and TROPIS, seem more suitable procedures for high-5 fistulas.

TROPIS provides a ray of hope, as it has been shown to have satisfactory results in these fistulas[2,3,16,24,41]. In the TROPIS procedure, the intersphincteric space is laid open in the anal canal and the resultant wound is allowed to heal by secondary intention[16,24]. The transsphincteric tracts (tracts lateral to the EAS in the ischiorectal fossa) are thoroughly curetted and cleaned[3,41]. Thus, the tracts on both sides of the EAS are managed separately (tracts inner to the EAS are laid open into the anal canal and tracts outside the EAS in the ischiorectal fossa are curetted and cleaned) and the EAS is not cut or damaged at all[16,24]. Due to this, it has been shown that there is no deterioration in continence after the TROPIS procedure[16,24].

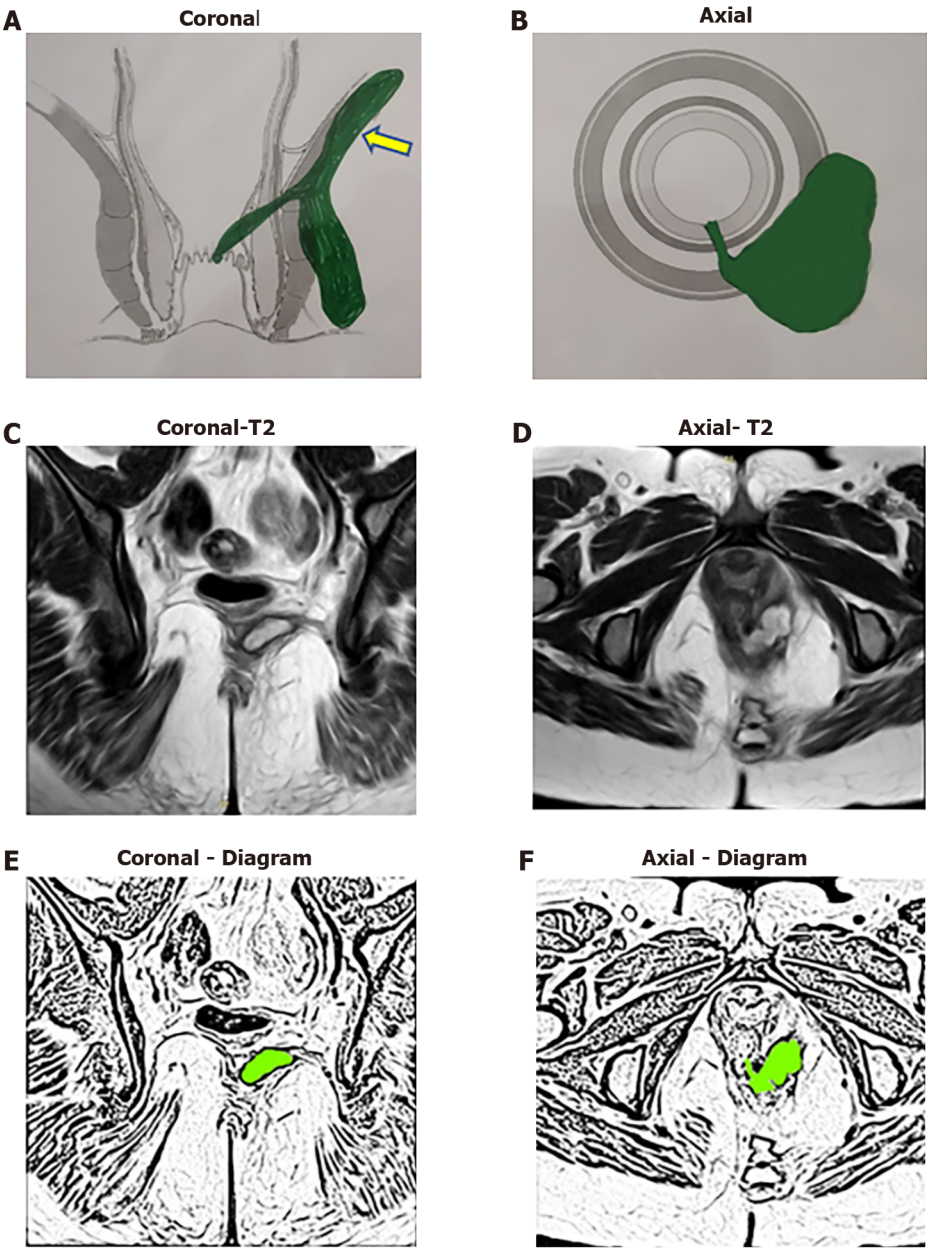

DOI: 10.3748/wjg.v28.i16.1608 **Copyright** ©The Author(s) 2022.

Figure 11 A 33-year-old female patient with a roof of ischiorectal fossa inside the levator ani muscle fistula on left side at 5 o'clock and internal opening at 6 o'clock position. A: Coronal section showing roof of ischiorectal fossa inside the levator ani muscle (RIFIL) fistula (yellow arrow) (schematic diagram); B: Axial section (schematic diagram); C: T2-weighted magnetic resonance imaging (MRI) Coronal section showing RIFIL fistula tract; D: T2-weighted MRI Axial section; E: Sketch of MRI Coronal section highlighting RIFIL fistula tract (light green color); F: Sketch of MRI Axial section highlighting fistula tract (light green color).

The reason for the higher success rate of the TROPIS procedure could be that, unlike other procedures, TROPIS adequately tackles the sepsis in the intersphincteric space[3,41]. It is now understood that the pus/sepsis in the intersphincteric part of the fistula tract is like an abscess in a closed space[24]. Therefore, this sepsis is best managed in the manner an abscess anywhere else in the body is managed-deroofing the abscess cavity and allowing it to heal by secondary intention[24].

Supralevator fistulas

A supralevator abscesses can be drained into the rectum with a moderate success rate[7,42-44]. The level of evidence for this is 2B with a grade of recommendation of B. For example, Garcia-Granero *et al*[7] drained the supralevator abscess into the rectum in four patients and all of them healed.

This not only leads to resolution of the acute symptoms, but also leads to fistula healing in many cases[7,44].

Fistulectomy with or without advancement flap may be done in selected cases with a moderate success rate[44]. The level of evidence is a -4, with the grade of recommendation a-D. Van Onkelen *et al*

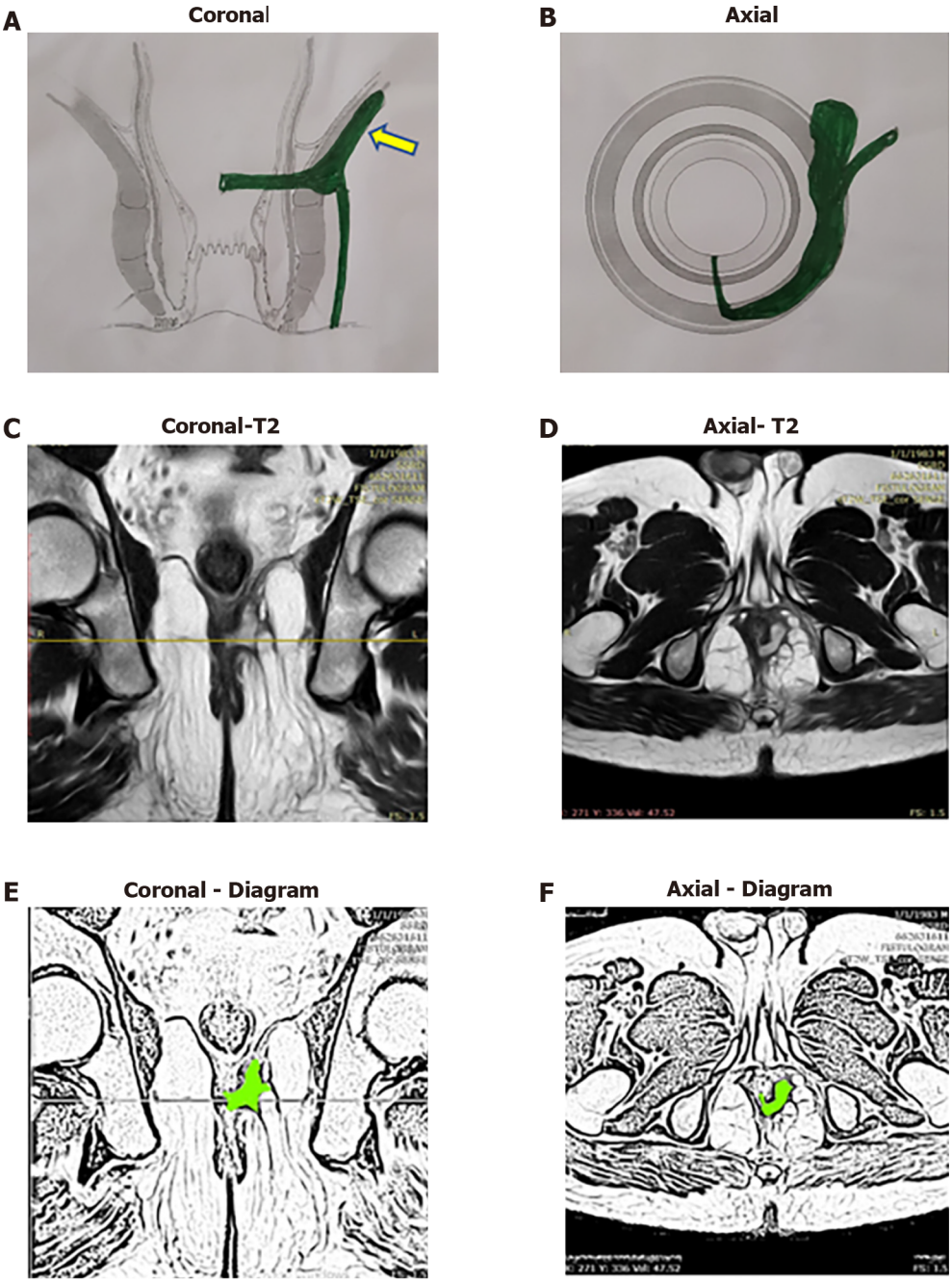

DOI: 10.3748/wjg.v28.i16.1608 **Copyright** ©The Author(s) 2022.

Figure 12 A 38-year-old male patient with a roof of ischiorectal fossa inside the levator ani muscle fistula on left side at 3 o'clock and internal opening at 6 o'clock position. A: Coronal section showing roof of ischiorectal fossa inside the levator ani muscle (RIFIL) fistula (yellow arrow) (schematic diagram); B: Axial section (schematic diagram); C: T2-weighted magnetic resonance imaging (MRI) Coronal section showing RIFIL fistula tract; D: T2-weighted MRI Axial section; E: Sketch of MRI Coronal section highlighting RIFIL fistula tract (light green color); F: Sketch of MRI Axial section highlighting fistula tract (light green color).

[44] performed advancement flap in three patients after draining the supralevator abscess. All patients healed but multiple surgeries were required in order to achieve fistula healing[44].

Supralevator fistula can be managed with laying open of the supralevator extension into the rectum through the transanal route (TROPIS) procedure with a satisfactory healing rate[6,16]. The level of evidence for this is 2B with a grade of recommendation of B. The success rate was 84.6% (11/13) in the initial series and 82.1% (92/112) on long-term follow-up (median 30 mo) in the same series[16].

LIFT and FPR can also be done in selected cases with good success rates (80%-91%) in high complex fistulas (the studies included supralevator fistulas)[45,46]. The level of evidence for this is 5 with a grade of recommendation of D. However, data for these two procedures specific to supralevator fistulas is not available.

Suprasphincteric fistulas

Advancement flap, fistulotomy/fistulectomy with primary sphincter repair and stem cells have moderate success rates, with a success rate range from 70%-85%, though the sample size was quite small [47]. The level of evidence for this is 2B with a grade of recommendation of D. Perez *et al*[47] compared advancement flap *vs* fistulotomy with sphincter reconstruction in suprasphincteric fistulas and the healing rate was 80% (4/5) and 83.3% (5/6) respectively[47]. However, the risk of cutting the entire EAS and then repairing the same seems a difficult option to most surgeons. Also, in the rare eventuality of suture dehiscence, the risk of incontinence would be very high.

Fibrin glue has a poor success rate in suprasphincteric fistulas. The level of evidence for this is 2B with a grade of recommendation of C. Garcia-Olmo *et al*[48] compared the healing rate of fibrin glue *vs* adipose stem cells in suprasphincteric fistulas. The healing rate in the fibrin glue group was 8% (2/16) while it was 71% (10/14) in the stem cells group[48].

The TROPIS procedure has had promising results with a good success rate with minimal impact on continence The level of evidence for this is 4 with a grade of recommendation of C. Out of 14 supras-phincteric fistulas, 78.6% (11/14) patients were cured with no deterioration in continence levels after surgery on long-term follow-up (median 30 mo)[16].

LIFT can be done in selected cases but is technically difficult. The level of evidence for this is 2B with a grade of recommendation of C.

There are studies in which LFT has shown a good success rate (80%-91%) in high complex fistulas[45, 46]. but data for LIFT exclusive to supralevator fistulas is not available. It is also expected that performing the LIFT procedure in suprasphincteric fistulas (ligating the intersphincteric tract high up in the intersphincteric plane) would be a technically demanding procedure.

Extrasphincteric fistulas

Temporary colostomy with management of the primary pathology can be used for extrasphincteric fisutlas. The level of evidence for this is 5 with a grade of recommendation of D.

Extrasphincteric fistulas are extremely rare these days, which means there is little data available on the management of these fistulas. As most of these fistulas are caused by secondary pelvic pathology or iatrogenic factors, a diverting stoma along with management of the underlying cause would be the mainstay of treatment[8].

High intra-rectal fistulas

Intra-anal fistulotomy (TROPIS procedure) has a high success rate with minimal impact on continence. The level of evidence for this is 4 with a grade of recommendation of B. These fistulas are perhaps the easiest to treat. Simple intra-rectal fistulotomy (laying open the fistula tract into the anorectum) would cure these fistulas with a high success rate (> 90%)[8,16].

RIFIL fistulas (fistula at the roof of ischiorectal fossa inside the levator ani muscle)

TROPIS has a moderate success rate with minimal impact on continence in RIFIL fistulas. The level of evidence for this is 2B with a grade of recommendation of B. RIFIL fistulas are challenging to manage because access to the RIFIL component might become difficult. TROPIS has shown a moderate success rate in RIFIL fistulas[9]. The healing rate in RIFIL fistulas by the TROPIS procedure was 69.4% (25/36) with a follow-up (median) of 12 mo[9]. There was no negative impact on continence following surgery.

LIFT and FPR are expected to have a moderate success rate; however, since RIFIL fistulas have been recently described[9] and till now, there are no studies of LIFT or FPR procedure in RIFIL fistulas. Conceptually it is expected that these procedures would also prove at least moderately effective for these fistulas. The level of evidence for this is 5 with a grade of recommendation of D.

CONCLUSION

Anal fistulas that reach up to the levator muscle and involve almost the complete EAS have been grouped together as high-5 fistulas. These comprise supralevator, supraphincteric, extrasphincteric, high intrarectal, and RIFIL fistulas. The diagnosis as well as the management of these five fistulas is quite challenging. Advanced radiological modalities, preferably MRI, are needed to accurately delineate these fistulas. Once diagnosed, care should be exercised to avoid sphincter-cutting procedures like fistulotomy or cutting seton in these fistulas as the risk of incontinence would be very high. Sphincter-sparing procedures like TROPIS or LIFT should be carried out in these fistulas. These guidelines may help improve understanding and outcomes in the management of these complex fistulas.

FOOTNOTES

Author contributions: Garg P conceived and designed the study, collected and analyzed the data, revised the data,

approved and submitted the final manuscript (guarantor of the review); Dawka S critically analyzed the data, reviewed and edited the manuscript, and approved and submitted the final manuscript; Kaur B and Yagnik VD collected and analyzed the data, revised the data, and approved and submitted the final manuscript; Menon GR analyzed the data, revised the data, and approved and submitted the final manuscript.

Conflict-of-interest statement: None of the authors, Pankaj Garg, Vipul D Yagnik, Baljit Kaur, Sushil Dawka, or Geetha R Menon, have any conflict of interest.

Open-Access: This article is an open-access article that was selected by an in-house editor and fully peer-reviewed by external reviewers. It is distributed in accordance with the Creative Commons Attribution NonCommercial (CC BY-NC 4.0) license, which permits others to distribute, remix, adapt, build upon this work non-commercially, and license their derivative works on different terms, provided the original work is properly cited and the use is non-commercial. See: https://creativecommons.org/Licenses/by-nc/4.0/

Country/Territory of origin: India

ORCID number: Pankaj Garg 0000-0002-0800-3578; Vipul D Yagnik 0000-0003-4008-6040; Sushil Dawka 0000-0002-9372-3683; Baljit Kaur 0000-0002-3882-7578; Geetha R Menon 0000-0003-2491-0650.

Corresponding Author's Membership in Professional Societies: American Society of Colon Rectum Surgeons; American Society of Gastrointestinal Endoscopic Surgeons; Association of Surgeons of India.

S-Editor: Fan JR
L-Editor: Filipodia
P-Editor: Yu HG

REFERENCES

1 **Ratto C**, Grossi U, Litta F, Di Tanna GL, Parello A, De Simone V, Tozer P, DE Zimmerman D, Maeda Y. Contemporary surgical practice in the management of anal fistula: results from an international survey. *Tech Coloproctol* 2019; **23**: 729-741 [PMID: 31368010 DOI: 10.1007/s10151-019-02051-5]
2 **Włodarczyk M**, Włodarczyk J, Sobolewska-Włodarczyk A, Trzciński R, Dziki Ł, Fichna J. Current concepts in the pathogenesis of cryptoglandular perianal fistula. *J Int Med Res* 2021; **49**: 300060520986669 [PMID: 33595349 DOI: 10.1177/0300060520986669]
3 **Li YB**, Chen JH, Wang MD, Fu J, Zhou BC, Li DG, Zeng HQ, Pang LM. Transanal Opening of Intersphincteric Space for Fistula-in-Ano. *Am Surg* 2021; 3134821989048 [PMID: 33517706 DOI: 10.1177/0003134821989048]
4 **Jeong HY**, Song SG, Nam WJ, Lee JK. Puborectalis Muscle Involvement on Magnetic Resonance Imaging in Complex Fistula: A New Perspective on Diagnosis and Treatment. *Ann Coloproctol* 2021; **37**: 51-57 [PMID: 32972097 DOI: 10.3393/ac.2020.08.26.1]
5 **Jayne DG**, Scholefield J, Tolan D, Gray R, Senapati A, Hulme CT, Sutton AJ, Handley K, Hewitt CA, Kaur M, Magill L; FIAT Trial Collaborative Group. A Multicenter Randomized Controlled Trial Comparing Safety, Efficacy, and Cost-effectiveness of the Surgisis Anal Fistula Plug Versus Surgeon's Preference for Transsphincteric Fistula-in-Ano: The FIAT Trial. *Ann Surg* 2021; **273**: 433-441 [PMID: 32516229 DOI: 10.1097/SLA.0000000000003981]
6 **Garg P**, R Menon G, Kaur B. Comparison of different methods to manage supralevator rectal opening in anal fistulas: A retrospective cohort study. *Cir Esp (Engl Ed)* 2021 [PMID: 33875192 DOI: 10.1016/j.ciresp.2021.03.011]
7 **Garcia-Granero A**, Granero-Castro P, Frasson M, Flor-Lorente B, Carreño O, Espí A, Puchades I, Garcia-Granero E. Management of cryptoglandular supralevator abscesses in the magnetic resonance imaging era: a case series. *Int J Colorectal Dis* 2014; **29**: 1557-1564 [PMID: 25339133 DOI: 10.1007/s00384-014-2028-2]
8 **Parks AG**, Gordon PH, Hardcastle JD. A classification of fistula-in-ano. *Br J Surg* 1976; **63**: 1-12 [PMID: 1267867 DOI: 10.1002/bjs.1800630102]
9 **Garg P**, Dawka S, Yagnik VD, Kaur B, Menon GR. Anal fistula at roof of ischiorectal fossa inside levator-ani muscle (RIFIL): a new highly complex anal fistula diagnosed on MRI. *Abdom Radiol (NY)* 2021; **46**: 5550-5563 [PMID: 34455464 DOI: 10.1007/s00261-021-03261-y]
10 **Liu X**, Wang Z, Ren H, Ren A, Wang W, Yang X, Shi S. Evaluating postoperative anal fistula prognosis by diffusion-weighted MRI. *Eur J Radiol* 2020; **132**: 109294 [PMID: 33038577 DOI: 10.1016/j.ejrad.2020.109294]
11 **Halligan S**, Tolan D, Amitai MM, Hoeffel C, Kim SH, Maccioni F, Morrin MM, Mortele KJ, Rafaelsen SR, Rimola J, Schmidt S, Stoker J, Yang J. ESGAR consensus statement on the imaging of fistula-in-ano and other causes of anal sepsis. *Eur Radiol* 2020; **30**: 4734-4740 [PMID: 32307564 DOI: 10.1007/s00330-020-06826-5]
12 **De Hous N**, Van den Broeck T, de Gheldere C. Fistulectomy and primary sphincteroplasty (FIPS) to prevent keyhole deformity in simple anal fistula: a single-center retrospective cohort study. *Acta Chir Belg* 2021; **121**: 308-313 [PMID: 32253992 DOI: 10.1080/00015458.2020.1753151]
13 **Ratto C**, Litta F, Marra AA, Campennì P, De Simone V, Parello A. Fistulotomy plus end-to-end primary sphincteroplasty - a video vignette. *Colorectal Dis* 2021; **23**: 2213-2214 [PMID: 34022114 DOI: 10.1111/codi.15745]
14 **Litta F**, Parello A, Ferri L, Torrecilla NO, Marra AA, Orefice R, De Simone V, Campennì P, Goglia M, Ratto C. Simple fistula-in-ano: is it all simple? *Tech Coloproctol* 2021; **25**: 385-399 [PMID: 33387100 DOI: 10.1007/s10151-020-02385-5]
15 **Fröhlich B**, Hötzinger H, Fritsch H. Tomographical anatomy of the pelvis, pelvic floor, and related structures. *Clin Anat* 1997; **10**: 223-230 [PMID: 9213037 DOI: 10.1002/(SICI)1098-2353(1997)10:4<223::AID-CA1>3.0.CO;2-T]

16 **Garg P**, Kaur B, Goyal A, Yagnik VD, Dawka S, Menon GR. Lessons learned from an audit of 1250 anal fistula patients operated at a single center: A retrospective review. *World J Gastrointest Surg* 2021; **13**: 340-354 [PMID: 33968301 DOI: 10.4240/wjgs.v13.i4.340]

17 **van Rijn KL**, Lansdorp CA, Tielbeek JAW, Nio CY, Buskens CJ, D'Haens GRAM, Löwenberg M, Stoker J. Evaluation of the modified Van Assche index for assessing response to anti-TNF therapy with MRI in perianal fistulizing Crohn's disease. *Clin Imaging* 2020; **59**: 179-187 [PMID: 31821976 DOI: 10.1016/j.clinimag.2019.10.007]

18 **Balcı S**, Onur MR, Karaosmanoğlu AD, Karçaaltıncaba M, Akata D, Konan A, Özmen MN. MRI evaluation of anal and perianal diseases. *Diagn Interv Radiol* 2019; **25**: 21-27 [PMID: 30582572 DOI: 10.5152/dir.2018.17499]

19 **Konan A**, Onur MR, Özmen MN. The contribution of preoperative MRI to the surgical management of anal fistulas. *Diagn Interv Radiol* 2018; **24**: 321-327 [PMID: 30272562 DOI: 10.5152/dir.2018.18340]

20 **Almeida IS**, Jayarajah U, Wickramasinghe DP, Samarasekera DN. Value of three-dimensional endoanal ultrasound scan (3D-EAUS) in preoperative assessment of fistula-in-ano. *BMC Res Notes* 2019; **12**: 66 [PMID: 30696490 DOI: 10.1186/s13104-019-4098-2]

21 **Youssef A**. The Ultrasound of Perianal External Opening. *Gastroenterol Hepatol Int J* 2017; **2**: 000128

22 **Lefrançois P**, Zummo-Soucy M, Olivié D, Billiard JS, Gilbert G, Garel J, Visée E, Manchec P, Tang A. Diagnostic performance of intravoxel incoherent motion diffusion-weighted imaging and dynamic contrast-enhanced MRI for assessment of anal fistula activity. *PLoS One* 2018; **13**: e0191822 [PMID: 29370278 DOI: 10.1371/journal.pone.0191822]

23 **Erden A**. MRI of anal canal: normal anatomy, imaging protocol, and perianal fistulas: Part 1. *Abdom Radiol (NY)* 2018; **43**: 1334-1352 [PMID: 28840368 DOI: 10.1007/s00261-017-1305-2]

24 **Garg P**, Sodhi SS, Garg N. Management of Complex Cryptoglandular Anal Fistula: Challenges and Solutions. *Clin Exp Gastroenterol* 2020; **13**: 555-567 [PMID: 33204136 DOI: 10.2147/CEG.S198796]

25 **Nottingham JM**, Rentea RM. Anal Fistulotomy. StatPearls. Treasure Island (FL), 2021

26 **Buhulaigah H**, Truong A, Zaghiyan K, Fleshner P. Clinical Factors Associated With Response to Fecal Diversion in Crohn's Disease. *Am Surg* 2020; **86**: 1277-1280 [PMID: 33150794 DOI: 10.1177/0003134820964223]

27 **Truong A**, Zaghiyan K, Fleshner P. Anorectal Crohn's Disease. *Surg Clin North Am* 2019; **99**: 1151-1162 [PMID: 31676054 DOI: 10.1016/j.suc.2019.08.012]

28 **Cao Y**, Su Q, Zhang B, Shen F, Li S. Efficacy of stem cells therapy for Crohn's fistula: a meta-analysis and systematic review. *Stem Cell Res Ther* 2021; **12**: 32 [PMID: 33413661 DOI: 10.1186/s13287-020-02095-7]

29 **Garg P**, Goyal A, Yagnik VD, Dawka S, Menon GR. Diagnosis of anorectal tuberculosis by polymerase chain reaction, GeneXpert and histopathology in 1336 samples in 776 anal fistula patients. *World J Gastrointest Surg* 2021; **13**: 355-365 [PMID: 33968302 DOI: 10.4240/wjgs.v13.i4.355]

30 **Guyatt G**, Gutterman D, Baumann MH, Addrizzo-Harris D, Hylek EM, Phillips B, Raskob G, Lewis SZ, Schünemann H. Grading strength of recommendations and quality of evidence in clinical guidelines: report from an american college of chest physicians task force. *Chest* 2006; **129**: 174-181 [PMID: 16424429 DOI: 10.1378/chest.129.1.174]

31 **Aguayo-Albasini JL**, Flores-Pastor B, Soria-Aledo V. [GRADE system: classification of quality of evidence and strength of recommendation]. *Cir Esp* 2014; **92**: 82-88 [PMID: 24361098 DOI: 10.1016/j.ciresp.2013.08.002]

32 **Chen Y**, Yang K, Marušic A, Qaseem A, Meerpohl JJ, Flottorp S, Akl EA, Schünemann HJ, Chan ES, Falck-Ytter Y, Ahmed F, Barber S, Chen C, Zhang M, Xu B, Tian J, Song F, Shang H, Tang K, Wang Q, Norris SL; RIGHT (Reporting Items for Practice Guidelines in Healthcare) Working Group. A Reporting Tool for Practice Guidelines in Health Care: The RIGHT Statement. *Ann Intern Med* 2017; **166**: 128-132 [PMID: 27893062 DOI: 10.7326/M16-1565]

33 **Appraisal of Guidelines for Research and Evaluation**. Global Rating Scale. [cited 16 September 2021]. Available from: https://www.agreetrust.org/wp-content/uploads/2017/11/AGREE-GRS.pdf

34 **Burns PB**, Rohrich RJ, Chung KC. The levels of evidence and their role in evidence-based medicine. *Plast Reconstr Surg* 2011; **128**: 305-310 [PMID: 21701348 DOI: 10.1097/PRS.0b013e318219c171]

35 **Brillantino A**, Iacobellis F, Reginelli A, Monaco L, Sodano B, Tufano G, Tufano A, Maglio M, De Palma M, Di Martino N, Renzi A, Grassi R. Preoperative assessment of simple and complex anorectal fistulas: Tridimensional endoanal ultrasound? *Radiol Med* 2019; **124**: 339-349 [PMID: 30607867 DOI: 10.1007/s11547-018-0975-3]

36 **Mathew RP**, Patel V, Low G. Caution in using 3D-EAUS as the first-line diagnostic tool in the preoperative work up for perianal fistulas. *Radiol Med* 2020; **125**: 155-156 [PMID: 31679127 DOI: 10.1007/s11547-019-01101-0]

37 **Grossberg SJ**, Harran N, Bebington B, Lutrin DL. Use of the OVESCO OTSC® Proctology Clip for closure of fistula-in-ano at Wits Donald Gordon Medical Centre - a single centre experience. *S Afr J Surg* 2020; **58**: 74-77 [PMID: 32644310]

38 **Mascagni D**, Pironi D, Grimaldi G, Romani AM, La Torre G, Eberspacher C, Palma R, Sorrenti S, Pontone S. OTSC® Proctology vs. fistulectomy and primary sphincter reconstruction as a treatment for low trans-sphincteric anal fistula in a randomized controlled pilot trial. *Minerva Chir* 2019; **74**: 1-6 [PMID: 29397638 DOI: 10.23736/S0026-4733.18.07617-4]

39 **Marinello F**, Kraft M, Ridaura N, Vallribera F, Espín E. Treatment of Fistula-in-ano With OTSC® Proctology Clip Device: Short-term Results. *Cir Esp (Engl Ed)* 2018; **96**: 369-374 [PMID: 29525123 DOI: 10.1016/j.ciresp.2018.02.003]

40 **Tao Y**, Zheng Y, Han JG, Wang ZJ, Cui JJ, Zhao BC, Yang XQ. Effects of an anal fistula plug on anal function after surgery for treatment of a trans-sphincteric anal fistula. *Langenbecks Arch Surg* 2021; **406**: 855-861 [PMID: 33174168 DOI: 10.1007/s00423-020-02024-5]

41 **Huang B**, Wang X, Zhou D, Chen S, Li B, Wang Y, Tai J. Treating highly complex anal fistula with a new method of combined intraoperative endoanal ultrasonography (IOEAUS) and transanal opening of intersphincteric space (TROPIS). *Wideochir Inne Tech Maloinwazyjne* 2021; **16**: 697-703 [PMID: 34950264 DOI: 10.5114/wiitm.2021.104368]

42 **Bevans DW Jr**, Westbrook KC, Thompson BW, Caldwell JT. Perirectal abscess: a potentically fatal illness. *Am J Surg* 1973; **126**: 765-768 [PMID: 4586132 DOI: 10.1016/s0002-9610(73)80067-4]

43 **Ferguson EF Jr**, Houston CH. Iatrogenic supralevator fistula. *South Med J* 1978; **71**: 490-495 [PMID: 644353 DOI: 10.1097/00007611-197805000-00004]

44 **van Onkelen RS**, Gosselink MP, Schouten WR. Treatment of anal fistulas with high intersphincteric extension. *Dis Colon Rectum* 2013; **56**: 987-991 [PMID: 23838868 DOI: 10.1097/DCR.0b013e3182908be6]

45 **Malakorn S**, Sammour T, Khomvilai S, Chowchankit I, Gunarasa S, Kanjanasilp P, Thiptanakij C, Rojanasakul A. Ligation of Intersphincteric Fistula Tract for Fistula in Ano: Lessons Learned From a Decade of Experience. *Dis Colon Rectum* 2017; **60**: 1065-1070 [PMID: 28891850 DOI: 10.1097/DCR.0000000000000880]

46 **Litta F**, Parello A, De Simone V, Grossi U, Orefice R, Ratto C. Fistulotomy and primary sphincteroplasty for anal fistula: long-term data on continence and patient satisfaction. *Tech Coloproctol* 2019; **23**: 993-1001 [PMID: 31538298 DOI: 10.1007/s10151-019-02093-9]

47 **Perez F**, Arroyo A, Serrano P, Sánchez A, Candela F, Perez MT, Calpena R. Randomized clinical and manometric study of advancement flap *vs* fistulotomy with sphincter reconstruction in the management of complex fistula-in-ano. *Am J Surg* 2006; **192**: 34-40 [PMID: 16769272 DOI: 10.1016/j.amjsurg.2006.01.028]

48 **Garcia-Olmo D**, Herreros D, Pascual I, Pascual JA, Del-Valle E, Zorrilla J, De-La-Quintana P, Garcia-Arranz M, Pascual M. Expanded adipose-derived stem cells for the treatment of complex perianal fistula: a phase II clinical trial. *Dis Colon Rectum* 2009; **52**: 79-86 [PMID: 19273960 DOI: 10.1007/DCR.0b013e3181973487]

49 **CEBM**. OCEBM levels of evidence. [cited 11 January 2022]. Available from: https://www.cebm.ox.ac.uk/resources/levels-of-evidence/ocebm-levels-of-evidence

World Journal of Gastroenterology

Submit a Manuscript: https://www.f6publishing.com

World J Gastroenterol 2022 April 28; 28(16): 1625-1640

DOI: 10.3748/wjg.v28.i16.1625

ISSN 1007-9327 (print) ISSN 2219-2840 (online)

REVIEW

Noninvasive imaging of hepatic dysfunction: A state-of-the-art review

Ting Duan, Han-Yu Jiang, Wen-Wu Ling, Bin Song

Specialty type: Radiology, nuclear medicine and medical imaging

Provenance and peer review: Invited article; Externally peer reviewed.

Peer-review model: Single blind

Peer-review report's scientific quality classification

Grade A (Excellent): 0
Grade B (Very good): 0
Grade C (Good): C, C
Grade D (Fair): 0
Grade E (Poor): 0

P-Reviewer: Duan S, China; Mogahed EA, Egypt

Received: March 18, 2021
Peer-review started: March 18, 2021
First decision: July 3, 2021
Revised: July 17, 2021
Accepted: March 27, 2022
Article in press: March 27, 2022
Published online: April 28, 2022

Ting Duan, Han-Yu Jiang, Bin Song, Department of Radiology, West China Hospital, Sichuan University, Chengdu 610041, Sichuan Province, China

Wen-Wu Ling, Department of Medical Ultrasound, West China Hospital of Sichuan University, Chengdu 610041, Sichuan Province, China

Corresponding author: Bin Song, MD, Chief Doctor, Professor, Department of Radiology, West China Hospital, Sichuan University, No. 37 Guoxue Alley, Chengdu 610041, Sichuan Province, China. anicesong@vip.sina.com

Abstract

Hepatic dysfunction represents a wide spectrum of pathological changes, which can be frequently found in hepatitis, cholestasis, metabolic diseases, and focal liver lesions. As hepatic dysfunction is often clinically silent until advanced stages, there remains an unmet need to identify affected patients at early stages to enable individualized intervention which can improve prognosis. Passive liver function tests include biochemical parameters and clinical grading systems (*e.g.*, the Child-Pugh score and Model for End-Stage Liver Disease score). Despite widely used and readily available, these approaches provide indirect and limited information regarding hepatic function. Dynamic quantitative tests of liver function are based on clearance capacity tests such as the indocyanine green (ICG) clearance test. However, controversial results have been reported for the ICG clearance test in relation with clinical outcome and the accuracy is easily affected by various factors. Imaging techniques, including ultrasound, computed tomography, and magnetic resonance imaging, allow morphological and functional assessment of the entire hepatobiliary system, hence demonstrating great potential in evaluating hepatic dysfunction noninvasively. In this article, we provide a state-of-the-art summary of noninvasive imaging modalities for hepatic dysfunction assessment along the pathophysiological track, with special emphasis on the imaging modality comparison and selection for each clinical scenario.

Key Words: Hepatic dysfunction; Ultrasound; Computed tomography; Magnetic resonance imaging

©The Author(s) 2022. Published by Baishideng Publishing Group Inc. All rights reserved.

Core Tip: Hepatic dysfunction can be frequently found in hepatitis, cholestasis, metabolic diseases, and focal liver lesions. It remains clinically silent until advanced stages, so there remains an unmet need to identify affected individuals at early stages. Imaging techniques, including ultrasound, computed tomography, and magnetic resonance imaging, allow morphological and functional assessment of the entire hepatobiliary system. In this article, we provide a state-of-the-art summary of noninvasive imaging modalities for assessing hepatic dysfunction in various clinical situations.

Citation: Duan T, Jiang HY, Ling WW, Song B. Noninvasive imaging of hepatic dysfunction: A state-of-the-art review. *World J Gastroenterol* 2022; 28(16): 1625-1640
URL: https://www.wjgnet.com/1007-9327/full/v28/i16/1625.htm
DOI: https://dx.doi.org/10.3748/wjg.v28.i16.1625

INTRODUCTION

Hepatic dysfunction is a common result of a wide variety of diseases, including hepatobiliary disorders and systemic diseases. The clinical symptoms of hepatic dysfunction (*e.g.*, jaundice, anorexia, and abdominal pain) are varied and nonspecific[1]. Liver biopsy is the gold standard for hepatic dysfunction currently. Accurate as it is, liver biopsy is invasive, and susceptible to sampling errors and inter-observer variation. Besides, liver biopsy is limited by various complications and operator expertise. Therefore, the introduction of noninvasive diagnostic approaches is pivotal to addressing the above limitations of liver biopsy. Hepatic dysfunction usually manifests as biochemical abnormalities of serum markers, typically involving hepatocyte damage, cholestasis, bilirubin, synthesis function, and liver fibrosis[2,3]. Nevertheless, it is worth noting that not all patients with abnormalities in the above markers have primary liver disease, highlighting the wide differential diagnosis spectrum of abnormal liver chemistry and metabolic functions[2]. Considering the limited value of single serum markers in hepatic dysfunction evaluation, clinical grading systems integrating biochemical parameters and clinical symptoms have been developed to reveal impaired liver function. Among them, the Child-Pugh score is a widely adopted clinical scoring system that is particularly useful in selecting surgical candidates with hepatocellular carcinoma (HCC) and cirrhosis[4]. The Model for End-Stage Liver Disease score was initially developed to predict short-term survival in patients undergoing transcutaneous intrahepatic portosystemic shunt procedures and has been later expanded to stratify patients with end-stage liver disease awaiting transplantation[5]. Nevertheless, the performances of these clinical grading systems are suboptimal in mild liver injuries. Furthermore, despite widely used and readily available, biochemical parameters and clinical grading systems only provide indirect information about the hepatic function [6]. In contrast, dynamic quantitative tests, such as the indocyanine green (ICG) clearance test[7], allows direct measurements of liver clearance capacity and hence has become a routine test in preoperative liver function evaluation. However, discrepancies have been reported on the performances of ICG clearance test in clinical outcome prediction[8]. In addition, the accuracy of ICG clearance is affected by operator's proficiency and the concentration of blood oxygen and other competitive agents[9].

Noninvasive imaging techniques, including ultrasound (US), computed tomography (CT), and magnetic resonance imaging (MRI), allow morphological and functional assessment of the entire hepatobiliary system (Table 1). These techniques permit qualitative and quantitative evaluation of hepatocyte quantity and function, fibrosis degree, type and severity of metabolic disorders, and excretory function of the biliary system. Therefore, through accurate hepatic dysfunction measurement and identification of affected individuals at early diseases stages, noninvasive imaging modalities offer appeal in individualized clinical decision-making and improving patient prognosis. Therefore, this review provides a state-of-the-art summary of noninvasive imaging modalities for assessing hepatic dysfunction along the pathophysiological track in various clinical situations.

HEPATITIS-INCLUDED HEPATIC DYSFUNCTION

Hepatitis is a major global public health problem affecting hundreds of millions of people. The common causes are the virus, bacteria, amoeba, and other infections. Other relatively rare causes include drug and food poisoning. Most deaths from viral hepatitis are due to hepatitis B and hepatitis C. An estimated 257 million people were living with hepatitis B and 71 million people were living with hepatitis C[10].

Acute hepatitis

In mild hepatitis, edema of hepatocytes and inflammatory cells gather in the portal area at pathology. At

Table 1 Noninvasive imaging modalities for hepatic dysfunction

Imaging modality		Target changes
US	B-mode ultrasonography	Echo intensity
		Morphological changes
	Color Doppler US	Phase and velocity of blood flow
	Contrast-enhanced US	Hemodynamic changes with better contrast than Doppler US
	Transient elastography	Liver stiffness
		Steatosis
	Point shear wave elastography	Liver stiffness
	2D-shear wave elastography	Liver stiffness
CT	Conventional CT	CT value
		Morphological changes
		Steatosis
	Dynamic enhanced CT	Portal hypertension
		Hemodynamic changes
	CT perfusion	Quantitative measurement hemodynamic changes
	Liver extracellular volume on CT	Fibrosis
MR	Conventional MRI	Morphological changes
	MR elastography	Liver stiffness
	Diffusion-weighted MRI	Brownian motion of water molecules
	Gadoxetate-enhanced MRI	Number and function of hepatocytes
	MR perfusion	Quantitative measurement hemodynamic changes
	Chemical-shift-encoded MRI	Steatosis
		Iron overload
	MR cholangiopancreatography	Biliary system
	Quantitative susceptibility mapping	Iron overload
	Liver extracellular volume on MRI	Fibrosis

US: Ultrasound; CT: Computed tomography; MR: Magnetic resonance; MRI: MR imaging.

this stage, the imaging findings are generally nonspecific, such as enhanced echo on US, slightly decreased density on CT, or increased signals on T2-weighted imaging.

With the aggravation of inflammation, histologic changes become more pronounced, including lobular disarray, acidophilic degeneration of hepatocytes, focal lobular necrosis, disruption of bile canaliculi with cholestasis, and portal and parenchymal infiltration of inflammatory cells (predominantly lymphocytes and macrophages)[11], as well as hypertrophy and hyperplasia of Kupffer cells and macrophages. These changes can lead to heterogeneous appearances of the liver parenchyma on pre-contrast imaging. Meanwhile, the microcirculation in the liver deteriorates, causing patchy enhancement or wedge-shaped enhancement pattern of the liver parenchyma on contrast-enhanced imaging. In addition, the "halo-ring sign" or "track sign" appears around the portal vein as a result of increased lymph inflow and blocked lymph backflow[12]. The transient portal hypertension (PH) leads to increased pressure in the gallbladder vein, causing subsequent subserosal edema of the gallbladder wall. With the gallbladder wall thickening and protruding into the cavity, a typical sign of "centripetal edema" appears[13]. Enlarged lymph node can be detected on US, CT, or MRI[14].

A high proportion of severe acute hepatitis cases can result in significant liver failure[15,16]. In these cases, extensive hepatocyte necrosis can lead to substantial bridging. Irregular necrosis is depicted as map-like low density on CT images. On contrast-enhanced images in the portal venous phase, the necrotic areas usually become hyper-attenuating compared with adjacent liver parenchyma due to infiltrates of inflammatory cells, increased arterial blood supply, and widened intercellular space. This sign is called "reverse enhancement", which is a characteristic manifestation of severe hepatitis. In addition, ascites can be detected frequently[15] (Figure 1). Grillet *et al*[15] reported that heterogeneous

DOI: 10.3748/wjg.v28.i16.1625 **Copyright** ©The Author(s) 2022.

Figure 1 Ultrasound and computed tomography images of a 19-year-old man with severe drug-induced hepatitis. A: High frequency ultrasound image showing increased and heterogenous echo intensity of the liver parenchyma; B: Pre-contrast computed tomography image showing map-like hypodense area in the liver parenchyma and moderate ascites; C: The hypodense areas on (B) became hyperattenuating on portal venous phase image, showing "reverse enhancement".

liver parenchyma on CT would be particularly beneficial for patients with acute severe autoimmune hepatitis as histological examinations could be technically challenging due to complications. They also reported heterogeneous CT features of severe alcoholic hepatitis, indicating that these imaging features were mainly associated with transient heterogeneous steatosis and liver perfusion disorders[15]. Furthermore, Tana *et al*[17] used texture analysis to quantify the heterogeneity of the liver parenchyma, and showed that texture features of the liver could provide important quantitative information in predicting the severity and outcomes of patients with acute alcohol-associated hepatitis.

In summary, ultrasound is recommended as the first-line imaging modality for morphologic evaluation in patients with acute hepatitis. Contrast-enhanced CT or MRI should be considered when intrahepatic necrosis is suspected.

Chronic hepatitis

Chronic hepatitis refers to a morphologic pattern that is usually observed in patients with chronic viral hepatitis, autoimmune hepatitis, drug-induced hepatitis, and alcoholic hepatitis. Chronic hepatitis is characterized by several pathologic changes. These include inflammations of the portal veins and sometimes of the bile ducts; periportal injury and inflammation; several degeneration and apoptosis of intra-acinar hepatocytes secondary to inflammatory response; and different forms of fibrosis[18]. The end-stage progression is cirrhosis. The image findings of liver fibrosis and cirrhosis are described in later sections.

Typical imaging characteristics of chronic hepatitis include unsmooth liver margin, blunt edge, widened portal vein, enlarged spleen, and thickened gallbladder wall[19] (Figure 2). Unfortunately, when the above signs appear, liver injury has usually occurred for a long time and become irreversible.

Many efforts have been devoted to capturing the early hepatic microcirculation and perfusion changes of chronic hepatitis using imaging techniques. The deposition of collagen in the space of Disse and sinusoidal capillarization result in increased resistance to incoming sinusoidal blood flow, leading to a decrease in portal venous flow to the liver and an increase in hepatic arterial flow, and subsequently the formation of intrahepatic and portosystemic shunts. Cao *et al*[20] reported a significant correlation between the ICG clearance rate and MR-based portal venous perfusion, suggesting that MR-based portal venous perfusion could be used as a surrogate for liver function assessment.

Another important cause for hepatic dysfunction in chronic hepatitis is the impaired hepatocytes. Active transport of MR hepatobiliary contrast agents (*e.g.*, gadoxetate and gadobenate dimeglumine) into the hepatocytes can reflect hepatocyte functions. Hepatobiliary phase (HBP) images can be acquired at about 20 min after contrast administration for gadoxetate and 1-2 h for gadobenate dimeglumine, with signal intensity on HBP images providing important information regarding liver function[21,22]. On this basis, studies further showed that T1 mapping could eliminate signal deviation and allow accurate liver function quantification[23-25].

Without proper and timely intervention, chronic hepatitis may progress to liver fibrosis (LF) and PH, which would be discussed in later sections.

CHOLESTASIS

Acute cholestasis

Acute cholestasis is characterized with mechanical biliary obstruction of any cause, such as choledocholithiasis, strictures (*e.g.*, neoplastic, inflammatory, or postoperative), pancreatitis, choledochal cysts,

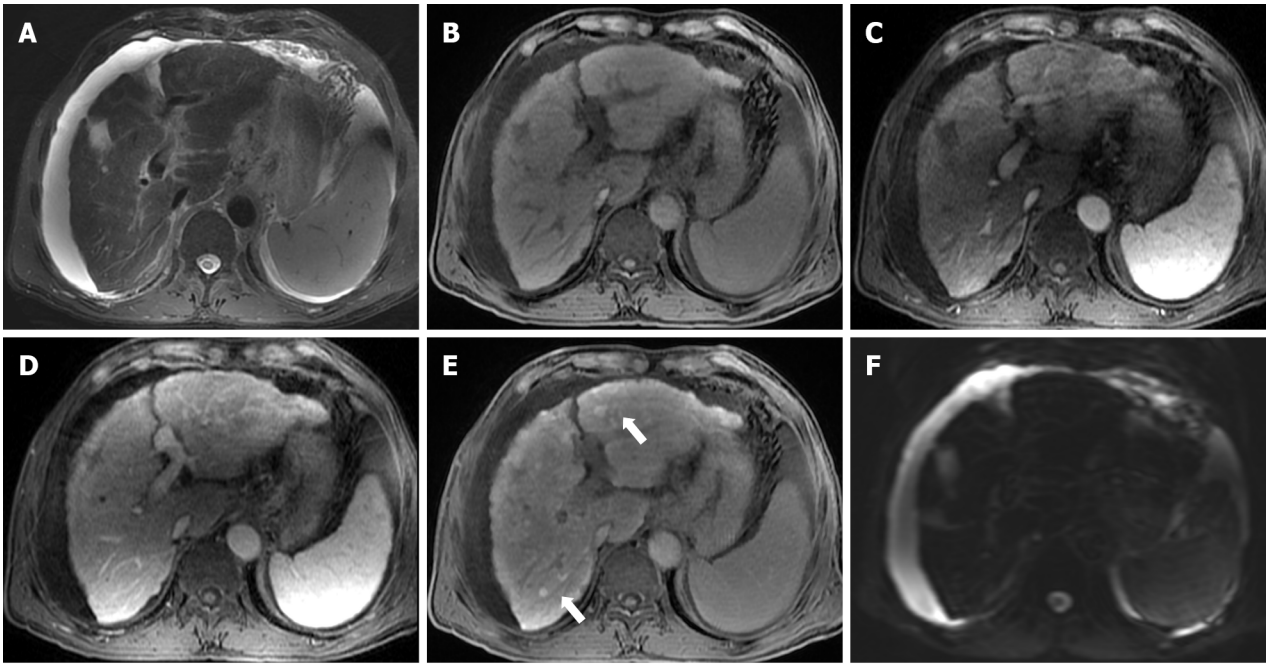

DOI: 10.3748/wjg.v28.i16.1625 **Copyright** ©The Author(s) 2022.

Figure 2 Gadoxetate-enhanced magnetic resonance images of a 70-year-old man with chronic hepatitis B. T2-weighted image (A) shows signal loss of the liver parenchyma, suggesting iron overload. T1-weighted pre-contrast (B), arterial phase (C), and portal venous phase (D) images show nodular contour and patchy enhancement of the liver parenchyma. Hepatobiliary phase image demonstrates diffuse hyperintense nodules (E, black arrows) without diffusion restriction on diffusion-weighted imaging (F), indicating regenerative nodules. Moderate ascites was also noted.

parasitic diseases (*e.g.*, ascariasis and fascioliasis), or even extrinsic pressure from enlarged lymph nodes [26]. US is promising for diagnosing early-stage acute cholestasis. However, magnetic resonance cholangiopancreatography (MRCP) is more sensitive in assessing the location, severity, cause, and extent of biliary obstruction[27]. MRCP images of a patient with suspected acute cholestasis can help: (1) Confirm the obstruction; (2) exclude other causes of jaundice; (3) determine the location of obstruction (intra- or extrahepatic ducts); (4) measure the approximate length of the biliary stricture; and (5) reveal the status of proximal bile ducts[28] (Figure 3).

Apart from MRCP, gadoxetate-enhanced MRI can also aid in evaluating acute cholestasis. Although less widely available than MRCP, it has a unique role in detecting bile leaks after biliary surgery or liver trauma[29].

Recently, elastography has also been applied in acute cholestasis. Kim *et al*[30] reported that liver stiffness measured by MRI elastography (MRE) is elevated with the increase of cholestasis, and can be predictive for the sufficiency of biliary decompression after biliary drainage.

Chronic cholestasis

Most chronic cholestatic disorders are insidious in onset, and chronic cholestasis progresses slowly over the course of years before it becomes clinically apparent. The most frequent causes of chronic cholestasis are primary sclerosing cholangitis (PSC) and primary biliary cirrhosis (PBC). Furthermore, allograft rejection can lead to bile duct damage and subsequent chronic cholestasis in patients who have undergone liver transplantation.

Characteristic imaging features of PSC include thickened concentric mural wall involving the extrahepatic biliary duct, with segmental intrahepatic biliary duct dilatation, preferentially affecting the left hepatic lobe. Gallbladder luminal sludge or stones and inflammatory polyps can also be depicted [31]. On MRCP, PSC can have typical features of biliary ductal changes, such as intrahepatic and extrahepatic short segmental bile duct strictures alternating with normal or mildly dilated bile ducts, giving rise to a beading appearance. At times, mild diffuse dilatation of the entire intrahepatic biliary system with a branching-tree appearance can be observed[32] (Figure 4).

On the other hand, PBC is characterized by chronic, non-suppurative lymphocytic cholangitis that predominantly affects small and interlobular bile ducts in the portal triads, leading to vanishing bile duct syndrome[33]. Diffuse hepatomegaly is the most pronounced morphological change. Patients usually develop micronodular or liver fibrosis. Most early PBCs had normal appearances on MRCP. As disease progresses, intrahepatic bile ducts become irregular. Thereafter, most peripheral branches of the intrahepatic bile ducts gradually become invisible, while medium-sized bile ducts present with reduced caliber and irregularity. These findings could be explained pathologically by destruction and disappearance of small intrahepatic bile ducts in PBC[34]. The assessments of liver function in PSC is

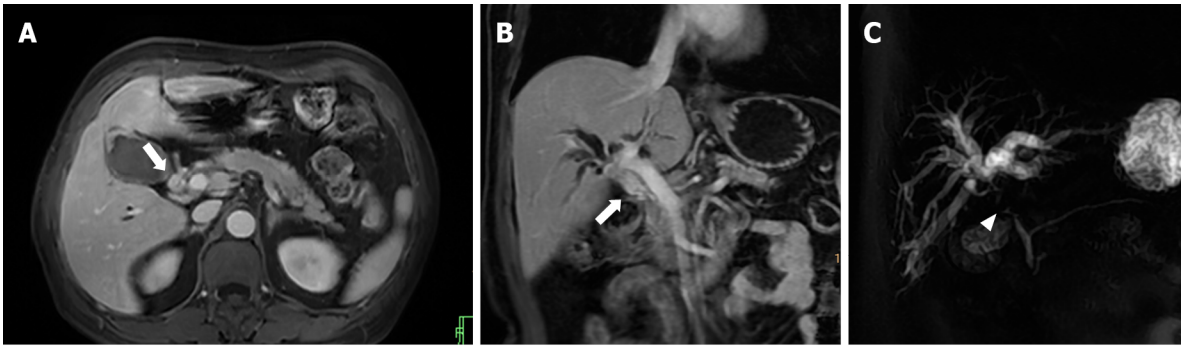

DOI: 10.3748/wjg.v28.i16.1625 **Copyright** ©The Author(s) 2022.

Figure 3 Magnetic resonance images of a 63-year-old man with hilar cholangiocarcinoma. Axial (A) and coronal (B) portal venous phase images demonstrate thickened hilar bile duct wall (white arrows). The extrahepatic bile duct is absent on magnetic resonance cholangiopancreatography image (C, white arrowhead), and the intrahepatic bile ducts are dilated and distorted ("vine-sign").

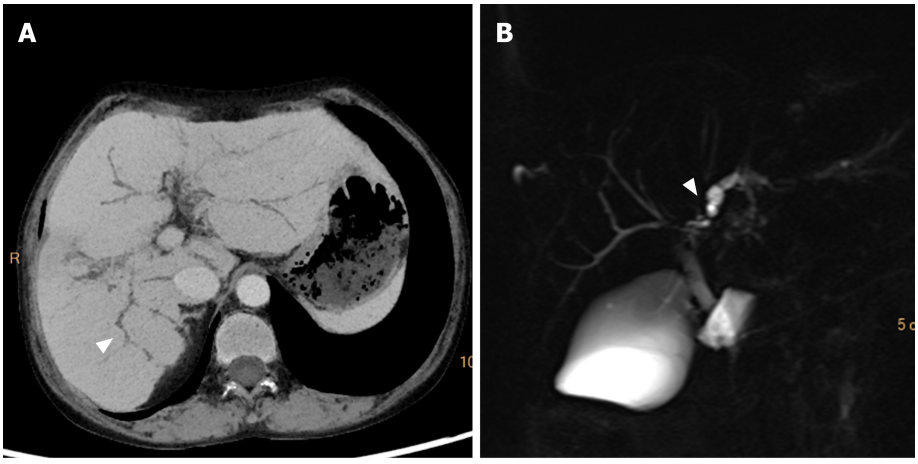

DOI: 10.3748/wjg.v28.i16.1625 **Copyright** ©The Author(s) 2022.

Figure 4 Computed tomography and magnetic resonance cholangiopancreatography images of a-42-year-old woman with primary sclerosing cholangitis. Minimum density projection computed tomography image of portal venous phase (A) and magnetic resonance cholangiopancreatography image (B) show a "beading appearance" of the intrahepatic bile ducts (white arrowheads).

similar to those in cirrhosis caused by chronic hepatitis[35].

In summary, when cholestasis is suspected, ultrasound is recommended for screening. When biliary obstruction or stricture is confirmed, MRI (MRCP in particular) is the preferred modality for further examinations.

METABOLIC DISEASES

Nonalcoholic fatty liver disease

Nonalcoholic fatty liver disease (NAFLD) is defined as liver fat exceeding 5%-10% by weight and exists as a spectrum from steatosis (usually stable) to nonalcoholic steatohepatitis (NASH) (characterized by cellular ballooning, necroapoptosis, inflammation, and fibrosis)[36]. Early detection and treatment of NAFLD can help prevent its progression to NASH and cirrhosis[37].

Among the imaging methods which enable liver fat quantification, transient elastography (TE) is the most widely studied US approach. A recent meta-analysis revealed that in NAFLD patients, the areas under the curve (AUC) of TE were 0.819 for S0 *vs* S1-S3 and 0·754 for S0-S1 *vs* S2-S3[38]. Another meta-analysis reported superior result of TE in the diagnosis of mild steatosis (AUC, 0.96) compared with severe steatosis (AUC, 0.70)[39]. Thus, an insufficient performance for TE in the diagnosis of moderate to severe steatosis should be noted.

The sensitivity and specificity of CT in detecting hepatic steatosis were reported ranging from 46% to 72% and from 88 to 95%, respectively[40]. However, given the potential additive radiation exposure, CT is not typically utilized as a screening test for NAFLD.

In addition, chemical-shift-encoded MRI-based proton density fat-fraction (PDFF) is increasingly accepted as an effective imaging modality in evaluating liver steatosis. A recent meta-analysis which included 2979 patients showed that MRI-PDFF offered pooled sensitivities of 0.71-0.91 and specificities of 0.88-0.93 for staging liver steatosis[41], with the optimal diagnostic performance achieved for detecting ≥ S1 (sensitivity, 0.92; specificity, 0.93) steatosis. Choi *et al*[42] compared the performance of MRI-PDFF and TE-based controlled attenuation parameter (CAP) in staging liver steatosis, and they found that MRI-PDFF correlated far better with hepatic fat measured (r = 0.978) than with CAP (r = 0.727). Besides, several clinical randomized controlled trials have shown that PDFF can be used to monitor and predict the therapeutic effect of NAFLD[43-45].

NASH is also characterized with a distinctive increase in liver extracellular fluid, which can be measured by an increase in T1 relaxation time. However, the accumulation of excess iron in liver tissue can be a confounding factor for T1 relaxation time. In this context, iron-corrected T1 can be generated to correct for this potential bias[46,47]. In a study of 50 patients undergoing standard-of-care liver biopsy for NAFLD, iron-corrected T1 has been demonstrated to correlate with ballooning and could accurately distinguish between steatosis and NASH patients[48].

Collectively, given the costs, availability, and diagnostic performances, US may be an appropriate modality to detect NAFLD. If accurate quantification of liver fat or monitoring of efficacy is needed, MRI PDFF should be a better choice.

Iron storage disorders

Iron storage disorders are characterized by unregulated iron increase or decrease in the liver[49]. An increase in systemic iron can be a consequence of: (1) Hereditary hemochromatosis; (2) ineffective erythropoiesis or chronic liver disease; and (3) parenteral iron administration. Excessive intracellular deposition of iron ultimately results in tissue and organ damage. The diagnosis of iron overload relies on serum iron studies (elevated transferrin saturation and elevated serum ferritin levels), genetic testing, and sometimes liver biopsy to assess the hepatic iron concentration and degree of liver injury [50].

The paramagnetic effect of liver iron on the neighborhood protons affects T2 and T2* relaxation times by accelerating the signal decay. Therefore, the presence of iron results in tissue signal loss on T2 and T2 * weighted images that is proportional to iron content, which is the basic principle of MRI in evaluating liver iron overload[51]. The MRI methods for liver iron quantification can be divided into signal intensity ratio methods and relaxometry methods.

With signal intensity ratios, studies showed that although these methods tended to overestimate mild to moderate hepatic iron overload, it might be more precise in severe iron overload, particularly on 3T MRI[52,53]. On the other hand, relaxometry techniques measure the MR signal decay resulting from the shortening of T2 or T2* relaxation times. For practical purposes, the inverse of T2 or T2* (the relaxation rates, R2 or R2*) is generally used instead, because the elevation in liver iron concentration directly increases the R2 and R2*[54]. The most known R2 relaxometry method is commercially available as FerriScan and is FDA-approved for 1.5T machines[55]. Well validated across different sites and platforms, liver R2 has an excellent correlation with liver iron concentration, with low inter-exam variability and good inter-machine reproducibility[56]. However, major limitations of this technique include long acquisition times and high cost. In contrast, R2* relaxometry is performed with fast, single breath-hold spoiled GRE multi-echo sequences in most MR scanners. Several studies demonstrated an excellent linear relationship between R2* and liver iron concentration[57,58] (Figure 5). However, R2* measurements may be affected by liver fibrosis and the coexistence of fat[59].

Quantitative susceptibility mapping (QSM) was first used in the nervous system. It is based on the concept of transforming hypointense blooming artifacts into precise quantitative measurements of spatial biodistributions. Therefore, it is not affected by liver fibrosis and the coexistence of fat[59]. Tipirneni-Sajja *et al*[60] applied a multispectral autoregressive moving average model in QSM to liver iron concentration. They found that autoregressive moving average-QSM showed a good association with an iron concentration in both phantom study and *in vivo* cohort, indicating that autoregressive moving average-QSM could provide a potentially confounder-free assessment of hepatic iron overload [60].

Therefore, the influence of iron on MRI signal makes MRI the most appropriate imaging modality for quantifying liver iron concentration, and QSM may be the most potential sequence to serve this purpose.

PROGRESSION OF DIFFUSE LIVER DISEASE

Liver fibrosis is a scarring response that occurs in almost all chronic liver injuries mentioned above. Ultimately, liver fibrosis can lead to cirrhosis, in which PH is a common and lethal complication. Early diagnosis and accurate staging of these conditions can facilitate timely patient care and optimize prognoses.

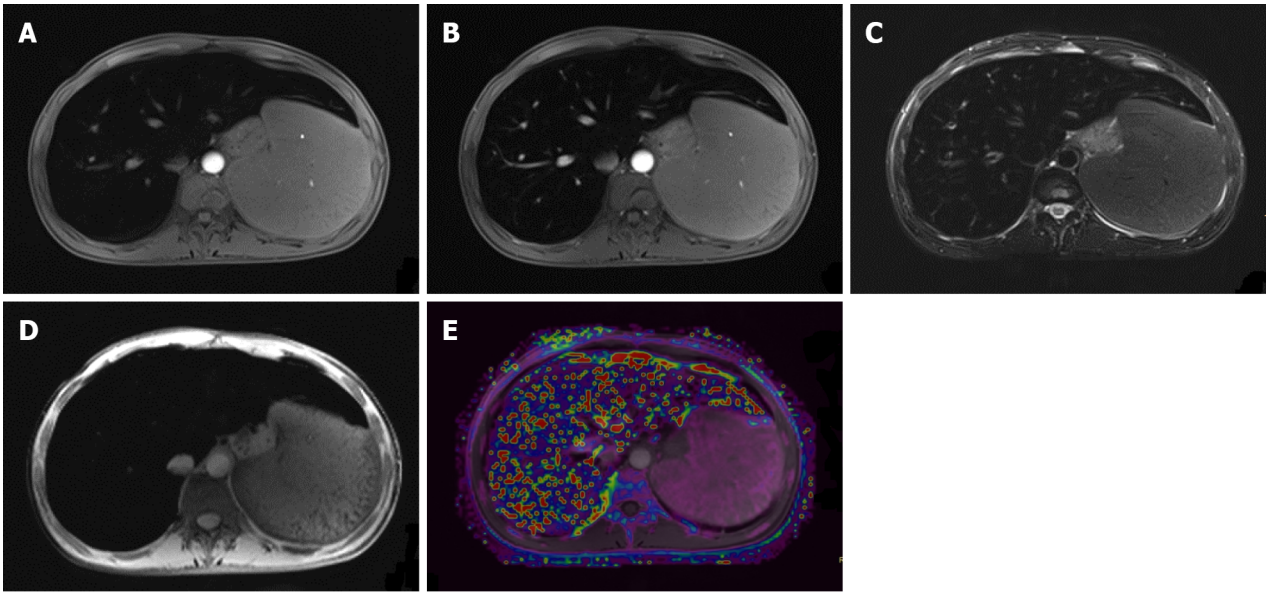

DOI: 10.3748/wjg.v28.i16.1625 **Copyright** ©The Author(s) 2022.

Figure 5 Magnetic resonance images of a 26-year-old man with hemochromatosis. Pre-contrast T1-weighted image (A), portal venous phase T1-weighted image (B), T2-weighted image (C), and SWI image (D) showed signal intensity in liver parenchyma, while $R2^*$ mapping (E) shows increased signal intensity in the liver, demonstrating severe iron overload. R2: Relaxation rate.

Liver fibrosis

With the deposition of collagen in the extracellular space, liver parenchyma stiffness increases as the disease progresses. These alterations can be measured by elastography techniques.

Among all elastography techniques, TE is the most widely used method to determine liver stiffness and may serve as a potential surrogate to assess liver fibrosis. The pooled AUC of TE for diagnosing liver fibrosis was 0.859 for NAFLD, 0.860 for chronic hepatitis B, and 0.830 for alcohol-related liver disease in previous meta-analyses[61-63]. In addition, shear wave elastography (SWE) was also reported with a high diagnostic accuracy for detecting early-stage liver fibrosis[64-66]. Petzold *et al*[67] found that a cutoff value of 8.05 kPa could differentiate patients with advanced fibrosis (F ≥ 3) from those with no or mild fibrosis (F0-F2) with AUCs ranging between 0.995 and 1.000. A meta-analysis revealed no significant difference between TE and SWE in the diagnosis of significant fibrosis, advanced fibrosis, and cirrhosis, but the proportion of failed measurements was over ten-fold greater with TE than SWE [68].

In addition to ultrasound-based elastography techniques, the MR-based elastography technique MRE is another promising noninvasive modality to assess liver fibrosis[69,70]. A prospective study of 67 PSC patients revealed a high sensitivity (87.5%) and specificity (96%) of MRE in detecting cirrhosis[71]. In another study, a significant discriminatory ability of MRE was confirmed when distinguishing between early to moderate and advanced liver fibrosis, shedding light on the incremental values of liver stiffness measurements on MRE in prognosis stratification[72]. Fu *et al*[73] found that the efficacy of MRE was superior compared with TE in detecting significant fibrosis (AUC: 0.965 *vs* 0.906) and advanced fibrosis (AUC: 0.957 *vs* 0.913). These results were confirmed by a meta-analysis in which the pooled AUC of MRE (0.97) was significantly higher than that of SWE (0.88) in detecting significant fibrosis[74].

As fibrosis progresses, the deposition of fibroglia can lead to enlarged extracellular space. Therefore, liver extracellular volume (LECV) measured by CT or MR T1 mapping can also be used to assess liver fibrosis[75-77]. In a cynomolgus monkey model of NASH, Lyu *et al*[78] found that LECV was significantly correlated with the fibrosis score (r = 0.949), and demonstrated an AUC of 0.945 in diagnosing liver fibrosis.

Diffusion-weighted imaging is a noninvasive technique based on the Brownian motion of water molecules in biological tissue and has shown potential in assessing liver fibrosis[79]. Studies showed that in chronic liver diseases, apparent diffusion coefficients in diffusion-weighted imaging decreased as the degree of fibrosis increased, but this relationship was not statistically significant due to confounding factor of blood microcirculation in the capillaries[80,81]. Recent studies have explored various diffusion models to avoid this influence. Lefebvre *et al*[82] reported that intravoxel incoherent motion parameter with 10 *b*-values was reproducible for liver tissue characterization and that perfusion fraction (f) provided good diagnostic performance for distinguishing dichotomized grades of inflammation. Park *et al*[83] showed that the distributed diffusion coefficient from the stretched exponential model was the most accurate diffusion-weighted imaging parameter for staging liver fibrosis as it could avoid the confounding effect by steatosis.

Besides, liver fibrosis can result in changes in hepatic microcirculation and perfusion. Fan *et al*[84] found that MR perfusion parameters, time to peak, and mean transit time in particular could reflect the degree of liver fibrosis. Similarly, Yoon *et al*[85] also found that portal blood flow was significantly lower in clinically significant hepatic fibrosis and that mean transit time and extracellular volume increased in cirrhosis.

In general, TE is the modality preferred for LF. SWE can be considered in patients who fail in TE examination. As a modality which is gaining increasingly popularity, MRE is preferred over sonographic elastography in patients with ascites and obesity, or requiring more comprehensive liver workup.

PH

PH is defined by values of hepatic venous pressure gradient (HVPG) > 5 mmHg, whereas clinically significant PH could be diagnosed if HVPG ≥ 10 mmHg. HVPG has been widely-validated as associated with variceal bleeding, hepatic decompensation, and mortality. However, its measurement is invasive and requires extensive expertise[86].

Characteristic imaging features of PH include portosystemic shunts, splenomegaly, ascites, and widening of the portal vein. However, these findings are often detectable at end stages of the disease, thus demonstrating limited sensitivities for diagnosing PH.

For quantitative methods, similar to liver fibrosis, elastography techniques have gained increasing attention in the assessment of PH[87]. Among ultrasound-based elastography techniques, TE was the most validated method for PH assessment. A meta-analysis involving 12 studies showed that liver stiffness measured on TE was well correlated with HVPG and demonstrated a sensitivity of 91.2% and specificity of 81.3% in diagnosing clinically significant PH (cut-off values 13.6-18.6 kPa)[88]. In contrast, despite much less applied than TE, SWE also exhibited encouraging profiles in predicting PH and esophageal varices (AUC: 0.86-0.89)[89-93].

Liver and spleen stiffness measured by MRE also showed promising performances in predicting PH and esophageal varices. A recent meta-analysis found that liver and spleen stiffness on MRE could serve as supplemental noninvasive assessment tools for detecting clinically significant PH and that spleen stiffness might be more specific and accurate than liver stiffness (AUC: 0.88 *vs* 0.92)[94].

Hemodynamic alteration is another distinct feature in PH. In patients with cirrhosis, decreased portal and total hepatic perfusion were observed[95,96]. Studies showed that mean portal vein velocity in cirrhosis was lower than that in normal subjects and decreased with the severity of liver cirrhosis and gastroesophageal varices[97,98]. The portal vein velocity measured by doppler US could be used as noninvasive triage tests before referral to endoscopy (sensitivity, 84%-97%), but the cutoff value varied from 16-19 cm/s[99,100]. Several MR techniques have also been proposed for liver hemodynamic assessment in PH. Chouhan *et al*[101] used phase-contrast MR to assess the portal vein and the infrahepatic and suprahepatic inferior vena cava. The hepatic artery flow was estimated by subtracting infrahepatic from suprahepatic inferior vena cava flow and portal vein flow, which showed significant positive correlations with HVPG[101]. Additionally, 4D flow MRI also demonstrated promising capacity in quantifying blood flow in the hepatic and splanchnic vasculature[102,103]. Motosugi *et al*[104] found that azygos flow > 0.1 L/min and portal venous flow less than the sum of splenic and superior mesenteric vein flow were useful markers to stratify the risk of gastroesophageal varices bleeding in patients with cirrhosis. Another study revealed that the combination of liver stiffness measured by MRE and perfusion metrics measured by contrast-enhanced-MRI had an AUC of 0.903 for diagnosing PH, and an AUC of 0.785 for detecting clinically significant PH[105].

In summary, TE and SWE are promising noninvasive approaches for preliminary PH screening. Nevertheless, for patients with increased risk for esophageal and gastric varices, multiparametric MRI may be a more accurate and comprehensive modality.

FOCAL LIVER LESIONS

Focal liver lesions include benign tumors, malignant tumors, and hepatic echinococcosis. The impact of focal liver lesions on liver function includes the decrease of normal liver volume and the reduced hepatocyte function, especially in surgical candidates with malignant liver tumors. Previous studies have shown that a high residual to total liver volume ratio (≥ 40%) was required for patients with an impaired liver function to tolerate resection[106-108]. Gadoxetate-enhanced MRI is also used to evaluate the hepatic function of patients with focal liver lesions. Yoon *et al*[109] reported that T1 mapping on gadoxetate-enhanced MRI provided information on global liver function and demonstrated functional heterogeneity in patients with HCC. Other studies have combined liver volume with hepatocyte function, and their results showed that combined T1 mapping and residual liver volume on gadoxetate-enhanced MRI could assess liver function with good diagnostic accuracy in patients with liver tumors [110-112]. Kim *et al*[113] and Wang *et al*[114] reported that the combination could predict post hepatectomy liver failure better than the ICG clearance test in patients with HCC who underwent hepatectomy.

To sum up, CT can be used to calculate the residual liver volume for surgical candidates. Gadoxetate-enhanced MRI can not only reflect residual liver volume, but also reveal the functional information of hepatocytes.

CONCLUSION

In this article, we provide a summary of noninvasive imaging modalities for assessing hepatic dysfunction in various clinical situations and case scenarios (Figure 6). Several challenges still exist in noninvasive imaging of hepatic dysfunction. First, many imaging parameters have inconsistencies on the device. Therefore, a unified threshold cannot be adopted. Second, quantification of sensitivity and specificity usually requires an effective reference standard (*e.g.*, liver biopsy) which may not be readily available. Furthermore, most of the current studies focus on the role of a single method or sequence, with limited multiparametric, multimodal, and multidisciplinary approaches to evaluate liver dysfunction.

The long-term goal in hepatic dysfunction imaging is to develop reliable, noninvasive, and comprehensive methods which could reveal not only the disease severities but also etiologies using safe and clinically available techniques. However, to accomplish this goal will require advances in imaging sciences (improved image modalities standardization and quantitation, further exploration of US, CT, and MR imaging methods, and combination of multiparametric and multimodal imaging techniques). On this basis, radiomics and artificial intelligence may provide further assistance in quantifying high-level imaging features beyond human eyes and help in constructing effective predictive models. A better understanding of the human genetic variation underlying differences in the liver will further contribute to this field. Furthermore, the potential value of combining imaging and serum biomarkers should also be explored.

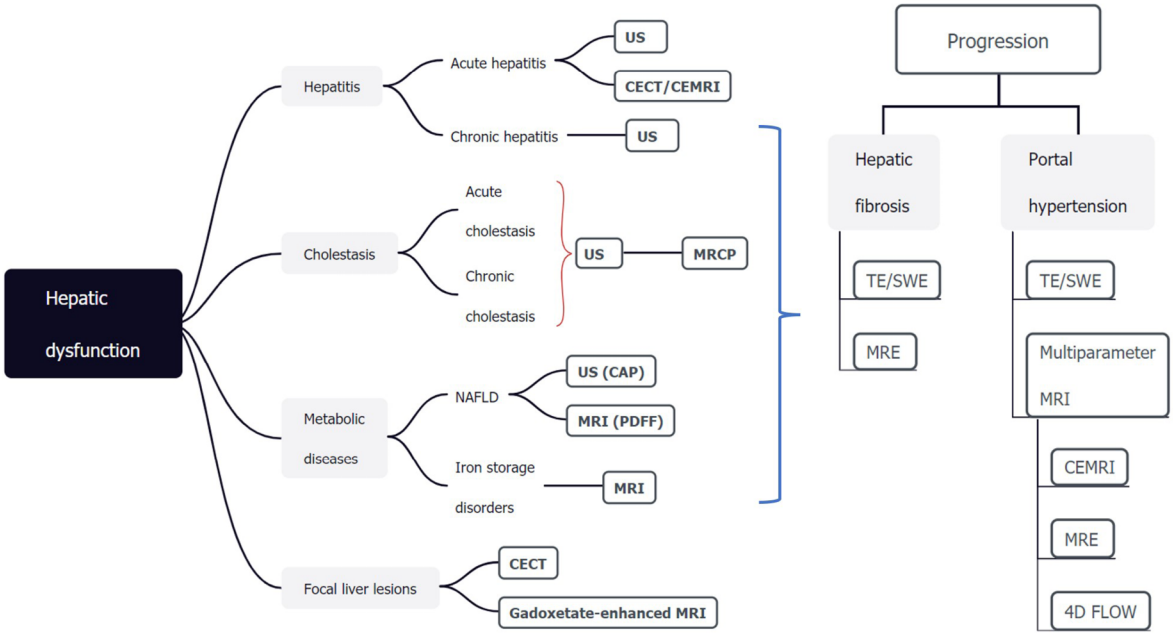

DOI: 10.3748/wjg.v28.i16.1625 **Copyright** ©The Author(s) 2022.

Figure 6 Noninvasive imaging modalities for assessing hepatic dysfunction. The TextTitle modalities are recommended and should be the first-line methods. US: Ultrasound; CT: Computed tomography; MRI: Magnetic resonance imaging; TE: Transient elastography; SWE: Shear wave elastography; MRE: MRI elastography; MRCP: Magnetic resonance cholangiopancreatography; NAFLD: Nonalcoholic fatty liver disease; PDFF: Proton density fat-fraction; CAP: Controlled attenuation parameter; CECT: Contrast-enhanced CT; CEMRI: Contrast-enhanced MRI.

FOOTNOTES

Author contributions: Duan T wrote the manuscript; Jiang HY contributed significantly to manuscript preparation and revision; Ling WW helped perform the analysis with constructive discussions; Jiang HY and Song B contributed to the conception of the study; all authors have read and approved the final manuscript.

Supported by Science and Technology Support Program of Sichuan Province, No. 2021YFS0021 and 2021YFS0141.

Conflict-of-interest statement: The authors have no conflict of interests related to this study.

Open-Access: This article is an open-access article that was selected by an in-house editor and fully peer-reviewed by external reviewers. It is distributed in accordance with the Creative Commons Attribution NonCommercial (CC BY-NC 4.0) license, which permits others to distribute, remix, adapt, build upon this work non-commercially, and license their derivative works on different terms, provided the original work is properly cited and the use is non-commercial. See: https://creativecommons.org/Licenses/by-nc/4.0/

Country/Territory of origin: China

ORCID number: Ting Duan 0000-0001-6694-4520; Han-Yu Jiang 0000-0002-7726-1618; Wen-Wu Ling 0000-0002-6449-3831; Bin Song 0000-0001-7007-6367.

S-Editor: Chang KL
L-Editor: Wang TQ
P-Editor: Chang KL

REFERENCES

1 **Helmke S**, Colmenero J, Everson GT. Noninvasive assessment of liver function. *Curr Opin Gastroenterol* 2015; **31**: 199-208 [PMID: 25714706 DOI: 10.1097/MOG.0000000000000167]
2 **Agrawal S**, Dhiman RK, Limdi JK. Evaluation of abnormal liver function tests. *Postgrad Med J* 2016; **92**: 223-234 [PMID: 26842972 DOI: 10.1136/postgradmedj-2015-133715]
3 **Dillon JF**, Miller MH, Robinson EM, Hapca A, Rezaeihemami M, Weatherburn C, McIntyre PG, Bartlett B, Donnan PT, Boyd KA, Dow E. Intelligent liver function testing (iLFT): A trial of automated diagnosis and staging of liver disease in primary care. *J Hepatol* 2019; **71**: 699-706 [PMID: 31226388 DOI: 10.1016/j.jhep.2019.05.033]
4 **Dhiman RK**, Agrawal S, Gupta T, Duseja A, Chawla Y. Chronic Liver Failure-Sequential Organ Failure Assessment is

better than the Asia-Pacific Association for the Study of Liver criteria for defining acute-on-chronic liver failure and predicting outcome. *World J Gastroenterol* 2014; **20**: 14934-14941 [PMID: 25356054 DOI: 10.3748/wjg.v20.i40.14934]

5 **Bajaj JS**, O'Leary JG, Reddy KR, Wong F, Biggins SW, Patton H, Fallon MB, Garcia-Tsao G, Maliakkal B, Malik R, Subramanian RM, Thacker LR, Kamath PS; North American Consortium For The Study Of End-Stage Liver Disease (NACSELD). Survival in infection-related acute-on-chronic liver failure is defined by extrahepatic organ failures. *Hepatology* 2014; **60**: 250-256 [PMID: 24677131 DOI: 10.1002/hep.27077]

6 **Rassam F**, Olthof PB, Bennink RJ, van Gulik TM. Current Modalities for the Assessment of Future Remnant Liver Function. *Visc Med* 2017; **33**: 442-448 [PMID: 29344518 DOI: 10.1159/000480385]

7 **Lisotti A**, Azzaroli F, Buonfiglioli F, Montagnani M, Cecinato P, Turco L, Calvanese C, Simoni P, Guardigli M, Arena R, Cucchetti A, Colecchia A, Festi D, Golfieri R, Mazzella G. Indocyanine green retention test as a noninvasive marker of portal hypertension and esophageal varices in compensated liver cirrhosis. *Hepatology* 2014; **59**: 643-650 [PMID: 24038116 DOI: 10.1002/hep.26700]

8 **Bolondi G**, Mocchegiani F, Montalti R, Nicolini D, Vivarelli M, De Pietri L. Predictive factors of short term outcome after liver transplantation: A review. *World J Gastroenterol* 2016; **22**: 5936-5949 [PMID: 27468188 DOI: 10.3748/wjg.v22.i26.5936]

9 **Kokudo T**, Hasegawa K, Shirata C, Tanimoto M, Ishizawa T, Kaneko J, Akamatsu N, Arita J, Demartines N, Uldry E, Kokudo N, Halkic N. Assessment of Preoperative Liver Function for Surgical Decision Making in Patients with Hepatocellular Carcinoma. *Liver Cancer* 2019; **8**: 447-456 [PMID: 31799202 DOI: 10.1159/000501368]

10 **Lanini S**, Ustianowski A, Pisapia R, Zumla A, Ippolito G. Viral Hepatitis: Etiology, Epidemiology, Transmission, Diagnostics, Treatment, and Prevention. *Infect Dis Clin North Am* 2019; **33**: 1045-1062 [PMID: 31668190 DOI: 10.1016/j.idc.2019.08.004]

11 **Kwong S**, Meyerson C, Zheng W, Kassardjian A, Stanzione N, Zhang K, Wang HL. Acute hepatitis and acute liver failure: Pathologic diagnosis and differential diagnosis. *Semin Diagn Pathol* 2019; **36**: 404-414 [PMID: 31405537 DOI: 10.1053/j.semdp.2019.07.005]

12 **Kim SW**, Shin HC, Kim IY. Diffuse pattern of transient hepatic attenuation differences in viral hepatitis: a sign of acute hepatic injury in patients without cirrhosis. *J Comput Assist Tomogr* 2010; **34**: 699-705 [PMID: 20861772 DOI: 10.1097/RCT.0b013e3181dbe5b2]

13 **Park SJ**, Kim JD, Seo YS, Park BJ, Kim MJ, Um SH, Kim CH, Yim HJ, Baik SK, Jung JY, Keum B, Jeen YT, Lee HS, Chun HJ, Kim CD, Ryu HS. Computed tomography findings for predicting severe acute hepatitis with prolonged cholestasis. *World J Gastroenterol* 2013; **19**: 2543-2549 [PMID: 23674857 DOI: 10.3748/wjg.v19.i16.2543]

14 **Feng IC**, Wang SJ, Sheu MJ, Koay LB, Lin CY, Ho CH, Sun CS, Kuo HT. Perihepatic nodes detected by point-of-care ultrasound in acute hepatitis and acute-on-chronic liver disease. *World J Gastroenterol* 2015; **21**: 12620-12627 [PMID: 26640338 DOI: 10.3748/wjg.v21.i44.12620]

15 **Grillet F**, Calame P, Cervoni JP, Weil D, Thevenot T, Ronot M, Delabrousse E. Non-invasive diagnosis of severe alcoholic hepatitis: Usefulness of cross-sectional imaging. *Diagn Interv Imaging* 2021; **102**: 247-254 [PMID: 33069642 DOI: 10.1016/j.diii.2020.09.009]

16 **Sonthalia N**, Rathi PM, Jain SS, Surude RG, Mohite AR, Pawar SV, Contractor Q. Natural History and Treatment Outcomes of Severe Autoimmune Hepatitis. *J Clin Gastroenterol* 2017; **51**: 548-556 [PMID: 28272079 DOI: 10.1097/MCG.0000000000000805]

17 **Tana MM**, McCoy D, Lee B, Patel R, Lin J, Ohliger MA. Texture features from computed tomography correlate with markers of severity in acute alcohol-associated hepatitis. *Sci Rep* 2020; **10**: 17980 [PMID: 33087739 DOI: 10.1038/s41598-020-74599-4]

18 **Seto WK**, Lo YR, Pawlotsky JM, Yuen MF. Chronic hepatitis B virus infection. *Lancet* 2018; **392**: 2313-2324 [PMID: 30496122 DOI: 10.1016/S0140-6736(18)31865-8]

19 **Shin SW**, Kim TY, Jeong WK, Kim Y, Kim J, Kim YH, Park HC, Sohn JH. Usefulness of B-mode and doppler sonography for the diagnosis of severe acute viral hepatitis A. *J Clin Ultrasound* 2015; **43**: 384-392 [PMID: 25195942 DOI: 10.1002/jcu.22234]

20 **Cao Y**, Wang H, Johnson TD, Pan C, Hussain H, Balter JM, Normolle D, Ben-Josef E, Ten Haken RK, Lawrence TS, Feng M. Prediction of liver function by using magnetic resonance-based portal venous perfusion imaging. *Int J Radiat Oncol Biol Phys* 2013; **85**: 258-263 [PMID: 22520476 DOI: 10.1016/j.ijrobp.2012.02.037]

21 **Van Beers BE**, Pastor CM, Hussain HK. Primovist, Eovist: what to expect? *J Hepatol* 2012; **57**: 421-429 [PMID: 22504332 DOI: 10.1016/j.jhep.2012.01.031]

22 **Choi Y**, Huh J, Woo DC, Kim KW. Use of gadoxetate disodium for functional MRI based on its unique molecular mechanism. *Br J Radiol* 2016; **89**: 20150666 [PMID: 26693795 DOI: 10.1259/bjr.20150666]

23 **Nakagawa M**, Namimoto T, Shimizu K, Morita K, Sakamoto F, Oda S, Nakaura T, Utsunomiya D, Shiraishi S, Yamashita Y. Measuring hepatic functional reserve using T1 mapping of Gd-EOB-DTPA enhanced 3T MR imaging: A preliminary study comparing with ^{99m}Tc GSA scintigraphy and signal intensity based parameters. *Eur J Radiol* 2017; **92**: 116-123 [PMID: 28624009 DOI: 10.1016/j.ejrad.2017.05.011]

24 **Pan S**, Wang XQ, Guo QY. Quantitative assessment of hepatic fibrosis in chronic hepatitis B and C: T1 mapping on Gd-EOB-DTPA-enhanced liver magnetic resonance imaging. *World J Gastroenterol* 2018; **24**: 2024-2035 [PMID: 29760545 DOI: 10.3748/wjg.v24.i18.2024]

25 **Liu MT**, Zhang XQ, Lu J, Zhang T, Chen Q, Jiang JF, Ding D, Du S, Chen WB. Evaluation of liver function using the hepatocyte enhancement fraction based on gadoxetic acid-enhanced MRI in patients with chronic hepatitis B. *Abdom Radiol (NY)* 2020; **45**: 3129-3135 [PMID: 32185444 DOI: 10.1007/s00261-020-02478-7]

26 **Di Serafino M**, Gioioso M, Severino R, Esposito F, Vezzali N, Ferro F, Pelliccia P, Caprio MG, Iorio R, Vallone G. Ultrasound findings in paediatric cholestasis: how to image the patient and what to look for. *J Ultrasound* 2020; **23**: 1-12 [PMID: 30756259 DOI: 10.1007/s40477-019-00362-9]

27 **Alsaigh S**, Aldhubayb MA, Alobaid AS, Alhajjaj AH, Alharbi BA, Alsudais DM, Alhothail HA, AlSaykhan MA. Diagnostic Reliability of Ultrasound Compared to Magnetic Resonance Cholangiopancreatography and Endoscopic

Retrograde Cholangiopancreatography in the Detection of Obstructive Jaundice: A Retrospective Medical Records Review. *Cureus* 2020; **12**: e10987 [PMID: 33209543 DOI: 10.7759/cureus.10987]

28 **Katabathina VS**, Dasyam AK, Dasyam N, Hosseinzadeh K. Adult bile duct strictures: role of MR imaging and MR cholangiopancreatography in characterization. *Radiographics* 2014; **34**: 565-586 [PMID: 24819781 DOI: 10.1148/rg.343125211]

29 **Hyodo T**, Kumano S, Kushihata F, Okada M, Hirata M, Tsuda T, Takada Y, Mochizuki T, Murakami T. CT and MR cholangiography: advantages and pitfalls in perioperative evaluation of biliary tree. *Br J Radiol* 2012; **85**: 887-896 [PMID: 22422383 DOI: 10.1259/bjr/21209407]

30 **Kim DK**, Choi JY, Park MS, Kim MJ, Chung YE. Clinical Feasibility of MR Elastography in Patients With Biliary Obstruction. *AJR Am J Roentgenol* 2018; **210**: 1273-1278 [PMID: 29629807 DOI: 10.2214/AJR.17.19085]

31 **Seo N**, Kim SY, Lee SS, Byun JH, Kim JH, Kim HJ, Lee MG. Sclerosing Cholangitis: Clinicopathologic Features, Imaging Spectrum, and Systemic Approach to Differential Diagnosis. *Korean J Radiol* 2016; **17**: 25-38 [PMID: 26798213 DOI: 10.3348/kjr.2016.17.1.25]

32 **Khoshpouri P**, Habibabadi RR, Hazhirkarzar B, Ameli S, Ghadimi M, Ghasabeh MA, Menias CO, Kim A, Li Z, Kamel IR. Imaging Features of Primary Sclerosing Cholangitis: From Diagnosis to Liver Transplant Follow-up. *Radiographics* 2019; **39**: 1938-1964 [PMID: 31626561 DOI: 10.1148/rg.2019180213]

33 **Crosignani A**, Battezzati PM, Invernizzi P, Selmi C, Prina E, Podda M. Clinical features and management of primary biliary cirrhosis. *World J Gastroenterol* 2008; **14**: 3313-3327 [PMID: 18528929 DOI: 10.3748/wjg.14.3313]

34 **Kovač JD**, Weber MA. Primary Biliary Cirrhosis and Primary Sclerosing Cholangitis: an Update on MR Imaging Findings with Recent Developments. *J Gastrointestin Liver Dis* 2016; **25**: 517-524 [PMID: 27981308 DOI: 10.15403/jgld.2014.1121.254.vac]

35 **Cebada Chaparro E**, Lloret Del Hoyo J, Méndez Fernández R. Chronic cholangitides: Differential diagnosis and role of MRI. *Radiologia (Engl Ed)* 2020; **62**: 452-463 [PMID: 33138982 DOI: 10.1016/j.rx.2020.08.004]

36 **Byrne CD**, Targher G. NAFLD: a multisystem disease. *J Hepatol* 2015; **62**: S47-S64 [PMID: 25920090 DOI: 10.1016/j.jhep.2014.12.012]

37 **Castera L**, Friedrich-Rust M, Loomba R. Noninvasive Assessment of Liver Disease in Patients With Nonalcoholic Fatty Liver Disease. *Gastroenterology* 2019; **156**: 1264-1281.e4 [PMID: 30660725 DOI: 10.1053/j.gastro.2018.12.036]

38 **Petroff D**, Blank V, Newsome PN, Shalimar, Voican CS, Thiele M, de Lédinghen V, Baumeler S, Chan WK, Perlemuter G, Cardoso AC, Aggarwal S, Sasso M, Eddowes PJ, Allison M, Tsochatzis E, Anstee QM, Sheridan D, Cobbold JF, Naveau S, Lupsor-Platon M, Mueller S, Krag A, Irles-Depe M, Semela D, Wong GL, Wong VW, Villela-Nogueira CA, Garg H, Chazouillères O, Wiegand J, Karlas T. Assessment of hepatic steatosis by controlled attenuation parameter using the M and XL probes: an individual patient data meta-analysis. *Lancet Gastroenterol Hepatol* 2021; **6**: 185-198 [PMID: 33460567 DOI: 10.1016/S2468-1253(20)30357-5]

39 **Pu K**, Wang Y, Bai S, Wei H, Zhou Y, Fan J, Qiao L. Diagnostic accuracy of controlled attenuation parameter (CAP) as a non-invasive test for steatosis in suspected non-alcoholic fatty liver disease: a systematic review and meta-analysis. *BMC Gastroenterol* 2019; **19**: 51 [PMID: 30961539 DOI: 10.1186/s12876-019-0961-9]

40 **Bohte AE**, van Werven JR, Bipat S, Stoker J. The diagnostic accuracy of US, CT, MRI and 1H-MRS for the evaluation of hepatic steatosis compared with liver biopsy: a meta-analysis. *Eur Radiol* 2011; **21**: 87-97 [PMID: 20680289 DOI: 10.1007/s00330-010-1905-5]

41 **Gu Q**, Cen L, Lai J, Zhang Z, Pan J, Zhao F, Yu C, Li Y, Chen C, Chen W, Shen Z. A meta-analysis on the diagnostic performance of magnetic resonance imaging and transient elastography in nonalcoholic fatty liver disease. *Eur J Clin Invest* 2021; **51**: e13446 [PMID: 33128454 DOI: 10.1111/eci.13446]

42 **Choi SJ**, Kim SM, Kim YS, Kwon OS, Shin SK, Kim KK, Lee K, Park IB, Choi CS, Chung DH, Jung J, Paek M, Lee DH. Magnetic Resonance-Based Assessments Better Capture Pathophysiologic Profiles and Progression in Nonalcoholic Fatty Liver Disease. *Diabetes Metab J* 2021; **45**: 739-752 [PMID: 33108854 DOI: 10.4093/dmj.2020.0137]

43 **Chalasani N**, Vuppalanchi R, Rinella M, Middleton MS, Siddiqui MS, Barritt AS 4th, Kolterman O, Flores O, Alonso C, Iruarrizaga-Lejarreta M, Gil-Redondo R, Sirlin CB, Zemel MB. Randomised clinical trial: a leucine-metformin-sildenafil combination (NS-0200) *vs* placebo in patients with non-alcoholic fatty liver disease. *Aliment Pharmacol Ther* 2018; **47**: 1639-1651 [PMID: 29696666 DOI: 10.1111/apt.14674]

44 **Yan J**, Yao B, Kuang H, Yang X, Huang Q, Hong T, Li Y, Dou J, Yang W, Qin G, Yuan H, Xiao X, Luo S, Shan Z, Deng H, Tan Y, Xu F, Xu W, Zeng L, Kang Z, Weng J. Liraglutide, Sitagliptin, and Insulin Glargine Added to Metformin: The Effect on Body Weight and Intrahepatic Lipid in Patients With Type 2 Diabetes Mellitus and Nonalcoholic Fatty Liver Disease. *Hepatology* 2019; **69**: 2414-2426 [PMID: 30341767 DOI: 10.1002/hep.30320]

45 **Jiang H**, Chen HC, Lafata KJ, Bashir MR. Week 4 Liver Fat Reduction on MRI as an Early Predictor of Treatment Response in Participants with Nonalcoholic Steatohepatitis. *Radiology* 2021; **300**: 361-368 [PMID: 34060937 DOI: 10.1148/radiol.2021204325]

46 **Mojtahed A**, Kelly CJ, Herlihy AH, Kin S, Wilman HR, McKay A, Kelly M, Milanesi M, Neubauer S, Thomas EL, Bell JD, Banerjee R, Harisinghani M. Reference range of liver corrected T1 values in a population at low risk for fatty liver disease-a UK Biobank sub-study, with an appendix of interesting cases. *Abdom Radiol (NY)* 2019; **44**: 72-84 [PMID: 30032383 DOI: 10.1007/s00261-018-1701-2]

47 **Imajo K**, Tetlow L, Dennis A, Shumbayawonda E, Mouchti S, Kendall TJ, Fryer E, Yamanaka S, Honda Y, Kessoku T, Ogawa Y, Yoneda M, Saito S, Kelly C, Kelly MD, Banerjee R, Nakajima A. Quantitative multiparametric magnetic resonance imaging can aid non-alcoholic steatohepatitis diagnosis in a Japanese cohort. *World J Gastroenterol* 2021; **27**: 609-623 [PMID: 33642832 DOI: 10.3748/wjg.v27.i7.609]

48 **Eddowes PJ**, McDonald N, Davies N, Semple SIK, Kendall TJ, Hodson J, Newsome PN, Flintham RB, Wesolowski R, Blake L, Duarte RV, Kelly CJ, Herlihy AH, Kelly MD, Olliff SP, Hübscher SG, Fallowfield JA, Hirschfield GM. Utility and cost evaluation of multiparametric magnetic resonance imaging for the assessment of non-alcoholic fatty liver disease. *Aliment Pharmacol Ther* 2018; **47**: 631-644 [PMID: 29271504 DOI: 10.1111/apt.14469]

49 **Bassett ML**, Hickman PE, Dahlstrom JE. The changing role of liver biopsy in diagnosis and management of

haemochromatosis. *Pathology* 2011; **43**: 433-439 [PMID: 21716156 DOI: 10.1097/PAT.0b013e3283490e04]
50 **Yan F**, He N, Lin H, Li R. Iron deposition quantification: Applications in the brain and liver. *J Magn Reson Imaging* 2018; **48**: 301-317 [PMID: 29897645 DOI: 10.1002/jmri.26161]
51 **Wells SA**. Quantification of hepatic fat and iron with magnetic resonance imaging. *Magn Reson Imaging Clin N Am* 2014; **22**: 397-416 [PMID: 25086936 DOI: 10.1016/j.mric.2014.04.010]
52 **Castiella A**, Alústiza JM, Emparanza JI, Zapata EM, Costero B, Díez MI. Liver iron concentration quantification by MRI: are recommended protocols accurate enough for clinical practice? *Eur Radiol* 2011; **21**: 137-141 [PMID: 20694471 DOI: 10.1007/s00330-010-1899-z]
53 **d'Assignies G**, Paisant A, Bardou-Jacquet E, Boulic A, Bannier E, Lainé F, Ropert M, Morcet J, Saint-Jalmes H, Gandon Y. Non-invasive measurement of liver iron concentration using 3-Tesla magnetic resonance imaging: validation against biopsy. *Eur Radiol* 2018; **28**: 2022-2030 [PMID: 29178028 DOI: 10.1007/s00330-017-5106-3]
54 **Sirlin CB**, Reeder SB. Magnetic resonance imaging quantification of liver iron. *Magn Reson Imaging Clin N Am* 2010; **18**: 359-381, ix [PMID: 21094445 DOI: 10.1016/j.mric.2010.08.014]
55 **St Pierre TG**, Clark PR, Chua-anusorn W, Fleming AJ, Jeffrey GP, Olynyk JK, Pootrakul P, Robins E, Lindeman R. Noninvasive measurement and imaging of liver iron concentrations using proton magnetic resonance. *Blood* 2005; **105**: 855-861 [PMID: 15256427 DOI: 10.1182/blood-2004-01-0177]
56 **St Pierre TG**, El-Beshlawy A, Elalfy M, Al Jefri A, Al Zir K, Daar S, Habr D, Kriemler-Krahn U, Taher A. Multicenter validation of spin-density projection-assisted R2-MRI for the noninvasive measurement of liver iron concentration. *Magn Reson Med* 2014; **71**: 2215-2223 [PMID: 23821350 DOI: 10.1002/mrm.24854]
57 **Sussman MS**, Ward R, Kuo KHM, Tomlinson G, Jhaveri KS. Impact of MRI technique on clinical decision-making in patients with liver iron overload: comparison of FerriScan- *vs* R2*-derived liver iron concentration. *Eur Radiol* 2020; **30**: 1959-1968 [PMID: 31953658 DOI: 10.1007/s00330-019-06450-y]
58 **Henninger B**, Plaikner M, Zoller H, Viveiros A, Kannengiesser S, Jaschke W, Kremser C. Performance of different Dixon-based methods for MR liver iron assessment in comparison to a biopsy-validated R2* relaxometry method. *Eur Radiol* 2021; **31**: 2252-2262 [PMID: 32965571 DOI: 10.1007/s00330-020-07291-w]
59 **Li J**, Lin H, Liu T, Zhang Z, Prince MR, Gillen K, Yan X, Song Q, Hua T, Zhao X, Zhang M, Zhao Y, Li G, Tang G, Yang G, Brittenham GM, Wang Y. Quantitative susceptibility mapping (QSM) minimizes interference from cellular pathology in R2* estimation of liver iron concentration. *J Magn Reson Imaging* 2018; **48**: 1069-1079 [PMID: 29566449 DOI: 10.1002/jmri.26019]
60 **Tipirneni-Sajja A**, Loeffler RB, Hankins JS, Morin C, Hillenbrand CM. Quantitative Susceptibility Mapping Using a Multispectral Autoregressive Moving Average Model to Assess Hepatic Iron Overload. *J Magn Reson Imaging* 2021; **54**: 721-727 [PMID: 33634923 DOI: 10.1002/jmri.27584]
61 **Nguyen-Khac E**, Thiele M, Voican C, Nahon P, Moreno C, Boursier J, Mueller S, de Ledinghen V, Stärkel P, Gyune Kim S, Fernandez M, Madsen B, Naveau S, Krag A, Perlemuter G, Ziol M, Chatelain D, Diouf M. Non-invasive diagnosis of liver fibrosis in patients with alcohol-related liver disease by transient elastography: an individual patient data meta-analysis. *Lancet Gastroenterol Hepatol* 2018; **3**: 614-625 [PMID: 29983372 DOI: 10.1016/S2468-1253(18)30124-9]
62 **Qi X**, An M, Wu T, Jiang D, Peng M, Wang W, Wang J, Zhang C; Chess Study Group OBOT. Transient Elastography for Significant Liver Fibrosis and Cirrhosis in Chronic Hepatitis B: A Meta-Analysis. *Can J Gastroenterol Hepatol* 2018; **2018**: 3406789 [PMID: 29977884 DOI: 10.1155/2018/3406789]
63 **Ooi GJ**, Mgaieth S, Eslick GD, Burton PR, Kemp WW, Roberts SK, Brown WA. Systematic review and meta-analysis: non-invasive detection of non-alcoholic fatty liver disease related fibrosis in the obese. *Obes Rev* 2018; **19**: 281-294 [PMID: 29119725 DOI: 10.1111/obr.12628]
64 **Dietrich CF**, Bamber J, Berzigotti A, Bota S, Cantisani V, Castera L, Cosgrove D, Ferraioli G, Friedrich-Rust M, Gilja OH, Goertz RS, Karlas T, de Knegt R, de Ledinghen V, Piscaglia F, Procopet B, Saftoiu A, Sidhu PS, Sporea I, Thiele M. EFSUMB Guidelines and Recommendations on the Clinical Use of Liver Ultrasound Elastography, Update 2017 (Long Version). *Ultraschall Med* 2017; **38**: e16-e47 [PMID: 28407655 DOI: 10.1055/s-0043-103952]
65 **Xiao G**, Zhu S, Xiao X, Yan L, Yang J, Wu G. Comparison of laboratory tests, ultrasound, or magnetic resonance elastography to detect fibrosis in patients with nonalcoholic fatty liver disease: A meta-analysis. *Hepatology* 2017; **66**: 1486-1501 [PMID: 28586172 DOI: 10.1002/hep.29302]
66 **Sande JA**, Verjee S, Vinayak S, Amersi F, Ghesani M. Ultrasound shear wave elastography and liver fibrosis: A Prospective Multicenter Study. *World J Hepatol* 2017; **9**: 38-47 [PMID: 28105257 DOI: 10.4254/wjh.v9.i1.38]
67 **Petzold G**, Bremer SCB, Knoop RF, Amanzada A, Raddatz D, Ellenrieder V, Ströbel P, Kunsch S, Neesse A. Noninvasive assessment of liver fibrosis in a real-world cohort of patients with known or suspected chronic liver disease using 2D-shear wave elastography. *Eur J Gastroenterol Hepatol* 2020; **32**: 1559-1565 [PMID: 31922976 DOI: 10.1097/MEG.0000000000001675]
68 **Jiang W**, Huang S, Teng H, Wang P, Wu M, Zhou X, Ran H. Diagnostic accuracy of point shear wave elastography and transient elastography for staging hepatic fibrosis in patients with non-alcoholic fatty liver disease: a meta-analysis. *BMJ Open* 2018; **8**: e021787 [PMID: 30139901 DOI: 10.1136/bmjopen-2018-021787]
69 **Venkatesh SK**, Yin M, Takahashi N, Glockner JF, Talwalkar JA, Ehman RL. Non-invasive detection of liver fibrosis: MR imaging features vs. MR elastography. *Abdom Imaging* 2015; **40**: 766-775 [PMID: 25805619 DOI: 10.1007/s00261-015-0347-6]
70 **Wang XP**, Wang Y, Ma H, Wang H, Yang DW, Zhao XY, Jin EH, Yang ZH. Assessment of liver fibrosis with liver and spleen magnetic resonance elastography, serum markers in chronic liver disease. *Quant Imaging Med Surg* 2020; **10**: 1208-1222 [PMID: 32550131 DOI: 10.21037/qims-19-849]
71 **Jhaveri KS**, Hosseini-Nik H, Sadoughi N, Janssen H, Feld JJ, Fischer S, Menezes R, Cheung AC. The development and validation of magnetic resonance elastography for fibrosis staging in primary sclerosing cholangitis. *Eur Radiol* 2019; **29**: 1039-1047 [PMID: 30051141 DOI: 10.1007/s00330-018-5619-4]
72 **Tafur M**, Cheung A, Menezes RJ, Feld J, Janssen H, Hirschfield GM, Jhaveri KS. Risk stratification in primary

sclerosing cholangitis: comparison of biliary stricture severity on MRCP *vs* liver stiffness by MR elastography and vibration-controlled transient elastography. *Eur Radiol* 2020; **30**: 3735-3747 [PMID: 32130494 DOI: 10.1007/s00330-020-06728-6]

73 **Fu F**, Li X, Chen C, Bai Y, Liu Q, Shi D, Sang J, Wang K, Wang M. Non-invasive assessment of hepatic fibrosis: comparison of MR elastography to transient elastography and intravoxel incoherent motion diffusion-weighted MRI. *Abdom Radiol (NY)* 2020; **45**: 73-82 [PMID: 31372777 DOI: 10.1007/s00261-019-02140-x]

74 **Dong BT**, Chen YP, Lyu GR, Wang HM, Lin GF, Gu JH. Diagnostic accuracy of two-dimensional shear wave elastography and magnetic resonance elastography for staging liver fibrosis in patients with chronic hepatitis B: A systematic review and meta-analysis. *J Gastroenterol Hepatol* 2021 [PMID: 33982301 DOI: 10.1111/jgh.15549]

75 **Morita K**, Nishie A, Ushijima Y, Takayama Y, Fujita N, Kubo Y, Ishimatsu K, Yoshizumi T, Maehara J, Ishigami K. Noninvasive assessment of liver fibrosis by dual-layer spectral detector CT. *Eur J Radiol* 2021; **136**: 109575 [PMID: 33548853 DOI: 10.1016/j.ejrad.2021.109575]

76 **Evrimler S**, Swensson JK, Are VS, Tirkes T, Vuppalanchi R, Akisik F. Quantitative assessment of disease severity of primary sclerosing cholangitis with T1 mapping and extracellular volume imaging. *Abdom Radiol (NY)* 2021; **46**: 2433-2443 [PMID: 33135100 DOI: 10.1007/s00261-020-02839-2]

77 **Bak S**, Kim JE, Bae K, Cho JM, Choi HC, Park MJ, Choi HY, Shin HS, Lee SM, Kim HO. Quantification of liver extracellular volume using dual-energy CT: utility for prediction of liver-related events in cirrhosis. *Eur Radiol* 2020; **30**: 5317-5326 [PMID: 32335746 DOI: 10.1007/s00330-020-06876-9]

78 **Lyu L**, Liu XL, Rui MP, Yang LC, Wang GZ, Fan D, Wang T, Zheng J. Liver extracellular volume fraction values obtained with magnetic resonance imaging can quantitatively stage liver fibrosis: a validation study in monkeys with nonalcoholic steatohepatitis. *Eur Radiol* 2020; **30**: 5748-5757 [PMID: 32377814 DOI: 10.1007/s00330-020-06902-w]

79 **Taouli B**, Koh DM. Diffusion-weighted MR imaging of the liver. *Radiology* 2010; **254**: 47-66 [PMID: 20032142 DOI: 10.1148/radiol.09090021]

80 **Tokgöz Ö**, Unal I, Turgut GG, Yildiz S. The value of liver and spleen ADC measurements in the diagnosis and follow up of hepatic fibrosis in chronic liver disease. *Acta Clin Belg* 2014; **69**: 426-432 [PMID: 25103596 DOI: 10.1179/2295333714Y.0000000062]

81 **Ding Y**, Rao SX, Chen C, Li R, Zeng MS. Assessing liver function in patients with HBV-related HCC: a comparison of T_1 mapping on Gd-EOB-DTPA-enhanced MR imaging with DWI. *Eur Radiol* 2015; **25**: 1392-1398 [PMID: 25523455 DOI: 10.1007/s00330-014-3542-x]

82 **Lefebvre T**, Hébert M, Bilodeau L, Sebastiani G, Cerny M, Olivié D, Gao ZH, Sylvestre MP, Cloutier G, Nguyen BN, Gilbert G, Tang A. Intravoxel incoherent motion diffusion-weighted MRI for the characterization of inflammation in chronic liver disease. *Eur Radiol* 2021; **31**: 1347-1358 [PMID: 32876833 DOI: 10.1007/s00330-020-07203-y]

83 **Park JH**, Seo N, Chung YE, Kim SU, Park YN, Choi JY, Park MS, Kim MJ. Noninvasive evaluation of liver fibrosis: comparison of the stretched exponential diffusion-weighted model to other diffusion-weighted MRI models and transient elastography. *Eur Radiol* 2021; **31**: 4813-4823 [PMID: 33439321 DOI: 10.1007/s00330-020-07600-3]

84 **Fan G**, Ya Y, Ni X, Hou J, Yu R. Application Value of Magnetic Resonance Perfusion Imaging in the Early Diagnosis of Rat Hepatic Fibrosis. *Biomed Res Int* 2019; **2019**: 5095934 [PMID: 31950040 DOI: 10.1155/2019/5095934]

85 **Yoon JH**, Lee JM, Yu MH, Hur BY, Grimm R, Sourbron S, Chandarana H, Son Y, Basak S, Lee KB, Yi NJ, Lee KW, Suh KS. Simultaneous evaluation of perfusion and morphology using GRASP MRI in hepatic fibrosis. *Eur Radiol* 2022; **32**: 34-45 [PMID: 34120229 DOI: 10.1007/s00330-021-08087-2]

86 **Engelmann C**, Clària J, Szabo G, Bosch J, Bernardi M. Pathophysiology of decompensated cirrhosis: Portal hypertension, circulatory dysfunction, inflammation, metabolism and mitochondrial dysfunction. *J Hepatol* 2021; **75** Suppl 1: S49-S66 [PMID: 34039492 DOI: 10.1016/j.jhep.2021.01.002]

87 **de Franchis R**; Baveno VI Faculty. Expanding consensus in portal hypertension: Report of the Baveno VI Consensus Workshop: Stratifying risk and individualizing care for portal hypertension. *J Hepatol* 2015; **63**: 743-752 [PMID: 26047908 DOI: 10.1016/j.jhep.2015.05.022]

88 **You MW**, Kim KW, Pyo J, Huh J, Kim HJ, Lee SJ, Park SH. A Meta-analysis for the Diagnostic Performance of Transient Elastography for Clinically Significant Portal Hypertension. *Ultrasound Med Biol* 2017; **43**: 59-68 [PMID: 27751595 DOI: 10.1016/j.ultrasmedbio.2016.07.025]

89 **Fofiu R**, Bende F, Popescu A, Şirli R, Miuțescu B, Sporea I. Assessing Baveno VI Criteria Using Liver Stiffness Measured with a 2D-Shear Wave Elastography Technique. *Diagnostics (Basel)* 2021; **11** [PMID: 33919033 DOI: 10.3390/diagnostics11050737]

90 **Fofiu R**, Bende F, Popescu A, Şirli R, Lupușoru R, Ghiuchici AM, Sporea I. Spleen and Liver Stiffness for Predicting High-Risk Varices in Patients with Compensated Liver Cirrhosis. *Ultrasound Med Biol* 2021; **47**: 76-83 [PMID: 33067019 DOI: 10.1016/j.ultrasmedbio.2020.09.004]

91 **Kang SH**, Baik SK, Kim MY. Application of Baveno Criteria and Modified Baveno Criteria with Shear-wave Elastography in Compensated Advanced Chronic Liver Disease. *J Korean Med Sci* 2020; **35**: e249 [PMID: 32743990 DOI: 10.3346/jkms.2020.35.e249]

92 **Yu JB**, Xiong H, Yuan XC, Zhou AY. Liver Stiffness Detected by Shear Wave Elastography Predicts Esophageal Varices in Cirrhotic Patients. *Ultrasound Q* 2019; **37**: 118-122 [PMID: 31299039 DOI: 10.1097/RUQ.0000000000000466]

93 **Yoo HW**, Kim YS, Kim SG, Yoo JJ, Jeong SW, Jang JY, Lee SH, Kim HS, Kim YD, Cheon GJ, Jun B, Kim BS. Usefulness of noninvasive methods including assessment of liver stiffness by 2-dimensional shear wave elastography for predicting esophageal varices. *Dig Liver Dis* 2019; **51**: 1706-1712 [PMID: 31281068 DOI: 10.1016/j.dld.2019.06.007]

94 **Singh R**, Wilson MP, Katlariwala P, Murad MH, McInnes MDF, Low G. Accuracy of liver and spleen stiffness on magnetic resonance elastography for detecting portal hypertension: a systematic review and meta-analysis. *Eur J Gastroenterol Hepatol* 2021; **32**: 237-245 [PMID: 32282542 DOI: 10.1097/MEG.0000000000001724]

95 **Ma R**, Hunter P, Cousins W, Ho H, Bartlett A, Safaei S. Anatomically based simulation of hepatic perfusion in the human liver. *Int J Numer Method Biomed Eng* 2019; **35**: e3229 [PMID: 31368204 DOI: 10.1002/cnm.3229]

96 **Donato H**, França M, Candelária I, Caseiro-Alves F. Liver MRI: From basic protocol to advanced techniques. *Eur J*

Radiol 2017; **93**: 30-39 [PMID: 28668428 DOI: 10.1016/j.ejrad.2017.05.028]
97 **Zironi G**, Gaiani S, Fenyves D, Rigamonti A, Bolondi L, Barbara L. Value of measurement of mean portal flow velocity by Doppler flowmetry in the diagnosis of portal hypertension. *J Hepatol* 1992; **16**: 298-303 [PMID: 1487606 DOI: 10.1016/s0168-8278(05)80660-9]
98 **Kayacetin E**, Efe D, Doğan C. Portal and splenic hemodynamics in cirrhotic patients: relationship between esophageal variceal bleeding and the severity of hepatic failure. *J Gastroenterol* 2004; **39**: 661-667 [PMID: 15293137 DOI: 10.1007/s00535-003-1362-x]
99 **Shastri M**, Kulkarni S, Patell R, Jasdanwala S. Portal vein Doppler: a tool for non-invasive prediction of esophageal varices in cirrhosis. *J Clin Diagn Res* 2014; **8**: MC12-MC15 [PMID: 25177589 DOI: 10.7860/JCDR/2014/8571.4589]
100 **Elkenawy YN**, Elarabawy RA, Ahmed LM, Elsawy AA. Portal vein flow velocity as a possible fast noninvasive screening tool for esophageal varices in cirrhotic patients. *JGH Open* 2020; **4**: 589-594 [PMID: 32782943 DOI: 10.1002/jgh3.12301]
101 **Chouhan MD**, Mookerjee RP, Bainbridge A, Punwani S, Jones H, Davies N, Walker-Samuel S, Patch D, Jalan R, Halligan S, Lythgoe MF, Taylor SA. Caval Subtraction 2D Phase-Contrast MRI to Measure Total Liver and Hepatic Arterial Blood Flow: Proof-of-Principle, Correlation With Portal Hypertension Severity and Validation in Patients With Chronic Liver Disease. *Invest Radiol* 2017; **52**: 170-176 [PMID: 27805917 DOI: 10.1097/RLI.0000000000000328]
102 **Roldán-Alzate A**, Frydrychowicz A, Niespodzany E, Landgraf BR, Johnson KM, Wieben O, Reeder SB. In vivo validation of 4D flow MRI for assessing the hemodynamics of portal hypertension. *J Magn Reson Imaging* 2013; **37**: 1100-1108 [PMID: 23148034 DOI: 10.1002/jmri.23906]
103 **Frydrychowicz A**, Roldan-Alzate A, Winslow E, Consigny D, Campo CA, Motosugi U, Johnson KM, Wieben O, Reeder SB. Comparison of radial 4D Flow-MRI with perivascular ultrasound to quantify blood flow in the abdomen and introduction of a porcine model of pre-hepatic portal hypertension. *Eur Radiol* 2017; **27**: 5316-5324 [PMID: 28656461 DOI: 10.1007/s00330-017-4862-4]
104 **Motosugi U**, Roldán-Alzate A, Bannas P, Said A, Kelly S, Zea R, Wieben O, Reeder SB. Four-dimensional Flow MRI as a Marker for Risk Stratification of Gastroesophageal Varices in Patients with Liver Cirrhosis. *Radiology* 2019; **290**: 101-107 [PMID: 30325278 DOI: 10.1148/radiol.2018180230]
105 **Wagner M**, Hectors S, Bane O, Gordic S, Kennedy P, Besa C, Schiano TD, Thung S, Fischman A, Taouli B. Noninvasive prediction of portal pressure with MR elastography and DCE-MRI of the liver and spleen: Preliminary results. *J Magn Reson Imaging* 2018; **48**: 1091-1103 [PMID: 29638020 DOI: 10.1002/jmri.26026]
106 **Wagener G**. Assessment of hepatic function, operative candidacy, and medical management after liver resection in the patient with underlying liver disease. *Semin Liver Dis* 2013; **33**: 204-212 [PMID: 23943101 DOI: 10.1055/s-0033-1351777]
107 **Blüthner E**, Jara M, Shrestha R, Faber W, Pratschke J, Stockmann M, Malinowski M. The predictive value of future liver remnant function after liver resection for HCC in noncirrhotic and cirrhotic patients. *HPB (Oxford)* 2019; **21**: 912-922 [PMID: 30733048 DOI: 10.1016/j.hpb.2018.11.012]
108 **Rahbari NN**, Mehrabi A, Mollberg NM, Müller SA, Koch M, Büchler MW, Weitz J. Hepatocellular carcinoma: current management and perspectives for the future. *Ann Surg* 2011; **253**: 453-469 [PMID: 21263310 DOI: 10.1097/SLA.0b013e31820d944f]
109 **Yoon JH**, Lee JM, Kim E, Okuaki T, Han JK. Quantitative Liver Function Analysis: Volumetric T1 Mapping with Fast Multisection B_1 Inhomogeneity Correction in Hepatocyte-specific Contrast-enhanced Liver MR Imaging. *Radiology* 2017; **282**: 408-417 [PMID: 27697007 DOI: 10.1148/radiol.2016152800]
110 **Yoon JH**, Choi JI, Jeong YY, Schenk A, Chen L, Laue H, Kim SY, Lee JM. Pre-treatment estimation of future remnant liver function using gadoxetic acid MRI in patients with HCC. *J Hepatol* 2016; **65**: 1155-1162 [PMID: 27476767 DOI: 10.1016/j.jhep.2016.07.024]
111 **Haimerl M**, Schlabeck M, Verloh N, Zeman F, Fellner C, Nickel D, Barreiros AP, Loss M, Stroszczynski C, Wiggermann P. Volume-assisted estimation of liver function based on Gd-EOB-DTPA-enhanced MR relaxometry. *Eur Radiol* 2016; **26**: 1125-1133 [PMID: 26186960 DOI: 10.1007/s00330-015-3919-5]
112 **Duan T**, Jiang H, Xia C, Chen J, Cao L, Ye Z, Wei Y, Song B, Lee JM. Assessing Liver Function in Liver Tumors Patients: The Performance of T1 Mapping and Residual Liver Volume on Gd-EOBDTPA-Enhanced MRI. *Front Med (Lausanne)* 2020; **7**: 215 [PMID: 32549039 DOI: 10.3389/fmed.2020.00215]
113 **Kim DK**, Choi JI, Choi MH, Park MY, Lee YJ, Rha SE, Jung SE. Prediction of Posthepatectomy Liver Failure: MRI With Hepatocyte-Specific Contrast Agent Versus Indocyanine Green Clearance Test. *AJR Am J Roentgenol* 2018; **211**: 580-587 [PMID: 29995498 DOI: 10.2214/AJR.17.19206]
114 **Wang Y**, Zhang L, Ning J, Zhang X, Li X, Chen G, Zhao X, Wang X, Yang S, Yuan C, Dong J, Chen H. Preoperative Remnant Liver Function Evaluation Using a Routine Clinical Dynamic Gd-EOB-DTPA-Enhanced MRI Protocol in Patients with Hepatocellular Carcinoma. *Ann Surg Oncol* 2021; **28**: 3672-3682 [PMID: 33230746 DOI: 10.1245/s10434-020-09361-1]

World Journal of Gastroenterology

Submit a Manuscript: https://www.f6publishing.com

World J Gastroenterol 2022 April 28; 28(16): 1641-1655

DOI: 10.3748/wjg.v28.i16.1641

ISSN 1007-9327 (print) ISSN 2219-2840 (online)

REVIEW

Small nucleolar RNA host gene 3 functions as a novel biomarker in liver cancer and other tumour progression

Dan-Dan Shan, Qiu-Xian Zheng, Jing Wang, Zhi Chen

Specialty type: Biochemistry and molecular biology

Provenance and peer review: Unsolicited article; Externally peer reviewed.

Peer-review model: Single blind

Peer-review report's scientific quality classification

Grade A (Excellent): 0
Grade B (Very good): B
Grade C (Good): C
Grade D (Fair): 0
Grade E (Poor): 0

P-Reviewer: Dalili S, Iran; Pang Y, China

Received: January 18, 2022
Peer-review started: January 18, 2022
First decision: February 7, 2022
Revised: February 9, 2022
Accepted: March 16, 2022
Article in press: March 16, 2022
Published online: April 28, 2022

Dan-Dan Shan, Qiu-Xian Zheng, Jing Wang, Zhi Chen, State Key Laboratory for Diagnosis and Treatment of Infectious Diseases, National Clinical Research Center for Infectious Diseases, National Medical Center for Infectious Diseases, Collaborative Innovation Center for Diagnosis and Treatment of Infectious Diseases, The First Affiliated Hospital, Zhejiang University School of Medicine, Hangzhou 310003, Zhejiang Province, China

Corresponding author: Zhi Chen, MD, PhD, Professor, State Key Laboratory for Diagnosis and Treatment of Infectious Diseases, National Clinical Research Center for Infectious Diseases, National Medical Center for Infectious Diseases, Collaborative Innovation Center for Diagnosis and Treatment of Infectious Diseases, The First Affiliated Hospital, Zhejiang University School of Medicine, No. 79 Qingchun Road, Shangcheng District, Hangzhou 310003, Zhejiang Province, China. zjuchenzhi@zju.edu.cn

Abstract

Cancer has become the most life-threatening disease in the world. Mutations in and aberrant expression of genes encoding proteins and mutations in noncoding RNAs, especially long noncoding RNAs (lncRNAs), have significant effects in human cancers. LncRNAs have no protein-coding ability but function extensively in numerous physiological and pathological processes. Small nucleolar RNA host gene 3 (SNHG3) is a novel lncRNA and has been reported to be differentially expressed in various tumors, such as liver cancer, gastric cancer, and glioma. However, the interaction mechanisms for the regulation between SNHG3 and tumor progression are poorly understood. In this review, we summarize the results of SNHG3 studies in humans, animal models, and cells to underline the expression and role of SNHG3 in cancer. SNHG3 expression is upregulated in most tumors and is detrimental to patient prognosis. SNHG3 expression in lung adenocarcinoma remains controversial. Concurrently, SNHG3 affects oncogenes and tumor suppressor genes through various mechanisms, including competing endogenous RNA effects. A deeper understanding of the contribution of SNHG3 in clinical applications and tumor development may provide a new target for cancer diagnosis and treatment.

Key Words: Small nucleolar RNA host gene 3; Long noncoding RNAs, Biomarker; Clinical characters; Molecular mechanism; Competing endogenous RNA; Liver cancer

©The Author(s) 2022. Published by Baishideng Publishing Group Inc. All rights reserved.

Core Tip: This review explores the differential expression of small nucleolar RNA host gene 3 (SNHG3) as a novel lncRNA in hepatocellular carcinoma as well as other tumours. SNHG3 is upregulated in most tumours and can influence tumourigenesis and progression through competing endogenous RNA effects and signalling pathways, thereby adversely affecting patient prognosis. Therefore, SNHG3 may become a new target for the diagnosis and treatment of many cancers, including hepatocellular carcinoma.

Citation: Shan DD, Zheng QX, Wang J, Chen Z. Small nucleolar RNA host gene 3 functions as a novel biomarker in liver cancer and other tumour progression. *World J Gastroenterol* 2022; 28(16): 1641-1655
URL: https://www.wjgnet.com/1007-9327/full/v28/i16/1641.htm
DOI: https://dx.doi.org/10.3748/wjg.v28.i16.1641

INTRODUCTION

Cancer has become one of the significant sources of mortality worldwide. Approximately 14.1 million individuals are newly diagnosed each year, and approximately 8.2 million deaths occurred in 2021 based on GLOBOCAN[1]. Despite considerable achievements and advances in clinical practices, cancer remains a dreadful illness with a poor prognosis and high health burden, which presents a global threat to health[2]. Cancer is a heterogeneous disease with substantial genotypic and phenotypic diversity[3]. Genomic regulation of the cancer genome plays a vital role in cancer initiation, progression, and metastasis[4,5]. It is of most importance to explore the intricate link underlying cancer development and progression.

Long noncoding RNAs (lncRNAs) are a class of noncoding RNAs (ncRNAs) with no protein-coding ability[6]. Evidence has shown that lncRNAs participate in genomic regulation at the transcriptional, translational, and epigenetic levels[6,7]. The regulatory functions of lncRNAs include activation and silencing of genes[8,9], recruitment of epigenetic regulator[10], modification of RNA interactions[11], transcriptional and posttranscriptional processes[12], mRNA decay[13], and protein recruitment[14]. LncRNA-associated regulatory functions are dynamically regulated in a cell-, tissue-, development- and distribution-specific manner[15]. LncRNAs in the cytoplasm may act as sponges, stabilizing mRNAs and regulating the mRNA translation process, thus modifying downstream target gene expression[16]. LncRNAs located in the nucleus may play "cis-acting" or "trans-acting" functions[17-19]. Recently, growing evidence demonstrates that lncRNAs are involved in various cancer functions and pathological processes, particularly in the initiation and progression of tumors[20]. LncRNAs regulate various malignant activities, including tumor progression, proliferation, apoptosis, migration, invasion, chromatin remodeling, metabolism[21-23].

More recently, small nucleolar RNAs can be encoded by several lncRNAs called small RNA host genes, which are significantly differentially expressed in many diseases, including cancers[24]. Studies have unveiled that small nucleolar RNA host gene 3 (SNHG3), which is affiliated with the lncRNA class, plays an influential regulatory role in cancer initiation, development, progression, and tumor-associated microenvironment formation. LncRNA SNHG3 is located in 1p35.3, as shown in Figure 1 (GeneCards, http://www.genecards.org). SNHG3 is mainly localized to the nucleus, mitochondrion, and extracellular space. Although many studies on SNHG3 and tumors have been published, clinical studies and research remains limited. This paper reviews the upregulation of SNHG3 expression in most human tumors and its relationship with negative prognosis as well as the role of SNHG3 in the mechanism of tumorigenesis. Finally, it was concluded that SNHG3 can function as a biomarker in the diagnosis and prognosis of different cancers.

CLINICAL CHARACTERS OF LNCRNA SNHG3

Growing evidence has demonstrated that SNHG3 acts as an oncogene and plays a critical regulatory role in the initiation and development of various cancers. SNHG3 exhibits characteristic oncogenic properties in multiple cancers. Studies have indicated that SNHG3 is significantly upregulated in hepatocellular carcinoma (HCC)[25,26] and other cancers, such as cervical cancer (CC)[27,28], and breast cancer (BC)[29-34]. Clear cell renal cell carcinoma (ccRCC)[35], colorectal cancer (CRC)[36-38], glioma [39,40], HCC[25,41,42], non-small cell lung cancer (NSCLC)[43-47], ovarian cancer (OC)[48-51], and papillary thyroid carcinoma (PTC)[52]. Different views exist on SNHG3 expression in lung adenocarcinoma, as shown in Table 1. Aberrant SNHG3 expression might represent a prognostic prediction value and therapeutic target in various cancers.

Table 1 The expression of small nucleolar RNA host gene 3 and its clinical significance in liver cancer and other cancers

Cancer types	Cases	Expression	Clinicopathologic parameters	PMID
Hepatocellular carcinoma	47 pairs	Upregulated	Tumor stage, lymph node metastasis, distant metastasis	31548493
Hepatocellular carcinoma	195 pairs	Upregulated	Tumor size, PVTT, relapse	26373735
Breast cancer	30 pairs	Upregulated		32495883
Breast cancer	60 pairs	Upregulated	Histological grade, TNM stage, lymph node metastasis, ER, Her-2	31586299
Breast cancer	60 pairs	Upregulated		32883233
Breast cancer	48 pairs	Upregulated		32945476
Cervical cancer	88 pairs	Upregulated	FIGO stage, metastasis	34816392
Clear cell renal cell carcinoma	36 pairs	Upregulated	Distant metastasis, T stage, pathological TNM stage, histologic grade	31505165
Colorectal cancer	58 pairs	Upregulated	Tumor stage, distant metastasis	32187965
	50 pairs	Upregulated		34661273
Esophageal cancer	384 pairs	Upregulated		33596916
Gastric cancer	60 pairs	Upregulated		32930970
Glioma	42 pairs	Upregulated	Tumor size, WHO grade	33817254
Glioma	8 low-grade and 8 high-grade and 8 normal tissues	Upregulated		34153159
Laryngeal carcinoma	18 pairs	Upregulated		31238052
Laryngeal carcinoma	25 pairs	Upregulated		32538668
Lung Adenocarcinoma	65 pairs	Downregulated	TNM stage, lymph node metastasis	32538668
Non-small-cell lung cancer	35 pairs	Upregulated	TNM stage, lymph node metastasis, tumor size	34132359
Non-small-cell lung cancer	32 pairs	Upregulated	TNM stage, lymph node metastasis, tumor size	31602642
Non-small-cell lung cancer	42 pairs	Upregulated	Stage, lymph node metastasis	33177840
Non-small-cell lung cancer	15 pairs	Upregulated		34032148
Oral squamous cell carcinoma	30 pairs	Upregulated		32989886
Osteosarcoma	54 pairs	Upregulated		30797154
Osteosarcoma	127 pairs	Upregulated		30791797
Ovarian cancer	18 pairs	Upregulated		29921511
Ovarian cancer	96 pairs	Upregulated	FIGO stage, histological grade, lymph node metastasis	33149611
Ovarian cancer	76 pairs	Upregulated	FIGO stage, lymph node metastasis	29758922
Ovarian cancer	40 patients with OC and 19 patients with benign OC	Upregulated		33552243
Papillary thyroid carcinoma	72 pairs	Upregulated	TNM stage, lymph node metastasis	32048306
Prostate cancer	50 pairs	Upregulated		33416420

PVTT: Portal vein tumor thrombosis; TNM: Tumor-node-metastasis; FIGO: International Federation of Gynecology and Obstetrics; WHO: World Health Organization.

HCC

HCC is one of the most widespread cancerous malignancies, ranking third in cancer-related deaths[53]. Cures for HCC tend to be more effective when used at an early stage[54]. However, patients at this stage

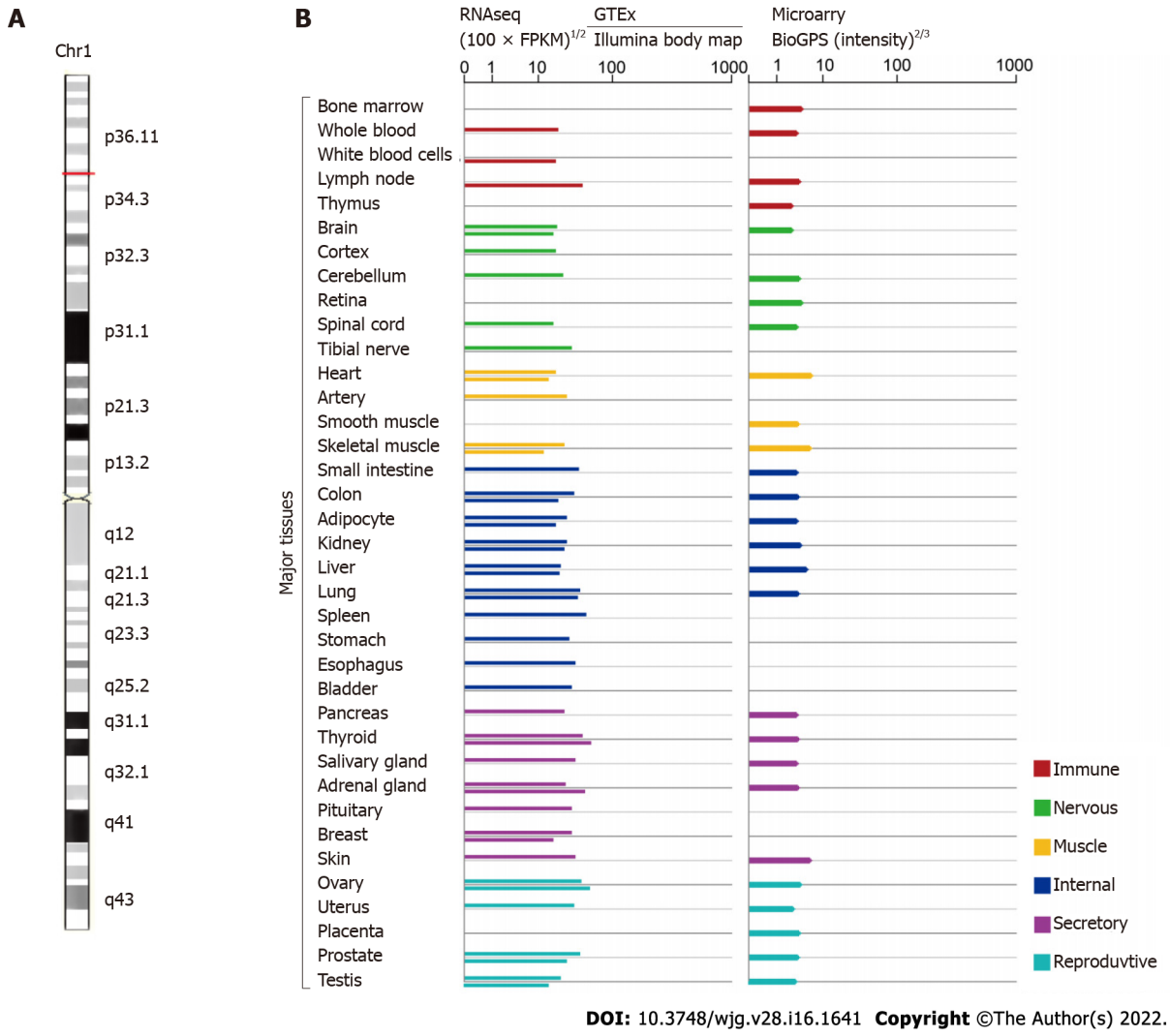

DOI: 10.3748/wjg.v28.i16.1641 **Copyright** ©The Author(s) 2022.

Figure 1 Small nucleolar RNA host gene 3 genomic information (GeneCards, http://www.genecards.org). A: The chromosomal localization of small nucleolar RNA host gene 3 (SNHG3); B: The expression level of SNHG3 in normal human tissues.

do not have specific symptoms or lack biomarkers for early diagnosis, which usually delays diagnosis. Accordingly, the development of biomarkers for early diagnosis and prognosis is urgent. Recent studies have shown that SNHG3 expression is upregulated in HCC tissues compared with normal tissues and positively correlates with tumor stage ($P < 0.001$), tumor size ($P = 0.003$), lymph node metastasis ($P < 0.001$), distant metastasis ($P < 0.001$), portal vein tumor thrombosis ($P = 0.014$), and relapse ($P = 0.038$) [25,26]. Based on the above evidence that SNHG3 influences HCC metastasis and growth, SNHG3 has the potential to be a reliable biomarker for the diagnosis and treatment of HCC.

BC

BC accounts for 30% of all female tumors and is the second leading contributor to cancer deaths in women[55]. Early detection of BC can reduce mortality and improve patient survival[56-58]. The discovery of a new biomarker appears critical. Ma *et al*[31] reported elevated SNHG3 expression in BC tissues and correlated it with tumor malignancy. They also reported that SNHG3 expression was associated with clinicopathological features, such as histological grade ($P = 0.016$), tumor-node-metastasis (TNM) stage ($P = 0.001$), lymph node metastasis ($P < 0.001$), estrogen receptor ($P = 0.009$), and Her-2 ($P = 0.001$)[31]. ER and Her-2 are major molecular targets in the pathogenesis of BC and are associated with prognosis and treatment options for BC[59]. Therefore, SNHG3 plays a carcinogenic role in the progression and prognosis of BC. Therefore, SNHG3 may play an oncogenic role in the progression and prognosis of BC.

CC

CC is the fourth most prevalent cancer among women worldwide in terms of incidence and mortality [53]. The survivability of patients with advanced CC is not desirable, and early diagnosis and treatment of CC improve its prognosis[60]. It is important to further explore the mechanisms of CC development

to develop new therapeutic approaches[61]. The function of SNHG3 in CC has been recognized in several studies. Zhu *et al*[27] published that SNHG3 expression was obviously upregulated in CC tissues, and high SNHG3 expression affected International Federation of Gynecology and Obstetrics (FIGO) stage (P = 0.011) and metastasis (P = 0.018), implying that SNHG3 is a possible prognostic biomarker and a target for treatment in CC.

ccRCC

With high morbidity and mortality, ccRCC is the most common and serious type of renal cell carcinoma [62]. Using TCGA and GEO databases, Zhang *et al*[35] found that lncRNA SNHG3 expression was elevated in ccRCC and positively correlated with many clinicopathological parameters. They further quantified the relative expression of SNHG3 in ccRCC tissues compared with normal tissues using qRT–PCR and discovered that the relative expression of SNHG3 was increased in ccRCC tissues[35]. These results revealed that upregulated SNHG3 expression may play an essential role in the ccRCC pathway.

CRC

CRC is a dominant reason for morbidity and mortality worldwide, yet greater than half of patients have progressed to stage II/III at the time of diagnosis. The treatment of CRC typically consists of curative resection *via* surgery followed by adjuvant chemotherapy to reduce the risk of recurrence[63]. Therefore, it is critical to further elucidate the mechanisms of CRC and to pursue the development of effective targeted therapies. SNHG3 expression was remarkably upregulated in CRC tissues compared to nearby normal tissues and correlated with poor outcomes in CRC[36-38]. Moreover, Wen *et al*[36] explored the connection between SNHG3 and clinicopathological parameters, and the results reflected a close association with tumor stage (P = 0.006) and distant metastasis (P = 0.0033). Overall, SNHG3 promotes the progression of CRC, leading to an unfavorable prognosis.

Glioma

Glioma is a fatal brain tumor that can be treated with radiation and surgery, but the median survival of patients is only approximately 14-17 mo[64]. Effective curative treatments for glioma are lacking. Thus, it is especially vital to determine the molecular mechanisms of glioma and identify novel strategies for treatment[65]. SNHG3 is highly expressed in glioma tissues compared to normal tissues[39,40]. Zhang *et al*[39] explored the relationship between SNHG3 expression and the clinicopathological features of GM patients, including tumor size (P = 0.0300) and World Health Organization classification (P = 0.0278). These studies indicated that SNHG3 offer new insights for the future treatment of glioma.

Lung cancer

Lung cancer is one of the cancers with the highest mortality and morbidity rates worldwide[66], with NSCLC accounting for 85% of lung cancer cases[67]. Shi *et al*[44] revealed that high expression of lncRNA SNHG3 in NSCLC tissues was associated with TNM stage (P = 0.0053), lymph node metastasis (P = 0.0006), and tumor size (P = 0.0005). Thus, elevated SNHG3 expression is relevant to the lower overall survival (OS) rate of NSCLC patients. Liu *et al*[67] analyzed the TCGA database as well as the GSE19804 public database and found high SNHG3 expression in lung adenocarcinoma. These researchers used Kaplan–Meier plotter database analysis to determine that high SNHG3 expression decreases the OS time of lung adenocarcinoma patients. However, Kang *et al*[68] used quantitative polymerase chain reaction to show that SNHG3 expression levels were decreased in lung adenocarcinoma tissues, and Kaplan–Meier analysis demonstrated that patients with low SNHG3 expression levels had a short OS. In conclusion, SNHG3 is associated with unfavorable prognosis in lung cancer patients, but the expression and function of SNHG3 in lung adenocarcinoma still requires further research.

Ovarian cancer

OC claims the lives of 151900 women worldwide each year and is one of the leading contributors to death in women[69]. Because there are no specific symptoms in the early stages, greater than 79% of OC patients reach stage III or IV[70]. The lack of effective biomarkers translates to a poor prognosis in OC patients. Recently, Hong *et al*[50] described high SNHG3 expression in OC tissues compared with normal tissues adjacent to cancer, and a high SNHG3 expression level was positively correlated with the FIGO stage (P = 0.007) and lymph node metastasis (P = 0.001) of OC patients. This finding suggests that high SNHG3 expression may be an individual prognostic factor affecting OS in OC patients.

Papillary thyroid carcinoma

PTC is the most common type of thyroid cancer, and the incidence of PTC is increasing[71]. The high rate of metastases in the cervical lymph nodes of PTC patients is closely related to the recurrence of PTC [72,73]. It seems relevant to study the mechanism of metastasis in PTC. Sui *et al*[52] analyzed 42 pairs of tissues and determined that SNHG3 expression was higher in PTC tissues compared with controls. High SNHG3 expression was positively correlated with TNM stage (P = 0.014) and lymph node metastasis (P

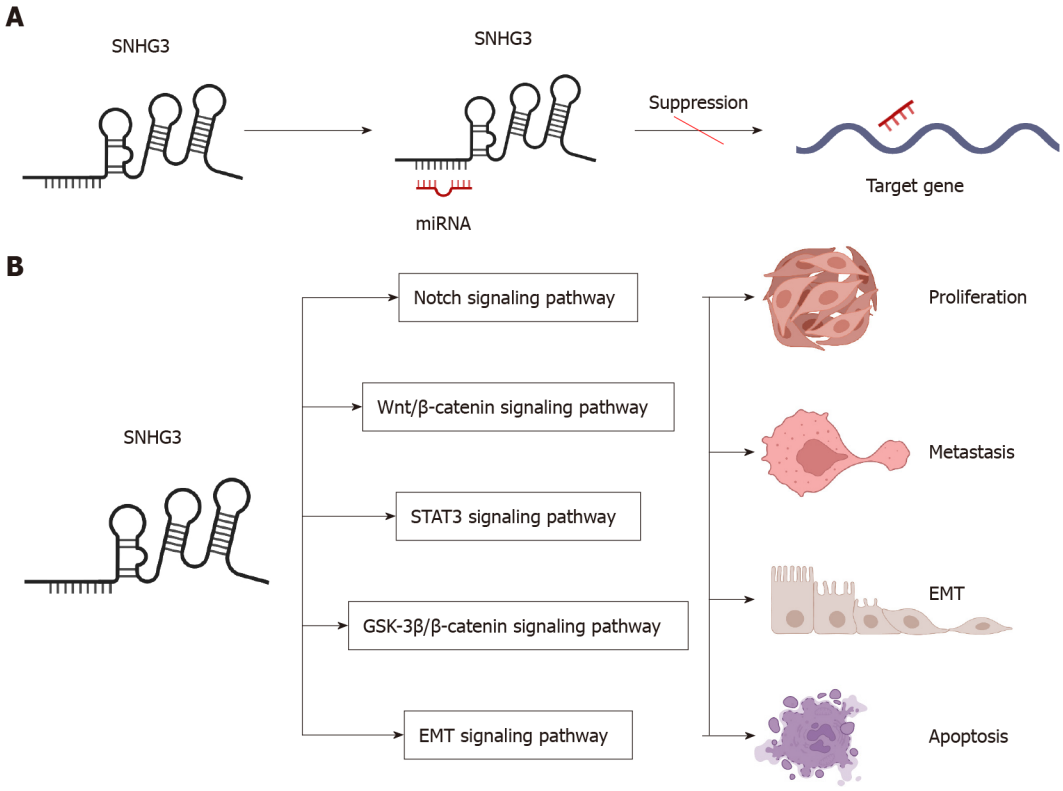

DOI: 10.3748/wjg.v28.i16.1641 **Copyright** ©The Author(s) 2022.

Figure 2 Small nucleolar RNA host gene 3-mediated mechanisms regulating cancer progression. A: Small nucleolar RNA host gene 3 (SNHG3) as a ceRNA; B: SNHG3 is involved in signaling pathways. SNHG3: Small nucleolar RNA host gene 3; EMT: Epithelial–mesenchymal transition.

= 0.0292) in advanced PTC. The above results suggest that SNHG3 could be a carcinogenic lncRNA in PTC.

Researchers have elucidated the high expression of SNHG3 in acute myeloid leukemia (AML)[74], esophageal cancer[75], gastric cancer (GC)[76-78], laryngeal carcinoma[79,80], oral squamous cell carcinoma[81,82], osteosarcoma[83,84], and prostate cancer[85,86], but have not yet explored the relationship between SNHG3 and clinicopathological features. Subsequent investigations into the biological mechanisms of SNHG3 in other diseases will further support the potential of SNHG3 as a new diagnostic and therapeutic biomarker.

SNHG3 *IN VIVO* STUDIES

SNHG3 may function as an oncogene and has the potential to become a novel potential therapeutic target for many cancers. Several studies have used animal models to explore the effect of SNHG3 *in vivo*. Zhao *et al*[25] assessed the role of SNHG3 in HCC growth *in vivo*. They injected stable SNHG3-depleted HepG2 cells subcutaneously into the right dorsum of female BALB/c nude mice and measured the volume of tumor. The results showed that SNHG3depleted tumors grew significantly slower than that of controls. HCC growth was inhibited *in vivo* due to the knockdown of the SNHG3 gene[25]. Similarly, SNHG3 gene knockdown inhibited the growth of other tumors, such as BC[34], CC[27], ccRCC[35], CRC [36,37], GC[77], glioma[40], laryngeal carcinoma[80], NSCLC[45,46], OC[49], PTC[52], prostate cancer [85]. Overall, SNHG3 promoted the progression of the abovementioned tumors.

BIOLOGICAL FUNCTION OF SNHG3 IN CANCER

In the following section, we will explore the biological function of SNHG3 in different cell lines. Many works have shown that SNHG3 affects cancer cell proliferation, epithelial-mesenchymal transition (EMT)[25,41,44,47,85-87], apoptosis, invasion, migration, and metabolism[29,48] specifically through the action of different molecular mechanisms. In HCC, SNHG3 affects cell proliferation, apoptosis, metastasis and invasion mainly by means of competing endogenous RNA (ceRNA) and EMT signaling pathway, as shown in Figure 2 and Table 2.

Table 2 Function and mechanism of small nucleolar RNA host gene 3 in liver cancer and other cancers

Cancer types	Assessed cancer cell lines	Expression	Related genes and pathways	Biological significance	PMID
Hepatocellular carcinoma	PLC/PRF/5, Hep3B, HepG2, MHCC97L, Huh7, SMMC-7721, HCCLM3	Up	miR-128, CD151	Invasion, EMT, sorafenib resistance	30132868
Hepatocellular carcinoma	HepG2, HCCLM3	Up	miR-326, SMAD3, ZEB1	Proliferation, migration, EMT, anti-apoptosis	31548493
Hepatocellular carcinoma	HepG2, HuH-7	Up	miR-214-3p, ASF1B		34336642
Acute myeloid leukemia	HL-60,THP-1,KG-1, NB4, MOLM-14	Up	miR-758-3p, SRGN	Proliferation, anti-apoptosis	31452272
Bladder cancer	5637,T24	Up	miR-515-5p, GINS2	Proliferation, migration, invasion, EMT	32596993
Breast cancer	MCF-7, MD-MBA-453	Up	miR-330, PKM	Proliferation, mitochondrial metabolism	31956955
Breast cancer	MDA-MB-231, BT-549, MDA-MB-468	Up	miR-326, ITGA5 Vav2/Rac1	Viability, migration, invasion, anti-apoptosis	32495883
Breast cancer	MDA-MB-231, MCF-7	Up	miR-384, HDGF	Proliferation, migration, invasion	31586299
Breast cancer	MCF-7, MDA-MB-231, HCC1937, BT474, SKBr-3	Up	miR-154-3p, Notch	Proliferation, migration, invasion	32883233
Breast cancer	MDA-MB-231, MCF-7	Up	miR-186-5p, ZEB1	Proliferation, migration, invasion	33594311
Breast cancer	MCF-7, MDA-MB-231, MDA-MB-468, BT-474	Up	miR-326	Proliferation, migration, invasion	32945476
Cervical cancer	C33A, HeLa, SiHa, CaSki and HCC94	Up	YAP1	Proliferation, migration, invasion	34816392
Cervical cancer	SiHa	Up		Proliferation, migration, invasion	34238747
Cholangiocarcinoma	HCCC9810, QBC939, RBE, HUCCT1	Up	miR-3173–5p, ERG	Proliferation, migration, invasion	34647226
Clear cell renal cell carcinoma	ACHN, A498, Caki-1	Up	miR-139-5p, TOP2A	Proliferation, migration, invasion	31505165
Colorectal cancer	HCT116, LoVo, SW480, and SW620	Up	miR-539, RUNX2	Proliferation, migration, invasion	32187965
Colorectal cancer	HT29, HCT116, SW480, and LoVo	Up	miR-182-5p, c-Myc	Proliferation, migration, invasion	28731158
Colorectal cancer	SW480, SW620, HCT8, HT29	Up	miR-370-5p, EZH1	Proliferation, migration, invasion	34661273
Esophageal cancer	KYSE-150, Eca-9706	Up	miR-186-5p, METTL3, m6A		33596916
Gastric cancer	MGC-803, AGS, BGC-823, SGC-7901, MKN-45, HGC-27	Up	EZH2, MED18	Proliferation, migration, invasion	31534128
Gastric cancer	SGC7901, BGC823	Up	IL-6, STAT3, SNHG3, miR-3619-5p, ARL2	Proliferation	32930970
Gastric cancer	HGC-27, GC9811-P	Up	miR-326, TWIST	Proliferation, migration, invasion	34257656
Glioma	A172, SHG44	Up	miR-384, HDGF	Proliferation, migration, invasion, anti-apoptosis	33817254
Glioma	U-87-MG, U-251-MG	Up	miR-485-5p, LMX1B	Proliferation, migration, invasion	34153159
Laryngeal carcinoma	16HBE, TU212, TU686	Up	miR-384, WEE1	Proliferation, migration, invasion	31238052
Laryngeal carcinoma	TU177, AMC-HN-8	Up	Wnt/β-catenin, miR-340-5p, YAP1	Proliferation, migration, anti-apoptosis, mitochondrial metabolism	32538668
Lung adenocarcinoma	A549, H1299	Up		Proliferation, cell cycle,anti-apoptosis	30154938
Lung adenocarcinoma	A549, H1299, H1975	Down	miR-890	Anti-proliferation, anti-migration, anti-invasion, apoptosis	34306585
Non-small-cell lung cancer	H1299, H358, A549, H1975	Up	miR-13433p, NFIX	Proliferation, migration, invasion	34132359

Non-small-cell lung cancer	CMT-167, LLC, CMT-170, CMT-181	Up	TGF-β pathway, IL-6, JAK2, STAT3 pathway	Proliferation, migration, EMT	31602642
Non-small-cell lung cancer	SPC-A1, A549, NCI-H23, NCI-H460	Up	miR-340-5p	Lymph node infiltration, distant metastases	33225676
Non-small-cell lung cancer	A549, H322, H1299, GLC-82, SPC-A1	Up	miR-216a, ZEB1	Proliferation, migration, invasion	33177840
Non-small-cell lung cancer	A549, HCC827, H2170, H520	Up	miR-515-5p, SUMO2	Proliferation, migration, invasion, EMT	34032148
Oral squamous cell carcinoma	SCC4, CAL-27	Up	miR-2682-5p, HOXB8	Proliferation, migration	32989886
Oral squamous cell carcinoma	SCC-15, SCC-9, CAL-27, HN5	Up	Wnt/β-catenin, NFYC	Proliferation, migration	31762107
Osteosarcoma	Saos2, MG63, U2OS, HOS	Up	miR-151a-3p, RAB22A	Proliferation, migration, invasion	30797154
Osteosarcoma	MG-63, 143B, HOS, SW-1353, Saos-2, U-2OS	Up	miR-196a-5p	Proliferation, colony formation	30791797
Ovarian cancer	SK-OV3, TOV-21G, and OVCAR-3	Up		Energy metabolism	29921511
Ovarian cancer	SKOV3, HeyA8, A2780	Up	miR-339-5p, TRPC3	Proliferation, anti-apoptosis	33149611
Ovarian cancer	SKOV3, 60OVCAR3, A2780, ES2	Up	GSK3β/β-catenin	Proliferation, migration	29758922
Ovarian cancer	A2780, SKOV3, OVCAR3, OV90	Up	miR-139-5p, Notch1	Proliferation, migration	33552243
Papillary thyroid carcinoma	BCPAP, TPC-1	Up	miR-214-3p, PSMD10	Migration, invasion, proliferation, and colony formation	32048306
Prostate cancer	PC3, DU145, 22RV1, NCaP	Up	miR-577, SMURF1	Proliferation, migration, EMT, anti-apoptosis	32248648
Prostate cancer	PC3, 22RV1, DU145, LNCaP	Up	miR-487a-3p,TRIM25	Viability, migration, invasion, EMT	33416420

EMT: Epithelial–mesenchymal transition.

SNHG3 function as a ceRNAs in cancers

LncRNAs and microRNAs (miRNAs) are ncRNAs. LncRNAs compete with miRNAs by acting as sponges for miRNAs to reduce the activity or expression of miRNAs[88]. These lncRNAs are called ceRNAs. Numerous studies have found that SNHG3 can function as a ceRNA by competitively binding to various miRNAs, including miR-758-3p[74], miR-515-5p[87], miR-330[29], miR-326[25,30,34,78], miR-384[31,39,79], miR-154-3p[32], miR-186-5p[33,75], miR3173–5p[89], miR-139-5p[35], miR-539[36], miR-182-5p[37], miR-370-5p[38], miR-3619-5p[76], miR-485-5p[40], miR-128[41], miR-214-3p[42,52], miR-340-5p[45,80], miR-890[68], miR-1343-3p[43], miR-216a[46], miR-515-5p[47], miR-2682-5p[81], miRNA-151a-3p[83], miR-196a-5p[84], miR-339-5p[49], miR-139-5p[51], miR-577[85], and miR-487a-3p[86]. In HCC SNHG3 plays its role as a ceRNA mainly by binding to miR-128[41], miR-326[25] and miR-214-3p[42]. SNHG3 acts as a sponge to bind to miRNAs, subsequently blocking the effects of miRNAs on their downstream target mRNAs. Thus, SNHG3 regulates the expression of oncogenes or tumor suppressor genes, such as *SRGN*[74], *PKM*[29], *HDGF*[31], and *c-Myc*[37], ultimately affecting cancer cell proliferation, apoptosis, metastasis, metabolism and EMT, as shown in Figures 3 and 4.

EMT signaling pathway

The EMT process has been shown to be critical in cancer[90,91]. Shi *et al*[44] showed that human lung cancer cells overexpressing the SNHG3 gene exhibited increased expression of mesenchymal markers (N-calmodulin and waveform protein) and reduced expression of epithelial cell markers (E-calmodulin) while also promoting cancer cell proliferation and metastasis through the TGF-β pathway. In addition, Zhao *et al*[25] learned that SNHG3 promotes cancer cell migration by upregulating the expression of ZEB1, a key transcription factor of EMT in HCC cells. The same conclusion was reached in BC[33] and NSCLC[46]. The above achievements point to the potential application of SNHG3 in the tumor EMT signaling pathway.

Notch signaling pathway

The Notch signaling pathway is a strongly conserved cellular signaling system in most multicellular organisms and is required for a variety of cellular processes, including stem cell functions, cell proliferation, differentiation, and cell death. Several lncRNAs have been proven to participate in the Notch signaling pathway. Zhang *et al*[51] demonstrated that SNHG3 promotes OC proliferation and migration by regulating Notch1. In addition, Jiang *et al*[32], suggested that SNHG3 promotes BC cell proliferation

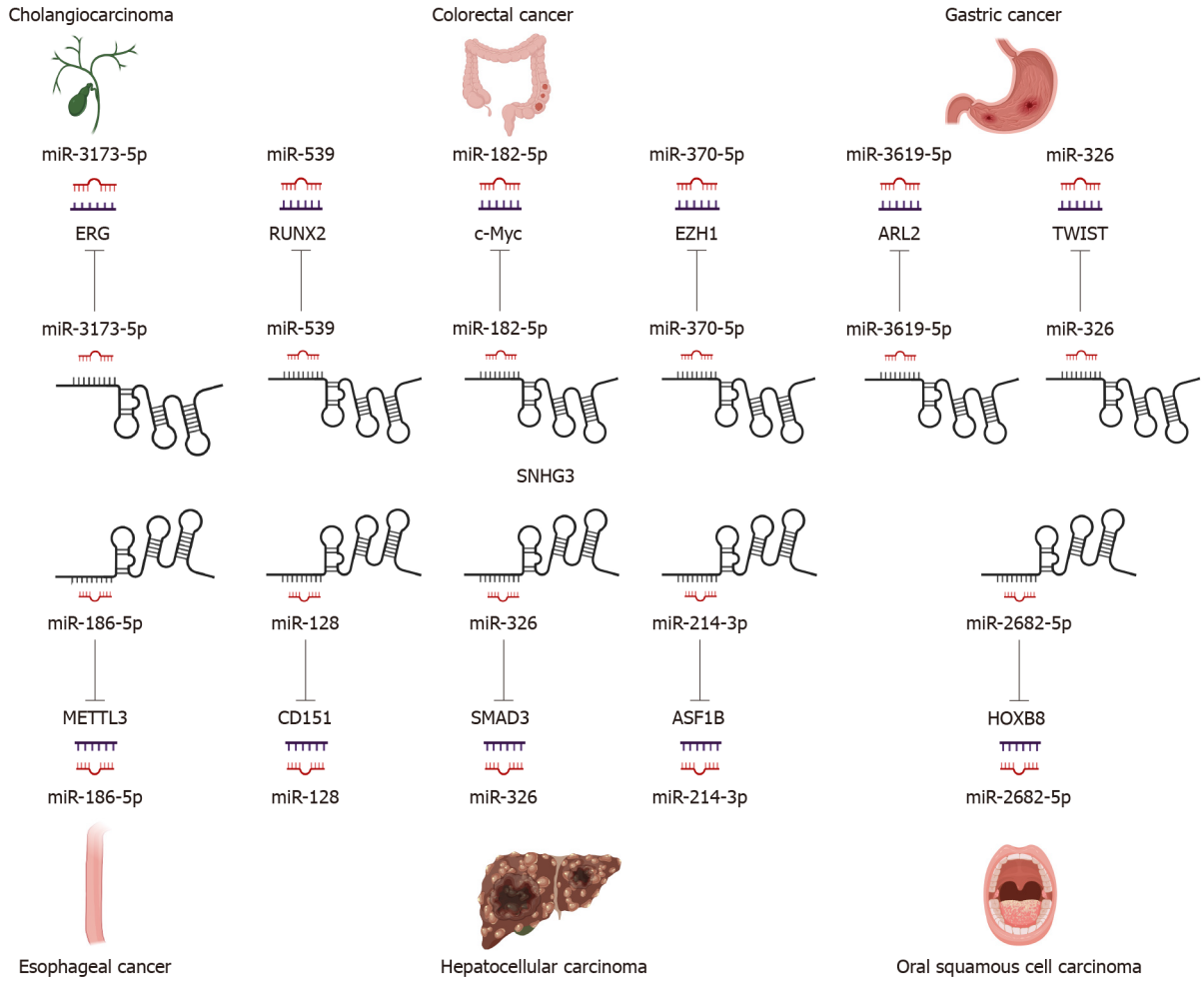

DOI: 10.3748/wjg.v28.i16.1641 **Copyright** ©The Author(s) 2022.

Figure 3 Small nucleolar RNA host gene 3 functions as a competing endogenous RNA in digestive system tumors.

and metastasis through upregulation of the Notch signaling pathway. These studies indicate that SNHG3 plays a crucial part in Notch pathways, which have the potential to develop novel therapeutic targets for cancer therapy.

Wnt/β-catenin signaling pathway

Aberrant activation of Wnt/β-catenin signaling was found in some tumors, and Wnt/β-catenin signaling can regulate oncogenes, such as *c-Myc* and *Bcl-2*, leading to tumorigenesis and cell proliferation. SNHG3 may upregulate the Wnt/β-catenin pathway by regulating miR-340-5p and YAP1 in laryngeal cancer cells[80]. In addition, SNHG3 may also promote the proliferation and metastasis of oral squamous carcinoma cells by upregulating the NFYC and Wnt/β-catenin pathways[82]. SNHG3 is involved in the Wnt/β-catenin signaling pathway that mediates tumor development and could represent a new tool for tumor therapy.

STAT3 signaling pathway

Tyrosine kinase signaling delivered by STAT3 is frequently activated in cancer cells, and the STAT3 signaling pathway plays an important role in cancer progression, where it can be activated by cytokines, such as IL-6[92], and growth factors[93,94]. STAT3 is phosphorylated by receptor-associated JAK and thus enters the nucleus to act as a transcriptional activator, regulating oncogene expression[95]. The impacts of STAT3 signaling in suppressing tumor immune surveillance have also been reported[96].

Sun *et al*[76] demonstrated that SNHG3 was overexpressed in GC tissues, and cellular experiments revealed that IL-6-activated STAT3 positively regulates SNHG3 and that SNHG3 promotes stem cell-like properties in GC cells. Shi *et al*[44] found that the IL-6/JAK2/STAT3 pathway activated SNHG3 in NSCLC and promoted cell proliferation and migration. This finding leads to the conclusion that the STAT3 signaling pathway involved in SNHG3 is a novel mechanism of carcinogenesis, suggesting that SNHG3 may represent a biomarker for the treatment of these carcinomas.

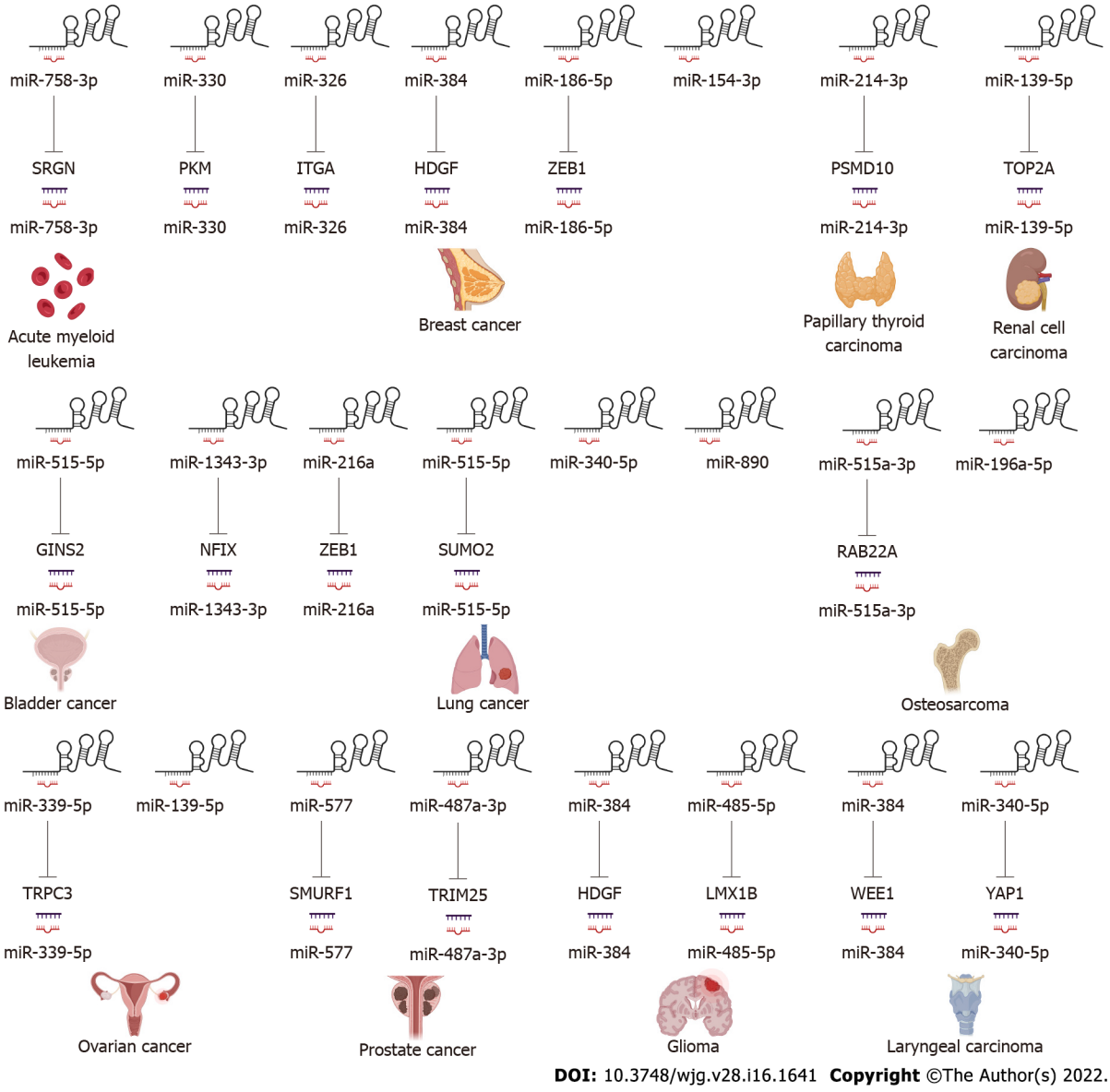

DOI: 10.3748/wjg.v28.i16.1641 **Copyright** ©The Author(s) 2022.

Figure 4 Small nucleolar RNA host gene 3 functions as a competing endogenous RNA in other systemic tumors.

GSK-3β/β-catenin signaling pathway

GSK-3β can negatively regulate β-catenin signaling, which is also implicated in cell proliferation[97]. Research has illustrated that GSK-3β/β-catenin signaling is, for example, one of the downstream drivers of SNHG3 in OC[50], and high expression of SNHG3 fosters cell proliferation and invasion *via* GSK-3β/β-catenin.

SNHG3 can revitalize multiple signaling pathways to promote human tumorigenesis, such as the Notch signaling pathway, Wnt/β-catenin signaling pathway, STAT3 signaling pathway, GSK-3β/β-catenin signaling pathway, and EMT signaling pathway. Thus, SNHG3 may become a target in the treatment of tumors.

CONCLUSION

LncRNAs function as multifunctional signaling modulators, facilitating tumor initiation, progression, and metastasis by regulating tumor cell proliferation, migration, apoptosis, cell cycle, drug resistance, epithelial-mesenchymal transition, metabolic reprogramming, and immune response[98-100]. Compelling studies have suggested that lncRNAs can act as diagnostic indices, prognostic biomarkers, and therapeutic targets for diseases[101,102]. These reports indicate that SNHG3 expression is upregulated in tumor tissues, such as HCC, GC, CC, PTC, and AML, compared to adjacent normal tissues. However, the expression of SNHG3 in lung adenocarcinoma has shown different results and

needs to be further explored. At the same time, SNHG3 has been associated with various clinicopathological parameters such as staging and distant metastasis. In addition, SNHG3 has been shown to promote tumour development in *in vivo* experiments, and at the cellular level, SNHG3 plays a significant role in promoting tumour cell proliferation, migration and metastasis, disrupting the cell cycle and inhibiting apoptosis in a variety of cancers through a variety of signalling pathways, resulting in a poor prognosis for patients.In short, these findings implied that SNHG3 might function as a new target in the diagnosis and treatment of tumours.

In summary, a better understanding of the function of SNHG3 in the clinicopathological features and mechanisms of tumor development may help to improve the efficiency and targeting of treatment. Further studies on SNHG3 and its regulatory mechanism may pave the way to improve prevention, cancer diagnosis, and treatment based on patients' biological and pathological characteristics.

ACKNOWLEDGEMENTS

The authors gratefully acknowledge all the people that have made this study.

FOOTNOTES

Author contributions: Chen Z carried out the concepts and designed the definition of intellectual content; Shan DD and Zheng QX carried out the literature search and manuscript editing; Wang J performed manuscript review; All authors have read and approved the content of the manuscript.

Supported by the National Science and Technology Major Project of China, No. 2018ZX10302206 and 2017ZX10202203.

Conflict-of-interest statement: The authors declare that there is no conflict of interests regarding the publication of this paper.

Open-Access: This article is an open-access article that was selected by an in-house editor and fully peer-reviewed by external reviewers. It is distributed in accordance with the Creative Commons Attribution NonCommercial (CC BY-NC 4.0) license, which permits others to distribute, remix, adapt, build upon this work non-commercially, and license their derivative works on different terms, provided the original work is properly cited and the use is non-commercial. See: https://creativecommons.org/Licenses/by-nc/4.0/

Country/Territory of origin: China

ORCID number: Dan-Dan Shan 0000-0003-4761-7385; Qiu-Xian Zheng 0000-0001-5609-7380; Jing Wang 0000-0001-6652-2854; Zhi Chen 0000-0002-0848-1502.

S-Editor: Zhang H
L-Editor: A
P-Editor: Zhang H

REFERENCES

1 **Sharma Y**, Miladi M, Dukare S, Boulay K, Caudron-Herger M, Groß M, Backofen R, Diederichs S. A pan-cancer analysis of synonymous mutations. *Nat Commun* 2019; **10**: 2569 [PMID: 31189880 DOI: 10.1038/s41467-019-10489-2]
2 **Nuevo-Tapioles C**, Santacatterina F, Stamatakis K, Núñez de Arenas C, Gómez de Cedrón M, Formentini L, Cuezva JM. Coordinate β-adrenergic inhibition of mitochondrial activity and angiogenesis arrest tumor growth. *Nat Commun* 2020; **11**: 3606 [PMID: 32681016 DOI: 10.1038/s41467-020-17384-1]
3 **Ni Y**, Schmidt KR, Werner BA, Koenig JK, Guldner IH, Schnepp PM, Tan X, Jiang L, Host M, Sun L, Howe EN, Wu J, Littlepage LE, Nakshatri H, Zhang S. Death effector domain-containing protein induces vulnerability to cell cycle inhibition in triple-negative breast cancer. *Nat Commun* 2019; **10**: 2860 [PMID: 31253784 DOI: 10.1038/s41467-019-10743-7]
4 **Dawson MA**, Kouzarides T. Cancer epigenetics: from mechanism to therapy. *Cell* 2012; **150**: 12-27 [PMID: 22770212 DOI: 10.1016/j.cell.2012.06.013]
5 **Paull EO**, Aytes A, Jones SJ, Subramaniam PS, Giorgi FM, Douglass EF, Tagore S, Chu B, Vasciaveo A, Zheng S, Verhaak R, Abate-Shen C, Alvarez MJ, Califano A. A modular master regulator landscape controls cancer transcriptional identity. *Cell* 2021; **184**: 334-351.e20 [PMID: 33434495 DOI: 10.1016/j.cell.2020.11.045]
6 **Statello L**, Guo CJ, Chen LL, Huarte M. Gene regulation by long non-coding RNAs and its biological functions. *Nat Rev Mol Cell Biol* 2021; **22**: 96-118 [PMID: 33353982 DOI: 10.1038/s41580-020-00315-9]
7 **Yao RW**, Wang Y, Chen LL. Cellular functions of long noncoding RNAs. *Nat Cell Biol* 2019; **21**: 542-551 [PMID:

31048766 DOI: 10.1038/s41556-019-0311-8]
8 **Dong H**, Hu J, Zou K, Ye M, Chen Y, Wu C, Chen X, Han M. Activation of LncRNA TINCR by H3K27 acetylation promotes Trastuzumab resistance and epithelial-mesenchymal transition by targeting MicroRNA-125b in breast Cancer. *Mol Cancer* 2019; **18**: 3 [PMID: 30621694 DOI: 10.1186/s12943-018-0931-9]
9 **Li L**, van Breugel PC, Loayza-Puch F, Ugalde AP, Korkmaz G, Messika-Gold N, Han R, Lopes R, Barbera EP, Teunissen H, de Wit E, Soares RJ, Nielsen BS, Holmstrøm K, Martínez-Herrera DJ, Huarte M, Louloupi A, Drost J, Elkon R, Agami R. LncRNA-OIS1 regulates DPP4 activation to modulate senescence induced by RAS. *Nucleic Acids Res* 2018; **46**: 4213-4227 [PMID: 29481642 DOI: 10.1093/nar/gky087]
10 **Wu H**, Qin W, Lu S, Wang X, Zhang J, Sun T, Hu X, Li Y, Chen Q, Wang Y, Zhao H, Piao H, Zhang R, Wei M. Long noncoding RNA ZFAS1 promoting small nucleolar RNA-mediated 2'-O-methylation *via* NOP58 recruitment in colorectal cancer. *Mol Cancer* 2020; **19**: 95 [PMID: 32443980 DOI: 10.1186/s12943-020-01201-w]
11 **Shen SN**, Li K, Liu Y, Yang CL, He CY, Wang HR. Down-regulation of long noncoding RNA PVT1 inhibits esophageal carcinoma cell migration and invasion and promotes cell apoptosis *via* microRNA-145-mediated inhibition of FSCN1. *Mol Oncol* 2019; **13**: 2554-2573 [PMID: 31369196 DOI: 10.1002/1878-0261.12555]
12 **Stojic L**, Niemczyk M, Orjalo A, Ito Y, Ruijter AE, Uribe-Lewis S, Joseph N, Weston S, Menon S, Odom DT, Rinn J, Gergely F, Murrell A. Transcriptional silencing of long noncoding RNA GNG12-AS1 uncouples its transcriptional and product-related functions. *Nat Commun* 2016; **7**: 10406 [PMID: 26832224 DOI: 10.1038/ncomms10406]
13 **Gong C**, Maquat LE. lncRNAs transactivate STAU1-mediated mRNA decay by duplexing with 3' UTRs *via* Alu elements. *Nature* 2011; **470**: 284-288 [PMID: 21307942 DOI: 10.1038/nature09701]
14 **McHugh CA**, Chen CK, Chow A, Surka CF, Tran C, McDonel P, Pandya-Jones A, Blanco M, Burghard C, Moradian A, Sweredoski MJ, Shishkin AA, Su J, Lander ES, Hess S, Plath K, Guttman M. The Xist lncRNA interacts directly with SHARP to silence transcription through HDAC3. *Nature* 2015; **521**: 232-236 [PMID: 25915022 DOI: 10.1038/nature14443]
15 **Sun Q**, Tripathi V, Yoon JH, Singh DK, Hao Q, Min KW, Davila S, Zealy RW, Li XL, Polycarpou-Schwarz M, Lehrmann E, Zhang Y, Becker KG, Freier SM, Zhu Y, Diederichs S, Prasanth SG, Lal A, Gorospe M, Prasanth KV. MIR100 host gene-encoded lncRNAs regulate cell cycle by modulating the interaction between HuR and its target mRNAs. *Nucleic Acids Res* 2018; **46**: 10405-10416 [PMID: 30102375 DOI: 10.1093/nar/gky696]
16 **Rashid F**, Shah A, Shan G. Long Non-coding RNAs in the Cytoplasm. *Genomics Proteomics Bioinformatics* 2016; **14**: 73-80 [PMID: 27163185 DOI: 10.1016/j.gpb.2016.03.005]
17 **Gil N**, Ulitsky I. Regulation of gene expression by cis-acting long non-coding RNAs. *Nat Rev Genet* 2020; **21**: 102-117 [PMID: 31729473 DOI: 10.1038/s41576-019-0184-5]
18 **Kopp F**, Mendell JT. Functional Classification and Experimental Dissection of Long Noncoding RNAs. *Cell* 2018; **172**: 393-407 [PMID: 29373828 DOI: 10.1016/j.cell.2018.01.011]
19 **Tuunanen TH**, Tervo TM. Excimer laser phototherapeutic keratectomy for corneal diseases: a follow-up study. *CLAO J* 1995; **21**: 67-72 [PMID: 7712612]
20 **Chen W**, Yang J, Fang H, Li L, Sun J. Relevance Function of Linc-ROR in the Pathogenesis of Cancer. *Front Cell Dev Biol* 2020; **8**: 696 [PMID: 32850817 DOI: 10.3389/fcell.2020.00696]
21 **Atianand MK**, Caffrey DR, Fitzgerald KA. Immunobiology of Long Noncoding RNAs. *Annu Rev Immunol* 2017; **35**: 177-198 [PMID: 28125358 DOI: 10.1146/annurev-immunol-041015-055459]
22 **Atianand MK**, Fitzgerald KA. Long non-coding RNAs and control of gene expression in the immune system. *Trends Mol Med* 2014; **20**: 623-631 [PMID: 25262537 DOI: 10.1016/j.molmed.2014.09.002]
23 **Mowel WK**, Kotzin JJ, McCright SJ, Neal VD, Henao-Mejia J. Control of Immune Cell Homeostasis and Function by lncRNAs. *Trends Immunol* 2018; **39**: 55-69 [PMID: 28919048 DOI: 10.1016/j.it.2017.08.009]
24 **Yang W**, Zhang K, Li L, Ma K, Hong B, Gong Y, Gong K. Discovery and validation of the prognostic value of the lncRNAs encoding snoRNAs in patients with clear cell renal cell carcinoma. *Aging (Albany NY)* 2020; **12**: 4424-4444 [PMID: 32126023 DOI: 10.18632/aging.102894]
25 **Zhao Q**, Wu C, Wang J, Li X, Fan Y, Gao S, Wang K. LncRNA SNHG3 Promotes Hepatocellular Tumorigenesis by Targeting miR-326. *Tohoku J Exp Med* 2019; **249**: 43-56 [PMID: 31548493 DOI: 10.1620/tjem.249.43]
26 **Zhang T**, Cao C, Wu D, Liu L. SNHG3 correlates with malignant status and poor prognosis in hepatocellular carcinoma. *Tumour Biol* 2016; **37**: 2379-2385 [PMID: 26373735 DOI: 10.1007/s13277-015-4052-4]
27 **Zhu H**, Zhu C, Feng X, Luo Y. Long noncoding RNA SNHG3 promotes malignant phenotypes in cervical cancer cells *via* association with YAP1. *Hum Cell* 2022; **35**: 320-332 [PMID: 34816392 DOI: 10.1007/s13577-021-00644-7]
28 **Sun Z**, Hu J, Hu K, Tang M, Sun S, Fang Y, Yu H, Zhang Y. [Role of long noncoding RNA SNHG3 in regulating proliferation, migration and invasion of cervical cancer SiHa cells]. *Nan Fang Yi Ke Da Xue Xue Bao* 2021; **41**: 931-936 [PMID: 34238747 DOI: 10.12122/j.issn.1673-4254.2021.06.17]
29 **Li Y**, Zhao Z, Liu W, Li X. SNHG3 Functions as miRNA Sponge to Promote Breast Cancer Cells Growth Through the Metabolic Reprogramming. *Appl Biochem Biotechnol* 2020; **191**: 1084-1099 [PMID: 31956955 DOI: 10.1007/s12010-020-03244-7]
30 **Wang P**, Liu GZ, Wang JF, Du YY. SNHG3 silencing suppresses the malignant development of triple-negative breast cancer cells by regulating miRNA-326/integrin α5 axis and inactivating Vav2/Rac1 signaling pathway. *Eur Rev Med Pharmacol Sci* 2020; **24**: 5481-5492 [PMID: 32495883 DOI: 10.26355/eurrev_202005_21333]
31 **Ma Q**, Qi X, Lin X, Li L, Chen L, Hu W. LncRNA SNHG3 promotes cell proliferation and invasion through the miR-384/hepatoma-derived growth factor axis in breast cancer. *Hum Cell* 2020; **33**: 232-242 [PMID: 31586299 DOI: 10.1007/s13577-019-00287-9]
32 **Jiang H**, Li X, Wang W, Dong H. Long non-coding RNA SNHG3 promotes breast cancer cell proliferation and metastasis by binding to microRNA-154-3p and activating the notch signaling pathway. *BMC Cancer* 2020; **20**: 838 [PMID: 32883233 DOI: 10.1186/s12885-020-07275-5]
33 **Wan Q**, Tang M, Sun SL, Hu J, Sun ZJ, Fang YT, He TC, Zhang Y. SNHG3 promotes migration, invasion, and epithelial-

mesenchymal transition of breast cancer cells through the miR-186-5p/ZEB1 axis. *Am J Transl Res* 2021; **13**: 585-600 [PMID: 33594311]

34 **Zhang H**, Wei N, Zhang W, Shen L, Ding R, Li Q, Li S, Du Y. lncRNA SNHG3 promotes breast cancer progression by acting as a miR326 sponge. *Oncol Rep* 2020; **44**: 1502-1510 [PMID: 32945476 DOI: 10.3892/or.2020.7690]

35 **Zhang C**, Qu Y, Xiao H, Xiao W, Liu J, Gao Y, Li M. LncRNA SNHG3 promotes clear cell renal cell carcinoma proliferation and migration by upregulating TOP2A. *Exp Cell Res* 2019; **384**: 111595 [PMID: 31505165 DOI: 10.1016/j.yexcr.2019.111595]

36 **Dacheng W**, Songhe L, Weidong J, Shutao Z, Jingjing L, Jiaming Z. LncRNA SNHG3 promotes the growth and metastasis of colorectal cancer by regulating miR-539/RUNX2 axis. *Biomed Pharmacother* 2020; **125**: 110039 [PMID: 32187965 DOI: 10.1016/j.biopha.2020.110039]

37 **Huang W**, Tian Y, Dong S, Cha Y, Li J, Guo X, Yuan X. The long non-coding RNA SNHG3 functions as a competing endogenous RNA to promote malignant development of colorectal cancer. *Oncol Rep* 2017; **38**: 1402-1410 [PMID: 28731158 DOI: 10.3892/or.2017.5837]

38 **Zhang Y**, Li L, Lu KX, Yu LB, Meng J, Liu CY. LncRNA SNHG3 is responsible for the deterioration of colorectal carcinoma through regulating the miR-370-5p/EZH1 axis. *Eur Rev Med Pharmacol Sci* 2021; **25**: 6131-6137 [PMID: 34661273 DOI: 10.26355/eurrev_202110_26891]

39 **Zhang X**, Zheng W, Jiang W, Lin R, Xing C. Long non-coding RNA SNHG3 accelerates progression in glioma by modulating miR-384/HDGF axis. *Open Life Sci* 2020; **15**: 654-664 [PMID: 33817254 DOI: 10.1515/biol-2020-0066]

40 **Guo X**, Zheng J, Yu MJ, Piao HZ, Zhao HY. Long noncoding RNA SNHG3 promotes glioma tumorigenesis by sponging miR-485-5p to upregulate LMX1B expression. *Kaohsiung J Med Sci* 2021; **37**: 851-862 [PMID: 34153159 DOI: 10.1002/kjm2.12411]

41 **Zhang PF**, Wang F, Wu J, Wu Y, Huang W, Liu D, Huang XY, Zhang XM, Ke AW. LncRNA SNHG3 induces EMT and sorafenib resistance by modulating the miR-128/CD151 pathway in hepatocellular carcinoma. *J Cell Physiol* 2019; **234**: 2788-2794 [PMID: 30132868 DOI: 10.1002/jcp.27095]

42 **Zhan T**, Gao X, Wang G, Li F, Shen J, Lu C, Xu L, Li Y, Zhang J. Construction of Novel lncRNA-miRNA-mRNA Network Associated With Recurrence and Identification of Immune-Related Potential Regulatory Axis in Hepatocellular Carcinoma. *Front Oncol* 2021; **11**: 626663 [PMID: 34336642 DOI: 10.3389/fonc.2021.626663]

43 **Zhao L**, Song X, Guo Y, Ding N, Wang T, Huang L. Long noncoding RNA SNHG3 promotes the development of nonsmall cell lung cancer *via* the miR13433p/NFIX pathway. *Int J Mol Med* 2021; **48** [PMID: 34132359 DOI: 10.3892/ijmm.2021.4980]

44 **Shi J**, Li J, Yang S, Hu X, Chen J, Feng J, Shi T, He Y, Mei Z, He W, Xie J, Li S, Jie Z, Tu S. LncRNA SNHG3 is activated by E2F1 and promotes proliferation and migration of non-small-cell lung cancer cells through activating TGF-β pathway and IL-6/JAK2/STAT3 pathway. *J Cell Physiol* 2020; **235**: 2891-2900 [PMID: 31602642 DOI: 10.1002/jcp.29194]

45 **He WW**, Ma HT, Guo X, Wu WM, Gao EJ, Zhao YH. lncRNA SNHG3 accelerates the proliferation and invasion of non-small cell lung cancer by downregulating miR-340-5p. *J Biol Regul Homeost Agents* 2020; **34**: 2017-2027 [PMID: 33225676 DOI: 10.23812/20-388-A]

46 **Zhao S**, Gao X, Zhong C, Li Y, Wang M, Zang S. SNHG3 Knockdown Suppresses Proliferation, Migration and Invasion, and Promotes Apoptosis in Non-Small Cell Lung Cancer Through Regulating miR-216a/ZEB1 Axis. *Onco Targets Ther* 2020; **13**: 11327-11336 [PMID: 33177840 DOI: 10.2147/OTT.S263637]

47 **Li Y**, Gao L, Zhang C, Meng J. LncRNA SNHG3 Promotes Proliferation and Metastasis of Non-Small-Cell Lung Cancer Cells Through miR-515-5p/SUMO2 Axis. *Technol Cancer Res Treat* 2021; **20**: 15330338211019376 [PMID: 34032148 DOI: 10.1177/15330338211019376]

48 **Li N**, Zhan X. The lncRNA SNHG3 regulates energy metabolism of ovarian cancer by an analysis of mitochondrial proteomes. *Gynecol Oncol* 2018; **150**: 343-354 [PMID: 29921511 DOI: 10.1016/j.ygyno.2018.06.013]

49 **Liu EL**, Zhou YX, Li J, Zhang DH, Liang F. Long-Chain Non-Coding RNA SNHG3 Promotes the Growth of Ovarian Cancer Cells by Targeting miR-339-5p/TRPC3 Axis. *Onco Targets Ther* 2020; **13**: 10959-10971 [PMID: 33149611 DOI: 10.2147/OTT.S249873]

50 **Hong L**, Chen W, Wu D, Wang Y. Upregulation of SNHG3 expression associated with poor prognosis and enhances malignant progression of ovarian cancer. *Cancer Biomark* 2018; **22**: 367-374 [PMID: 29758922 DOI: 10.3233/CBM-170710]

51 **Zhang L**, Li G, Wang X, Zhang Y, Huang X, Wu H. lncRNA SNHG3 acts as oncogene in ovarian cancer through miR-139-5p and Notch1. *Oncol Lett* 2021; **21**: 122 [PMID: 33552243 DOI: 10.3892/ol.2020.12383]

52 **Sui G**, Zhang B, Fei D, Wang H, Guo F, Luo Q. The lncRNA SNHG3 accelerates papillary thyroid carcinoma progression *via* the miR-214-3p/PSMD10 axis. *J Cell Physiol* 2020; **235**: 6615-6624 [PMID: 32048306 DOI: 10.1002/jcp.29557]

53 **Bray F**, Ferlay J, Soerjomataram I, Siegel RL, Torre LA, Jemal A. Global cancer statistics 2018: GLOBOCAN estimates of incidence and mortality worldwide for 36 cancers in 185 countries. *CA Cancer J Clin* 2018; **68**: 394-424 [PMID: 30207593 DOI: 10.3322/caac.21492]

54 **Ren Z**, Li A, Jiang J, Zhou L, Yu Z, Lu H, Xie H, Chen X, Shao L, Zhang R, Xu S, Zhang H, Cui G, Sun R, Wen H, Lerut JP, Kan Q, Li L, Zheng S. Gut microbiome analysis as a tool towards targeted non-invasive biomarkers for early hepatocellular carcinoma. *Gut* 2019; **68**: 1014-1023 [PMID: 30045880 DOI: 10.1136/gutjnl-2017-315084]

55 **Siegel RL**, Miller KD, Fuchs HE, Jemal A. Cancer Statistics, 2021. *CA Cancer J Clin* 2021; **71**: 7-33 [PMID: 33433946 DOI: 10.3322/caac.21654]

56 **Teh YC**, Tan GH, Taib NA, Rahmat K, Westerhout CJ, Fadzli F, See MH, Jamaris S, Yip CH. Opportunistic mammography screening provides effective detection rates in a limited resource healthcare system. *BMC Cancer* 2015; **15**: 405 [PMID: 25972043 DOI: 10.1186/s12885-015-1419-2]

57 **O'Mahony M**, Comber H, Fitzgerald T, Corrigan MA, Fitzgerald E, Grunfeld EA, Flynn MG, Hegarty J. Interventions for raising breast cancer awareness in women. *Cochrane Database Syst Rev* 2017; **2**: CD011396 [PMID: 28185268 DOI: 10.1002/14651858.CD011396.pub2]

58 **Coleman C**. Early Detection and Screening for Breast Cancer. *Semin Oncol Nurs* 2017; **33**: 141-155 [PMID: 28365057 DOI: 10.1016/j.soncn.2017.02.009]

59 **Waks AG**, Winer EP. Breast Cancer Treatment: A Review. *JAMA* 2019; **321**: 288-300 [PMID: 30667505 DOI: 10.1001/jama.2018.19323]

60 **Frumovitz M**, Querleu D, Gil-Moreno A, Morice P, Jhingran A, Munsell MF, Macapinlac HA, Leblanc E, Martinez A, Ramirez PT. Lymphadenectomy in locally advanced cervical cancer study (LiLACS): Phase III clinical trial comparing surgical with radiologic staging in patients with stages IB2-IVA cervical cancer. *J Minim Invasive Gynecol* 2014; **21**: 3-8 [PMID: 23911560 DOI: 10.1016/j.jmig.2013.07.007]

61 **Wang L**, Zhao Y, Wang Y, Wu X. The Role of Galectins in Cervical Cancer Biology and Progression. *Biomed Res Int* 2018; **2018**: 2175927 [PMID: 29854732 DOI: 10.1155/2018/2175927]

62 **Siegel RL**, Miller KD, Jemal A. Cancer statistics, 2019. *CA Cancer J Clin* 2019; **69**: 7-34 [PMID: 30620402 DOI: 10.3322/caac.21551]

63 **Glaire MA**, Domingo E, Sveen A, Bruun J, Nesbakken A, Nicholson G, Novelli M, Lawson K, Oukrif D, Kildal W, Danielsen HE, Kerr R, Kerr D, Tomlinson I, Lothe RA, Church DN. Tumour-infiltrating $CD8^+$ lymphocytes and colorectal cancer recurrence by tumour and nodal stage. *Br J Cancer* 2019; **121**: 474-482 [PMID: 31388185 DOI: 10.1038/s41416-019-0540-4]

64 **Reifenberger G**, Wirsching HG, Knobbe-Thomsen CB, Weller M. Advances in the molecular genetics of gliomas - implications for classification and therapy. *Nat Rev Clin Oncol* 2017; **14**: 434-452 [PMID: 28031556 DOI: 10.1038/nrclinonc.2016.204]

65 **Riabovol OO**, Tsymbal DO, Minchenko DO, Lebid-Biletska KM, Sliusar MY, Rudnytska OV, Minchenko OH. Effect of glucose deprivation on the expression of genes encoding glucocorticoid receptor and some related factors in ERN1-knockdown U87 glioma cells. *Endocr Regul* 2019; **53**: 237-249 [PMID: 31734653 DOI: 10.2478/enr-2019-0024]

66 **Youlden DR**, Cramb SM, Baade PD. The International Epidemiology of Lung Cancer: geographical distribution and secular trends. *J Thorac Oncol* 2008; **3**: 819-831 [PMID: 18670299 DOI: 10.1097/JTO.0b013e31818020eb]

67 **Liu L**, Ni J, He X. Upregulation of the Long Noncoding RNA SNHG3 Promotes Lung Adenocarcinoma Proliferation. *Dis Markers* 2018; **2018**: 5736716 [PMID: 30154938 DOI: 10.1155/2018/5736716]

68 **Kang B**, Qiu C, Zhang Y. The Effect of lncRNA SNHG3 Overexpression on Lung Adenocarcinoma by Regulating the Expression of miR-890. *J Healthc Eng* 2021; **2021**: 1643788 [PMID: 34306585 DOI: 10.1155/2021/1643788]

69 **Torre LA**, Bray F, Siegel RL, Ferlay J, Lortet-Tieulent J, Jemal A. Global cancer statistics, 2012. *CA Cancer J Clin* 2015; **65**: 87-108 [PMID: 25651787 DOI: 10.3322/caac.21262]

70 **Torre LA**, Trabert B, DeSantis CE, Miller KD, Samimi G, Runowicz CD, Gaudet MM, Jemal A, Siegel RL. Ovarian cancer statistics, 2018. *CA Cancer J Clin* 2018; **68**: 284-296 [PMID: 29809280 DOI: 10.3322/caac.21456]

71 **Seib CD**, Sosa JA. Evolving Understanding of the Epidemiology of Thyroid Cancer. *Endocrinol Metab Clin North Am* 2019; **48**: 23-35 [PMID: 30717905 DOI: 10.1016/j.ecl.2018.10.002]

72 **Wang X**, Lei J, Wei T, Zhu J, Li Z. Clinicopathological characteristics and recurrence risk of papillary thyroid microcarcinoma in the elderly. *Cancer Manag Res* 2019; **11**: 2371-2377 [PMID: 31114316 DOI: 10.2147/CMAR.S198451]

73 **Zheng X**, Peng C, Gao M, Zhi J, Hou X, Zhao J, Wei X, Chi J, Li D, Qian B. Risk factors for cervical lymph node metastasis in papillary thyroid microcarcinoma: a study of 1,587 patients. *Cancer Biol Med* 2019; **16**: 121-130 [PMID: 31119052 DOI: 10.20892/j.issn.2095-3941.2018.0125]

74 **Peng L**, Zhang Y, Xin H. lncRNA SNHG3 facilitates acute myeloid leukemia cell growth *via* the regulation of miR-758-3p/SRGN axis. *J Cell Biochem* 2020; **121**: 1023-1031 [PMID: 31452272 DOI: 10.1002/jcb.29336]

75 **Zhang M**, Bai M, Wang L, Lu N, Wang J, Yan R, Cui M, Yan H, Zhang L. Targeting SNHG3/miR-186-5p reverses the increased m6A level caused by platinum treatment through regulating METTL3 in esophageal cancer. *Cancer Cell Int* 2021; **21**: 114 [PMID: 33596916 DOI: 10.1186/s12935-021-01747-9]

76 **Sun B**, Han Y, Cai H, Huang H, Xuan Y. Long non-coding RNA SNHG3, induced by IL-6/STAT3 transactivation, promotes stem cell-like properties of gastric cancer cells by regulating the miR-3619-5p/ARL2 axis. *Cell Oncol (Dordr)* 2021; **44**: 179-192 [PMID: 32930970 DOI: 10.1007/s13402-020-00560-2]

77 **Xuan Y**, Wang Y. Long non-coding RNA SNHG3 promotes progression of gastric cancer by regulating neighboring MED18 gene methylation. *Cell Death Dis* 2019; **10**: 694 [PMID: 31534128 DOI: 10.1038/s41419-019-1940-3]

78 **Rao J**, Fu J, Meng C, Huang J, Qin X, Zhuang S. LncRNA SNHG3 Promotes Gastric Cancer Cells Proliferation, Migration, and Invasion by Targeting miR-326. *J Oncol* 2021; **2021**: 9935410 [PMID: 34257656 DOI: 10.1155/2021/9935410]

79 **Wang L**, Su K, Wu H, Li J, Song D. LncRNA SNHG3 regulates laryngeal carcinoma proliferation and migration by modulating the miR-384/WEE1 axis. *Life Sci* 2019; **232**: 116597 [PMID: 31238052 DOI: 10.1016/j.lfs.2019.116597]

80 **Kang R**, Yao DF, Xu GZ, Zhou YH. The knockdown of SNHG3 inhibits the progression of laryngeal squamous cell carcinoma by miR-340-5p/YAP1 axis and Wnt/β-catenin pathway. *Neoplasma* 2020; **67**: 1094-1105 [PMID: 32538668 DOI: 10.4149/neo_2020_191022N1073]

81 **Lu N**, Yin Y, Yao Y, Zhang P. SNHG3/miR-2682-5p/HOXB8 promotes cell proliferation and migration in oral squamous cell carcinoma. *Oral Dis* 2021; **27**: 1161-1170 [PMID: 32989886 DOI: 10.1111/odi.13656]

82 **Liu Z**, Tao H. Small nucleolar RNA host gene 3 facilitates cell proliferation and migration in oral squamous cell carcinoma *via* targeting nuclear transcription factor Y subunit gamma. *J Cell Biochem* 2020; **121**: 2150-2158 [PMID: 31762107 DOI: 10.1002/jcb.29421]

83 **Zheng S**, Jiang F, Ge D, Tang J, Chen H, Yang J, Yao Y, Yan J, Qiu J, Yin Z, Ni Y, Zhao L, Chen X, Li H, Yang L. LncRNA SNHG3/miRNA-151a-3p/RAB22A axis regulates invasion and migration of osteosarcoma. *Biomed Pharmacother* 2019; **112**: 108695 [PMID: 30797154 DOI: 10.1016/j.biopha.2019.108695]

84 **Chen J**, Wu Z, Zhang Y. LncRNA SNHG3 promotes cell growth by sponging miR-196a-5p and indicates the poor survival in osteosarcoma. *Int J Immunopathol Pharmacol* 2019; **33**: 2058738418820743 [PMID: 30791797 DOI: 10.1177/2058738418820743]

85 **Li T**, Xing Y, Yang F, Sun Y, Zhang S, Wang Q, Zhang W. LncRNA SNHG3 sponges miR-577 to up-regulate SMURF1 expression in prostate cancer. *Cancer Med* 2020; **9**: 3852-3862 [PMID: 32248648 DOI: 10.1002/cam4.2992]

86 **Yu L**, Ren Y. Long Noncoding RNA Small Nucleolar RNA Host Gene 3 Mediates Prostate Cancer Migration, Invasion, and Epithelial-Mesenchymal Transition by Sponging *miR-487a-3p* to Regulate *TRIM25*. *Cancer Biother Radiopharm* 2021 [PMID: 33416420 DOI: 10.1089/cbr.2020.3988]

87 **Dai G**, Huang C, Yang J, Jin L, Fu K, Yuan F, Zhu J, Xue B. LncRNA SNHG3 promotes bladder cancer proliferation and metastasis through miR-515-5p/GINS2 axis. *J Cell Mol Med* 2020; **24**: 9231-9243 [PMID: 32596993 DOI: 10.1111/jcmm.15564]

88 **Zhang H**, Lu B. The Roles of ceRNAs-Mediated Autophagy in Cancer Chemoresistance and Metastasis. *Cancers (Basel)* 2020; **12** [PMID: 33050642 DOI: 10.3390/cancers12102926]

89 **Sun ZP**, Tan ZG, Peng C, Yi WM. LncRNA SNHG3 Facilitates the Malignant Phenotype of Cholangiocarcinoma Cells *via* the miR-3173-5p/ERG Axis. *J Gastrointest Surg* 2021 [PMID: 34647226 DOI: 10.1007/s11605-021-05160-5]

90 **Li Z**, Chen Y, An T, Liu P, Zhu J, Yang H, Zhang W, Dong T, Jiang J, Zhang Y, Jiang M, Yang X. Nuciferine inhibits the progression of glioblastoma by suppressing the SOX2-AKT/STAT3-Slug signaling pathway. *J Exp Clin Cancer Res* 2019; **38**: 139 [PMID: 30922391 DOI: 10.1186/s13046-019-1134-y]

91 **Scanlon CS**, Van Tubergen EA, Inglehart RC, D'Silva NJ. Biomarkers of epithelial-mesenchymal transition in squamous cell carcinoma. *J Dent Res* 2013; **92**: 114-121 [PMID: 23128109 DOI: 10.1177/0022034512467352]

92 **Heinrich PC**, Behrmann I, Müller-Newen G, Schaper F, Graeve L. Interleukin-6-type cytokine signalling through the gp130/Jak/STAT pathway. *Biochem J* 1998; **334** (Pt 2): 297-314 [PMID: 9716487 DOI: 10.1042/bj3340297]

93 **Miscia S**, Marchisio M, Grilli A, Di Valerio V, Centurione L, Sabatino G, Garaci F, Zauli G, Bonvini E, Di Baldassarre A. Tumor necrosis factor alpha (TNF-alpha) activates Jak1/Stat3-Stat5B signaling through TNFR-1 in human B cells. *Cell Growth Differ* 2002; **13**: 13-18 [PMID: 11801527]

94 **Park OK**, Schaefer TS, Nathans D. In vitro activation of Stat3 by epidermal growth factor receptor kinase. *Proc Natl Acad Sci U S A* 1996; **93**: 13704-13708 [PMID: 8942998 DOI: 10.1073/pnas.93.24.13704]

95 **Yang L**, Lin S, Xu L, Lin J, Zhao C, Huang X. Novel activators and small-molecule inhibitors of STAT3 in cancer. *Cytokine Growth Factor Rev* 2019; **49**: 10-22 [PMID: 31677966 DOI: 10.1016/j.cytogfr.2019.10.005]

96 **Miklossy G**, Hilliard TS, Turkson J. Therapeutic modulators of STAT signalling for human diseases. *Nat Rev Drug Discov* 2013; **12**: 611-629 [PMID: 23903221 DOI: 10.1038/nrd4088]

97 **Soda M**, Willert K, Kaushansky K, Geddis AE. Inhibition of GSK-3beta promotes survival and proliferation of megakaryocytic cells through a beta-catenin-independent pathway. *Cell Signal* 2008; **20**: 2317-2323 [PMID: 18804163 DOI: 10.1016/j.cellsig.2008.09.001]

98 **Hu Q**, Egranov SD, Lin C, Yang L. Long noncoding RNA loss in immune suppression in cancer. *Pharmacol Ther* 2020; **213**: 107591 [PMID: 32473960 DOI: 10.1016/j.pharmthera.2020.107591]

99 **Sun H**, Huang Z, Sheng W, Xu MD. Emerging roles of long non-coding RNAs in tumor metabolism. *J Hematol Oncol* 2018; **11**: 106 [PMID: 30134946 DOI: 10.1186/s13045-018-0648-7]

100 **Zhang L**, Xu X, Su X. Noncoding RNAs in cancer immunity: functions, regulatory mechanisms, and clinical application. *Mol Cancer* 2020; **19**: 48 [PMID: 32122338 DOI: 10.1186/s12943-020-01154-0]

101 **Liu K**, Gao L, Ma X, Huang JJ, Chen J, Zeng L, Ashby CR Jr, Zou C, Chen ZS. Long non-coding RNAs regulate drug resistance in cancer. *Mol Cancer* 2020; **19**: 54 [PMID: 32164712 DOI: 10.1186/s12943-020-01162-0]

102 **Zhang X**, Xie K, Zhou H, Wu Y, Li C, Liu Y, Liu Z, Xu Q, Liu S, Xiao D, Tao Y. Role of non-coding RNAs and RNA modifiers in cancer therapy resistance. *Mol Cancer* 2020; **19**: 47 [PMID: 32122355 DOI: 10.1186/s12943-020-01171-z]

World Journal of Gastroenterology

Submit a Manuscript: https://www.f6publishing.com

World J Gastroenterol 2022 April 28; 28(16): 1656-1670

DOI: 10.3748/wjg.v28.i16.1656

ISSN 1007-9327 (print) ISSN 2219-2840 (online)

ORIGINAL ARTICLE

Basic Study

LncRNA cancer susceptibility 20 regulates the metastasis of human gastric cancer cells *via* the miR-143-5p/MEMO1 molecular axis

Ke-Shu Shan, Wei-Wei Li, Wang Ren, Shuai Kong, Li-Pan Peng, Hong-Qing Zhuo, Shu-Bo Tian

Specialty type: Gastroenterology and hepatology

Provenance and peer review: Unsolicited article; Externally peer reviewed.

Peer-review model: Single blind

Peer-review report's scientific quality classification

Grade A (Excellent): A
Grade B (Very good): 0
Grade C (Good): C
Grade D (Fair): 0
Grade E (Poor): 0

P-Reviewer: Senchukova M, Russia; Tanabe S, Japan

Received: October 19, 2021
Peer-review started: October 19, 2021
First decision: December 12, 2021
Revised: December 26, 2021
Accepted: March 25, 2022
Article in press: March 25, 2022
Published online: April 28, 2022

Ke-Shu Shan, Shuai Kong, Li-Pan Peng, Hong-Qing Zhuo, Shu-Bo Tian, Department of Gastrointestinal Surgery, Shandong Provincial Hospital Affiliated to Shandong First Medical University, Jinan 250021, Shandong Province, China

Ke-Shu Shan, Shuai Kong, Li-Pan Peng, Hong-Qing Zhuo, Shu-Bo Tian, Department of Gastrointestinal Surgery, Shandong Provincial Hospital Affiliated to Shandong University, Jinan 250021, Shandong Province, China

Wei-Wei Li, Department of Critical Care Medicine, The 960th Hospital of the People's Liberation Army Joint Logistics Support Force, Jinan 250031, Shandong Province, China

Wang Ren, Department of General Surgery, People's Hospital of Sishui County, Jining 273200, Shandong Province, China

Corresponding author: Shu-Bo Tian, PhD, Chief Doctor, Department of Gastrointestinal Surgery, Shandong Provincial Hospital Affiliated to Shandong First Medical University, Department of Gastrointestinal Surgery, Shandong Provincial Hospital Affiliated to Shandong University, Jinan 250021, Shandong Province, China. ttkl_bo@126.com

Abstract

BACKGROUND

Gastric cancer (GC) is considered as one of the most widespread malignancies. Emerging evidence has shown that lncRNAs can function as important oncogenes or tumor suppressors during GC progression.

AIM

To investigate the effect and mechanism of lncRNA cancer susceptibility 20 (CASC20) in the proliferation and metastasis of GC cells.

METHODS

Data mining and clinical samples were used to evaluate the expression of CASC20 in GC and adjacent tissues. CASC20 was down-regulated in GC cells by short-interfering RNA. Cell proliferation was evaluated by CCK-8 assay, and cell migration and invasion were detected by wound healing and Transwell assays. The expressions of proteins related to epithelial-mesenchymal transition were detected by western blot assay.

RESULTS

The expression of CASC20 was increased in GC tumor tissues and various GC cell lines. High CASC20 expression was correlated with a high risk of lymphatic metastasis and poor prognosis in GC patients. In vitro assays showed that silencing CASC20 reduced cell proliferation, migration, and invasion in GC cells. Mechanistic studies revealed that CASC20 exhibits oncogenic functions by regulating MEMO1 expression through competitive endogenous binding to miR-143-5p, leading to induction of epithelial-mesenchymal transition.

CONCLUSION

Our findings indicate that CASC20 serves as a tumor promoter by regulating metastasis in GC *via* the miR-143-5p/MEMO1 axis. CASC20 may be a potential therapeutic target for GC.

Key Words: Gastric cancer; LncRNA; Cancer susceptibility 20; miR-143-5p; MEMO1; Epithelial-mesenchymal transition

©The Author(s) 2022. Published by Baishideng Publishing Group Inc. All rights reserved.

Core Tip: LncRNA cancer susceptibility 20 (CASC20) is upregulated in gastric cancer (GC) and associated with a higher risk of lymphatic metastasis and poor prognosis of patients. CASC20 can promote the proliferation, invasion and metastasis of GC cells by absorbing miR-143-5p to upregulate MEMO1, thereby induced epithelial-mesenchymal transition *in vitro*.

Citation: Shan KS, Li WW, Ren W, Kong S, Peng LP, Zhuo HQ, Tian SB. LncRNA cancer susceptibility 20 regulates the metastasis of human gastric cancer cells *via* the miR-143-5p/MEMO1 molecular axis. *World J Gastroenterol* 2022; 28(16): 1656-1670

URL: https://www.wjgnet.com/1007-9327/full/v28/i16/1656.htm

DOI: https://dx.doi.org/10.3748/wjg.v28.i16.1656

INTRODUCTION

In 2020, gastric cancer (GC) was the fifth most common cancer and the fourth for mortality of cancer-related in the world[1]. Many patients are already at an advanced stage when diagnosed with GC. Surgical resection is the main treatment for GC. However, postoperative metastasis is the main cause of death from GC[2]. In 2011, Robert A. Weinberg published an article classifying metastasis as one of the top ten characteristics of cancer[3]. Therefore, finding effective molecular markers and therapeutic targets for metastasis is important for developing treatments for GC. The mechanisms underlying metastasis in GC have not yet been fully clarified and require further elucidation.

LncRNAs are RNA molecules more than 200 nucleotides in length that are located in the nucleus or cytoplasm and lack any protein-coding ability. Increasing studies have shown that lncRNAs play important roles in chromosome silencing, chromatin epigenetic modification, gene transcription, protein translation and protein localization[4,5]. In addition, lncRNAs have been shown to function in tumor progression[6,7]. Some lncRNAs function as competing endogenous RNA (ceRNA) and regulate the expression of target genes by binding miRNA elements in target miRNAs and "sponging" miRNAs[8]. MiRNAs can specifically target the 3'UTR of target mRNAs, thereby inhibiting mRNA translation. LncRNA 00473 is highly expressed in GC tissues and is closely related to lymph node metastasis and late TNM staging. LncRNA 00473 regulates the expression of CCND2 by adsorbing miR-16-5p to promote the proliferation and metastasis of GC cells[9]. LncRNAs also play emerging roles in endothelial-mesenchymal transition (EMT) process of GC[10]. The process of EMT involves downregulation of the epithelial cell specific proteins and upregulation of the mesenchymal cell specific proteins and it is an important cause of tumor metastasis[11]. LncRNA CASC19 is highly expressed in colorectal cancer, and CASC19 overexpression increased the invasion and migration ability of colorectal cancer cells. CASC19 regulates cell migration inducing hyaluronidase 1 (CEMIP) by targeting miR-140-5p and affecting the EMT process[12].

Several studies have revealed key roles for lncRNAs in GC progression, and multiple lncRNAs have been identified as diagnostic and prognostic markers or treatment targets for GC[4]. A recent study identified the HOXC-AS3 lncRNA as highly expressed in GC tissues. HOXC-AS3 binds YBX1 protein to regulate downstream gene transcription and participates in GC progression[13]. The lncRNA CASC9 is highly expressed in GC tissues and cells. CASC9 negatively regulates miR-370 and promotes the progression of GC through the EGFR/AKT pathway[14]. However, the precise mechanisms and roles of lncRNAs in GC progression are still unclear.

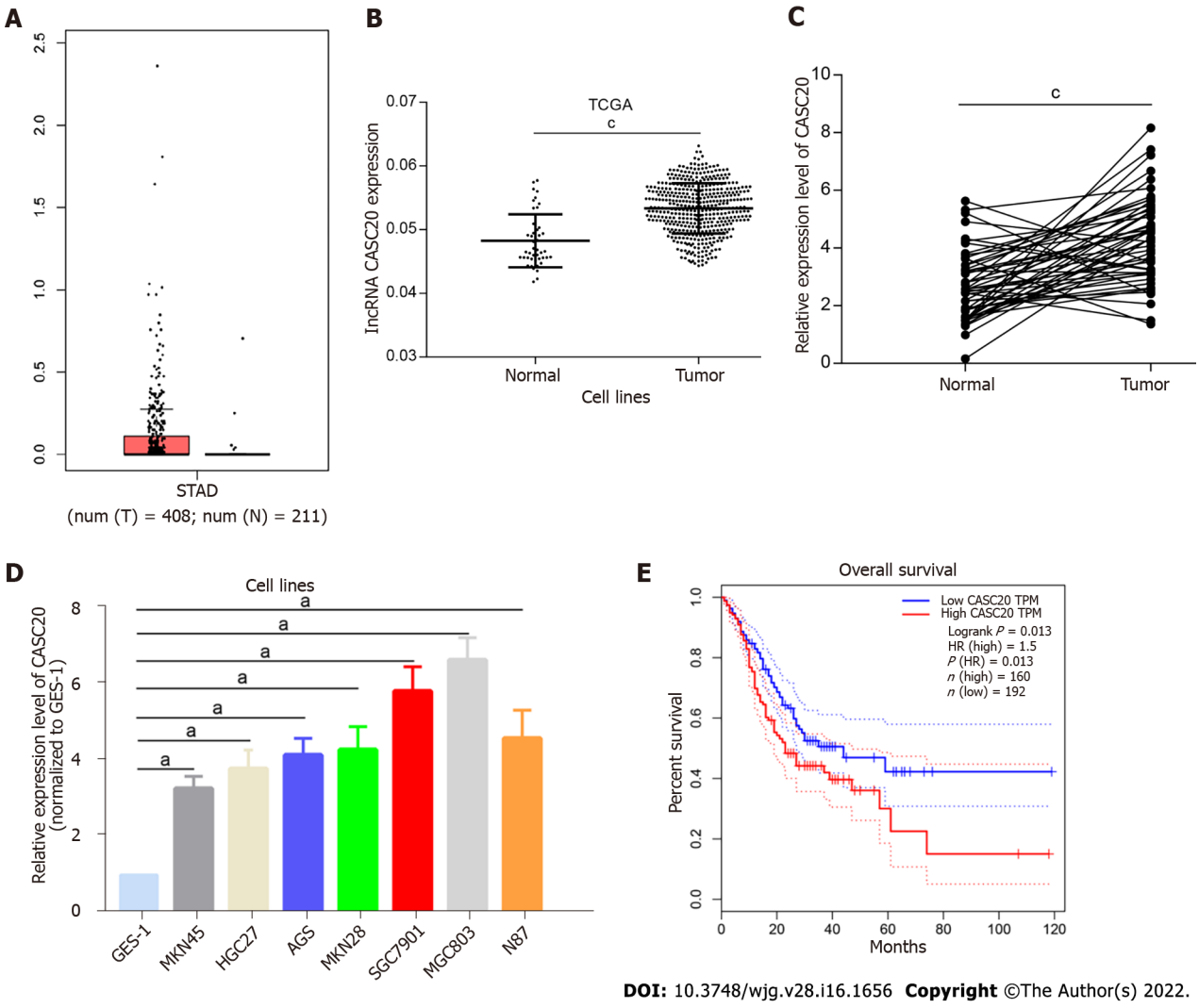

DOI: 10.3748/wjg.v28.i16.1656 **Copyright** ©The Author(s) 2022.

Figure 1 High level of cancer susceptibility 20 in gastric cancer tissues and cell lines. A and B: Cancer susceptibility 20 (CASC20) expression in gastric cancer (GC) samples and normal samples from TCGA GC database; C: CASC20 expression in 50 pairs of clinically collected gastric cancer tissues and normal tissue samples; D: CASC20 expression in GC cell lines and GES-1 cell line was analyzed by quantitative real-time polymerase chain reaction; E: Overall survival curves of TCGA GC patients with different CASC20 expression. $^{a}P < 0.05$ and $^{c}P < 0.001$ *vs* control.

Cancer susceptibility 20 (CASC20) is a 1484 bp lncRNA mapped to chromosome 20p12.3. In this study, we explored the role and possible mechanism of the lncRNA CASC20 in GC metastasis to gain more insights into the mechanism of GC metastasis. We found that the CASC20 lncRNA is highly expressed in GC and closely associated with lymph node metastasis and poor prognosis of GC patients. Through *in vitro* and *in vivo* experiments, we found that CASC20 promotes the proliferation, migration and invasion of GC cells. Mechanistic studies revealed that CASC20 "sponges" miR-143-5p and promotes EMT by regulating MEMO1. This function of CASC20 plays an important role in the metastasis of GC.

MATERIALS AND METHODS

Tissue specimens

All clinical samples and information in this study were from the Department of Gastrointestinal Surgery, Provincial Hospital Affiliated to Shandong First Medical University. Fresh pathological specimens (GC and adjacent normal tissues) were from patients undergoing radical GC surgery at our hospital. All patients provided informed consent and were approved by the Medical Ethics Committee.

Cell culture and transfection

Human GC cell lines (MKN45, MKN28, HGC27, MGC803, N87, AGS and SGC7901) and the immortalized gastric mucosa cell line (GES-1) were provided by the Cell Center of the Chinese Academy of Medical Sciences. All cell lines were cultured in RPMI-1640 medium supplemented with

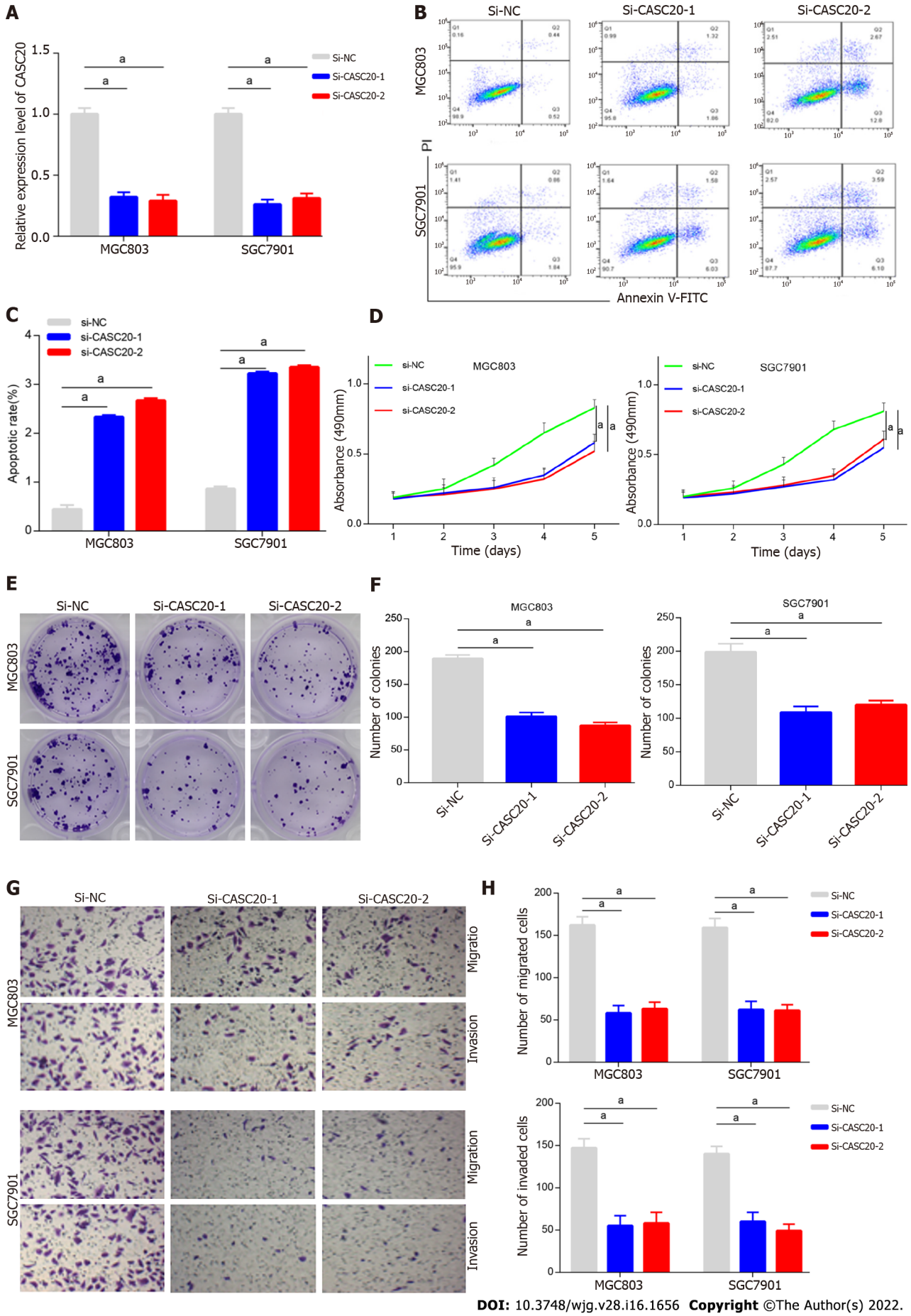

DOI: 10.3748/wjg.v28.i16.1656 **Copyright** ©The Author(s) 2022.

Figure 2 Konckdown of cancer susceptibility 20 inhibits the apoptosis, proliferation and metastasis of gastric cancer cells. A: Efficacy assessment of cancer susceptibility 20 (CASC20) silence through quantitative real-time polymerase chain reaction method in MGC803 and SGC7901 cells; B and C: Cell apoptosis evaluation in transfected cells through flow cytometry; D: Cell viability was verified by CCK-8 experiments after transfection with si-CASC20; E and F: Colony formation assay was used to detect the cell proliferation ability after transfection with si-CASC20; G and H: Transwell assay was employed for examining the effect of CASC20 low-expression on gastric cancer cell migration and invasion. $^{a}P < 0.05$ *vs* control.

10% fetal bovine serum (FBS, Gibco, United States). Cells were cultured in incubator at 37 °C and 5% CO_2. Cells were passaged when they were 70% confluent.

The miR-143-5p mimics and inhibitor were purchased from RiboBio (Guangzhou, China). siRNAs targeting CASC20 (si-CASC20) and MEMO1 (si-MEMO1) were designed and synthesized by RiboBio (Guangzhou, China). Lipofectamine2000 (Invitrogen, United States) was used to transfect siRNA or miRNA mimics/inhibitor into cells following the manufacturer's instructions. GC cells in logarithmic phase were collected and inoculated in a 6-well plate. Cells were transfected with siRNAs when cell confluence reached approximately 50%.

RNA extraction and quantitative real-time polymerase chain reaction

Trizol reagent (Invitrogen, United States) was used to extract total RNA from GC tissues and cells. RNA integrity was determined by evaluating the absorbance at $OD_{260}/280$ using a NanoDrop analyzer and confirmed at 1.8–2.0. Total RNA was reverse transcribed into cDNA using a reverse transcription kit (Takara, Dalian, China) in accordance with the manufacturer's instructions. The quantitative real-time polymerase chain reaction (qRT-PCR) three-step method was used, and the $2^{-\Delta\Delta Ct}$ method was used to calculate the relative expression levels of CASC20 and miR-143-5p. The primer sequences are as follows: CASC20, Forward 5′-ATAACCACCCTCCCCTCCTC-3′, Reverse 5′-GCTCCTCCCACTTTAACCCC-3′; miR-143-5p, Forward 5′-ATGGTTCGTGGGGTCCAGTTTTCCCAG-3′, Reverse 5′-GTGTCGTG-GAGTCGGCAATTC-3′; MEMO1, Forward, 5′-GCTTCGGCAGCACATATACTAAAAT-3′, Reverse 5'-CGCTTCACGAATTTGCGTGTCAT-3′; and β-actin, Forward 5′-TGGCACCCAGCACAATGAA-3′, Reverse 5′-CTAAGTCATAGTCCGCCTAGAAGCA-3′. U6, Forward 5′-CAGCACATATACTAAAAT-TGGAACG-3′ Reverse 5′-ACGAATTTGCGTGTCATCC-3′. β-actin (cytoplasm control) and U6 (nucleus control) were used for normalization.

CCK-8 assay

GC cells were inoculated into 96-well plate at 5×10^3 cells *per* well. At 24 h, 48 h, 72 h, 96 h and 120 h after transfection, 90 μL of fresh culture medium containing 10% FBS and 10 μL of CCK-8 reagent (Dojindo, Mashikimachi, Japan) were simultaneously added to each well. Cells were cultured for another 4 h. The OD value of each well at 450 nm was measured and proliferation curves were drawn.

Flow cytometric analysis

GC cells were collected after trypsin digestion and centrifuged at 1000 rpm/min for 5 min. The cells were washed twice with phosphate buffer solution, and 500 μL binding buffer was added to adjust the cell concentration to 1×10^6 cells/mL. Annexin V-FITC (5 μL) and propidium iodide solution (10 μL) (NeoBioscience, China) were added to the cell suspension, and cells were analyzed on a flow cytometer (BD Accuri C6).

Colony formation assay

After 48 h of transfection, cells were collected and the cell density was adjusted to 1×10^5 cells/mL. The cell suspension was inoculated into a 6-well plate at 100 μL/well and the plates were incubated for 14 d. Cells were washed twice with phosphate buffered saline and fixed with 4% paraformaldehyde for 15 min; the cells were then stained with 0.1% crystal violet staining solution for 10 min. We counted the number of cell clones in five fields under the microscope and determined the clone formation rate as follows: Clone formation rate (%) = (number of clones/number of inoculated cells) × 100%. The experiment was repeated three times.

Wound healing assay

GC cells were cultured in a 6-well plate at 5×10^5 cells *per* well. Linear scratch wounds were created in the cell monolayer with a sterile 100 μL pipette tip. Cells were cultured for 24 h, and the wound widths were photographed and measured.

Transwell experiment

Assays using a Transwell chamber (8 μm, Corning, United States) were used to evaluate cell migration and invasion abilities. GC cells were collected and resuspended in serum-free RPMI 1640 medium at 1.5×10^4 cells/mL, and 200 μL of the cell suspension was inoculated into the upper chambers. Complete medium containing 10% FBS was added to the lower chamber. After culturing for 24 h, the cells were fixed with methanol. Cells in the upper chamber were removed with cotton swabs, and cells in the

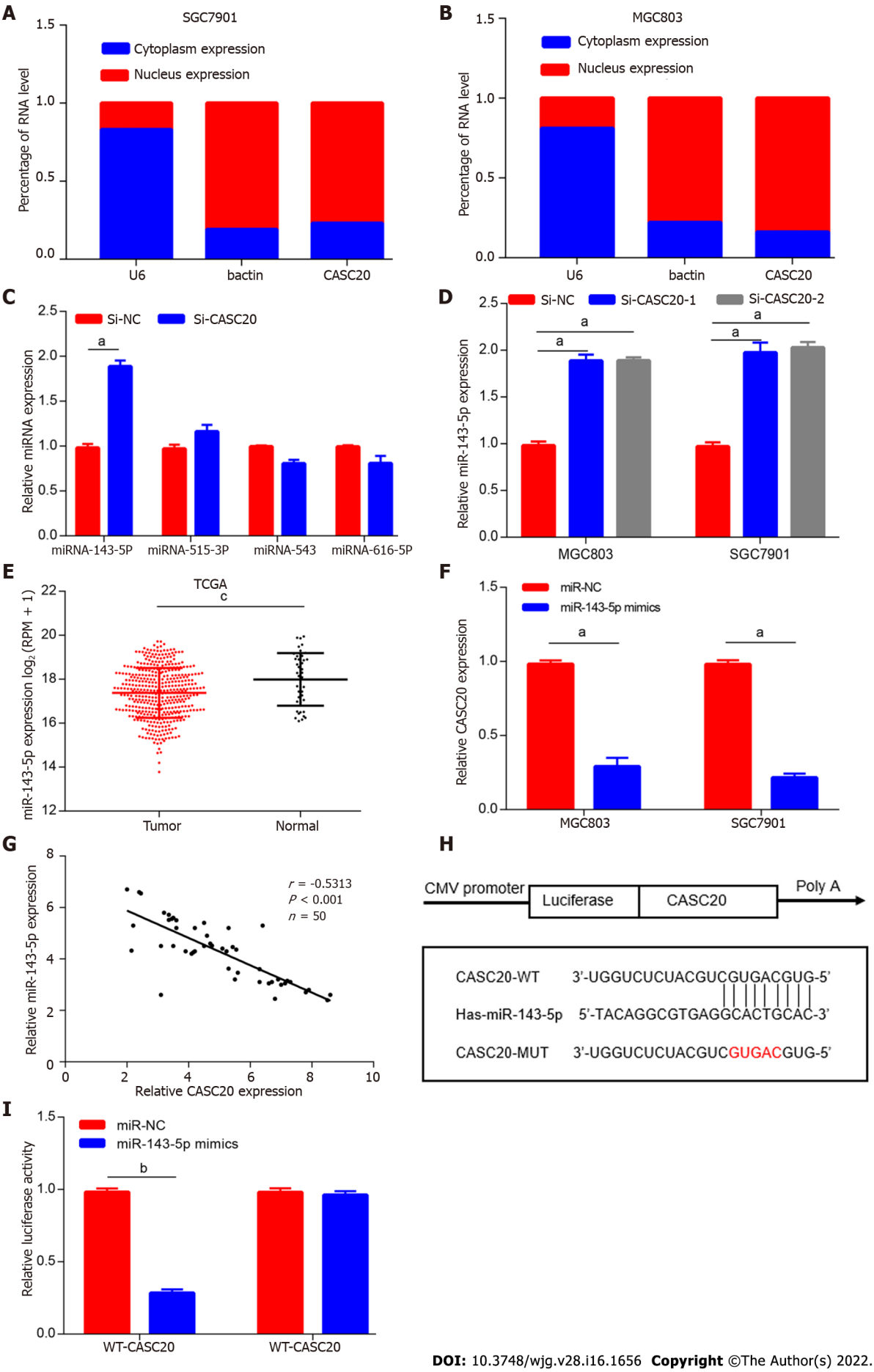

DOI: 10.3748/wjg.v28.i16.1656 **Copyright** ©The Author(s) 2022.

Figure 3 miR-143-5p served as a target of cancer susceptibility 20 in gastric cancer cells. A and B: Relative cancer susceptibility 20 (CASC20) expression levels in nucleus and cytoplasm of SGC7901 and MGC803 cells; C: The relative expressions of miRNAs in gastric cancer (GC) cells after downregulation of CASC20; D: The expression of miR-143-5p was detected by quantitative real-time polymerase chain reaction in GC cells after transfection with si-CASC20; E: The expression levels of miR-143-5p in GC from TCGA database; F: The detection of CASC20 expression after transfection of miR-143-5p mimics; G: The correlation analysis between miR-143-5p expression and CASC20 expression in 50 GC tissues; H: Bioinformatics presentation of CASC20 and miR-143-5p binding sites; I: The verification of CASC20 and miR-143-5p interaction by luciferase report assay. $^{a}P < 0.05$, $^{b}P < 0.01$ and $^{c}P < 0.001$ *vs* control.

lower chambers were stained with 0.1% crystal violet solution for 30 min. The cells were observed under a microscope and photographed; five random fields were obtained to count the number of migrated cells. Each experimental group was performed in triplicate, and the average value was taken. For the invasion experiment, the upper chamber was coated with Matrigel; the assay was then conducted following the methods for the migration assay.

Bioinformatics analysis

The online tool lncRNASNP2 was used to predict miRNAs that potentially bind to CASC20. We used miRDB, Targetscan, and miRTarbase to predict putative target genes of miR-143-5p.

Dual-luciferase reporter assay

Luciferase reporter pGL3 vectors with wild-type CASC20 (termed WT-CASC20), wild-type MEMO1 (MEMO1-WT), mutant CASC20 (MUT-CASC20) and mutant MEMO1 (MEMO1-MUT) were constructed (Promega, Madison, United States). The reporter plasmids were transfected into MGC803 cells along with miR-143-5p mimics. At 48 h after transfection, the luciferase activity was measured using the Dual Luciferase Reporter Assay system (Promega, United States) in accordance with the manufacturer's instructions.

Western blot analysis

Cells were collected and lysed with RIPA lysis buffer (Beyotime, Shanghai, China). After lysates were centrifuged, the supernatant was collected and protein concentration was evaluated by the BCA method. The samples (60 μg/well) were separated by 10% sodium dodecyl sulfate polyacrylamide gel electrophoresis and electro-transferred to a polyvinylidene difluoride membrane (Millipore, Billerica, MA, United States). After blocking in 5% skim milk at room temperature for 2 h, the membrane was incubated with primary antibody overnight at 4 °C. The membrane was then washed three times with Tris buffered saline tween and incubated with the secondary antibody at room temperature for 2 h. ECL luminescent solution was used for chemiluminescence and Image J software was used to analyze the protein expression level. MEMO1 and β-actin monoclonal antibodies were obtained from Sigma-Aldrich (St Louis, MO, United States). The other antibodies were purchased from Abcam (Cambridge, England).

Statistical analysis

Statistical analyses were performed using GraphPad Prism (version 7.0; GraphPad Prism software, San Diego, CA, United States). Data are shown as mean ± SD. For measurement data, the difference between two or more groups was calculated using the Student's t-test or one-way ANOVA analysis. Chi-square test was used to analyze the correlation between CASC20 and clinicopathological parameters of GC patients. The survival curve was determined by the Kaplan–Meier method and log-rank test. $P < 0.05$ was considered statistically significant.

RESULTS

LncRNA CASC20 is highly expressed in GC tissues and cells

Analysis of TCGA database revealed that CASC20 expression was significantly higher in 408 GC tumor tissues than that in 211 normal gastric tissues ($P < 0.01$, Figure 1A and B). We performed qRT-PCR to assess the expression of CASC20 in 50 cases of GC tissues and paired normal gastric mucosa tissues adjacent to tumors. The results showed that the expression of CASC20 in GC tissues was significantly higher than that in normal adjacent gastric mucosa tissues ($P < 0.01$, Figure 1C). We further found that the expression of CASC20 in seven GC cell lines was significantly higher than that of GES-1 normal gastric mucosal epithelial cells (Figure 1D). We next analyzed the relationship between CASC20 expression and the survival rate of GC patients in TCGA database. The results indicated that the survival rate of GC patients with high expression of CASC20 was significantly lower than that of patients with low expression (Figure 1E). Together these data indicate that CASC20 is highly expressed in GC and may play an important role in the development of GC.

Next, we examined the correlation between CASC20 expression and the pathological characteristics of 50 GC patients. GC patients were divided into high and low CASC20 expression groups based on the

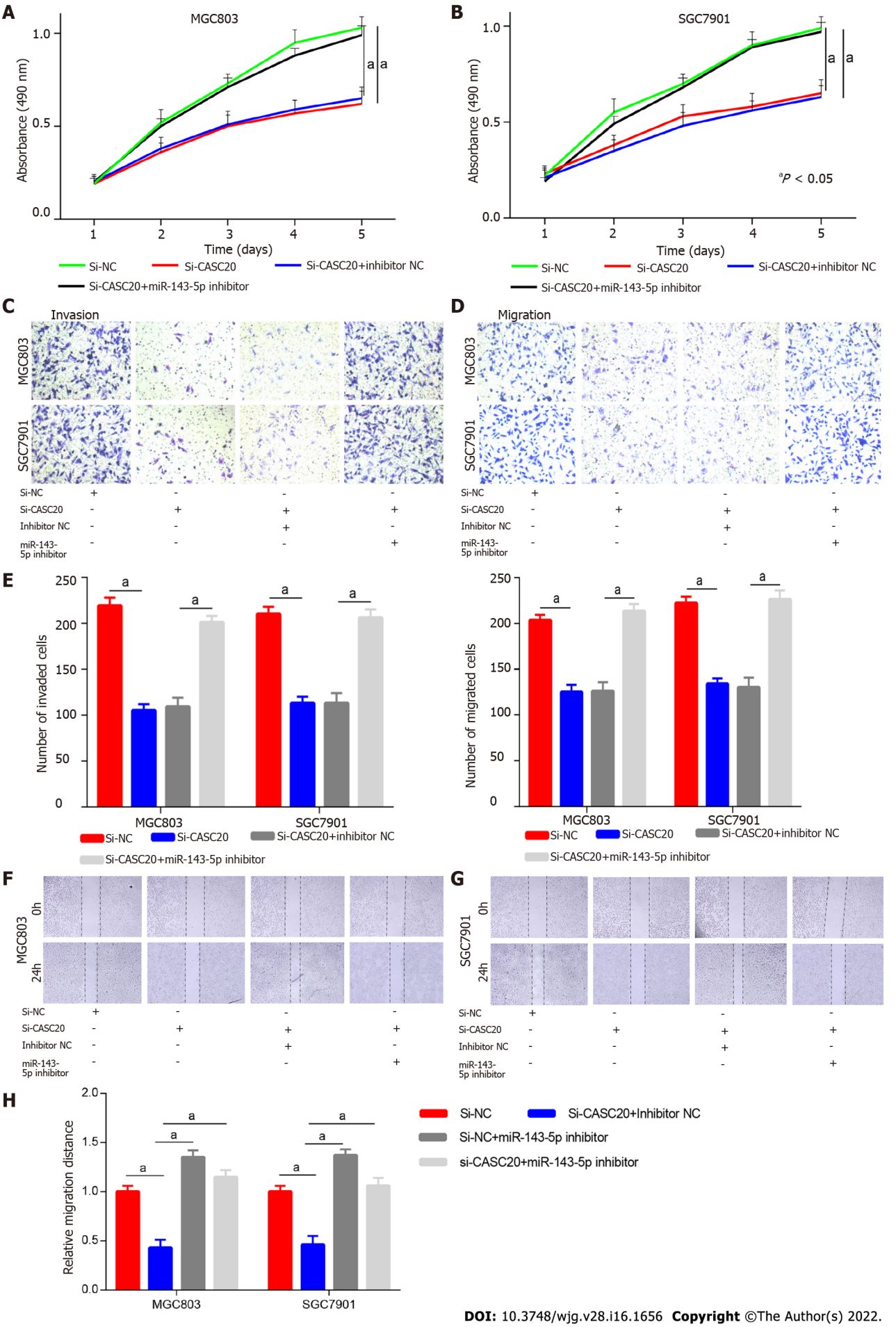

DOI: 10.3748/wjg.v28.i16.1656 **Copyright** ©The Author(s) 2022.

Figure 4 The regulation of cancer susceptibility 20 on gastric cancer cells is mediated by miR-143-5p. A and B: Gastric cancer (GC) cells were treated with si-NC, si-cancer susceptibility 20 (CASC20), si-CASC20 + inhibitor NC, si-CASC20 + miR-143-5p inhibitor, CCK-8 assays evaluated the proliferation; C-E: Transwell assays tested invasion and migration abilities of transfected cells; F-H: GC cells were treated with si-NC, si-CASC20 + inhibitor NC, si-NC + miR-143-5p inhibitor, si-CASC20 + miR-143-5p inhibitor, wound healing assay was used to detect migration ability. $^{a}P < 0.05$ *vs* control.

median ratio of relative CASC20 expression. High CASC20 expression in GC patients was significantly correlated with a higher risk of lymphatic metastasis ($P = 0.011$), but did not show associations with age, gender, TNM stage and differentiation degree (Table 1). These results suggest that CASC20 is closely related to the malignant biological behavior of GC.

Knockdown of CASC20 inhibits GC cell proliferation, invasion and metastasis and induces apoptosis

We next evaluated the role and effects of CASC20 in GC cells. We transfected siRNA targeting CASC20 into GC cells and qRT-PCR confirmed that the expression of CASC20 was significantly down-regulated after siRNA transfection (Figure 2A). Flow cytometry results showed that knockdown of CASC20 significantly increased the apoptosis rate of SGC7901 and MGC803 GC cells compared with the control cells (Figure 2B and C). CCK8 assays demonstrated that knockdown of CASC20 significantly inhibited the proliferation of SGC7901 and MGC803 cells (Figure 2D). Colony formation experiments revealed that inhibiting CASC20 expression resulted in decreased clonogenic survival (Figure 2E and F). Transwell experiments showed that knocking down CASC20 significantly reduced the numbers of invading and migrating GC cells (Figure 2G and H). Together, these findings show that knockdown of CASC20 inhibits the malignant phenotype of GC cells, suggesting that CASC20 exhibits oncogenic functions in GC.

CASC20 adsorbs miR-143-5p in GC cells

To gain better insights into the function of CASC20, we first determined the subcellular location of CASC20 by GeneCards software (https://www.genecards.org). The results showed that CASC20 is mainly located in the cytoplasm. The results of nuclear cytoplasmic experiments further confirmed that CASC20 mostly localizes in the cytoplasm (Figure 3A and B), suggesting that CASC20 may function as a ceRNA to "sponge" miRNA.

We next used bioinformatics tools (lncRNASNP2) to predict miRNAs with potential binding sites for CASC20 and the results identified miR-143-5p, miR-515-3p, miR-543 and miR-616-5p. We evaluated the expressions of these miRNAs in cells transfected with si-CASC20 and found that the expression of miR-143-5p was up-regulated when CASC20 was knocked down, while miR-515-3p, miR-543 and miR-616-5p showed no significant changes (Figure 3C and D). We thus selected miR-143-5p for further analyses.

TCGA database analysis showed that miR-143-5p was expressed at low levels in GC tissues (Figure 3E), which was consistent with previous studies on miR-143-5p[15]. We transfected miR-143-5p mimics into GC cells and observed significantly decreased expression of CASC20 (Figure 3F). In addition, we identified a negative correlation between CASC20 and miR-143-5p in 50 GC tissues (Figure 3G).

To further determine the regulatory mechanism between CASC20 and miR-143-5p, we performed dual luciferase reporter assays. The results showed that transfection of miR-143-5p mimics decreased the luciferase activity of the WT-CASC20 reporter in MGC803 cells, while miR-143-5p mimics had no impact on the MUT-CASC20 reporter activity (Figure 3H and I). This result suggests that the regulatory relationship of CASC20 and miR-143-5p in GC cells involves interactions between CASC20 and miR-143-5p.

CASC20 inhibits miR-143-5p to regulate the malignant phenotype of GC cells

To determine whether miR-143-5p played a role in the effects of CASC20 in GC cells, we co-transfected si-CASC20 and miR-143-5p inhibitor into SGC7901 and MGC803 cells. CCK8 assays showed that si-CASC20 transfection inhibited GC cell proliferation, and co-transfection of miR-143-5p inhibitor restored proliferation (Figure 4A and B). Transwell experiments showed while transfection of si-CASC20 inhibited the invasion and migration of GC cells, co-transfection of miR-143-5p inhibitor restored the invasion and migration abilities (Figure 4C–E). Wound healing assays also confirmed that co-transfection of miR-143-5p inhibitor partly rescued the inhibitory effect of knockdown of CASC20 on GC cells (Figure 4F–H). These results indicate that CASC20 regulates GC cell activities through miR-143-5p.

MEMO1 mRNA is a target of miR-143-5p, and miR-143-5p regulates MEMO1 mRNA expression

To further explore the role of miR-143-5p in GC, we screened and identified the potential target mRNAs of miR-143-5p. Bioinformatics tools miRDB, Targetscan and miRTarbase predicted several mRNAs (HDAC7, ZNF85, ZNF347, MEMO1, ESCO1, MLXIP, MAP3K2 and DYRK1A mRNAs) that potentially interact with miR-143-5p (Figure 5A). Among them, MEMO1 was selected as the target gene of miR-143-5p because it had the highest score in the prediction analysis.

Table 1 The correlation between cancer susceptibility 20 expression and the clinicopathological factors of 50 gastric patients

Characteristics	Number of cases	CASC20 expression		*P* value
		High (*n* = 26)	Low (*n* = 24)	
Gender				0.382
Male	23	14	9	
Female	27	12	15	
Age				0.546
≤ 55	22	13	9	
> 55	28	13	15	
TNM stage				0.262
I + II	24	10	14	
III	26	16	10	
Lymphatic metastasis				0.011[a]
Positive	25	18	7	
Negative	25	8	17	
Differentiation				0.073
Moderate/well	30	12	18	
Poor	20	14	6	

[a]*P* < 0.05 was considered significant. CASC20: Cancer susceptibility 20.

TCGA database analysis showed that MEMO1 was highly expressed in GC tissues (Figure 5B). In addition, the mRNA expression of MEMO1 was significantly increased in 50 GC tissues compared with its expression in adjacent tissues (Figure 5C).

We next designed luciferase reporter vectors containing the wild-type 3′UTR of MEMO1 mRNA or the 3′UTR with mutated binding sites (Figure 5D). Dual luciferase reporter assay showed that miR-143-5p significantly reduced the luciferase activity of the reporter vector with the wild-type 3′UTR of MEMO1 mRNA but had no effects on the mutated reporter (Figure 5E), suggesting that MEMO1 mRNA may be a target gene of miR-143-5p. We then transfected miR-143-5p mimics into MGC803 cells and found that the expression of MEMO1 was significantly reduced at both gene and protein levels (Figure 5F). These data indicate that miR-143-5p regulates MEMO1 mRNA expression.

We also found that the expression of CASC20 was positively correlated to MEMO1 expression in GC tissues (Figure 5G). In cells with CASC20 knockdown, MEMO1 expression was downregulated, suggesting a positive regulatory relationship between CASC20 and MEMO1 (Figure 5H).

To explore the role of MEMO1 in GC, we transfected siRNA targeting MEMO1 into GC cells. Scratch experiments and Transwell experiments revealed that knockdown of MEMO1 inhibited the invasion and migration of GC cells. The migration and invasion abilities were partially rescued by co-transfection with miR-143-5p inhibitor (Figure 6A–G), indicating that miR-143-5p inhibition reversed the effects of MEMO1 knockdown.

CASC20 regulates EMT through miR-143-5p/MEMO1 to promote the invasion and migration of GC cells

To investigate whether CASC20 regulates MEMO1 through miR-143-5p, we transfected si-CASC20 and miR-143-5p inhibitor into MGC803 cells. Western blot results indicated that MEMO1 expression decreased in GC cells after transfection with si-CASC20, while MEMO1 expression was restored after co-transfection with si-CASC20 and miR-143-5p inhibitor (Figure 6H).

We next evaluated the effects of CASC20 on EMT. In MGC803 cells with CASC20 knockdown, the expression level of the epithelial protein marker E-cadherin was up-regulated, while the expression levels of the mesenchymal protein markers Vimentin and ZEB1 were down-regulated. After transfection with miR-143-5p inhibitor, the expressions of MEMO1, Vimentin and ZEB1 were up-regulated, and the expression of E-cadherin was down-regulated (Figure 6H and I).

Together these results indicated that CASC20 may sequester miR-143-5p to increase the MEMO1 expression, leading to the induction of EMT and metastasis of GC.

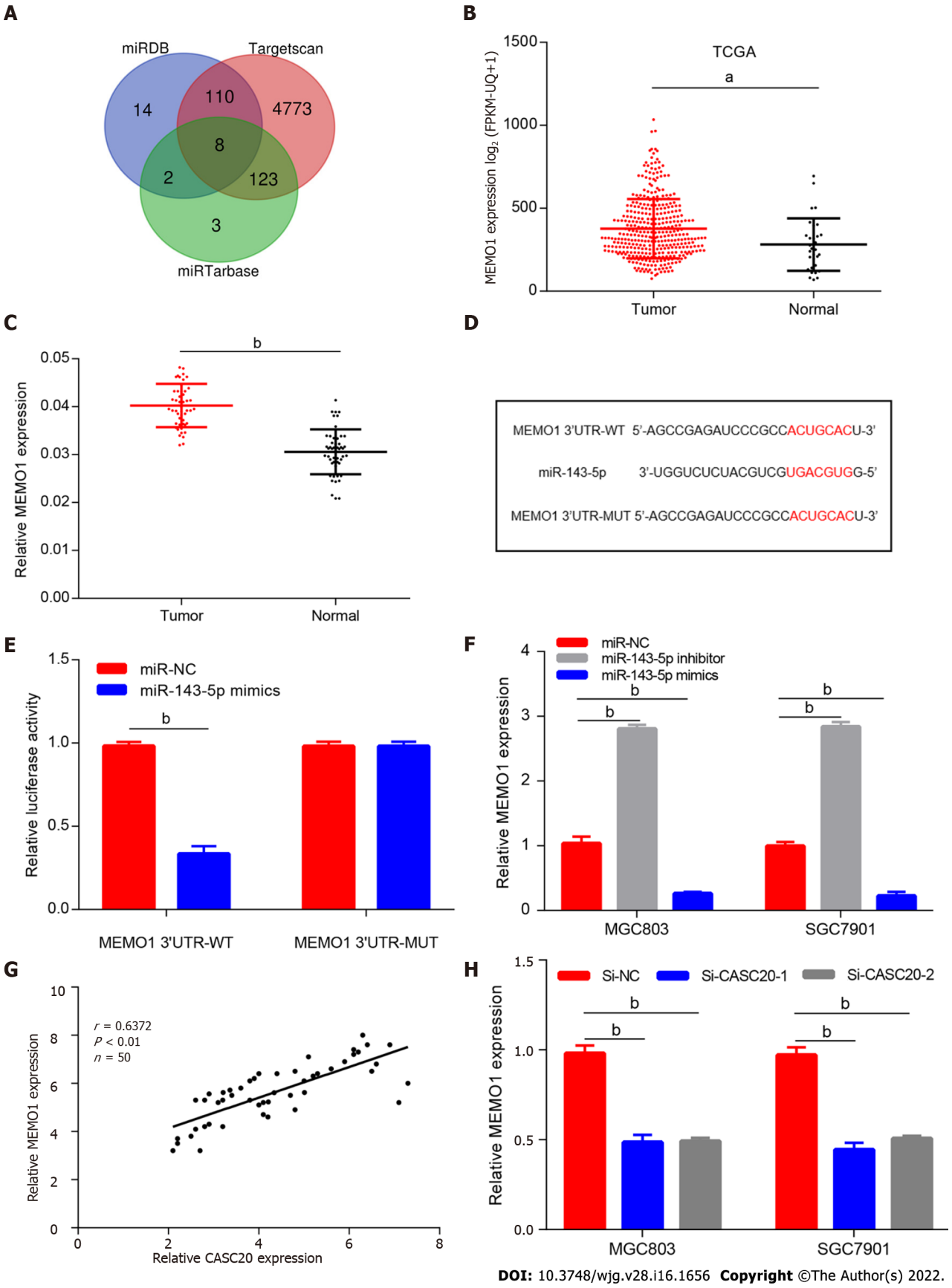

DOI: 10.3748/wjg.v28.i16.1656 **Copyright** ©The Author(s) 2022.

Figure 5 Cancer susceptibility 20 regulates the miR-143-5p target MEMO1. A: Bioinformatic tools were used to predict the potential target mRNA of miR-143-5p; B: The expression levels of MEMO1 in gastric cancer (GC) from TCGA STAD database; C: MEMO1 expression in 50 pairs of gastric cancer tissues and normal tissue samples; D: Putative miR-143-5p binding sequence and mutation sequence of MEMO1 mRNA were as shown; E: Dual luciferase reporter assays were used to confirm the direct target between miR-143-5p and MEMO1; F: MEMO1 expression was decreased in GC cells transfected by miR-143-5p mimics; G: The correlation analysis between cancer susceptibility 20 (CASC20) and MEMO1 expression in 50 GC tissues; H: MEMO1 expression was decreased after knockdown of

CASC20. [a]*P* < 0.05, [b]*P* < 0.01 *vs* control.

DISCUSSION

Mounting evidence confirmed that lncRNAs play extensive regulatory roles in the initiation and progression of human cancers. A complex ceRNA crosstalk mechanism has been identified in GC[16]. However, only a small fraction of lncRNAs has been thoroughly studied, with no research on CASC20 in tumors. We analyzed the TCGA GC database and found that CASC20 is highly expressed in GC and associated with poor prognosis of GC patients. Functional experiments revealed that knock down of CASC20 significantly inhibited the proliferation, invasion, and migration of GC cells. These findings indicate a potential oncogenic function of CASC20 in GC.

miRNAs are 18–24 nt in length and negatively regulate gene expression by interacting with mRNA, thereby playing important physiological functions in several cellular processes. In tumors, the combination of miRNA and the 3'UTR of the target gene can function as an oncogene or tumor suppressor gene by regulating its expression[17,18]. miRNAs may thus become potential therapeutic targets for cancer metastasis, and the application of miRNA mimics and their antagonists for therapeutic purposes is expanding[19].

Our study showed that CASC20 was mainly distributed in the cytoplasm in GC cells, which suggested that CASC20 may function as a ceRNA for sponging miRNA. LncRNASNP2 was used to predict miRNAs that potentially bind CASC20, and our *in vitro* experiments indicated that CASC20 acts as a molecular sponge for miR-143-5p.

miR-143-5p is located in the human 5q32 chromosome region. Wu *et al*[15] found that miR-143-5p is expressed at low levels in GC and functions as tumor suppressor gene by targeting COX-2[15]. The lncRNA ZEB2-AS is highly expressed in GC tissues and cell lines, and ZEB2-AS was shown to promote the proliferation and metastasis of GC cells through the miR-143-5p/HIF-1α pathway[20]. These studies have shown that miR-143-5p is expressed at low levels in GC and exhibits tumor suppressor functions. Our qRT-PCR results showed that miR-143-5p was markedly down-regulated in GC tissues, and its expression level was negatively correlated with CASC20. Downregulation of miR-143-5p partially reversed the effects of CASC20 knockdown on the proliferation, invasion and migration of GC cells.

Bioinformatics analysis predicted that miR-143-5p interacts with the 3′UTR of MEMO1 (mediator of ErbB2-driven cell motility 1), a key mediator of receptor tyrosine kinase activation. MEMO1 plays an important role in breast cancer cell invasion and migration by activating the PI3K/Akt signaling pathway, leading to up-regulated Snail1 and induction of the EMT program[21]. MEMO1 is highly expressed in colon cancer tissues and cells, and miR-219a-1 regulates the proliferation, invasion and metastasis of colon cancer cells by targeting MEMO1, thereby functioning as a tumor suppressor gene [22]. The role of MEMO1 in the progression of GC has not yet been reported. In this study, we found that MEMO1 is highly expressed in GC in TCGA GC database and clinical samples. Overexpression of miR-143-5p reduced the expression of MEMO1 at the gene and protein level. Dual luciferase reporter assay was performed to reveal the regulatory relationship between miR-143-5p and MEMO1. Reduced migration and migration abilities of GC cells caused by MEMO1 knockdown were reversed by miR-143-5p inhibitor. EMT is a prerequisite for distant metastasis of malignant tumor cells, and many studies reported roles for lncRNAs in the tumor EMT process[23]. Our western blot results showed that CASC20 expression resulted in decreased expression of the epithelial cell marker E-cadherin and increased expression of the mesenchymal cell marker Vimentin. Together, our results indicate that CASC20 functions as ceRNA to sponge miR-143-5p, leading to up-regulated MEMO1 expression and initiation of the EMT process in GC.

This study has several limitations. Only 50 GC tissues were collected and analyzed in this study. The small clinical sample size may be one of the reasons why CASC20 expression was only related to lymph node metastasis, but showed no significant association with tumor size and clinical stage. In addition, *in vivo* experiments are required to further establish the biological function of CASC20 in GC.

CONCLUSION

In summary, this study identified the lncRNA CASC20/miR-143-5p/MEMO1 axis in GC and provided insights into the mechanistic relationships among CASC20, miR-143-5p and MEMO. These findings enrich the molecular regulatory network driving the occurrence and development of GC and deepen our understanding of the function and mechanism of CASC20 in cancer. Our results suggest that CASC20 may be a potential therapeutic target and clinical prognostic marker for GC.

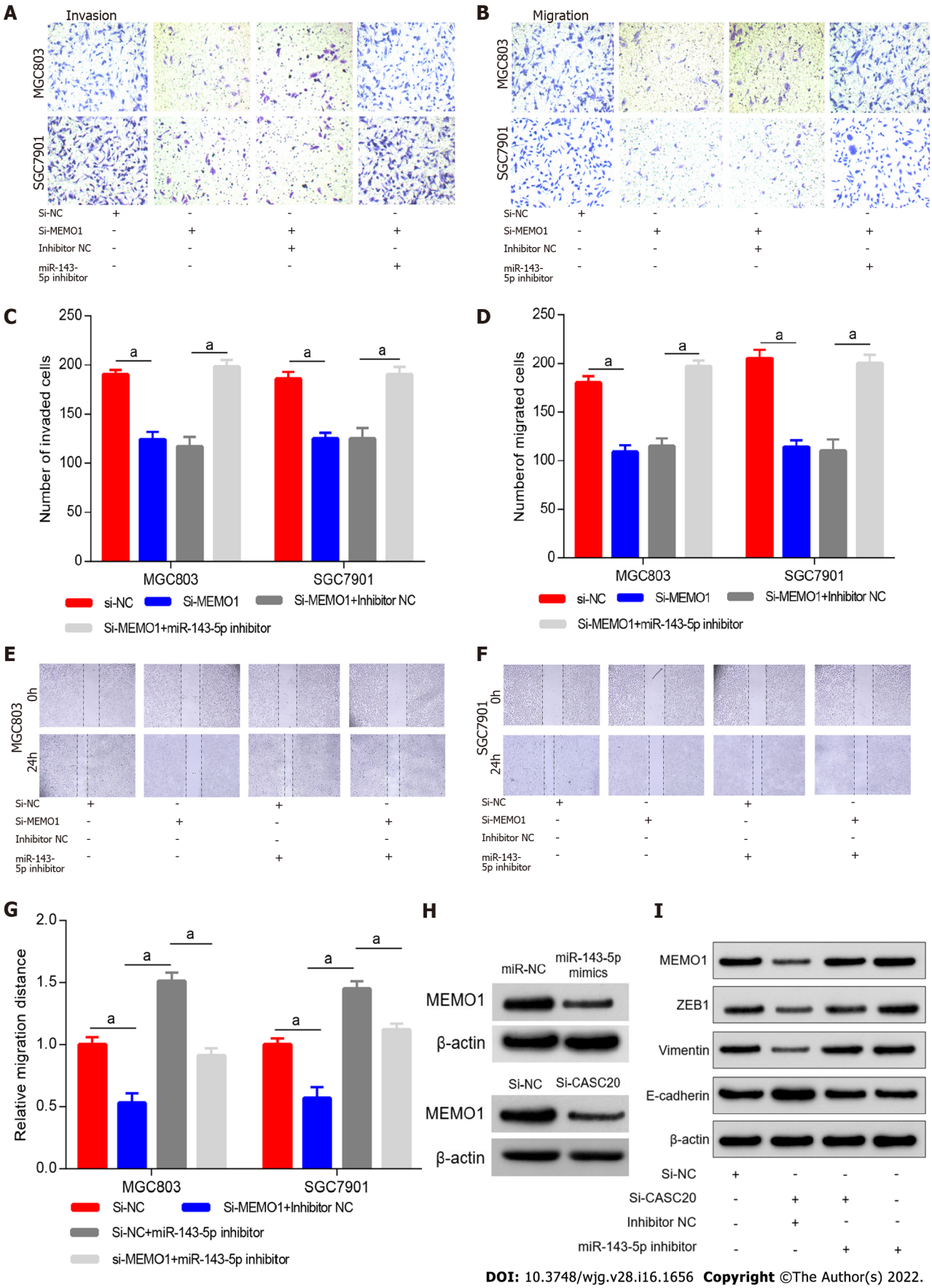

DOI: 10.3748/wjg.v28.i16.1656 **Copyright** ©The Author(s) 2022.

Figure 6 Inhibition of miR-143-5p blocked the function of MEMO1 knockdown in gastric cancer cells. A-D: MGC803 and SGC7901 cells were transfected with si-NC, si-MEMO1, si-MEMO1 + inhibitor NC, si-MEMO1 + miR-143-5p inhibitor, respectively. Transwell assay was employed for the detection of cell invasion and migration ability; E-G: MGC803 and SGC7901 cells were transfected with si-NC, si-MEMO1 + inhibitor NC, si-NC + miR-143-5p inhibitor, si-MEMO1 +

miR-143-5p inhibitor, respectively. Wound healing assay was used to detect migration ability; H: The protein expression of MEMO1 was detected by western blot assay after transfecting with miR-143-5p mimics or si-cancer susceptibility 20; I: Western blot was utilized to detect the expressions of EMT-related proteins (ZEB1, Vimentin and E-cadherin). $^{a}P < 0.05$ *vs* control.

ARTICLE HIGHLIGHTS

Research background

LncRNAs have been indicated to play critical roles in gastric cancer (GC) tumorigenesis and progression. However, their roles in GC remain to be further elucidated.

Research motivation

To discover promising diagnostic and therapeutic targets for GC.

Research objectives

To investigate the underlying mechanisms of the lncRNA cancer susceptibility 20 (CASC20) in GC.

Research methods

The expression of CASC20, miR-143-5p and MEMO1 genes were detected by quantitative real-time polymerase chain reaction. The oncogenic functions of CASC20 was investigated by experiments including cell counting kit-8, colony formation, wound-healing and Transwell assays in GC cells in vitro. Bioinformatics and dual-luciferase report assay were performed for determining the regulatory relationship of lncRNA-miRNA-mRNA.

Research results

We found that the expression of lncRNA CASC20 was significantly upregulated in GC tissues and cell lines, and increased expression of CASC20 was positively correlated with lymph node metastasis in patients with GC. Additionally, knockdown of CASC20 could inhibit GC cells growth, migration and invasion, whereas its overexpression could reverse these effects. Mechanistically, CASC20 specifically inhibited miR-143-5p expression, thus up-regulating MEMO1 expression.

Research conclusions

CASC20 promotes GC cell metastasis *via* adsorbing miR-143-5p and up-regulating MEMO1, it plays an important oncogenic function in GC.

Research perspectives

This study identified the lncRNA CASC20/miR-143-5p/MEMO1 axis in GC and provided insights into the mechanistic relationships among CASC20, miR-143-5p and MEMO. The results of our research suggest that CASC20 may act as a promising diagnostic marker for GC.

FOOTNOTES

Author contributions: Shan KS and Li WW contributed equally to this work; Tian SB and Shan KS designed the study; Shan KS, Li WW and Ren W performed all experiments; Kong S and Peng LP collected tissue samples and the clinical data; Shan KS and Li WW analyzed and interpreted the data; Tian SB and Zhuo HQ drafted the manuscript; all authors read and approved the final manuscript.

Supported by Shandong Province Medicine and Health Science and Technology Development Plan Project, No. 2019WS477.

Institutional review board statement: The study was reviewed and approved by the Shandong Provincial Hospital Institutional Review Board, No. SZRJJ: NO. 2020.

Conflict-of-interest statement: The authors declare no conflict of interest.

Data sharing statement: No additional data are available.

Open-Access: This article is an open-access article that was selected by an in-house editor and fully peer-reviewed by external reviewers. It is distributed in accordance with the Creative Commons Attribution NonCommercial (CC BY-NC 4.0) license, which permits others to distribute, remix, adapt, build upon this work non-commercially, and license their derivative works on different terms, provided the original work is properly cited and the use is non-commercial. See: https://creativecommons.org/Licenses/by-nc/4.0/

Country/Territory of origin: China

ORCID number: Ke-Shu Shan 0000-0001-5907-2189; Wei-Wei Li 0000-0003-3201-6739; Wang Ren 0000-0001-6607-7519; Shuai Kong 0000-0003-3751-6679; Li-Pan Peng 0000-0003-1221-3524; Hong-Qing Zhuo 0000-0003-0829-5563; Shu-Bo Tian 0000-0001-6022-6288.

S-Editor: Fan JR
L-Editor: A
P-Editor: Yu HG

REFERENCES

1 **Sung H**, Ferlay J, Siegel RL, Laversanne M, Soerjomataram I, Jemal A, Bray F. Global Cancer Statistics 2020: GLOBOCAN Estimates of Incidence and Mortality Worldwide for 36 Cancers in 185 Countries. *CA Cancer J Clin* 2021; **71**: 209-249 [PMID: 33538338 DOI: 10.3322/caac.21660]
2 **Xie Y**, Shi L, He X, Luo Y. Gastrointestinal cancers in China, the USA, and Europe. *Gastroenterol Rep (Oxf)* 2021; **9**: 91-104 [PMID: 34026216 DOI: 10.1093/gastro/goab010]
3 **Hanahan D**, Weinberg RA. Hallmarks of cancer: the next generation. *Cell* 2011; **144**: 646-674 [PMID: 21376230 DOI: 10.1016/j.cell.2011.02.013]
4 **Yu H**, Rong L. Emerging role of long non-coding RNA in the development of gastric cancer. *World J Gastrointest Oncol* 2018; **10**: 260-270 [PMID: 30254721 DOI: 10.4251/wjgo.v10.i9.260]
5 **McDonel P**, Guttman M. Approaches for Understanding the Mechanisms of Long Noncoding RNA Regulation of Gene Expression. *Cold Spring Harb Perspect Biol* 2019; **11** [PMID: 31791999 DOI: 10.1101/cshperspect.a032151]
6 **Chi Y**, Wang D, Wang J, Yu W, Yang J. Long Non-Coding RNA in the Pathogenesis of Cancers. *Cells* 2019; **8** [PMID: 31480503 DOI: 10.3390/cells8091015]
7 **Huang Y**, Guo Q, Ding XP, Wang X. Mechanism of long noncoding RNAs as transcriptional regulators in cancer. *RNA Biol* 2020; **17**: 1680-1692 [PMID: 31888402 DOI: 10.1080/15476286.2019.1710405]
8 **Salmena L**, Poliseno L, Tay Y, Kats L, Pandolfi PP. A ceRNA hypothesis: the Rosetta Stone of a hidden RNA language? *Cell* 2011; **146**: 353-358 [PMID: 21802130 DOI: 10.1016/j.cell.2011.07.014]
9 **Zhuo S**, Sun M, Bai R, Lu D, Di S, Ma T, Zou Z, Li H, Zhang Z. Long intergenic non-coding RNA 00473 promotes proliferation and migration of gastric cancer *via* the miR-16-5p/CCND2 axis and by regulating AQP3. *Cell Death Dis* 2021; **12**: 496 [PMID: 33993193 DOI: 10.1038/s41419-021-03775-9]
10 **Landeros N**, Santoro PM, Carrasco-Avino G, Corvalan AH. Competing Endogenous RNA Networks in the Epithelial to Mesenchymal Transition in Diffuse-Type of Gastric Cancer. *Cancers (Basel)* 2020; **12** [PMID: 32987716 DOI: 10.3390/cancers12102741]
11 **Hanly DJ**, Esteller M, Berdasco M. Interplay between long non-coding RNAs and epigenetic machinery: emerging targets in cancer? *Philos Trans R Soc Lond B Biol Sci* 2018; **373** [PMID: 29685978 DOI: 10.1098/rstb.2017.0074]
12 **Wang XD**, Lu J, Lin YS, Gao C, Qi F. Functional role of long non-coding RNA CASC19/miR-140-5p/CEMIP axis in colorectal cancer progression *in vitro*. *World J Gastroenterol* 2019; **25**: 1697-1714 [PMID: 31011255 DOI: 10.3748/wjg.v25.i14.1697]
13 **Zhang E**, He X, Zhang C, Su J, Lu X, Si X, Chen J, Yin D, Han L, De W. A novel long noncoding RNA HOXC-AS3 mediates tumorigenesis of gastric cancer by binding to YBX1. *Genome Biol* 2018; **19**: 154 [PMID: 30286788 DOI: 10.1186/s13059-018-1523-0]
14 **Li C**, Zhang J, Zhou Y, Li B. Long non-coding RNA CASC9 promotes the progression and development of gastric cancer *via* regulating miR-370/EGFR axis. *Dig Liver Dis* 2021; **53**: 509-516 [PMID: 33478874 DOI: 10.1016/j.dld.2020.12.115]
15 **Wu XL**, Cheng B, Li PY, Huang HJ, Zhao Q, Dan ZL, Tian DA, Zhang P. MicroRNA-143 suppresses gastric cancer cell growth and induces apoptosis by targeting COX-2. *World J Gastroenterol* 2013; **19**: 7758-7765 [PMID: 24616567 DOI: 10.3748/wjg.v19.i43.7758]
16 **Ye J**, Li J, Zhao P. Roles of ncRNAs as ceRNAs in Gastric Cancer. *Genes (Basel)* 2021; **12** [PMID: 34356052 DOI: 10.3390/genes12071036]
17 **Bartel DP**. Metazoan MicroRNAs. *Cell* 2018; **173**: 20-51 [PMID: 29570994 DOI: 10.1016/j.cell.2018.03.006]
18 **Mori MA**, Ludwig RG, Garcia-Martin R, Brandão BB, Kahn CR. Extracellular miRNAs: From Biomarkers to Mediators of Physiology and Disease. *Cell Metab* 2019; **30**: 656-673 [PMID: 31447320 DOI: 10.1016/j.cmet.2019.07.011]
19 **Rupaimoole R**, Slack FJ. MicroRNA therapeutics: towards a new era for the management of cancer and other diseases. *Nat Rev Drug Discov* 2017; **16**: 203-222 [PMID: 28209991 DOI: 10.1038/nrd.2016.246]
20 **Wu F**, Gao H, Liu K, Gao B, Ren H, Li Z, Liu F. The lncRNA ZEB2-AS1 is upregulated in gastric cancer and affects cell proliferation and invasion *via* miR-143-5p/HIF-1α axis. *Onco Targets Ther* 2019; **12**: 657-667 [PMID: 30705594 DOI: 10.2147/OTT.S175521]
21 **Sorokin AV**, Chen J. MEMO1, a new IRS1-interacting protein, induces epithelial-mesenchymal transition in mammary epithelial cells. *Oncogene* 2013; **32**: 3130-3138 [PMID: 22824790 DOI: 10.1038/onc.2012.327]
22 **Xu K**, Shi J, Mo D, Yang Y, Fu Q, Luo Y. miR-219a-1 inhibits colon cancer cells proliferation and invasion by targeting *MEMO1*. *Cancer Biol Ther* 2020; **21**: 1163-1170 [PMID: 33218285 DOI: 10.1080/15384047.2020.1843897]
23 **De Craene B**, Berx G. Regulatory networks defining EMT during cancer initiation and progression. *Nat Rev Cancer* 2013; **13**: 97-110 [PMID: 23344542 DOI: 10.1038/nrc3447]

World Journal of Gastroenterology

Submit a Manuscript: https://www.f6publishing.com

World J Gastroenterol 2022 April 28; 28(16): 1671-1680

DOI: 10.3748/wjg.v28.i16.1671

ISSN 1007-9327 (print) ISSN 2219-2840 (online)

ORIGINAL ARTICLE

Retrospective Cohort Study

Aspartate transferase-to-platelet ratio index-plus: A new simplified model for predicting the risk of mortality among patients with COVID-19

Ali Madian, Ahmed Eliwa, Hytham Abdalla, Haitham A Azeem Aly

Specialty type: Gastroenterology and hepatology

Provenance and peer review: Unsolicited article; Externally peer reviewed.

Peer-review model: Single blind

Peer-review report's scientific quality classification

Grade A (Excellent): A
Grade B (Very good): B
Grade C (Good): 0
Grade D (Fair): 0
Grade E (Poor): 0

P-Reviewer: Al-Ani RM, Iraq; Omar BJ, India

Received: November 16, 2021
Peer-review started: November 16, 2021
First decision: January 11, 2022
Revised: January 21, 2022
Accepted: March 16, 2022
Article in press: March 16, 2022
Published online: April 28, 2022

Ali Madian, Haitham A Azeem Aly, Department of Internal Medicine, Faculty of Medicine, Al-Azhar University-Assiut, Assiut 71524, Egypt

Ahmed Eliwa, Department of Internal Medicine, Faculty of Medicine, Al-Azhar University-Cairo, Cairo 11754, Egypt

Hytham Abdalla, Department of Chest Diseases, Faculty of Medicine, Al-Azhar University-Assiut, Assiut 71524, Egypt

Corresponding author: Ali Madian, MD, MSc, Lecturer, Department of Internal Medicine, Faculty of Medicine, Al-Azhar University-Assiut, Assiut 71524, Egypt.
a.madian@azhar.edu.eg

Abstract

BACKGROUND

Coronavirus disease 2019 (COVID-19) has a spectrum of clinical syndromes with serious involvement of the lung and frequent effection of the liver and hemostatic system. Blood biomarkers are affordable, rapid, objective, and useful in the evaluation and prognostication of COVID-19 patients.

AIM

To investigate the association between aspartate transferase-to-platelet ratio index (APRI) and in-hospital mortality to develop a COVID-19 mortality prediction model.

METHODS

A multicenter cohort study with a retrospective design was conducted. Medical records of all consecutive adult patients admitted to Al-Azhar University Hospital (Assiut, Egypt) and Chest Hospital (Assiut, Egypt) with confirmed COVID-19 from July 1, 2020 to October 1, 2020, were retrieved and analyzed. The patient cohort was classified into the following two categories based on the APRI: (1) COVID-19 presenting with APRI ≤ 0.5; and (2) COVID-19 presenting with APRI (> 0.5 and ≤ 1.5). The association between APRI and all-cause in-hospital mortality was analyzed, and the new model was developed through logistic regression analyses.

RESULTS

Of the 353 patients who satisfied the inclusion criteria, 10% were admitted to the intensive care unit (n = 36) and 7% died during the hospital stay (n = 25). The median age was 40 years and 50.7% were male. On admission, 49% had aspartate transferase-dominant liver injury. On admission, APRI (> 0.5 and ≤ 1.5) was independently associated with all-cause in-hospital mortality in unadjusted regression analysis and after adjustment for age and sex; after stepwise adjustment for several clinically relevant confounders, APRI was still significantly associated with all-cause in-hospital mortality. On admission, APRI (> 0.5 and ≤ 1.5) increased the odds of mortality by five-times (P < 0.006). From these results, we developed a new predictive model, the APRI-plus, which includes the four predictors of age, aspartate transferase, platelets, and serum ferritin. Performance for mortality was very good, with an area under the receiver operating curve of 0.90.

CONCLUSION

APRI-plus is an accurate and simplified prediction model for mortality among patients with COVID-19 and is associated with in-hospital mortality, independent of other relevant predictors.

Key Words: COVID-19; Aspartate transferase-to-platelet ratio index; Aspartate transferase; All-cause in-hospital mortality; Serum ferritin; SARS-CoV-2

©The Author(s) 2022. Published by Baishideng Publishing Group Inc. All rights reserved.

Core Tip: Aspartate transferase-to-platelet ratio index-plus can be used to predict the severity of coronavirus disease 2019. The performance of the model for mortality was very good, with an area under the receiver operating curve of 0.90. This new prediction model could help in estimating the risk of mortality and may, therefore, assist in triaging patients. Moreover, our study confirmed that an aspartate transferase-dominant pattern, diabetes mellites, leukocytosis, and increased ferritin levels are associated with fatal outcomes.

Citation: Madian A, Eliwa A, Abdalla H, A Azeem Aly H. Aspartate transferase-to-platelet ratio index-plus: A new simplified model for predicting the risk of mortality among patients with COVID-19. *World J Gastroenterol* 2022; 28(16): 1671-1680

URL: https://www.wjgnet.com/1007-9327/full/v28/i16/1671.htm

DOI: https://dx.doi.org/10.3748/wjg.v28.i16.1671

INTRODUCTION

The coronavirus disease 2019 (COVID-19) pandemic has prompted a global race to develop a variety of vaccine platforms. As a result, the first vaccine had been approved for emergency use by approximately 1 year from the beginning of the outbreak[1]. However, the ongoing limited availability of vaccines, particularly in low-income countries, means that the approach will not be sufficient to achieve global herd immunity. Therefore, effective and efficient allocation of health care resources is essential during the management of COVID-19 patients.

Blood biomarkers are affordable, rapid, readily available, and objective. It has been proven that blood biomarkers are useful in the evaluation and prognostication of COVID-19 patients. Many studies have demonstrated lymphopenia and thrombocytopenia among COVID-19 patients on hospital admission[2,3]. Furthermore, both lymphopenia[3,4] and thrombocytopenia[5] have been shown as predictive of COVID-19 severity and mortality.

Previously, many reports have cited hepatocellular injury with an aspartate aminotransferase (AST)-dominant pattern at hospital admission[6,7]. In addition, it has been demonstrated that AST elevation at admission is associated with severe COVID-19 disease status and poor outcomes, including intensive care admission, need for mechanical ventilation[7], and all-cause in-hospital mortality[6]. It has also been reported that elevated serum ferritin on admission is associated with fatal outcomes in patients with COVID-19[8,9].

Patients with COVID-19 associated with thrombocytopenia and hepatocellular injury progress to severe disease and poor outcomes. Previously, a simple scoring system, the AST-to-platelet ratio index (APRI), was developed to predict fibrosis in patients with chronic hepatitis C, being based upon routine blood biomarkers, including AST and platelets[10]. Using this as a premise, we hypothesized that it is possible to build a similar prediction model for patients with COVID-19 using objective, inexpensive, and readily available items.

The aim of the current study was to investigate whether APRI is associated with all-cause in-hospital mortality among patients with COVID-19 and develop a predictive model using objective and readily available factors.

MATERIALS AND METHODS

We conducted a multicenter retrospective cohort study using medical records of all consecutive adult patients admitted to Al-Azhar University Hospital in Assiut, Egypt and Chest Hospital in Assiut, Egypt with confirmed COVID-19 from July 1, 2020 to October 1, 2020, as the Egyptian Ministry of Health had allocated both hospitals for the management of COVID-19 patients. The inclusion criteria for patients were complete medical record data, hospitalized adults of ages ≥ 18 years, and COVID-19 diagnosis established by examination of nasopharyngeal swab specimens using reverse-transcriptase PCR [*CerTest* Viasure® SARS-CoV-2 Real Time PCR Detection Kit (CerTest; Biotec, Spain)] for severe acute respiratory syndrome coronavirus 2 (SARS-CoV-2). All laboratory tests were operated in the accredited laboratories at the Clinical Pathology Departments (Microbiology and Immunology units) in Al-Azhar University Hospital and Chest Hospital. The exclusion criteria were pediatric patients of ages < 18 years, patients with known chronic liver disease or newly diagnosed with chronic liver disease at hospital admission, pregnant females, patients with incomplete data, patients with splenomegaly, splenectomy, chemotherapy, or radiotherapy within 1 mo of hospital admission, and patients on immunosuppressive therapy. In addition, we excluded any patient with marked fibrosis, as determined by both APRI and fibrosis-4 (FIB-4) scores (FIB-4 > 2.67 and APRI > 1.5). The institutional review boards approved the study protocol.

Cohort assignment

AST and platelets were measured within 24 h of hospital admission. The normal upper limit for AST was 40 U/L, and the normal upper limit and lower limit for platelets were 350 ´ 10^9/L and 150 ´ 10^9/L, respectively. APRI was calculated according to the following equation: "AST Level/ULN ÷ Platelet count × 100"[10]. We categorized our patient cohort into the following two categories based on APRI: (1) COVID-19 presenting with APRI ≤ 0.5; and (2) COVID-19 presenting with APRI (> 0.5 and ≤ 1.5).

Covariates

For every participant of our cohort, demographic criteria, including age, sex, and smoking status, comorbidities, including as diabetes mellites (DM), hypertension (HTN), chronic kidney disease (CKD), chronic obstructive pulmonary disease (COPD), and Deyo-Charlson index, and laboratory biomarkers, including complete blood count, liver enzymes, serum albumin, serum total bilirubin, blood urea, and serum creatinine and creatine kinase, were retrieved and analyzed. The FIB-4 was calculated by the following equation:

Age (year) × AST(U/L) ÷ Platelets (1000/μL) × √ALT(U/L)[11].

Outcome measurement

The primary outcome of interest was all-cause in-hospital mortality. The vital status of each patient in the study cohort was confirmed from hospital records. Follow-up of outcome was ended on October 15, 2020.

Statistical analysis

We summarized continuous variables as medians and interquartile ranges, and categorical variables were summarized as absolute numbers and percentages. We utilized unadjusted binary logistic regression for analyses of group differences. We performed a stepwise analysis adjusted for age and sex, as well as for relevant confounding factors, to investigate clinical confounders. Spearman's correlation coefficients were utilized to analyze the relationships between variables. All *P* values calculated were two-tailed; values less than 0.05 were considered as indicative of statistical significance. Prediction performance was evaluated by the area under the curve of the receiver operating curve (AUROC). Overall fit of the models was evaluated by the Hosmer-Lemeshow test and the Bayesian information criterion. We used Stata Software (Stata Statistical Software: Release 16. College Station, TX, United States: Stata Corp LP) for data visualization and analysis.

RESULTS

Out of the 396 patients considered, 353 satisfied the inclusion criteria. Among those, 10% of the study cohort was admitted to the intensive care unit (n = 36) and 7% of the study participants succumbed during hospitalization (n = 25) (Figure 1). The median age at hospital admission was 40 years [interquartile range (IQR): 28-55 years], and 50.7% were males (n = 179) (Table 1). The frequency of

Table 1 Baseline demographic, clinical and laboratory characteristics of survivors and non-survivors' groups

Characteristics	Survivors, *n* = 328	Non-survivors, *n* = 25	Unadjusted OR	*P* value
Age in yr, median (IQR)				
< 40	178 (98.89)	2 (1.11)	Ref.	
40-60	112 (94.92)	6 (5.08)	4.76 (0.94-24.03)	0.05
> 60	38 (69.09)	17 (30.91)	39.81 (8.82-179.59)	0.0001
Male sex, *n* (%)	167 (93.30)	12 (6.70)	0.88 (0.39-2.00)	0.77
Comorbidities				
Chronic kidney disease, *n* (%)	4 (44.44)	5 (55.56)	20.25 (5.04-81.31)	0.0001
Diabetes mellites, *n* (%)	55 (77.46)	16 (22.54)	8.82 (3.70-20.98)	0.0001
Chronic obstructive pulmonary disease, *n* (%)	55 (88.71)	7 (11.29)	1.93 (0.76-4.84)	0.16
Hypertension, *n* (%)	84 (84.00)	16 (16.00)	5.16 (2.19-12.12)	0.0001
Deyo-Charlson index, *n* (%)				
0-1	267 (97.45)	7 (2.55)	Ref.	
2-3	60 (80.00)	15 (20.00)	9.53 (3.72-24.40)	0.0001
> 3	1 (25.00)	3 (75.00)	114.42 (10.54-1241.77)	0.0001
Laboratory biomarkers				
Hemoglobin < 12 mg/dL, *n* (%)	125 (92.59)	10 (7.41)	1.08 (0.47-2.48)	0.85
Total leukocytic count > 11 × 10^9/L, *n* (%)	50 (80.65)	12 (19.35)	5.13 (2.21-11.89)	0.0001
Platelet				
150-350	248 (93.58)	17 (6.42)	Ref.	
< 150 × 10^9/L, *n* (%)	32 (94.12)	2 (5.88)	0.91 (0.20-4.13)	0.90
> 350 × 10^9/L, *n* (%)	48 (88.89)	6 (11.11)	1.82 (0.68-4.86)	0.23
Serum AST, *n* (%)				
< 40 U/L	239 (97.15)	7 (2.85)	Ref.	
40-80 U/L	81 (84.38)	15 (15.63)	6.32 (2.49-16.05)	0.0001
> 80 U/L	8 (72.73)	3 (27.27)	12.80 (2.78-58.83)	0.001
Serum ALT, *n* (%)				
< 40 U/L	217 (93.94)	14 (6.06)	Ref.	
40-80 U/L	90 (90.00)	10 (10.00)	1.72 (0.73-4.02)	0.20
> 80 U/L	21 (95.45)	1 (4.55)	0.73 (0.09-5.89)	0.77
Serum albumin < 3.5 g/dL, *n* (%)	112 (86.15)	18 (13.85)	4.95 (2.01-12.22)	0.001
Serum total bilirubin > 1.5 mg/dL, *n* (%)	2 (40.00)	3 (60.00)	22.22 (3.52-140.03)	0.001
Serum creatinine > 1.1 mg/dL for males; > 0.95 mg/dL for females, *n* (%)	64 (80.00)	16 (20.00)	7.33 (3.09-17.34)	0.0001
Serum ferritin > 400 μg/L for males; > 150 μg/L for females, *n* (%)	169 (87.56)	24 (12.44)	22.57 (3.01-168.86)	0.002
D-dimer > 0.5 μg/mL	319 (92.73)	25 (7.27)	1	-
C-reactive protein ≥ 1 mg/L, *n* (%)	330 (92.70)	26 (7.30)	1	-
Creatine kinase > 117 IU/L, *n* (%)	0.00 (100.00)	0.00 (0.00)	-	-
APRI, *n* (%)				
≤ 0.5	254 (95.85)	11 (4.15)	Ref.	
> 0.5	74 (84.09)	14 (15.19)	4.36 (1.90-10.02)	0.001

FIB-4, *n* (%)				
≤ 2	300 (96.15)	12 (3.85)	Ref.	
> 2	17 (73.91)	6 (26.09)	8.82 (2.95-26.37)	0.0001
> 2.67	11 (61.11)	7 (38.89)	15.90 (5.24-48.24)	0.0001

Odds ratios were calculated by univariate logistic regression. Univariate logistic regression was used to calculate *P* value for the characteristics' differences between survivors and survivors. ALT: Alanine transferase; APRI: AST-to-platelet ratio index; AST: Aspartate transferase; CRP: C-reactive protein; FIB-4: Fibrosis-4 score; IQR: Interquartile range; OR: Odds ratio.

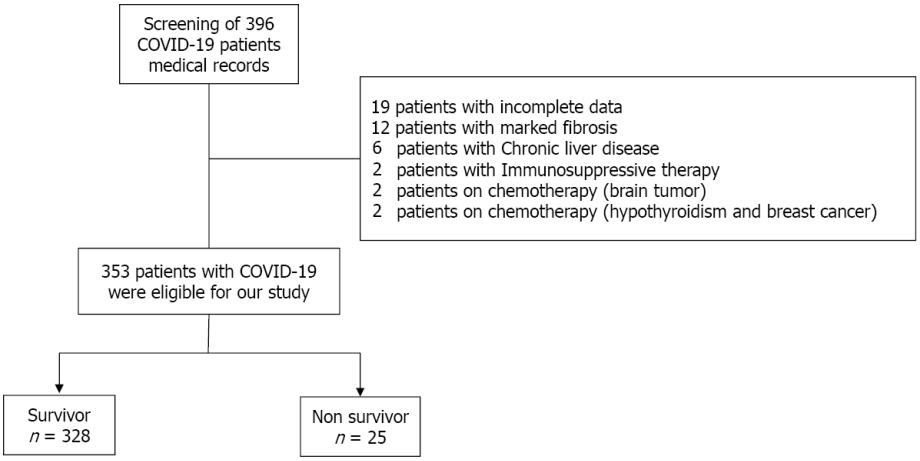

DOI: 10.3748/wjg.v28.i16.1671 **Copyright** ©The Author(s) 2022.

Figure 1 Flowchart of the studied cohort. COVID-19: Coronavirus disease 2019.

thrombocytopenia was 9.6% (*n* = 34). Thrombocytosis was reported among 15% (*n* = 54) of the study cohort. However, there was no statistically significant difference in platelet count between the survivor and death groups (Table 1). On admission, 49% of study participants had AST-dominant liver injury (*n* = 174). Study participants were grouped based on all-cause in-hospital death into survivor and nonsurvivor groups, and their features are provided in Table 1.

Predictors of the primary outcome

Variables associated with in-hospital mortality were first assessed by univariate analysis. Significant variables from univariate analysis ($P < 0.05$) or clinically relevant variables were then utilized for multivariate analysis by forward logistic regression to identify independent predictors associated with in-hospital death among patients with COVID-19.

Regression analysis: (1) Binary logistic regression analysis. Age, Deyo-Charlson index, CKD, DM, and HTN were the clinical predictors significantly associated with hospital mortality. Additionally, the unadjusted regression demonstrated that APRI, serum ferritin, total leukocytic count, serum total bilirubin, serum creatinine, serum AST, and serum albumin levels were significant biochemical markers associated with hospital death. There was no association between hospital mortality and sex, COPD, hemoglobin, platelets, serum alanine transferase (ALT), C-reactive protein (CRP), creatine kinase, or D-dimer levels (Table 1). (2) Multivariable logistic regression analysis. The APRI (> 0.5 - ≤ 1.5) at admission was significantly associated with hospital mortality in the unadjusted binary logistic regression analysis and remained a significant predictor of the odds of hospital mortality in model 1 adjusted for age and sex (Table 2). In addition, in model 2, after adjustment for several covariates, APRI was still a significant predictor of hospital mortality and associated with increased odds of hospital mortality by five times ($P < 0.005$) (Table 2).

Variables in the best model (full model) for the prediction of death among patients with COVID-19 included APRI, age, CKD, DM, total leukocytic count, and serum ferritin. The AUROC for the prediction of death among patients with COVID-19 was 0.94 [95% confidence interval (CI): 0.90-0.98]. When the prediction model comprised APRI alone (APRI model), the AUROC for the prediction of mortality was 0.66 (95%CI: 0.56-0.76). The model with APRI, age, and serum ferritin (APRI-plus model) had better accuracy than the APRI model, and the AUROC became 0.90 (95%CI: 0.86-0.95) ($P < 0.0001$) (Figure 2). In addition, the APRI-plus model showed good calibration (Hosmer-Lemeshow $\chi^2 = 1.7$, $P = 0.97$) and was a better-fitting model than the full model (Bayesian information criterion 148.4) (Table 3).

Table 2 Odds ratios of aspartate transferase-to-platelet ratio index associated mortality and 95% confidence intervals

	Unadjusted			Model I (Adjusted for age and sex)			Model II		
APRI	OR	CI	*P* value	OR	CI	*P* value	OR	CI	*P* value
≤ 0.5	Ref.			Ref.			Ref.		
> 0.5 - ≤ 1.5	4.36	1.90-10.02	0.001	3.23	1.29-8.12	0.01	5.03	1.63-15.52	0.005
						Covariates			
						Age in yr			
						< 40	Ref.		
						40-60	1.75	0.25-11.89	0.56
						> 60	10.45	1.51-72.09	0.01
						Sex	1.19	0.39-3.65	0.75
						CKD	8.24	1.37-49.53	0.02
						DM	7.77	1.82-33.04	0.006
						HTN	0.25	0.05-1.11	0.07
						WBC	4.20	1.32-13.32	0.01
						Albumin	1.17	0.33-4.09	0.81
						Bilirubin	10.10	0.97-104.45	0.05
						Ferritin	12.94	1.38-121.08	0.02

Adjusted odds ratios for hospital mortality. Model 1 adjusted for age and sex; Model 2 adjusted for age, sex, diabetes mellites, chronic kidney disease, hypertension, white blood cells, serum albumin, serum total bilirubin, and serum ferritin. APRI: Aspartate transferase-to-platelet ratio index; CKD: Chronic kidney disease; CI: Confidence interval; DM: Diabetes mellites; HTN: Hypertension; IQR: Interquartile range; WBCs: White blood cells.

Table 3 Comparison of full model and aspartate transferase-to-platelet ratio index-plus in prediction of mortality among patients with coronavirus disease 2019 in the study cohort

	AUROC	HL-χ^2	BIC
APRI-plus model	0.90 (95%CI: 0.86–0.95)	0.97	148.4
Full model	0.94 (95%CI: 0.90–0.98)	0.95	164.9

AUROC: Area under the receiver operating characteristic curve; BIC: Bayesian information criterion; CI: Confidence interval; HL-χ^2: Hosmer-Lemeshow χ^2 goodness-of-fit test.

The adjusted equation for the APRI-plus in patients with COVID-19 was *P* (in-hospital mortality) = -0.18 + 0.06 × (APRI > 0.5 and ≤ 1.5) (yes = 1, no = 0) + 0.004 × age + 0.00013 × ferritin.

Comparison with FIB-4

The AUROC for FIB-4 score was 0.72 (95%CI: 0.61-0.82). Upon comparison of the APRI-plus with FIB-4, the AUROC was significantly higher for APRI-plus, at 0.92 (95%CI: 0.86-0.98) ($P < 0.0001$) (Figure 3).

Association of D-dimer with inflammatory markers

D-dimer was examined as a marker of thrombosis. On admission, platelets, serum ferritin, CRP, total leukocytic count, and AST were correlated with D-dimer ($r = 0.1$; $P < 0.03$, $r = 0.4$; $P < 0.0001$, $r = 0.4$; $P < 0.0001$, $r = 0.1$; $P < 0.01$, and $r = 0.1$; $P < 0.03$, respectively).

Association of APRI components with markers of inflammation

Serum ferritin, CRP, and total leukocytic count were investigated as inflammatory markers. Serum levels of AST were correlated with serum ferritin ($r = 0.2$; $P < 0.0001$), CRP ($r = 0.2$; $P < 0.0001$), and total leucocytic count ($r = 0.1$; $P < 0.007$). Platelets were correlated with serum ferritin ($r = 0.1$; $P = 0.04$), CRP ($r = 0.07$; $P = 0.1$), and total leukocytic count ($r = 0.1$; $P = 0.05$).

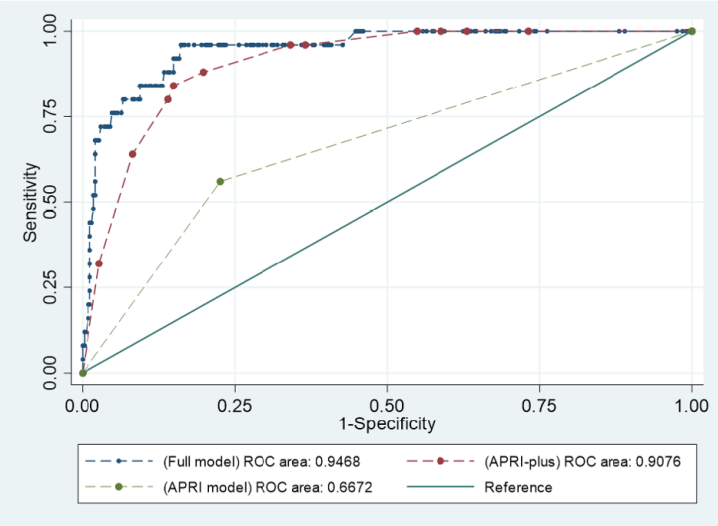

DOI: 10.3748/wjg.v28.i16.1671 **Copyright** ©The Author(s) 2022.

Figure 2 Receiver operating characteristic curves comparing full model, aspartate transferase-to-platelet ratio index and aspartate transferase-to-platelet ratio index-plus in prediction of mortality among patients with coronavirus disease 2019 in the study cohort. APRI: Aspartate transferase-to-platelet ratio index; COVID-19: Coronavirus disease 2019.

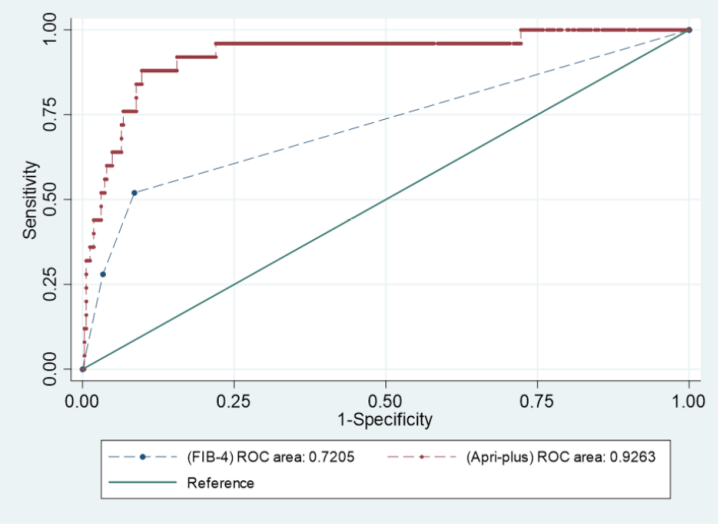

DOI: 10.3748/wjg.v28.i16.1671 **Copyright** ©The Author(s) 2022.

Figure 3 Receiver operating characteristic curves comparing aspartate transferase-to-platelet ratio index-plus with the fibrosis-4 score in prediction of mortality among patients with coronavirus disease 2019 in the study cohort. APRI: Aspartate transferase-to-platelet ratio index; COVID-19: Coronavirus disease 2019; FIB-4: Fibrosis-4.

DISCUSSION

In the current study, we developed APRI-plus, a new, simple, inexpensive, and objective clinical score that is significantly associated with mortality among patients with COVID-19. APRI (> 0.5 and ≤ 1.5) increased the odds of mortality by five-fold. Since patients with chronic liver disease were excluded from participation in our analysis, this association is likely due to inflammation related to COVID-19 and the direct impact of SARS-Cov-2 on the liver and hemostatic system.

We observed a significant difference in AST between survivors and nonsurvivors at hospital admission. The AST-dominant pattern of hepatocellular injury among patients with COVID-19 has been reported many times in previous studies[6,7]. Likewise, the levels of serum ferritin were significantly higher among nonsurvivors. Platelets have been reported to be one of the strongest indicators of adverse outcomes and mortality among patients with COVID-19[2,3]. However, in our cohort, we did not find any statistically significant difference in platelets between survivors and nonsurvivors. Thus, platelets alone are less ideal in predicting outcomes among patients with COVID-19.

APRI includes AST in the numerator and platelets in the denominator. These criteria make the APRI score a better predictor of COVID-19 outcomes than AST or platelets alone. Regarding its accuracy in predicting mortality among patients with COVID-19, the APRI has an AUROC of 0.66. However, when age and serum ferritin were incorporated in the regression model (APRI-plus model), the performance of the model had an AUROC of 0.90. In contrast, compared with another noninvasive score, FIB-4 (composed of AST, ALT, age, and platelets), we found that the AUROC was significantly lower for FIB-4 (0.72). In line with our findings, the reported AUROC in an earlier study for FIB-4 was 0.79[11]. Using APRI-plus, it is possible to predict mortality among patients with COVID-19 with good performance.

Liver stiffness among patients with COVID-19 is likely to be multifactorial. Hepatic congestion, hepatocellular injury, and systemic inflammation may all play a role in the development of liver stiffness among patients with COVID-19. It has been reported that COVID-19 is associated with increased pressure within the right ventricle[12]; thus, this may result in hepatic venous congestion and liver stiffness[11].

Severe liver injury caused by SARS-CoV-2 Likely results in mitochondrial damage and defective clearance of AST, leading to an AST-dominant pattern. At the onset of severe SARS-CoV-2 infection, severe liver injury is likely associated with extensive inflammation, hepatocyte swelling, and tissue edema, especially among patients with an AST-dominant pattern. Similar to acute viral hepatitis, extensive necroinflammatory activity among patients with COVID-19 increases liver stiffness[13].

Our cohort revealed that platelet count did not have a significant association with mortality. Interestingly, not all previous studies have found platelet counts to be a predictor of COVID-19 mortality[14]. Inflammatory mediators associated with SARS-CoV-2 infection may result in the activation of platelets. Activated platelets have two pathways. First, enhanced platelet clearance/sequestration from circulation by the spleen results in thrombocytopenia. Second, consumptive coagulopathy, such as inflammation-mediated endothelial damage/activation in addition to platelet activation, leads to the formation of platelet aggregates through systemic circulation and/or pulmonary circulation[15]. Therefore, we can speculate that the early phase of SARS-CoV-2 infection results in the activation of platelets followed by thrombocytopenia. Our results support this speculation, as inflammatory markers (CRP, serum ferritin, and leukocytosis) were correlated with D-dimer. This may suggest that the mechanism and progression of platelet activation rather than platelet number were associated with worse outcomes.

The rising question is why we did not find a significant difference in D-dimer between the survivor and nonsurvivor groups. This could be explained by COVID-19-associated coagulopathy. Coagulation changes associated with COVID-19 have the following three proposed stages: stage 1 presents with raised D-dimer; stage 2 presents with raised D-dimer together with modestly increased prothrombin time/international normalization ratio, activated partial thromboplastin time, and mild thrombocytopenia; and stage 3 presents with critical illness and laboratory markers, directing towards classic disseminated intravascular coagulopathy[14]. Therefore, our data may be retrieved early during platelet activation and before firing of stage 1 COVID-19-associated coagulopathy.

Limitations of the current study

The retrospective design of the study reflected the association between APRI-plus and risk of mortality among patients with COVID-19 but did not reflect causality. We used APRI at the time of admission for group categorization without knowing follow-up changes. Because of the lack of follow-up, we do not know whether these necroinflammatory changes were self-limiting or progressive. Moreover, we do not know the extent and duration of resolution. We did not evaluate platelet activity, fibrin degradation products, or coagulation profiles. Elastography should be evaluated in different age groups to dissect the impact of age from COVID-19 on liver stiffness. Validation of the APRI-plus is required.

CONCLUSION

The current study showed that, on admission, APRI-plus among patients with COVID-19 has good performance in predicting mortality. A prediction model could help stratify the risk of mortality. This association may be explained by the impact of SARS-CoV-2 infection on the liver and hemostatic system. Further studies are required to investigate this association.

ARTICLE HIGHLIGHTS

Research background

Coronavirus disease 2019 (COVID-19) has a spectrum of clinical syndromes with serious involvement of the lung and frequent effection of the liver and hemostatic system.

Research motivation

Development of a prediction model using objective, inexpensive, and readily available items is needed for patients with COVID-19.

Research objectives

To investigate whether the aspartate transferase-to-platelet ratio index (APRI) is associated with all-cause in-hospital mortality among patients with COVID-19 and develop a predictive model using objective and readily available factors.

Research methods

A retrospective cohort study was carried out with 353 consecutive adult patients admitted to Al-Azhar University Hospital (Assiut, Egypt) and Chest Hospital (Assiut, Egypt) with confirmed COVID-19 from July 1, 2020 to October 1, 2020.

Research results

The prediction model comprised APRI alone (APRI model), and the area under the receiver operating curve (AUROC) for the prediction of mortality was 0.66 [95% confidence interval (CI): 0.56-0.76]. A modified model of APRI that included age and serum ferritin (APRI-plus model) had better accuracy than the APRI model, as the AUROC became 0.90 (95%CI: 0.86-0.95) ($P < 0.0001$).

Research conclusions

APRI-plus among patients with COVID-19 showed good performance in predicting mortality. A prediction model could help stratify the risk of mortality.

Research perspectives

Further studies are required to investigate this association. Validation of the APRI-plus is required.

ACKNOWLEDGEMENTS

We appreciate the effort of all medical staff and technicians who agreed to participate in this study.

FOOTNOTES

Author contributions: Madian A was responsible for the study conception and design, the data acquisition, analysis and interpretation, the statistical analysis, and writing of the first draft of the manuscript; Eliwa A and Abdalla H contributed to the data collection; Azeem HA reviewed the manuscript and provided critical scientific input; all authors approved the final manuscript.

Institutional review board statement: The study was approved by the Ethics Committee of Faculty of Medicine, Al-Azhar University, Assiut, Egypt.

Informed consent statement: No informed consent was required, as patient identity is not revealed in the retrospective analysis.

Conflict-of-interest statement: No benefits in any form have been received or will be received from a commercial party related directly or indirectly to the subject of this article.

Data sharing statement: The original anonymous dataset is available on request from the corresponding author at a.madian@azhar.edu.eg.

STROBE statement: The authors have read the STROBE Statement—checklist of items, and the manuscript was prepared and revised according to the STROBE Statement—checklist of items.

Open-Access: This article is an open-access article that was selected by an in-house editor and fully peer-reviewed by external reviewers. It is distributed in accordance with the Creative Commons Attribution NonCommercial (CC BY-NC 4.0) license, which permits others to distribute, remix, adapt, build upon this work non-commercially, and license their derivative works on different terms, provided the original work is properly cited and the use is non-commercial. See: https://creativecommons.org/Licenses/by-nc/4.0/

Country/Territory of origin: Egypt

ORCID number: Ali Madian 0000-0002-8322-7504; Ahmed Eliwa 0000-0003-0818-3086; Hytham Abdalla 0000-0001-5377-6572; Haitham A Azeem Aly 0000-0001-5732-5277.

S-Editor: Wu YXJ
L-Editor: A
P-Editor: Wu YXJ

REFERENCES

1 **Lamb YN**. BNT162b2 mRNA COVID-19 Vaccine: First Approval. *Drugs* 2021; **81**: 495-501 [PMID: 33683637 DOI: 10.1007/s40265-021-01480-7]
2 **Guan WJ**, Ni ZY, Hu Y, Liang WH, Ou CQ, He JX, Liu L, Shan H, Lei CL, Hui DSC, Du B, Li LJ, Zeng G, Yuen KY, Chen RC, Tang CL, Wang T, Chen PY, Xiang J, Li SY, Wang JL, Liang ZJ, Peng YX, Wei L, Liu Y, Hu YH, Peng P, Wang JM, Liu JY, Chen Z, Li G, Zheng ZJ, Qiu SQ, Luo J, Ye CJ, Zhu SY, Zhong NS; China Medical Treatment Expert Group for Covid-19. Clinical Characteristics of Coronavirus Disease 2019 in China. *N Engl J Med* 2020; **382**: 1708-1720 [PMID: 32109013 DOI: 10.1056/NEJMoa2002032]
3 **Huang C**, Wang Y, Li X, Ren L, Zhao J, Hu Y, Zhang L, Fan G, Xu J, Gu X, Cheng Z, Yu T, Xia J, Wei Y, Wu W, Xie X, Yin W, Li H, Liu M, Xiao Y, Gao H, Guo L, Xie J, Wang G, Jiang R, Gao Z, Jin Q, Wang J, Cao B. Clinical features of patients infected with 2019 novel coronavirus in Wuhan, China. *Lancet* 2020; **395**: 497-506 [PMID: 31986264 DOI: 10.1016/S0140-6736(20)30183-5]
4 **Yang X**, Yu Y, Xu J, Shu H, Xia J, Liu H, Wu Y, Zhang L, Yu Z, Fang M, Yu T, Wang Y, Pan S, Zou X, Yuan S, Shang Y. Clinical course and outcomes of critically ill patients with SARS-CoV-2 pneumonia in Wuhan, China: a single-centered, retrospective, observational study. *Lancet Respir Med* 2020; **8**: 475-481 [PMID: 32105632 DOI: 10.1016/S2213-2600(20)30079-5]
5 **Yang X**, Yang Q, Wang Y, Wu Y, Xu J, Yu Y, Shang Y. Thrombocytopenia and its association with mortality in patients with COVID-19. *J Thromb Haemost* 2020; **18**: 1469-1472 [PMID: 32302435 DOI: 10.1111/jth.14848]
6 **Madian A**, Eliwa A, Abdalla H, Aly HAA. Hepatocellular injury and the mortality risk among patients with COVID-19: A retrospective cohort study. *World J Hepatol* 2021; **13**: 939-948 [PMID: 34552700 DOI: 10.4254/wjh.v13.i8.939]
7 **Weber S**, Hellmuth JC, Scherer C, Muenchhoff M, Mayerle J, Gerbes AL. Liver function test abnormalities at hospital admission are associated with severe course of SARS-CoV-2 infection: a prospective cohort study. *Gut* 2021; **70**: 1925-1932 [PMID: 33514597 DOI: 10.1136/gutjnl-2020-323800]
8 **Deng F**, Zhang L, Lyu L, Lu Z, Gao D, Ma X, Guo Y, Wang R, Gong S, Jiang W. [Increased levels of ferritin on admission predicts intensive care unit mortality in patients with COVID-19]. *Med Clin (Barc)* 2021; **156**: 324-331 [PMID: 33422296 DOI: 10.1016/j.medcli.2020.11.030]
9 **Vargas-Vargas M**, Cortés-Rojo C. Ferritin levels and COVID-19. *Rev Panam Salud Publica* 2020; **44**: e72 [PMID: 32547616 DOI: 10.26633/RPSP.2020.72]
10 **Wai CT**, Greenson JK, Fontana RJ, Kalbfleisch JD, Marrero JA, Conjeevaram HS, Lok AS. A simple noninvasive index can predict both significant fibrosis and cirrhosis in patients with chronic hepatitis C. *Hepatology* 2003; **38**: 518-526 [PMID: 12883497 DOI: 10.1053/jhep.2003.50346]
11 **Li Y**, Regan J, Fajnzylber J, Coxen K, Corry H, Wong C, Rosenthal A, Atyeo C, Fischinger S, Gillespie E, Chishti R, Baden L, Yu XG, Alter G, Kim A, Li JZ. Liver Fibrosis Index FIB-4 Is Associated With Mortality in COVID-19. *Hepatol Commun* 2021; **5**: 434-445 [PMID: 34553511 DOI: 10.1002/hep4.1650]
12 **Li Y**, Li H, Zhu S, Xie Y, Wang B, He L, Zhang D, Zhang Y, Yuan H, Wu C, Sun W, Li M, Cui L, Cai Y, Wang J, Yang Y, Lv Q, Zhang L, Xie M. Prognostic Value of Right Ventricular Longitudinal Strain in Patients With COVID-19. *JACC Cardiovasc Imaging* 2020; **13**: 2287-2299 [PMID: 32654963 DOI: 10.1016/j.jcmg.2020.04.014]
13 **Arena U**, Vizzutti F, Corti G, Ambu S, Stasi C, Bresci S, Moscarella S, Boddi V, Petrarca A, Laffi G, Marra F, Pinzani M. Acute viral hepatitis increases liver stiffness values measured by transient elastography. *Hepatology* 2008; **47**: 380-384 [PMID: 18095306 DOI: 10.1002/hep.22007]
14 **Wool GD**, Miller JL. The Impact of COVID-19 Disease on Platelets and Coagulation. *Pathobiology* 2021; **88**: 15-27 [PMID: 33049751 DOI: 10.1159/000512007]
15 **Connors JM**, Levy JH. COVID-19 and its implications for thrombosis and anticoagulation. *Blood* 2020; **135**: 2033-2040 [PMID: 32339221 DOI: 10.1182/blood.2020006000]

World Journal of Gastroenterology

Submit a Manuscript: https://www.f6publishing.com

World J Gastroenterol 2022 April 28; 28(16): 1681-1691

DOI: 10.3748/wjg.v28.i16.1681

ISSN 1007-9327 (print) ISSN 2219-2840 (online)

ORIGINAL ARTICLE

Retrospective Study

Association of maternal obesity and gestational diabetes mellitus with overweight/obesity and fatty liver risk in offspring

Jing Zeng, Feng Shen, Zi-Yuan Zou, Rui-Xu Yang, Qian Jin, Jing Yang, Guang-Yu Chen, Jian-Gao Fan

Specialty type: Pediatrics

Provenance and peer review: Unsolicited article; Externally peer reviewed.

Peer-review model: Single blind

Peer-review report's scientific quality classification

Grade A (Excellent): 0
Grade B (Very good): B
Grade C (Good): C
Grade D (Fair): 0
Grade E (Poor): 0

P-Reviewer: Popova PV, Russia; Pustozerov EA, Russia

Received: August 29, 2021
Peer-review started: August 29, 2021
First decision: October 16, 2021
Revised: October 30, 2021
Accepted: March 16, 2022
Article in press: March 16, 2022
Published online: April 28, 2022

Jing Zeng, Feng Shen, Zi-Yuan Zou, Rui-Xu Yang, Qian Jin, Jing Yang, Guang-Yu Chen, Jian-Gao Fan, Department of Gastroenterology, Xinhua Hospital, Shanghai Jiao Tong University School of Medicine, Shanghai 200092, China

Jian-Gao Fan, Shanghai Key Lab of Pediatric Gastroenterology and Nutrition, Shanghai 200092, China

Corresponding author: Jian-Gao Fan, MD, PhD, Professor, Department of Gastroenterology, Xinhua Hospital, Shanghai Jiao Tong University School of Medicine, No. 1665 Kongjiang Road, Shanghai 200092, China. fanjiangao@xinhuamed.com.cn

Abstract

BACKGROUND

Childhood obesity and fatty liver are associated with adverse outcomes such as diabetes, metabolic syndrome, and cardiovascular diseases in adulthood. It is very important to identify relevant risk factors and intervene as early as possible. At present, the relationship between maternal and offspring metabolic factors is conflicting.

AIM

To estimate the association of maternal obesity and gestational diabetes mellitus (GDM) with overweight/obesity and fatty liver risk in offspring at 8 years of age.

METHODS

The prospective study included mothers who all had a 75-g oral glucose tolerance test at 24-28 wk of gestation and whose offspring completed follow-up at 8 years of age. Offspring birth weight, sex, height, weight, and body mass index (BMI) were measured and calculated. FibroScan-502 examination with an M probe (Echosens, Paris, France) was prospectively conducted in offspring aged 8 years from the Shanghai Prenatal Cohort Study.

RESULTS

A total of 430 mother-child pairs were included in the analysis. A total of 62 (14.2%) mothers were classified as obese, and 48 (11.1%) were classified as having GDM. The mean age of the offspring at follow-up was 8 years old. Thirty-seven (8.6%) offspring were overweight, 14 (3.3%) had obesity, and 60 (14.0%) had fatty liver. The prevalence of overweight, obesity and fatty liver in offspring increased significantly across maternal BMI quartiles (all $P < 0.05$). Among offspring of

mothers with GDM, 12 (25.0%) were overweight, 4 (8.3%) were obese, and 12 (25.0%) had fatty liver vs. 25 (6.5%), 10 (2.6%) and 48 (12.6%), respectively, for offspring of mothers without GDM (all $P < 0.05$). In multiple logistic regression, after adjustment for variables, the OR for fatty liver in offspring was 8.26 (95%CI: 2.38-28.75) for maternal obesity and GDM.

CONCLUSION

This study showed that maternal obesity can increase the odds of overweight/obesity and fatty liver in offspring, and GDM status also increases the odds of overweight/obesity in offspring. Weight management and glycemic control before and during pregnancy need to be highlighted in primary prevention of pediatric obesity and fatty liver.

Key Words: Maternal obesity; Gestational diabetes mellitus; Offspring overweight/obesity; Offspring fatty liver; FibroScan

©The Author(s) 2022. Published by Baishideng Publishing Group Inc. All rights reserved.

Core Tip: It is very important to identify relevant risk factors for childhood obesity and fatty liver and intervene as early as possible, considering their adverse outcomes. In this work, we reported the association of maternal obesity and gestational diabetes mellitus (GDM) with overweight/obesity and fatty liver risk in offspring at 8 years of age. This study showed that maternal obesity can increase the odds of overweight/obesity and fatty liver in offspring, and GDM status also increases the odds of overweight/obesity in offspring. Weight management and glycemic control before and during pregnancy need to be highlighted in primary prevention of pediatric obesity and fatty liver.

Citation: Zeng J, Shen F, Zou ZY, Yang RX, Jin Q, Yang J, Chen GY, Fan JG. Association of maternal obesity and gestational diabetes mellitus with overweight/obesity and fatty liver risk in offspring. *World J Gastroenterol* 2022; 28(16): 1681-1691

URL: https://www.wjgnet.com/1007-9327/full/v28/i16/1681.htm

DOI: https://dx.doi.org/10.3748/wjg.v28.i16.1681

INTRODUCTION

With economic development and changing living and eating habits, the prevalence of obesity in children has been rapidly increasing in recent decades[1]. It is alarming because it is also associated with health consequences such as metabolic syndrome, diabetes, cardiovascular diseases, and even many types of cancers in adulthood[2,3]. The incidence of fatty liver in children is also rising, due, in part, to the increasing prevalence of childhood obesity. At present, there is still no effective noninvasive means for diagnosing fatty liver in children. Recently, some novel noninvasive techniques for the assessment of liver fat have been developed. Transient elastography (TE) is one of these new techniques based on inducing a shear wave to the liver and measuring the velocity of the wave. The device (FibroScan-502, Echosens, Paris, France) was developed using the TE technique, and controlled attenuation parameter (CAP) and liver stiffness measurement (LSM) can be obtained simultaneously by the device in a rapid, noninvasive, reproducible, and painless way. FibroScan-502 has also been used in the assessment of liver fat and fibrosis in pediatric individuals with liver diseases, and the reference values of CAP have been studied in our previous article[4].

Recent studies have suggested that maternal body mass index (BMI) is associated with the birth weight of offspring and is a risk factor for offspring obesity[5,6]. Gestational diabetes mellitus (GDM) is the occurrence of glucose intolerance during pregnancy and usually resolves after birth[7]. Meanwhile, many studies have shown that GDM can increase the incidence of impaired glucose tolerance in offspring and increase the risk of offspring obesity[8,9].

Therefore, in this article, we aimed to assess whether maternal BMI and in utero exposure to GDM are associated with a long-term risk of overweight/obese and fatty liver among offspring 8 years postpartum.

MATERIALS AND METHODS

Study population

The individuals included in the prospective study were 430 maternal-child pairs from the Shanghai Prenatal Cohort Study, which is a prospective study that enrolled 1043 Han maternal-child pairs between January 2012 and December 2013 at Xinhua Hospital and International Peace Maternity and Child Hospital in Shanghai. The offspring were followed up at the age of 8 years (94 to 98 mo) with medical examinations. The exclusion criteria for the study population were as follows: (1) Non-Shanghai residents; (2) lost to follow-up; (3) missing some of the mothers' clinical information on prepregnancy and the offspring's anthropometric data; (4) mothers' medical history of diabetes (diagnosed before the index pregnancy) and other participants whose fasting glucose was ≥ 7.0 mmol/L before 12 gestational weeks; and (5) failure of FibroScan-502 measurement with an M probe. Ethics approval was obtained by the Ethics Committees (XHEC-C-2012-023). The parents of all the participating children were required to give informed consent for study participation and sign the written documents.

Clinical and laboratory data collection

All mothers' heights and weights were measured in light indoor clothing and without shoes during early pregnancy. The oral glucose tolerance test (OGTT) was conducted between 24 and 28 wk gestation among those mothers. All followed-up offspring underwent annual medical examination at the health examination center in Xinhua Hospital. Stadiometers (Seca 416 Infantmeter, United States) were used to measure height to the nearest 0.1 cm. Digital scales (Detector 6745 Baby Scale, United States) were used to measure body weight to the nearest 0.1 kg. Participant characteristics and anthropometric indices, including age, sex, body weight, height, chest circumference, waist circumference, hip circumference and BMI, were obtained.

Following a fast of at least 6 h, all offspring underwent FibroScan-502 examination with an M-probe (3.5 MHz) (Echosens, Paris, France) by the same physician. The device estimates liver stiffness in kilopascals (kPa) and liver steatosis in decibels/meter (dB/m). CAP in dB/m and LSM in kPa were obtained simultaneously by each examination. A TE examination was considered successful when 10 valid measurements with a success rate of at least 60% were conducted and the interquartile range (IQR) was less than 30% of the median LSM value[10]. Subjects with unsuccessful examinations were excluded from the analyses.

Work definitions

Maternal obese, overweight and lean: A BMI during the early pregnancy greater than 25 kg/m^2 was used to define the obese population, and a BMI less than 25 kg/m^2 was used to define the nonobese population. The nonobese population was further divided into lean (< 23 kg/m^2) and overweight (23-25 kg/m^2) groups.

GDM: All mothers without diagnosed diabetes were screened for GDM by a one-step approach undergoing a 75g OGTT after fasting overnight between 24 and 28 wk gestation according to the guideline from Obstetrics and Gynecology Branch of Chinese Medical Association[11]. GDM was diagnosed when the glucose level that met or exceeded any of the following standards: a blood glucose value of 92, 180 or 153 mg/dL before or one or two hours after taking a 75 g glucose tolerance test, respectively.

Offspring overweight/obesity were defined by using the International Obesity Task Force age- and sex-specific cutoff points[12].

Offspring fatty liver: The offspring were considered to have fatty liver when the CAP value exceeded the normal value of 214.53 dB/m[4].

Statistical analysis

Continuous variables are expressed as the mean ± SD for a normal distribution and as the median ± IQR for a skewed distribution. General linear models for continuous variables were used to compare means of characteristics, and the χ^2 test for categorical variables was applied to compare offspring proportions across quartiles of maternal BMI during early pregnancy. We further explored the effects of maternal GDM status on such associations by a stratified analysis according to GDM status. Multivariate logistic regression models were used to examine the relationship between maternal BMI during early pregnancy and GDM status and offspring overweight/obesity status and fatty liver prevalence. Multiple logistic regression was used for continuous outcomes, and the results are reported as odds ratios (ORs) with 95%CIs. Three multivariate-adjusted models were included in these analyses. Significance tests were two tailed, and a P value < 0.05 was considered statistically significant. The data analysis for this article was generated using SAS Version 9.4.

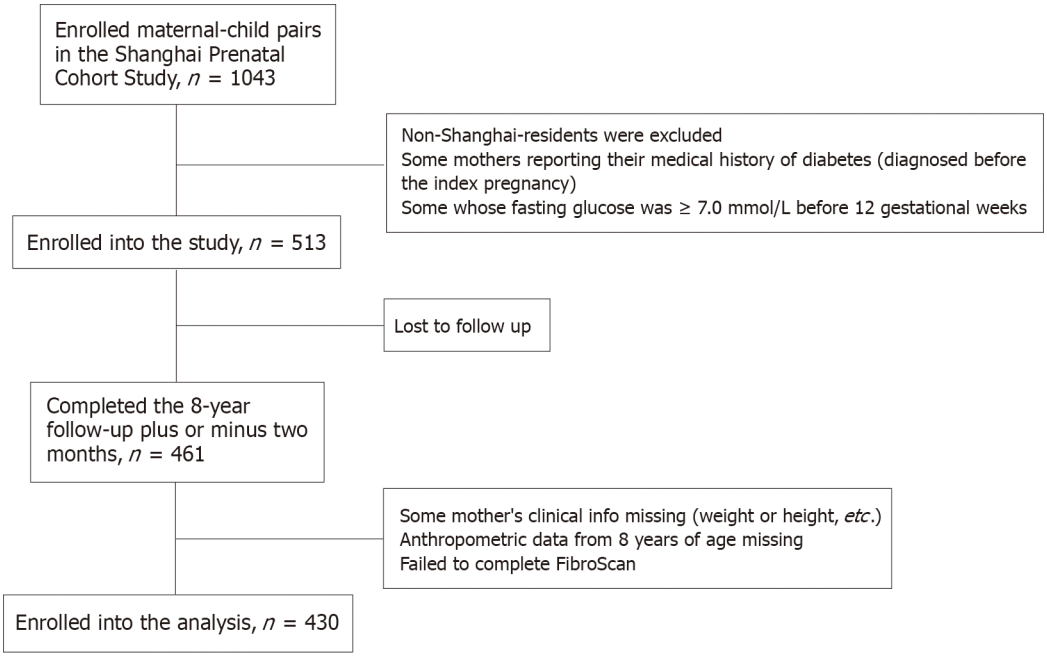

DOI: 10.3748/wjg.v28.i16.1681 **Copyright** ©The Author(s) 2022.

Figure 1 Flow diagram of participants included in this study.

RESULTS

Participant characteristics

A total of 513 maternal-child pairs from the Shanghai Prenatal Cohort Study were prospectively followed for 8 years. Of these individuals, 430 mothers and their offspring were included in the analysis (Figure 1).

The characteristics of participating mothers and offspring are shown in Table 1. The mean maternal age before pregnancy was 29 (4.9) years (20 to 42 years old). The mean maternal BMI was 21.55 (3.59) kg/m^2. A total of 62 (14.2%) mothers were classified as obese, and 48 (11.1%) were classified as having GDM. The mean birth weight of the offspring was 3.40 ± 0.48 kg and 210 (48.8%) were boys. A total of 37 (8.6%) offspring were classified as overweight, 14 (3.3%) offspring were classified as obese, and 60 (14.0%) had fatty liver (Table 1).

Maternal BMI and the characteristics of the mothers and offspring

Across maternal BMI quartiles, mothers in higher maternal BMI quartiles were more likely to have a greater weight and GDM. The offspring of mothers in higher maternal BMI quartiles were also more likely to have greater birth weight, BMI, waist circumference, hip circumference, chest circumference and CAP values and to be more prone to overweight/obese and fatty liver (Table 1).

The association of maternal BMI with outcomes for offspring

The fatty liver risk of these offspring increased progressively from the lowest to the highest quartiles of maternal BMI, with odds ratios (ORs) of 5.84 (95%CI: 0.67-50.67), 9.76 (95%CI: 1.21-78.83), and 26.3 (95%CI: 3.21-215.3), respectively, after controlling for the sex and age of the offspring (Model 1). Further adjusting for maternal age, nulliparity (Model 2), GDM status of the mothers and birth weight (Model 3) did not change the associations (Table 2).

The OR of the offspring overweight/obesity risk in the highest quartile of maternal BMI was 10.6 (95%CI: 2.17-51.76) after controlling for the sex and age of the children (Model 1) (Table 2).

Association of maternal GDM status with offspring overweight/obesity and CAP values

As shown in Table 3, mothers with GDM weighed more, had higher maternal BMIs and had a higher prevalence of maternal obesity than mothers without GDM (all $P < 0.05$). The offspring of mothers with GDM had higher BMI, chest circumference, hip circumference, and CAP values (all $P < 0.05$). Among offspring whose mothers had GDM, 4 (8.3%) were obese, compared with 10 (2.6%) offspring whose mothers did not have GDM ($P < 0.000$). However, there were no significant differences in birth weight, sex distribution, weight at follow-up, waist circumference, or LSM values between the offspring of mothers with and without GDM (Table 3).

Table 1 Characteristics of mothers and their offspring stratified into groups based on maternal body mass index quartiles at follow-up

Variables	All (*n* = 430)	Quartiles of maternal BMI (kg/m²)				
		Q1 (*n* = 108): 15.00-19.13	Q2 (*n* = 105): 19.14-20.76	Q3 (*n* = 115): 20.77-23.44	Q4 (*n* = 102): 23.45-42.00	*P* value
Maternal characteristics						
Age, yr	29.33 ± 4.89	29.21 ± 4.59	28.97 ± 3.14	29.59 ± 3.73	29.44 ± 7.36	0.805
Height, cm	162.97 ± 16.46	162.77 ± 5.09	161.84 ± 4.93	161.61 ± 4.29	162.26 ± 6.18	0.358
Weight, kg	56.73 ± 9.77	47.48 ± 3.45	52.21 ± 3.53	57.76 ± 3.53	69.9 ± 9.1	0.000
BMI, kg/m^2	21.55 ± 3.59	17.92 ± 0.97	19.91 ± 0.43	22.1 ± 0.79	26.57 ± 3.3	0.000
GDM, *n* (%)	48 (11.2)	6 (5.6)	8 (7.6)	11 (9.6)	23 (22.5)	0.000
Offspring characteristics						
Birth weight, kg	3.40 ± 0.48	3.33 ± 0.42	3.34 ± 0.39	3.42 ± 0.55	3.51 ± 0.51	0.021
Boy, *n* (%)	210 (48.8)	47 (43.5)	53 (50.5)	53 (46.1)	57 (55.9)	0.304
Height, cm	122.78 ± 29.93	121.59 ± 31.31	129.03 ± 4.91	118.81 ± 36.96	123.35 ± 31.01	0.242
Weight, kg	25.58 ± 10.57	22.98 ± 8.83	26.37 ± 7.8	25.18 ± 10.25	28.15 ± 13.12	0.070
BMI, kg/m^2	15.89 ± 4.42	14.58 ± 3.81	15.70 ± 4.00	16.20 ± 3.69	17.25 ± 5.81	0.025
Waist circumference, cm	58.70 ± 10.79	54.33 ± 12.76	58.33 ± 7.08	59.15 ± 9.32	63.13 ± 9.42	0.000
Hip circumference, cm	69.04 ± 13.73	65.3 ± 14.55	69.17 ± 13.47	69.39 ± 7.36	72.14 ± 13.39	0.041
Chest circumference, cm	56.19 ± 21.03	49.79 ± 22.55	53.44 ± 22.62	56.72 ± 16.15	63.41 ± 14.73	0.003
Waist-height ratio	0.46 ± 0.05	0.44 ± 0.05	0.45 ± 0.05	0.46 ± 0.04	0.48 ± 0.06	0.000
Waist-hip ratio	0.84 ± 0.08	0.83 ± 0.06	0.84 ± 0.07	0.84 ± 0.06	0.86 ± 0.12	0.292
Chest-height ratio	0.44 ± 0.14	0.4 ± 0.16	0.44 ± 0.12	0.41 ± 0.17	0.48 ± 0.11	0.023
CAP, dB/m	167.71 ± 46.09	151.76 ± 37.01	164.33 ± 41.45	169.97 ± 40.76	188.38 ± 58.89	0.001
LSM, kPa	3.36 ± 0.75	3.31 ± 0.8	3.52 ± 0.8	3.35 ± 0.73	3.4 ± 0.71	0.480
Overweight, *n* (%)	37 (8.6)	4 (3.7)	7 (6.7)	5 (4.4)	21 (20.6)	0.000
Obesity, *n* (%)	14 (3.3)	0 (0)	0 (0)	2 (1.7)	12 (11.8)	0.000
Fatty liver, *n* (%)	60 (14.0)	2 (1.9)	10 (9.5)	19 (16.5)	29 (28.4)	0.001

BMI: Body max index; GDM: Gestational diabetes mellitus; CAP: Controlled attenuation parameter; LSM: Liver stiffness measurement.

The CAP values of the offspring gradually increased in the mothers with neither obesity nor GDM (163.62 ± 44.41) dB/m, GDM but no obesity (173.43 ± 34.57) dB/m, obesity but no GDM (190.73 ± 49.74) dB/m to both obesity and GDM (202.15 ± 61.55) dB/m (all $P < 0.05$) (Figure 2).

Association of maternal obesity and GDM with outcomes for offspring

Maternal obesity was positively associated with childhood fatty liver with OR 4.57 (95%CI: 1.96-10.67) and childhood overweight/obesity with OR 5.73 (95%CI: 2.18-15.10) (Model 1). Further adjustment for maternal age, nulliparity (Model 2), GDM status of the mother and birth weight (Model 3) did not change the associations (Table 4).

Maternal GDM was also positively associated with childhood overweight/obesity, with an OR of 4.70 (95%CI: 1.72-12.81) (Model 1). Additionally, further adjustment for maternal age, nulliparity (Model 2), and offspring birth weight (Model 3) did not change the associations. In addition, the association of maternal GDM with childhood fatty liver was not statistically significant, with an OR of 2.39 (95%CI: 0.91-6.29) (Model 1) (Table 4).

Table 2 Adjusted odds ratios (95% confidence interval) of offspring overweight/obesity and fatty liver according to quartiles of maternal body max index

	Quartiles of BMI	Model 1		*P* value	Model 2		*P* value	Model 3		*P* value
		OR	95%CI		OR	95%CI		OR	95%CI	
Offspring fatty liver		1.21	1.1-1.33	0.000	1.21	1.1-1.34	0.000	1.23	1.11-1.36	0.000
	Q1	Reference			Reference			Reference		
	Q2	5.84	0.67-50.67	0.109	5.70	0.65-49.77	0.115	5.52	0.63-48.36	0.123
	Q3	9.76	1.21-78.83	0.033	9.60	1.18-77.79	0.034	9.50	1.17-77.33	0.035
	Q4	26.3	3.21-215.3	0.002	26.95	3.27-222.23	0.002	26.09	3.08-220.72	0.003
Offspring overweight/obesity		1.19	1.07-1.33	0.002	1.19	1.07-1.33	0.002	1.20	1.07-1.34	0.002
	Q1	Reference			Reference			Reference		
	Q2	2.09	0.37-11.60	0.401	2.23	0.40-12.57	0.364	2.17	0.38-12.5	0.385
	Q3	1.30	0.22-7.62	0.770	1.43	0.24-8.49	0.694	1.43	0.24-8.58	0.696
	Q4	10.6	2.17-51.76	0.004	11.66	2.34-58.14	0.003	10.75	2.05-56.28	0.005

Model 1: Adjusted for offspring age and sex; Model 2: Further adjusted for maternal age and nulliparous; Model 3: Further adjusted for gestational diabetes mellitus status of the mothers included in the model and offspring birth weight. OR: Odds ratio; CI: Confidence interval; BMI: Body mass index.

DISCUSSION

In this prospective birth cohort, we assessed the causal association of maternal metabolic disorders with offspring overweight/obesity and fatty liver in Han Chinese populations. This study demonstrated that high maternal BMI increased the odds of both childhood overweight/obesity and fatty liver, independent of maternal age, offspring birth weight, and childhood waist circumference at 8 years of age. Furthermore, maternal pregnancy glucose concentrations were positively correlated with offspring CAP values at school age. These two findings corroborated that the negative impacts of maternal obesity and impaired glucose metabolism on offspring livers are long-term and not merely limited to infancy.

More impressively, the negative effects of maternal obesity and impaired glucose metabolism might vary in degree. A recent cohort study based on magnetic resonance imaging found that maternal early-pregnancy glucose levels were associated with a 1.95-fold increase in odds of offspring non-alcoholic fatty liver disease (NAFLD) only among mothers of European ancestry[13]. In our study, maternal blood samples were collected in the second trimester. We observed that maternal mid-pregnancy glucose levels had only a weak relation with offspring fatty liver among Han Chinese populations, while maternal obesity was more strongly associated with offspring fatty liver than GDM.

Maternal obesity and impaired glucose metabolism have lasting impacts on offspring hepatic health through epigenetic, dietary, and metabolic factors[14,15]. A sibling comparison cohort reported that maternal weight gain was aligned with the odds of offspring obesity[16], suggesting that maternal overnutrition may be a predisposing factor for offspring metabolic dysbiosis. This conclusion was also validated in some animal models, such as macaques and mice, and investigators found that reversing the high-fat diet to a low-fat diet during the subsequent pregnancy alleviated offspring hepatic lipid accumulation[17-19]. In terms of mechanisms, one study demonstrated that maternal obesity might render innate immunity dysfunctional, and another study observed that maternal obesity accelerated the progression of offspring NAFLD through activation of lipogenesis and oxidative stress pathways[20,21].

Our observations were mutually verified with previous studies and have several differences as follows. Two studies focused on the relation between maternal factors and infant hepatic fat[22,23]. Modi *et al*[23] observed that increasing maternal BMI might initiate lipid accumulation in infant livers. Subsequently, Brumbaugh and colleagues reported that infants of GDM mothers had greater hepatic steatosis than infants of non-GDM mothers[22]. In contrast, our study revealed the relatively long-term health outcomes in school-age children to corroborate that such associations might predispose children to fatty liver later in life.

Another study in obese mothers observed a positive relation with offspring ultrasound-diagnosed NAFLD during adolescence. However, ultrasound has limited power to detect mild steatosis and cannot quantify histological characteristics such as hepatic lipid content and liver stiffness. In our studies, we assessed pediatric liver pathology through TE, which is a reliable noninvasive diagnostic tool for fibrosis assessment in NAFLD[24]. Meanwhile, a biopsy-confirmed study reported that an association

Table 3 Characteristics of mothers with and without gestational diabetes mellitus and their offspring at follow-up

Variables	Mother without GDM (*n* = 382)	Mother with GDM (*n* = 48)	*P* value
Maternal characteristics			
Age, yr	29.25 ± 5.1	29.98 ± 3.17	0.172
Height, cm	163.12 ± 17.48	162.02 ± 4.96	0.336
Weight, kg	56.16 ± 9.65	61 ± 9.47	0.001
BMI, kg/m^2	21.33 ± 3.59	23.22 ± 3.28	0.000
Obesity, *n* (%)	42 (11.0)	20 (41.7)	0.000
Children characteristics			
Birth weight, kg	3.41 ± 0.45	3.37 ± 0.61	0.653
Boy, *n* (%)	186 (49.1)	25 (52.1)	0.699
Height, cm	122.19 ± 30.67	125.07 ± 25.75	0.597
Weight, kg	25.13 ± 10.28	29.15 ± 10.38	0.058
BMI, kg/m^2	15.74 ± 4.43	17.72 ± 3.94	0.024
Waist circumference, cm	58.2 ± 10.79	61.39 ± 10.23	0.148
Hip circumference, cm	68.15 ± 13.73	73.83 ± 7.94	0.003
Chest circumference, cm	54.38 ± 21.03	64.48 ± 7.96	0.000
Waist-height ratio	0.46 ± 0.05	0.47 ± 0.07	0.202
Waist-hip ratio	0.85 ± 0.08	0.83 ± 0.07	0.265
Chest-height ratio	0.43 ± 0.15	0.49 ± 0.05	0.024
CAP, dB/m	166.49 ± 45.65	187.26 ± 50.59	0.029
LSM, kPa	3.36 ± 0.75	3.53 ± 0.77	0.303
Overweight, *n* (%)	25 (6.5)	12 (25.0)	0.000
Obesity, *n* (%)	10 (2.6)	4 (8.3)	0.000
Fatty liver, *n* (%)	48 (12.6)	12 (25.0)	0.073

BMI: Body max index; GDM: Gestational diabetes mellitus; CAP: Controlled attenuation parameter; LSM: Liver stiffness measurement.

between parental obesity and offspring liver fibrosis was found in Italians[25]. As maternal impaired glucose metabolism was only related to offspring NAFLD in Europeans[13], the association between maternal obesity and progression of NAFLD in offspring may also differ across ethnic groups and the possible mechanisms need to be explored[26,27].

To the best of our knowledge, the present study is the first prospective birth cohort to assess the causal relationship between maternal metabolic dysbiosis and the odds of fatty liver in offspring. After adjustment for multiple regression models, the results were rigorous and trustworthy. Nonetheless, there are still several limitations that are worthy of discussion. First, to date, there is no widely accepted threshold of TE to detect childhood liver steatosis and fibrosis[28]. We used the 95th percentile cutoff values reported in a large health check-up cohort of preschool children as a surrogate threshold for this study[4]. Second, in this cohort, only 11.1% of mothers developed GDM during pregnancy, which reflected the true prevalence of GDM in the Chinese population. However, the small number of mothers with GDM might lead to type-2 statistical errors. Further nested case-control studies can address this issue and are recommended. Ultimately, single nucleotide polymorphisms of the patatin-like phospholipase domain containing 3, transmembrane 6 superfamily member 2, glucokinase regulatory protein, and several other susceptibility genes were not determined in this cohort. Further studies are needed to explore whether a predisposed genetic background mediates the influence of maternal metabolic dysbiosis on offspring NAFLD.

With the rapid spread of childhood fatty liver, it is urgent to develop preventive strategies against childhood fatty liver. In this regard, the current observations could be applied to the primary prevention of childhood obesity and fatty liver. The earliest timepoints of primary prevention of pediatric fatty liver could be before pregnancy. Weight management and glycemic control before and during pregnancy may help to promote liver and metabolic health status in children. Furthermore, lifestyle intervention before pregnancy is worth further investigation.

Table 4 Adjusted odds ratios for the association of maternal obesity and gestational diabetes mellitus with outcomes among children in a follow-up study

Outcomes	Risk factors	Model 1		*P* value	Model 2		*P* value	Model 3		*P* value
		OR	95%CI		OR	95%CI		OR	95%CI	
Fatty liver	Maternal obesity	4.57	1.96-10.67	0.000	4.79	2.03-11.31	0.000	4.64	1.82-11.87	0.001
	GDM	2.39	0.91-6.29	0.077	2.45	0.93-6.49	0.071	2.49	0.94-6.61	0.068
	Maternal obesity and GDM	7.19	2.15-24.13	0.001	7.72	2.25-26.46	0.001	8.26	2.38-28.75	0.001
Overweight/obesity	Maternal obesity	5.73	2.18-15.10	0.000	5.69	2.14-15.10	0.000	4.15	1.44-11.97	0.009
	GDM	4.70	1.72-12.81	0.003	4.85	1.76-13.37	0.002	4.84	1.76-13.36	0.002
	Maternal obesity and GDM	16.97	4.07-70.88	0.000	16.97	4.07-70.88	0.000	17.22	4.08-72.79	0.000

Model 1: Adjusted for offspring age and sex; Model 2: Further adjusted for maternal age and nulliparity; Model 3: Further adjusted for offspring birth weight. OR: Odds ratio; CI: Confidence interval; BMI: Body mass index; GDM: Gestational diabetes mellitus.

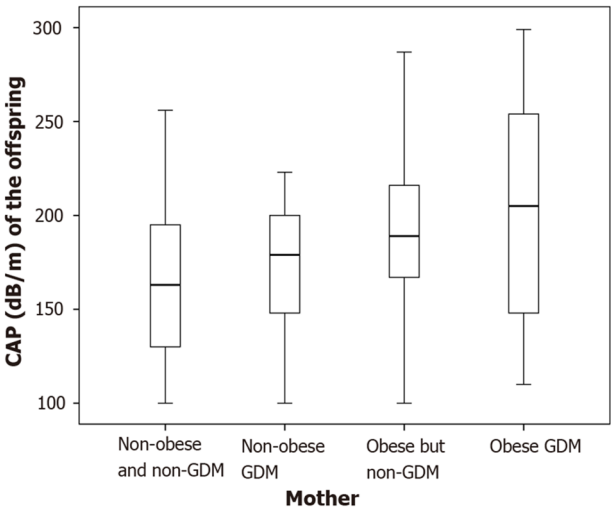

DOI: 10.3748/wjg.v28.i16.1681 **Copyright** ©The Author(s) 2022.

Figure 2 Controlled attenuation parameter values of the children of mothers with or without gestational diabetes mellitus and/or obesity. CAP: Controlled attenuation parameter; GDM: Gestational diabetes mellitus.

CONCLUSION

In this study, maternal obesity increased the odds of both fatty liver and obesity in offspring, independent of maternal age, GDM status and offspring birth weight at 8 years of age. On another note, the association between maternal GDM and childhood fatty liver trended toward significance in the Chinese population, and this association needs to be confirmed in studies with larger sample sizes. To prevent these intergenerational predisposing factors, weight management and glycemic control before and during pregnancy need to be highlighted for primary prevention of pediatric fatty liver.

ARTICLE HIGHLIGHTS

Research background

Associations were found among childhood obesity, fatty liver and adverse outcomes such as diabetes, metabolic syndrome, and cardiovascular diseases in adulthood. It is important to identify relevant risk factors and intervene as early as possible.

Research motivation

We aimed to discover the possible relationship between metabolic factors in mothers and offspring.

Research objectives
We aimed to estimate the association of maternal obesity and gestational diabetes mellitus (GDM) with overweight/obesity and fatty liver risk in offspring.

Research methods
The mothers in the study all underwent a 75 g oral glucose tolerance test at 24-28 wk of gestation, and their offspring completed follow-up at 8 years of age. An examination was prospectively conducted in offspring using a FibroScan-502 with an M probe (Echosens, Paris, France).

Research results
A total of 430 mother-child pairs were included in the analysis. The prevalence of overweight, obesity and fatty liver in offspring increased significantly across maternal BMI quartiles and among mothers with GDM (all $P < 0.05$). In the multiple logistic regression analysis, after adjustment for variables, the OR for fatty liver in offspring was 8.26 (95%CI: 2.38-28.75) for participants with maternal obesity and GDM.

Research conclusions
Maternal obesity can increase the odds of overweight/obesity and fatty liver in offspring, and GDM status also increases the odds of overweight/obesity in offspring.

Research perspectives
To prevent these intergenerational predisposing factors, weight management and glycemic control before and during pregnancy need to be emphasized for primary prevention of pediatric fatty liver.

FOOTNOTES

Author contributions: Zeng J and Shen F contributed equally to this work; Zeng J, Shen F, and Yang RX carried out the experiments; Zeng J, Shen F, Yang RX, Jin Q, Yang J, and Chen GY contributed to acquisition, analysis, or interpretation of the data; Zeng J and Zou ZY wrote the paper; Fan JG made critical revision of the manuscript for important intellectual content.

Supported by Collaborative Innovation Program of Shanghai Municipal Health Commission, No. 2020CXJQ01; National Natural Science Foundation of China, No. 81873565 and No. 82100605; SJTU Trans-med Awards Research, No. 20190104; Star Program of Shanghai Jiao Tong University, No. YG2021QN54; WBE Liver Fibrosis Foundation, No. CFHPC2020061; and Hospital Funded Clinical Research, Xinhua Hospital Affiliated to Shanghai Jiao Tong University School of Medicine, No. 17CSK04 and No. 15LC06.

Institutional review board statement: The study was reviewed and approved by the ethics committees of all hospitals involved. All procedures were performed in accordance with the ethical standards of the responsible committee on human experimentation (institutional and national) and with the Helsinki Declaration of 1975, as revised in 2008.

Informed consent statement: Informed consent was obtained from all individual participants included in the study.

Conflict-of-interest statement: The authors declare that they have no conflict of interest.

Data sharing statement: No additional data are available.

Open-Access: This article is an open-access article that was selected by an in-house editor and fully peer-reviewed by external reviewers. It is distributed in accordance with the Creative Commons Attribution NonCommercial (CC BY-NC 4.0) license, which permits others to distribute, remix, adapt, build upon this work non-commercially, and license their derivative works on different terms, provided the original work is properly cited and the use is non-commercial. See: http://creativecommons.org/Licenses/by-nc/4.0/

Country/Territory of origin: China

ORCID number: Jing Zeng 0000-0001-7764-155X; Feng Shen 0000-0001-7782-2211; Zi-Yuan Zou 0000-0001-9566-5045; Rui-Xu Yang 0000-0001-9384-6408; Qian Jin 0000-0002-6077-9437; Jing Yang 0000-0001-8255-1903; Guang-Yu Chen 0000-0002-9564-8971; Jian-Gao Fan 0000-0001-7443-5056.

S-Editor: Yan JP
L-Editor: A
P-Editor: Yan JP

REFERENCES

1 **NCD Risk Factor Collaboration (NCD-RisC)**. Worldwide trends in body-mass index, underweight, overweight, and obesity from 1975 to 2016: a pooled analysis of 2416 population-based measurement studies in 128·9 million children, adolescents, and adults. *Lancet* 2017; **390**: 2627-2642 [PMID: 29029897 DOI: 10.1016/S0140-6736(17)32129-3]

2 **Pothuraju R**, Rachagani S, Junker WM, Chaudhary S, Saraswathi V, Kaur S, Batra SK. Pancreatic cancer associated with obesity and diabetes: an alternative approach for its targeting. *J Exp Clin Cancer Res* 2018; **37**: 319 [PMID: 30567565 DOI: 10.1186/s13046-018-0963-4]

3 **Sonntag D**. Why Early Prevention of Childhood Obesity Is More Than a Medical Concern: A Health Economic Approach. *Ann Nutr Metab* 2017; **70**: 175-178 [PMID: 28301840 DOI: 10.1159/000456554]

4 **Zeng J**, Zhang X, Sun C, Pan Q, Lu WY, Chen Q, Huang LS, Fan JG. Feasibility study and reference values of FibroScan 502 with M probe in healthy preschool children aged 5 years. *BMC Pediatr* 2019; **19**: 129 [PMID: 31018838 DOI: 10.1186/s12887-019-1487-6]

5 **Drake AJ**, Reynolds RM. Impact of maternal obesity on offspring obesity and cardiometabolic disease risk. *Reproduction* 2010; **140**: 387-398 [PMID: 20562299 DOI: 10.1530/REP-10-0077]

6 **Tyrrell J**, Richmond RC, Palmer TM, Feenstra B, Rangarajan J, Metrustry S, Cavadino A, Paternoster L, Armstrong LL, De Silva NM, Wood AR, Horikoshi M, Geller F, Myhre R, Bradfield JP, Kreiner-Møller E, Huikari V, Painter JN, Hottenga JJ, Allard C, Berry DJ, Bouchard L, Das S, Evans DM, Hakonarson H, Hayes MG, Heikkinen J, Hofman A, Knight B, Lind PA, McCarthy MI, McMahon G, Medland SE, Melbye M, Morris AP, Nodzenski M, Reichetzeder C, Ring SM, Sebert S, Sengpiel V, Sørensen TI, Willemsen G, de Geus EJ, Martin NG, Spector TD, Power C, Järvelin MR, Bisgaard H, Grant SF, Nohr EA, Jaddoe VW, Jacobsson B, Murray JC, Hocher B, Hattersley AT, Scholtens DM, Davey Smith G, Hivert MF, Felix JF, Hyppönen E, Lowe WL Jr, Frayling TM, Lawlor DA, Freathy RM; Early Growth Genetics (EGG) Consortium. Genetic Evidence for Causal Relationships Between Maternal Obesity-Related Traits and Birth Weight. *JAMA* 2016; **315**: 1129-1140 [PMID: 26978208 DOI: 10.1001/jama.2016.1975]

7 **Kim C**. Gestational diabetes: risks, management, and treatment options. *Int J Womens Health* 2010; **2**: 339-351 [PMID: 21151681 DOI: 10.2147/IJWH.S13333]

8 **Wang J**, Wang L, Liu H, Zhang S, Leng J, Li W, Zhang T, Li N, Baccarelli AA, Hou L, Hu G. Maternal gestational diabetes and different indicators of childhood obesity: a large study. *Endocr Connect* 2018; **7**: 1464-1471 [PMID: 30508416 DOI: 10.1530/EC-18-0449]

9 **Dabelea D**. The predisposition to obesity and diabetes in offspring of diabetic mothers. *Diabetes Care* 2007; **30** Suppl 2: S169-S174 [PMID: 17596467 DOI: 10.2337/dc07-s211]

10 **Cho Y**, Tokuhara D, Morikawa H, Kuwae Y, Hayashi E, Hirose M, Hamazaki T, Tanaka A, Kawamura T, Kawada N, Shintaku H. Transient Elastography-Based Liver Profiles in a Hospital-Based Pediatric Population in Japan. *PLoS One* 2015; **10**: e0137239 [PMID: 26398109 DOI: 10.1371/journal.pone.0137239]

11 **Obstetrics and gynecology branch of Chinese medical association**; Perinatal Medicine Branch of Chinese Medical Association. Guidelines for the diagnosis and treatment of pregnancy complicated with diabetes. *honghua Fuchanke Zazhi* 2014; **8**: 561-569 [DOI: 10.3760/cma.j.issn.0529-567x.2014.08.001]

12 **Cole TJ**, Bellizzi MC, Flegal KM, Dietz WH. Establishing a standard definition for child overweight and obesity worldwide: international survey. *BMJ* 2000; **320**: 1240-1243 [PMID: 10797032 DOI: 10.1136/bmj.320.7244.1240]

13 **Geurtsen ML**, Wahab RJ, Felix JF, Gaillard R, Jaddoe VWV. Maternal Early-Pregnancy Glucose Concentrations and Liver Fat Among School-Age Children. *Hepatology* 2021; **74**: 1902-1913 [PMID: 34008183 DOI: 10.1002/hep.31910]

14 **Nobili V**, Alisi A, Valenti L, Miele L, Feldstein AE, Alkhouri N. NAFLD in children: new genes, new diagnostic modalities and new drugs. *Nat Rev Gastroenterol Hepatol* 2019; **16**: 517-530 [PMID: 31278377 DOI: 10.1038/s41575-019-0169-z]

15 **Goldner D**, Lavine JE. Nonalcoholic Fatty Liver Disease in Children: Unique Considerations and Challenges. *Gastroenterology* 2020; **158**: 1967-1983.e1 [PMID: 32201176 DOI: 10.1053/j.gastro.2020.01.048]

16 **Lawlor DA**, Lichtenstein P, Fraser A, Långström N. Does maternal weight gain in pregnancy have long-term effects on offspring adiposity? *Am J Clin Nutr* 2011; **94**: 142-148 [PMID: 21562086 DOI: 10.3945/ajcn.110.009324]

17 **McCurdy CE**, Bishop JM, Williams SM, Grayson BE, Smith MS, Friedman JE, Grove KL. Maternal high-fat diet triggers lipotoxicity in the fetal livers of nonhuman primates. *J Clin Invest* 2009; **119**: 323-335 [PMID: 19147984 DOI: 10.1172/JCI32661]

18 **Gregorio BM**, Souza-Mello V, Carvalho JJ, Mandarim-de-Lacerda CA, Aguila MB. Maternal high-fat intake predisposes nonalcoholic fatty liver disease in C57BL/6 offspring. *Am J Obstet Gynecol* 2010; **203**: 495.e1-495.e8 [PMID: 20822767 DOI: 10.1016/j.ajog.2010.06.042]

19 **Oben JA**, Mouralidarane A, Samuelsson AM, Matthews PJ, Morgan ML, McKee C, Soeda J, Fernandez-Twinn DS, Martin-Gronert MS, Ozanne SE, Sigala B, Novelli M, Poston L, Taylor PD. Maternal obesity during pregnancy and lactation programs the development of offspring non-alcoholic fatty liver disease in mice. *J Hepatol* 2010; **52**: 913-920 [PMID: 20413174 DOI: 10.1016/j.jhep.2009.12.042]

20 **Mouralidarane A**, Soeda J, Visconti-Pugmire C, Samuelsson AM, Pombo J, Maragkoudaki X, Butt A, Saraswati R, Novelli M, Fusai G, Poston L, Taylor PD, Oben JA. Maternal obesity programs offspring nonalcoholic fatty liver disease by innate immune dysfunction in mice. *Hepatology* 2013; **58**: 128-138 [PMID: 23315950 DOI: 10.1002/hep.26248]

21 **Bruce KD**, Cagampang FR, Argenton M, Zhang J, Ethirajan PL, Burdge GC, Bateman AC, Clough GF, Poston L, Hanson MA, McConnell JM, Byrne CD. Maternal high-fat feeding primes steatohepatitis in adult mice offspring, involving mitochondrial dysfunction and altered lipogenesis gene expression. *Hepatology* 2009; **50**: 1796-1808 [PMID: 19816994 DOI: 10.1002/hep.23205]

22 **Brumbaugh DE**, Tearse P, Cree-Green M, Fenton LZ, Brown M, Scherzinger A, Reynolds R, Alston M, Hoffman C, Pan Z, Friedman JE, Barbour LA. Intrahepatic fat is increased in the neonatal offspring of obese women with gestational diabetes. *J Pediatr* 2013; **162**: 930-6.e1 [PMID: 23260099 DOI: 10.1016/j.jpeds.2012.11.017]

23 **Modi N**, Murgasova D, Ruager-Martin R, Thomas EL, Hyde MJ, Gale C, Santhakumaran S, Doré CJ, Alavi A, Bell JD. The influence of maternal body mass index on infant adiposity and hepatic lipid content. *Pediatr Res* 2011; **70**: 287-291 [PMID: 21629154 DOI: 10.1203/PDR.0b013e318225f9b1]

24 **Serra-Burriel M**, Graupera I, Torán P, Thiele M, Roulot D, Wai-Sun Wong V, Neil Guha I, Fabrellas N, Arslanow A, Expósito C, Hernández R, Lai-Hung Wong G, Harman D, Darwish Murad S, Krag A, Pera G, Angeli P, Galle P, Aithal GP, Caballeria L, Castera L, Ginès P, Lammert F; investigators of the LiverScreen Consortium. Transient elastography for screening of liver fibrosis: Cost-effectiveness analysis from six prospective cohorts in Europe and Asia. *J Hepatol* 2019; **71**: 1141-1151 [PMID: 31470067 DOI: 10.1016/j.jhep.2019.08.019]

25 **Mosca A**, De Cosmi V, Parazzini F, Raponi M, Alisi A, Agostoni C, Nobili V. The Role of Genetic Predisposition, Programing During Fetal Life, Family Conditions, and Post-natal Diet in the Development of Pediatric Fatty Liver Disease. *J Pediatr* 2019; **211**: 72-77.e4 [PMID: 31128886 DOI: 10.1016/j.jpeds.2019.04.018]

26 **Popova P**, Vasilyeva L, Tkachuck A, Puzanov M, Golovkin A, Bolotko Y, Pustozerov E, Vasilyeva E, Li O, Zazerskaya I, Dmitrieva R, Kostareva A, Grineva E. A Randomised, Controlled Study of Different Glycaemic Targets during Gestational Diabetes Treatment: Effect on the Level of Adipokines in Cord Blood and ANGPTL4 Expression in Human Umbilical Vein Endothelial Cells. *Int J Endocrinol* 2018; **2018**: 6481658 [PMID: 29861725 DOI: 10.1155/2018/6481658]

27 **Popova PV**, Vasileva LB, Tkachuk AS, Puzanov MV, Bolotko YA, Pustozerov EA, Gerasimov AS, Zazerskaya IE, Li OA, Vasilyeva EY, Kostareva AA, Dmitrieva RI, Grineva EN. Association of tribbles homologue 1 gene expression in human umbilical vein endothelial cells with duration of intrauterine exposure to hyperglycaemia. *Genet Res (Camb)* 2018; **100**: e3 [PMID: 29502537 DOI: 10.1017/S0016672318000010]

28 **Vos MB**, Abrams SH, Barlow SE, Caprio S, Daniels SR, Kohli R, Mouzaki M, Sathya P, Schwimmer JB, Sundaram SS, Xanthakos SA. NASPGHAN Clinical Practice Guideline for the Diagnosis and Treatment of Nonalcoholic Fatty Liver Disease in Children: Recommendations from the Expert Committee on NAFLD (ECON) and the North American Society of Pediatric Gastroenterology, Hepatology and Nutrition (NASPGHAN). *J Pediatr Gastroenterol Nutr* 2017; **64**: 319-334 [PMID: 28107283 DOI: 10.1097/MPG.0000000000001482]

World Journal of Gastroenterology

Submit a Manuscript: https://www.f6publishing.com

World J Gastroenterol 2022 April 28; 28(16): 1692-1704

DOI: 10.3748/wjg.v28.i16.1692

ISSN 1007-9327 (print) ISSN 2219-2840 (online)

ORIGINAL ARTICLE

Retrospective Study

Evaluating the accuracy of American Society for Gastrointestinal Endoscopy guidelines in patients with acute gallstone pancreatitis with choledocholithiasis

Supisara Tintara, Ishani Shah, William Yakah, Awais Ahmed, Cristina S Sorrento, Cinthana Kandasamy, Steven D Freedman, Darshan J Kothari, Sunil G Sheth

Specialty type: Gastroenterology and hepatology

Provenance and peer review: Invited article; Externally peer reviewed.

Peer-review model: Single blind

Peer-review report's scientific quality classification

Grade A (Excellent): 0
Grade B (Very good): B, B
Grade C (Good): 0
Grade D (Fair): 0
Grade E (Poor): 0

P-Reviewer: Chow WK, Taiwan; Miyabe K, Japan

Received: December 10, 2021
Peer-review started: December 10, 2021
First decision: January 27, 2022
Revised: February 7, 2022
Accepted: March 16, 2022
Article in press: March 16, 2022
Published online: April 28, 2022

Supisara Tintara, Cristina S Sorrento, Cinthana Kandasamy, Department of Internal Medicine, Beth Israel Deaconess Medical Center, Harvard Medical School, Boston, MA 02215, United States

Ishani Shah, William Yakah, Awais Ahmed, Steven D Freedman, Sunil G Sheth, Division of Gastroenterology & Hepatology, Beth Israel Deaconess Medical Center, Harvard Medical School, Boston, MA 02215, United States

Darshan J Kothari, Division of Gastroenterology, Duke University Medical Center, Durham, NC 27710, United States

Darshan J Kothari, Division of Gastroenterology, Durham VA Medical Center, Durham, NC 27705, United States

Corresponding author: Sunil G Sheth, AGAF, FACG, FASGE, MBBS, MD, Associate Professor, Division of Gastroenterology & Hepatology, Beth Israel Deaconess Medical Center, Harvard Medical School, 330 Brookline Ave, Boston, MA 02215, United States.
ssheth@bidmc.harvard.edu

Abstract

BACKGROUND

Acute gallstone pancreatitis (AGP) is the most common cause of acute pancreatitis (AP) in the United States. Patients with AGP may also present with choledocholithiasis. In 2010, the American Society for Gastrointestinal Endoscopy (ASGE) suggested a management algorithm based on probability for choledocholithiasis, recommending additional imaging for patients at intermediate risk and endoscopic retrograde cholangiopancreatography (ERCP) for patients at high risk of choledocholithiasis. In 2019, the ASGE guidelines were updated using more specific criteria to categorize individuals at high risk for choledocholithiasis. Neither ASGE guideline has been studied in AGP to determine the probability of having choledocholithiasis.

AIM

To determine compliance with ASGE guidelines, assess outcomes, and compare

2019 *vs* 2010 ASGE criteria for suspected choledocholithiasis in AGP.

METHODS

We conducted a retrospective cohort study of 882 patients admitted with AP to a single tertiary care center from 2008-2018. AP was diagnosed using revised Atlanta criteria and AGP was defined as the presence of gallstones on imaging or with cholestatic pattern of liver injury in the absence of another cause. Patients with chronic pancreatitis and pancreatic malignancy were excluded as were those who went directly to cholecystectomy prior to assessment for choledocholithiasis. Patients were assigned low, intermediate or high risk based on ASGE guidelines. Our primary outcomes of interest were the proportion of patients in the intermediate risk group undergoing magnetic resonance cholangiopancreatography (MRCP) first and the proportion of patients in the high risk group undergoing ERCP directly without preceding imaging. Secondary outcomes of interest included outcome differences based on if guidelines were not adhered to. We then evaluated the diagnostic accuracy of 2019 in comparison to the 2010 ASGE criteria for patients with suspected choledocholithiasis. We performed the *t* test or Wilcoxon rank sum test, as appropriate, to analyze if there were outcome differences based on if guidelines were not adhered to. Kappa coefficients were calculated to measure the degree of agreement between pairs of variables.

RESULTS

In this cohort, we identified 235 patients with AGP of which 79 patients were excluded as they went directly to surgery for cholecystectomy without prior MRCP or ERCP. Of the remaining 156 patients, 79 patients were categorized as intermediate risk and 77 patients were high risk for choledocholithiasis according to the 2010 ASGE guidelines. Among 79 intermediate risk patients, 54 (68%) underwent MRCP first whereas 25 patients (32%) went directly to ERCP. For the 54 patients with intermediate risk who had MRCP first, 36 patients had no choledocholithiasis while 18 patients had evidence of choledocholithiasis prompting ERCP. Of these patients, ERCP confirmed stone disease in 11 patients. Of the 25 intermediate risk patients who directly underwent ERCP, 18 patients had stone disease. One patient with a normal ERCP developed post ERCP pancreatitis. Patients undergoing MRCP in this group had a significantly longer length of stay (5.0 *vs* 4.0 d, $P = 0.02$). In the high risk group, 64 patients (83%) had ERCP without preceding imaging, of which, 53 patients had findings consistent with choledocholithiasis, of which 13 patients (17%) underwent MRCP before ERCP, all of which showed evidence of stone disease. Furthermore, all of these patients ultimately had an ERCP, of which 8 patients had evidence of stones and 5 had normal examination.

RESULTS

Our cohort also demonstrated that 58% of all 156 patients with AGP had confirmed choledocholithiasis (79% of the high risk group and 37% of the intermediate group when risk was assigned based on the 2010 ASGE guidelines). When the updated 2019 ASGE guidelines were applied instead of the original 2010 guidelines, there was moderate agreement between the 2010 and 2019 guidelines (kappa = 0.46, 95%CI: 0.34-0.58). Forty-two of 77 patients were still deemed to be high risk and 35 patients were downgraded to intermediate risk. Thirty-five patients who were originally assigned high risk were reclassified as intermediate risk. For these 35 patients, 26 patients had ERCP findings consistent with choledocholithiasis and 9 patients had a normal examination. Based on the 2019 criteria, 9/35 patients who were downgraded to intermediate risk had an unnecessary ERCP with normal findings (without a preceding MRCP).

CONCLUSION

Two-thirds in intermediate risk and 83% in high risk group followed ASGE guidelines for choledocholithiasis. One intermediate-group patient with normal ERCP had post-ERCP AP, highlighting the risk of unnecessary procedures.

Key Words: American Society for Gastrointestinal Endoscopy guidelines; Choledocholithiasis; Acute gallstone pancreatitis; Endoscopic retrograde cholangiopancreatography; Magnetic resonance cholangiopancreatography

©The Author(s) 2022. Published by Baishideng Publishing Group Inc. All rights reserved.

Core Tip: We demonstrated that more than half of patients with acute gallstone pancreatitis (AGP) have choledocholithiasis. We also found that approximately 2/3 of patients in the intermediate group and 83% of patients in the high risk group followed American Society for Gastrointestinal Endoscopy guidelines for management of choledocholithiasis in the setting of AGP. There was associated longer length of stay for patients undergoing magnetic resonance cholangiopancreatography (MRCP) in both groups. Importantly, one patient who had a normal endoscopic retrograde cholangiopancreatography (ERCP) in the intermediate group without preceding MRCP suffered from post ERCP pancreatitis, highlighting the risk of unnecessary procedures.

Citation: Tintara S, Shah I, Yakah W, Ahmed A, Sorrento CS, Kandasamy C, Freedman SD, Kothari DJ, Sheth SG. Evaluating the accuracy of American Society for Gastrointestinal Endoscopy guidelines in patients with acute gallstone pancreatitis with choledocholithiasis. *World J Gastroenterol* 2022; 28(16): 1692-1704
URL: https://www.wjgnet.com/1007-9327/full/v28/i16/1692.htm
DOI: https://dx.doi.org/10.3748/wjg.v28.i16.1692

INTRODUCTION

Acute gallstone pancreatitis (AGP) is the most common cause of acute pancreatitis (AP) in the United States[1]. Patients with AGP may also present with choledocholithiasis as the occurrence of common bile duct (CBD) stones is present in up to 15% of patients with gallstones[2]. The diagnosis of choledocholithiasis is challenging and requires a high degree of suspicion as it often cannot be made conclusively without invasive procedures like endoscopic retrograde cholangiopancreatography (ERCP)[3]. In 2010, the American Society for Gastrointestinal Endoscopy (ASGE) suggested a management algorithm based on probability for choledocholithiasis to assist in risk stratifying patients[4]. These guidelines stratify patients into those with high, intermediate, and low risk based on clinical criteria, liver tests, and abdominal ultrasound. High risk (> 50% probability of choledocholithiasis) is defined as the presence of any very strong predictor (clinical ascending cholangitis, CBD stone seen on ultrasound, and/or total bilirubin > 4 mg/dL) or the presence of both strong predictors (CBD dilated more than 6 mm and bilirubin 1.8-4 mg/dL). Intermediate risk (10%-50% probability of choledocholithiasis) is defined as presence of age > 55, clinical gallstone pancreatitis, any other abnormal liver test. Finally, low risk patients do not have any of these features[4].

These guidelines aim to provide evidence-based recommendations with the goal of optimizing the efficacy and safety of patient care by minimizing the morbidity and cost from unnecessary invasive biliary evaluation. Furthermore, they recommend imaging [*i.e.* magnetic resonance cholangiopancreatography (MRCP) or endoscopic ultrasound (EUS)] for patients with intermediate risk and ERCP for patients with high probability of choledocholithiasis[4].

In 2019, the ASGE guidelines were updated using more specific criteria to categorize individuals at high-risk for choledocholithiasis[5]. These updated criteria propose that high-risk patients are those with elevated total bilirubin > 4 mg/dL and dilated CBD. The presence of only elevated total bilirubin > 4 or total bilirubin 1.8-4 with dilated CBD are no longer in the criteria for the high-risk group. These guidelines still recommend ERCP for those with high risk and imaging (MRCP or EUS) for those with intermediate risk for choledocholithiasis[6]. Additionally, clinical gallstone pancreatitis was removed as one of the criteria for assigning intermediate risk[6].

Neither ASGE guideline has been studied in AGP to determine the probability of having choledocholithiasis. Thus, our study aimed to determine the true incidence of choledocholithiasis in patients with AGP and determine compliance with the guidelines at our institution and assess outcomes when guidelines were not adhered to. In our patient population of AGP, we also evaluated the performance and diagnostic accuracy of 2019 *vs* 2010 ASGE criteria for suspected choledocholithiasis in patients with AGP.

MATERIALS AND METHODS

Data source, patient selection and study design

This retrospective observational cohort study was approved by Beth Israel Deaconess Medical Center institutional review board. This manuscript adheres to the applicable STROBE reporting guidelines for cohort studies.

We performed a review of all adult (age > 18) patients with a discharge diagnosis of AP who were admitted to our tertiary center between January 1, 2008 and December 31, 2018. The diagnosis of AP was confirmed by a review of the electronic medical record to ensure all patients met the 2012 Revised

Atlanta Criteria for the diagnosis of AP (at least two of the following three criteria: epigastric pain, elevation of serum lipase level > three times the upper limit of normal, and/or evidence of pancreatitis on cross-sectional imaging)[7]. Patients with chronic pancreatitis or known pancreatic malignancy were excluded from the study. AGP was defined as the presence of gallstones on imaging or with cholestatic pattern of liver injury in the absence of another cause. Patients who directly went to surgery for cholecystectomy without having either MRCP or ERCP were excluded.

Several parameters including demographic, clinical, laboratory, and radiologic data of the study population were collected. The severity of AP was defined based on the 2012 Revised Atlanta Criteria with mild defined as AP without any local or systemic complications, moderately severe as AP with transient (< 48 h) end-organ failure with or without local complications), and severe as AP with persistent (> 48 h) end-organ damage with or without local complications)[7]. The severity of AP in each patient was also characterized based on the bedside index for severity of AP (BISAP) score[8,9].

Study groups and outcomes of interest

Our cohort of interest was divided based on their risk for choledocholithiasis. These included: low, intermediate or high risk based on the 2010 ASGE guidelines. Since the guidelines defined AGP as at least intermediate risk, no patients were in the low risk category, thus leaving only two groups. We then compared demographic characteristics, comorbidities, and outcomes between the two groups.

Our primary outcomes of interest were the proportion of patients in the intermediate risk group undergoing MRCP first and the proportion of patients in the high risk group undergoing ERCP directly without preceding imaging. Secondary outcomes of interest included outcome differences based on if guidelines were not adhered to. We then evaluated the diagnostic accuracy of the 2019 in comparison to the 2010 ASGE criteria for patients with suspected choledocholithiasis. Additionally, we calculated the sensitivity and specificity of the 2010 and 2019 ASGE guidelines for patients categorized as high risk and intermediate risk for choledocholithiasis. Evidence of choledocholithiasis on ERCP was used as the gold standard for true positives.

Statistical analysis

All data analysis was performed using R software (version 3.6.1, R Core Team 2018a) within RStudio (version 1.1463, RStudio, Inc) *via* the tidyverse (Wickham, 2017) package. Continuous variables were presented as means with range and standard deviation. These were analyzed using the *t*-test or Wilcoxon rank sum test, as appropriate. Categorical variables were presented as frequencies (%) and analyzed using the Pearson χ^2 test or Fisher's exact test, as deemed appropriate. Univariate analyses comparing several characteristics and outcomes between the two groups were performed. A significant *P* value was assigned at 0.05. To determine concordance between the 2019 and 2010 guidelines, Kappa coefficients were calculated to measure the degree of agreement between pairs of variables.

RESULTS

Patient characteristics

In our cohort, 882 patients with AP were hospitalized of which 235 patients had AGP. Seventy-nine patients were excluded as they went directly to surgery for cholecystectomy without prior MRCP or ERCP. These 79 patients had mild AP with resolution of abdominal pain and rapid normalization of liver enzymes suggesting that CBD stones had likely already passed. Moreover, these patients had abdominal ultrasound that showed normal size CBD. Thus, these patients directly underwent cholecystectomy without preceding ERCP or MRCP.

Of the remaining 156 patients, 79 patients were categorized as intermediate risk (Tables 1 and 2) and 77 patients were high risk (Tables 3 and 4) for choledocholithiasis according to the 2010 ASGE guidelines.

Baseline characteristics and demographics are summarized in Table 5. When comparing demographics between the intermediate risk and high risk groups, there was no difference in age, gender, race, Charlson Comorbidity Index, severity of pancreatitis and baseline BISAP. Patients in the high risk group had a higher BMI than those in the intermediate group (29.0 *vs* 29.6, $P = 0.05$). While most of the baseline laboratory data were similar in both groups, total bilirubin was significantly higher in the high risk group (4.04 mg/dL *vs* 1.32 mg/dL, $P < 0.01$). Further, alanine aminotransferase and alkaline phosphatase were higher in the high risk groups and approached significance (335 IU/L *vs* 241 IU/L, $P = 0.06$ and 196 IU/L *vs* 156 IU/L, $P = 0.07$, respectively) (Table 5).

Intermediate risk

Seventy-nine patients were assigned to have intermediate risk of choledocholithiasis based on the 2010 ASGE criteria. In this group, 45 were older than 55 years-old, 73 had abnormal liver tests and 22 had dilated CBD or total bilirubin of 1.8-4.0mg/dL (Table 1). Thirty-three patients met all 4 criteria for intermediate risk group, while 45 patients met 3 criteria, 1 patient met 2 criteria and no patients met

Table 1 Patients categorized as intermediate risk for choledocholithiasis, *n* = 79

	Number of patients meeting criteria
Dilated common bile duct greater than 6 mm or total bilirubin 1.8-4.0 mg/dL (only one)	22
Abnormal liver biochemical other than bilirubin	73
Age greater than 55 yr	45
Acute gallstone pancreatitis	79

Table 2 Number of criteria met for patients categorized as intermediate risk for choledocholithiasis, *n* = 79

	Number of patients
1 criterion	0
2 criteria	1
3 criteria	45
4 criteria	33

Table 3 Patients categorized as high risk for choledocholithiasis, *n* = 77

	Numbers patients meeting criteria
Cholangitis	1
Common bile duct stone on imaging	12
Total Bilirubin greater than 4.0 mg/dL	38
Dilated common bile duct greater than 6 mm and total bilirubin 1.8-4.0 mg/dL	31

Table 4 Number of criteria met for patients categorized as high risk for choledocholithiasis, *n* = 77

	Number of patients
1 criterion	75
2 criteria	2
3 criteria	0
4 criteria	0

only 1 criterion (Table 2).

Among 79 intermediate risk patients, 54 (68%) underwent MRCP first whereas 25 patients (32%) went directly to ERCP (Figure 1). For the 54 patients with intermediate risk who had MRCP first, 18 patients had evidence of choledocholithiasis prompting ERCP, while 36 patients had imaging that did not show choledocholithiasis. Of the 18 patients undergoing ERCP after MRCP, 11 patients had choledocholithiasis, whereas 7 patients had normal examinations. There were no complications from ERCP noted in this group.

Of the 25 intermediate risk patients who directly underwent ERCP, 18 patients had choledocholithiasis whereas 7 patients had a normal ERCP (Figure 1). Notably, one of these patients with a normal ERCP developed post ERCP pancreatitis. Patients undergoing MRCP first in this group had a significantly longer length of stay (LOS, 5.0 *vs* 4.0 d, P = 0.02). They also had higher incidence of pancreatic necrosis (33% *vs* 8%, P = 0.03) and higher rate of 1-year readmission (52% *vs* 20%, P = 0.02) (Table 6). There were multiple causes of readmissions in our cohort such as diverticulitis, autonomic dysfunction, pneumonia and urinary tract infection. The 1-year readmission rates for recurrence of acute gallstone pancreatitis or choledocholithiasis were 9% for patients who had MRCP first and 8% for those who directly underwent ERCP, likely because some of them refused or did not undergo cholecystectomy.

High risk

Seventy-seven patients were assigned to have high risk of choledocholithiasis based on the 2010 ASGE

Table 5 Demographics of gallstone pancreatitis patients with intermediate and high risk for choledocholithiasis

	Intermediate risk (*n* = 79)	High risk (*n* = 77)	*P* value
Age (yr) mean ± SD	58.6 ± 19.2	58.1 ± 17.3	0.86
BMI (kg/m^2) mean ± SD	29.0 ± 6.83	29.6 ± 9.82	0.05
Female	44 (60%)	45 (58%)	0.95
Race			0.70
White	50 (72%)	51 (68%)	
Black	15 (22%)	15 (20%)	
Other	4 (6%)	9 (12%)	
Charlson Comorbidity Index			0.60
0	17 (23%)	19 (25%)	
1 to 2	24 (33%)	20 (26%)	
3 to 5	21 (29%)	29 (38%)	
6 and above	11 (15%)	9 (12%)	
Baseline laboratory			
Creatinine (mg/dL) mean ± SD	0.98 ± 0.55	0.94 ± 0.68	0.71
White blood cell count (K/L) mean ± SD	11.4 ± 4.64	12.1 ± 7.27	0.49
Lactate (mmol/L) mean ± SD	1.60 ± 1.33	1.75 ± 1.44	0.63
Lipase (IU/L) mean ± SD	4012 ± 5264	3576 ± 4699	0.60
ALT (IU/L) mean ± SD	241 ± 269	335 ± 324	0.06
AST (IU/L) mean ± SD	232 ± 280	294 ± 269	0.18
Alkaline phosphatase (IU/L) mean ± SD	156 ± 130	196 ± 140	0.07
Total bilirubin (mg/dL) mean ± SD	1.32 ± 0.78	4.04 ± 2.06	< 0.01
Presence of gallstone on imaging	79 (100%)	77 (100%)	0.91
Severity of pancreatitis			
Mean BISAP ± SD	0.90 ± 0.91	0.88 ± 0.88	0.90
Modified Atlanta Criteria			0.13
Mild	57 (72%)	63 (83%)	
Moderate	21 (27%)	10 (13%)	
Severe	1 (1%)	3 (4%)	

BMI: Body mass index; ALT: Alanine aminotransferase; AST: Aspartate aminotransferase; BISAP: Bedside index of severity in acute pancreatitis.

criteria. In this group, 1 patient was suspected to have cholangitis, 38 patients had total bilirubin > 4.0 mg/dL, 12 patients had CBD stone on imaging, and 31 patients had dilated CBD with total bilirubin 1.8-4.0 mg/dL (Table 3). Seventy-five patients met 1 criterion for high risk group and 2 patients met 2 criteria. No patient met 3 or more criteria (Table 4).

In this group, 64 patients (83%) had ERCP without preceding imaging, of which, 53 patients had findings consistent with choledocholithiasis (27 patients with stones and 26 patients with sludge) while 10 had a normal examination (Figure 2). In comparison, 13 patients in this group (17%) underwent MRCP before ERCP, all of which showed evidence of stone disease. Furthermore, all of these patients ultimately had an ERCP, of which 8 patients had evidence of choledocholithiasis and 5 had normal examination (Figure 2). Two of the 13 patients who underwent imaging first due to altered luminal anatomy and body habitus. For the remaining 11 patients, there was no identifiable reason for not directly proceeding to ERCP.

As with the intermediate group, for the high risk group, the MRCP-first group had longer LOS compared to ERCP-first group which approached significance (4.28 *vs* 3.00 days, $P = 0.08$). There were no significant differences in outcomes such as readmission rate, 1-year mortality between the two groups (Table 6).

Table 6 Outcomes of patients with intermediate and high risk for choledocholithiasis

	Intermediate risk (*n* = 79)			High risk (*n* = 77)		
Outcomes	**ERCP first (*n* = 25)**	**MRCP first (*n* = 54)**	***P* value**	**ERCP first (*n* = 64)**	**MRCP first (*n* = 13)**	***P* value**
Mean length of stay (Q1; Q3)	4.00 (2.74; 5.00)	5.00 (4.00; 8.00)	0.02	3.00 (2.54; 5.00)	4.38 (4.00; 6.00)	0.08
30-d readmission (%)	3 (12.0%)	11 (20.8%)	0.53	6 (9.52%)	2 (16.7%)	0.61
1-yr readmission (%)	5 (20.0%)	28 (51.9%)	0.02	19 (29.7%)	7 (53.8%)	0.11
1-yr mortality (%)	0 (0.00%)	1 (1.85%)	0.09	1 (1.56%)	0 (0.00%)	1.00
Pancreas necrosis (%)	2 (8.0%)	18 (33.3%)	0.03	6 (10.7%)	3 (35.0%)	0.19
Days to enteral nutrition (Q1; Q3)	2.00 (1.00; 2.50)	2.50 (1.00; 4.00)	0.16	2.00 (1.00; 2.00)	3.00 (2.00; 4.00)	0.10

ERCP: Endoscopic retrograde cholangiopancreatography; MRCP: Magnetic resonance cholangiopancreatography.

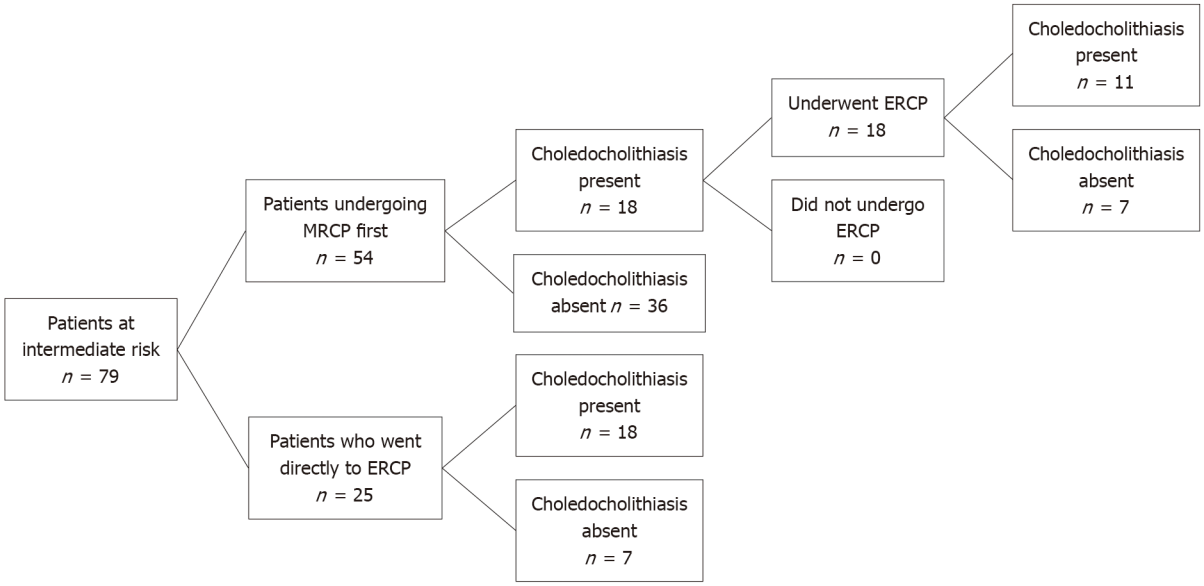

DOI: 10.3748/wjg.v28.i16.1692 **Copyright** ©The Author(s) 2022.

Figure 1 Patients at intermediate risk for choledocholithiasis. MRCP: Magnetic resonance cholangiopancreatography; ERCP: Endoscopic retrograde cholangiopancreatography.

Incidence of confirmed choledocholithiasis in patients with AGP

Our cohort also demonstrated that of all 156 patients with AGP, 90 (58%) were found to have choledocholithiasis on ERCP. When stratified by assigned choledocholithiasis risk based on the 2010 ASGE guidelines, 61 of 77 patients in the high risk group (79%) and 29 of 79 patients in the intermediate risk group (37%) were found to have choledocholithiasis (Figure 3).

Comparison to the 2019 ASGE guidelines

Our cohort of patients was admitted to the hospital between 2008 and 2018, thus the 2010 ASGE guideline were used in the above analysis. We then applied the 2019 criteria to this group to see how results may have changed. There was moderate agreement between the classifications by the 2010 and 2019 guidelines (kappa = 0.46, 95%CI: 0.34-0.58). When the 2019 ASGE guidelines were applied to our 79 patients with intermediate risk for choledocholithiasis, all of these patients were still assigned intermediate risk. Among the 77 patients in the high risk group, when the updated 2019 ASGE guidelines were applied instead of the original 2010 guidelines, 42 patients were still deemed to be high risk and 35 patients were downgraded to intermediate risk. In the high risk group, 34 of 42 who still remained high risk went directly to ERCP of which showed 28 patients had a confirmatory findings of choledocholithiasis and 5 patients had a normal examination (Figure 4).

Thirty-five patients who were originally assigned high risk were then reclassified as intermediate risk (Figure 4). For these 35 patients, 26 patients had ERCP findings consistent with choledocholithiasis and 9 patients had a normal examination. In further review of those patients with a normal ERCP, 5 patients had a bilirubin of > 4 mg/dL and 4 patients had a dilated CBD and a bilirubin of 1.8 to 4 mg/dL. Hence,

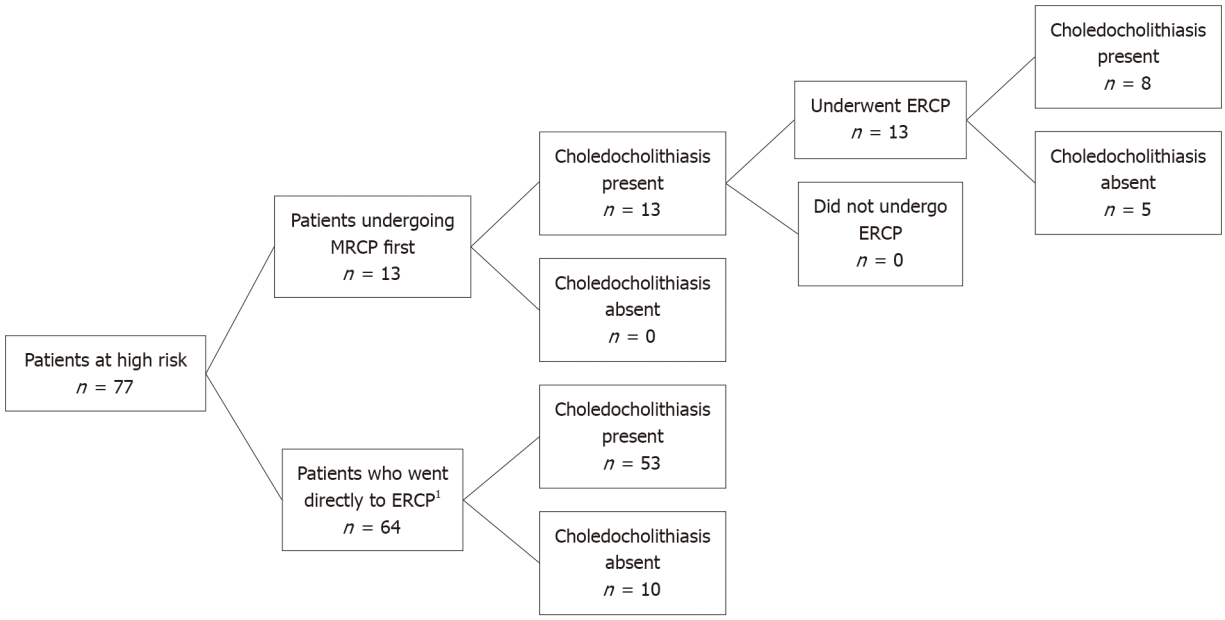

DOI: 10.3748/wjg.v28.i16.1692 **Copyright** ©The Author(s) 2022.

Figure 2 Patients categorized as high risk by American Society for Gastrointestinal Endoscopy guidelines. MRCP: Magnetic resonance cholangiopancreatography; ERCP: Endoscopic retrograde cholangiopancreatography. [1]One patient's procedure could not be completed due to failure of bile duct cannulization.

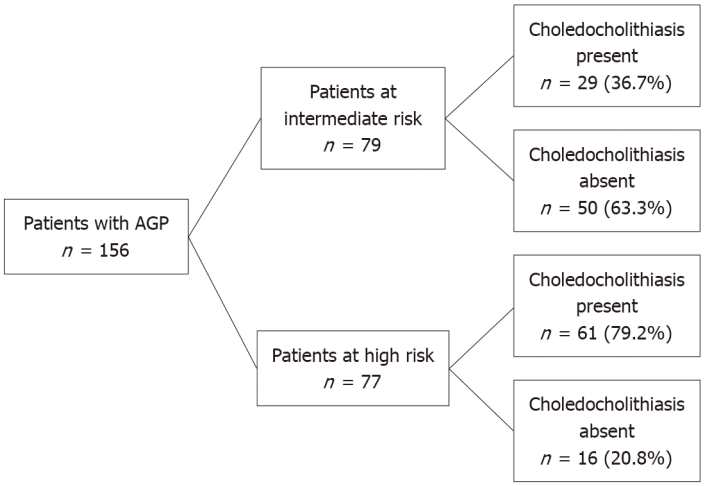

DOI: 10.3748/wjg.v28.i16.1692 **Copyright** ©The Author(s) 2022.

Figure 3 Patients with choledocholithiasis. AGP: Acute gallstone pancreatitis.

based on the 2019 criteria, 9 out of 35 patients who were downgraded to intermediate risk had an unnecessary ERCP with normal findings (without a preceding MRCP).

Finally, the sensitivity and specificity of the 2010 and 2019 ASGE guidelines in assessing choledocholithiasis were calculated (Tables 7-10). In our cohort of patients with AGP, the 2010 ASGE criteria for predicting high risk for choledocholithiasis had a sensitivity of 67.8% and specificity of 75.8%. On the other hand, the 2019 ASGE criteria for predicting high risk for choledocholithiasis had a sensitivity of 38.2% and specificity of 89.4%.

DISCUSSION

AGP is the most common cause of AP in the United States accounting for approximately one-third of all cases[1]. Furthermore, given the potential for comorbid choledocholithiasis, patients with AGP should be evaluated for CBD stone disease[2]. In our cohort of patients with AGP, 37% of patients with intermediate risk and 79.2% of patients with high risk for choledocholithiasis based on the 2010 ASGE

Table 7 Sensitivity and specificity of 2010 American Society for Gastrointestinal Endoscopy guidelines for predicting high risk of choledocholithiasis in patients with acute gallstone pancreatitis

	Choledocholithiasis present	Choledocholithiasis not present
Positive for high risk criteria	61	16
Negative for high risk criteria	29	50

Sensitivity = 67.8%; specificity = 75.8%.

Table 8 Sensitivity and specificity of 2010 American Society for Gastrointestinal Endoscopy guidelines for predicting intermediate risk of choledocholithiasis in patients with acute gallstone pancreatitis

	Choledocholithiasis present	Choledocholithiasis not present
Positive for intermediate risk criteria	29	50
Negative for intermediate risk criteria	61	16

Sensitivity = 82.9%; specificity = 24.2%.

Table 9 Sensitivity and specificity of 2019 American Society for Gastrointestinal Endoscopy guidelines for predicting high risk of choledocholithiasis in patients with acute gallstone pancreatitis

	Choledocholithiasis present	Choledocholithiasis not present
Positive for intermediate risk criteria	34	8
Negative for intermediate risk criteria	55	59

Sensitivity = 38.2%; specificity = 88.1%.

Table 10 Sensitivity and specificity of 2019 American Society for Gastrointestinal Endoscopy guidelines for predicting intermediate risk of choledocholithiasis in patients with acute gallstone pancreatitis

	Choledocholithiasis present	Choledocholithiasis not present
Positive for intermediate risk criteria	55	59
Negative for intermediate risk criteria	34	8

Sensitivity = 61.8%; specificity = 11.9%.

guidelines had documented CBD stone disease. When combined, our data demonstrated that the true incidence of choledocholithiasis in patients with AGP is 58%. The overall high prevalence of concurrent choledocholithiasis in patients with AGP may help explain the relatively high risk of recurrent pancreatitis in patients with AGP[10].

The ASGE published guidelines in 2010 which proposed a risk stratification system to clarify how to best manage patients with suspected choledocholithiasis, categorizing patients into low, intermediate and high risk[4].

In this scheme, patients at high risk are recommended to undergo ERCP directly without further imaging and those at intermediate risk should have additional imaging with MRCP or EUS. Those at low risk require no further evaluation. In this study, we aimed to apply these guidelines to patients admitted with AGP to a single tertiary care center over 10 years and determine what effect deviation had on outcomes.

In our cohort of 156 patients, approximately one-half of patients were either classified as intermediate or high risk. Since all patients in our cohort had AGP and the presence of AGP was a criteria for at least intermediate risk for choledocholithiasis according to the 2010 ASGE guidelines, no patients in our cohort were considered low risk for choledocholithiasis. After applying the guidelines to these groups, 76% of patients (54 patients in the intermediate group and 64 patients in the high risk group) were managed in accordance to the ASGE recommendations and 24% of patients (25 patients in the

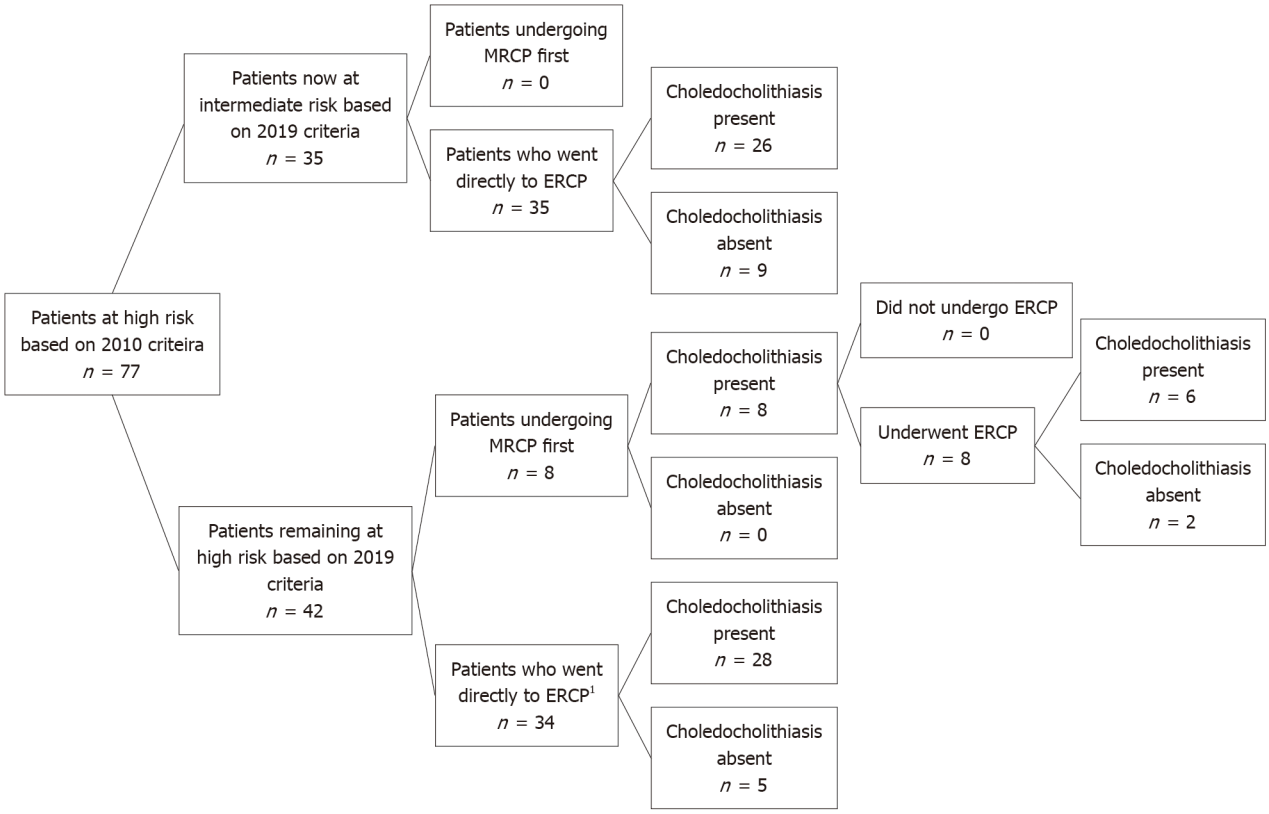

DOI: 10.3748/wjg.v28.i16.1692 **Copyright** ©The Author(s) 2022.

Figure 4 Patients at high risk based on 2010 American Society for Gastrointestinal Endoscopy guidelines now re-stratified based on 2019 guidelines. MRCP: Magnetic resonance cholangiopancreatography; ERCP: Endoscopic retrograde cholangiopancreatography. [1]One patient's procedure could not be completed due to failure of bile duct cannulization.

intermediate group and 13 patients in the high risk group) deviated from the guidelines. Specifically in the intermediate group, 7 patients who had an ERCP first had a normal examination suggesting that an inappropriate procedure was performed and importantly, one of these patients suffered from post-ERCP pancreatitis. These 7 intermediate risk patents who directly underwent ERCP and had normal findings did not receive EUS or MRCP. Thus, it may be prudent to consider EUS to evaluate for choledocholithiasis to prevent unnecessary ERCPs. Furthermore, all 13 of the patients in the high risk group who underwent MRCP prior to ERCP had a positive finding, suggesting an unnecessary test (*i.e.* MRCP) was performed first. Importantly, patients who underwent MRCP prior to ERCP were found to have longer hospital lengths of stay and delays in initiation of enteral feeding.

The ASGE guidelines provide evidence-based recommendations with the goal of optimizing the efficacy and safety of patient care. Additionally, a study has shown that adherence to ASGE guidelines also result in cost-saving from unnecessary imaging studies[3]. Accordingly, patients with intermediate risk (10%-50%) should undergo additional imaging because the risk of choledocholithiasis is too low to warrant proceeding directly to ERCP[6]. MRCP is often preferred in patients with pancreatitis who have intermediate risk for choledocholithiasis because it has high sensitivity in detecting CBD stones without procedural risks[11]. While ERCP is highly sensitive and specific in diagnosis and effective in therapeutic management of choledocholithiasis[12], the procedure also has a number of associated risks such as post-ERCP pancreatitis and post-endoscopic sphincterotomy bleeding[13,14]. One of the intermediate risk patients in our cohort who went directly to ERCP which showed normal findings developed worsening of pancreatitis thought to be related to post ERCP AP. This highlights that unnecessary invasive procedure and adverse outcome could have been prevented by adhering to the guidelines.

In 2019, the ASGE updated guidelines on management of choledocholithiasis, which further fine-tuned the criteria needed for the high risk group[6]. Specifically, patients now required the presence of a bilirubin greater than 4 mg/dL and imaging with a dilated CBD to qualify as high risk and thus those patients with a total bilirubin of 1.8-4.0 mg/dL with CBD dilation on imaging were downgraded to intermediate risk. The impetus for these changes were largely driven by studies that demonstrated that up to 30% of patients had ERCPs without evidence of CBD stones[15,16]. In our study, we found that approximately 26% (9/35) of patients categorized as high risk by 2019 criteria had a normal ERCP.

Since the cohort we studied was prior to the update, the 2010 guidelines were used in the initial analysis. In our subsequent analysis we aimed to determine concordance in categorization between the 2010 and 2019 guidelines. After applying the 2019 guidelines, we found that all patients in the intermediate group remained the intermediate group, whereas there was less concordance in the high risk group which was largely due to the group of patients who had lower total bilirubin levels. Importantly, using the newer guidelines, 9 patients may have been spared an ERCP. We also found that while the 2010 ASGE guidelines in predicting high risk for choledocholithiasis had a specificity of 75.8%, using the 2019 ASGE guidelines led to an improved specificity of 89.4%. This demonstrated that the use of the revised guidelines in assessing risk for choledocholithiasis in AGP patients can lead to a decrease in unnecessary invasive and costly procedures. Moreover, although AGP was removed from the intermediate risk criteria, all patients in our intermediate cohort remained intermediate suggesting that AGP implicitly increases the risk to the intermediate level for choledocholithiasis. This was verified in our cohort where 58% of patients with AGP were confirmed to have choledocholithiasis. Thus, clinicians should remain vigilant for concurrent choledocholithiasis in patients admitted with AGP.

We recognize that our study also has several limitations. First, this is a retrospective cohort study which has a potential for selection bias. The smaller size and retrospective nature of this study may limit the assessment of the degree of adherence to the ASGE guidelines. As the decision to proceed with MRCP or ERCP were at the discretion of the physician on service, the detailed reasoning behind selecting each modality was not always apparent in the medical record. Our results may not be generalizable to all medical settings as this study was done at a single tertiary care center at an academic institution located in a large metropolitan city. Further work is needed to determine the influencing factors driving deviation from the guidelines.

CONCLUSION

In the study cohort, we demonstrated that more than half of patients with AGP have choledocholithiasis. We also found that approximately two thirds of patients in the intermediate group and 83% of patients in the high risk group followed ASGE guidelines for management of choledocholithiasis in the setting of AGP. There was associated longer LOS for patients undergoing MRCP in both groups. Importantly, one patient who had a normal ERCP in the intermediate group without preceding MRCP suffered from post ERCP AP, highlighting the risk of unnecessary procedures. Further work is needed to determine the influencing factors driving deviation from the guidelines.

ARTICLE HIGHLIGHTS

Research background

Acute gallstone pancreatitis (AGP) is the most common cause of acute pancreatitis (AP) in the United States. Patients with AGP may also present with choledocholithiasis. In 2010, the American Society for Gastrointestinal Endoscopy (ASGE) suggested a management algorithm based on probability for choledocholithiasis. In 2019, the ASGE guidelines were updated.

Research motivation

Neither 2010 nor 2019 ASGE guidelines has been studied in AGP to determine the probability of having choledocholithiasis.

Research objectives

Our study aimed to determine compliance with ASGE guidelines, assess outcomes, and compare 2019 *vs* 2010 ASGE criteria for suspected choledocholithiasis in AGP.

Research methods

We conducted a retrospective cohort study of 882 patients admitted with AP to a single tertiary care center from 2008-2018. Patients with AGP were assigned low, intermediate or high risk for choledocholithiasis based on ASGE guidelines. Our primary outcomes of interest were the proportion of patients in the intermediate risk group undergoing magnetic resonance cholangiopancreatography (MRCP) first and the proportion of patients in the high risk group undergoing endoscopic retrograde cholangiopancreatography (ERCP) directly without preceding imaging. Secondary outcomes of interest included outcome differences based on if guidelines were not adhered to. We then evaluated the diagnostic accuracy of 2019 in comparison to the 2010 ASGE criteria for patients with suspected choledocholithiasis.

Research results

Among 79 intermediate risk patients according to the 2010 ASGE guidelines, 54 (68%) underwent MRCP first whereas 25 patients (32%) went directly to ERCP. Of the 25 intermediate risk patients who directly underwent ERCP, 18 patients had stone disease. One patient with a normal ERCP developed post ERCP pancreatitis. In the high risk group, 64 patients (83%) had ERCP without preceding imaging. When the updated 2019 ASGE guidelines were applied instead of the original 2010 guidelines, there was moderate agreement between the 2010 and 2019 guidelines (kappa = 0.46, 95%CI: 0.34-0.58). Based on the 2019 criteria, 9/35 patients who were downgraded to intermediate risk had an unnecessary ERCP with normal findings (without a preceding MRCP).

Research conclusions

In the study cohort, we demonstrated that more than half of patients with AGP have choledocholithiasis. We also found that approximately two thirds of patients in the intermediate group and 83% of patients in the high risk group followed ASGE guidelines for management of choledocholithiasis in the setting of AGP. Importantly, one patient who had a normal ERCP in the intermediate group without preceding MRCP suffered from post ERCP pancreatitis, highlighting the risk of unnecessary procedures. We also found that while the 2010 ASGE guidelines in predicting high risk for choledocholithiasis had a specificity of 75.8%, using the 2019 ASGE guidelines led to an improved specificity of 89.4%.

Research perspectives

Further work is needed to determine the influencing factors driving deviation from the guidelines.

ACKNOWLEDGEMENTS

The authors would like to thank the Harvard Catalyst Biostatistics Consulting Program at Beth Israel Deaconess Medical Center for reviewing statistical methods and reporting of results.

FOOTNOTES

Author contributions: Tintara S, Shah I, Ahmed A, Freedman SD, Kothari DJ and Sheth SG contributed to the study design and coordination; Tintara S contributed to the acquisition and interpretation of data, and primarily drafting the manuscript; Shah I assisted in drafting the manuscript; Yakah W contributed to the acquisition and interpretation of data and statistical analysis; Ahmed A, Sorrento CS and Kandasamy C contributed to the acquisition of data; Freedman SD contributed to revision of manuscript for intellectual content; Kothari DJ and Sheth SG contributed to the interpretation and analysis of data, revision of manuscript for intellectual content, and study supervision; All authors have approved the final draft submitted.

Institutional review board statement: This retrospective observational cohort study was approved by Beth Israel Deaconess Medical Center institutional review board.

Informed consent statement: Informed written consent was obtained fromthe patient for publication of this report and any accompanying images.

Conflict-of-interest statement: The authors of this study have no relevant conflict of interests to declare.

Data sharing statement: Statistical code, and dataset available from the corresponding author at ssheth@bidmc.harvard.edu. This retrospective observational cohort study was approved by the Beth Israel Deaconess Medical Center institutional review board which did not require individual patient consent for retrospective chart review.

STROBE statement: This manuscript adheres to the applicable Strengthening the Reporting of Observational Studies in Epidemiology (STROBE) reporting guidelines for cohort studies.

Open-Access: This article is an open-access article that was selected by an in-house editor and fully peer-reviewed by external reviewers. It is distributed in accordance with the Creative Commons Attribution NonCommercial (CC BY-NC 4.0) license, which permits others to distribute, remix, adapt, build upon this work non-commercially, and license their derivative works on different terms, provided the original work is properly cited and the use is non-commercial. See: https://creativecommons.org/Licenses/by-nc/4.0/

Country/Territory of origin: United States

ORCID number: Supisara Tintara 0000-0002-9427-2845; Ishani Shah 0000-0003-2916-1089; William Yakah 0000-0003-3264-5404; Awais Ahmed 0000-0001-7254-5921; Cristina S Sorrento 0000-0002-1111-5271; Cinthana Kandasamy 0000-0002-4235-

6932; Steven D Freedman 0000-0003-1255-9701; Darshan J Kothari 0000-0002-6835-218X; Sunil G Sheth 0000-0003-0602-8509.

S-Editor: Zhang H
L-Editor: A
P-Editor: Zhang H

REFERENCES

1 **Forsmark CE**, Baillie J; AGA Institute Clinical Practice and Economics Committee; AGA Institute Governing Board. AGA Institute technical review on acute pancreatitis. *Gastroenterology* 2007; **132**: 2022-2044 [PMID: 17484894 DOI: 10.1053/j.gastro.2007.03.065]
2 **Rosseland AR**, Glomsaker TB. Asymptomatic common bile duct stones. *Eur J Gastroenterol Hepatol* 2000; **12**: 1171-1173 [PMID: 11111771 DOI: 10.1097/00042737-200012110-00001]
3 **Singhvi G**, Ampara R, Baum J, Gumaste V. ASGE guidelines result in cost-saving in the management of choledocholithiasis. *Ann Gastroenterol* 2016; **29**: 85-90 [PMID: 26752953]
4 **ASGE Standards of Practice Committee**, Maple JT, Ben-Menachem T, Anderson MA, Appalaneni V, Banerjee S, Cash BD, Fisher L, Harrison ME, Fanelli RD, Fukami N, Ikenberry SO, Jain R, Khan K, Krinsky ML, Strohmeyer L, Dominitz JA. The role of endoscopy in the evaluation of suspected choledocholithiasis. *Gastrointest Endosc* 2010; **71**: 1-9 [PMID: 20105473 DOI: 10.1016/j.gie.2009.09.041]
5 **Chandran A**, Rashtak S, Patil P, Gottlieb A, Bernstam E, Guha S, Ramireddy S, Badillo R, DaVee RT, Kao LS, Thosani N. Comparing diagnostic accuracy of current practice guidelines in predicting choledocholithiasis: outcomes from a large healthcare system comprising both academic and community settings. *Gastrointest Endosc* 2021; **93**: 1351-1359 [PMID: 33160977 DOI: 10.1016/j.gie.2020.10.033]
6 **ASGE Standards of Practice Committee**, Buxbaum JL, Abbas Fehmi SM, Sultan S, Fishman DS, Qumseya BJ, Cortessis VK, Schilperoort H, Kysh L, Matsuoka L, Yachimski P, Agrawal D, Gurudu SR, Jamil LH, Jue TL, Khashab MA, Law JK, Lee JK, Naveed M, Sawhney MS, Thosani N, Yang J, Wani SB. ASGE guideline on the role of endoscopy in the evaluation and management of choledocholithiasis. *Gastrointest Endosc* 2019; **89**: 1075-1105.e15 [PMID: 30979521 DOI: 10.1016/j.gie.2018.10.001]
7 **Banks PA**, Bollen TL, Dervenis C, Gooszen HG, Johnson CD, Sarr MG, Tsiotos GG, Vege SS; Acute Pancreatitis Classification Working Group. Classification of acute pancreatitis--2012: revision of the Atlanta classification and definitions by international consensus. *Gut* 2013; **62**: 102-111 [PMID: 23100216 DOI: 10.1136/gutjnl-2012-302779]
8 **Wu BU**, Johannes RS, Sun X, Tabak Y, Conwell DL, Banks PA. The early prediction of mortality in acute pancreatitis: a large population-based study. *Gut* 2008; **57**: 1698-1703 [PMID: 18519429 DOI: 10.1136/gut.2008.152702]
9 **Charlson ME**, Pompei P, Ales KL, MacKenzie CR. A new method of classifying prognostic comorbidity in longitudinal studies: development and validation. *J Chronic Dis* 1987; **40**: 373-383 [PMID: 3558716 DOI: 10.1016/0021-9681(87)90171-8]
10 **Hwang SS**, Li BH, Haigh PI. Gallstone pancreatitis without cholecystectomy. *JAMA Surg* 2013; **148**: 867-872 [PMID: 23884515 DOI: 10.1001/jamasurg.2013.3033]
11 **Scheiman JM**, Carlos RC, Barnett JL, Elta GH, Nostrant TT, Chey WD, Francis IR, Nandi PS. Can endoscopic ultrasound or magnetic resonance cholangiopancreatography replace ERCP in patients with suspected biliary disease? *Am J Gastroenterol* 2001; **96**: 2900-2904 [PMID: 11693324 DOI: 10.1111/j.1572-0241.2001.04245.x]
12 **Prat F**, Amouyal G, Amouyal P, Pelletier G, Fritsch J, Choury AD, Buffet C, Etienne JP. Prospective controlled study of endoscopic ultrasonography and endoscopic retrograde cholangiography in patients with suspected common-bileduct lithiasis. *Lancet* 1996; **347**: 75-79 [PMID: 8538344 DOI: 10.1016/s0140-6736(96)90208-1]
13 **ASGE Standards of Practice Committee**, Chandrasekhara V, Khashab MA, Muthusamy VR, Acosta RD, Agrawal D, Bruining DH, Eloubeidi MA, Fanelli RD, Faulx AL, Gurudu SR, Kothari S, Lightdale JR, Qumseya BJ, Shaukat A, Wang A, Wani SB, Yang J, DeWitt JM. Adverse events associated with ERCP. *Gastrointest Endosc* 2017; **85**: 32-47 [PMID: 27546389 DOI: 10.1016/j.gie.2016.06.051]
14 **ASGE Standards of Practice Committee**, Anderson MA, Fisher L, Jain R, Evans JA, Appalaneni V, Ben-Menachem T, Cash BD, Decker GA, Early DS, Fanelli RD, Fisher DA, Fukami N, Hwang JH, Ikenberry SO, Jue TL, Khan KM, Krinsky ML, Malpas PM, Maple JT, Sharaf RN, Shergill AK, Dominitz JA. Complications of ERCP. *Gastrointest Endosc* 2012; **75**: 467-473 [PMID: 22341094 DOI: 10.1016/j.gie.2011.07.010]
15 **Adams MA**, Hosmer AE, Wamsteker EJ, Anderson MA, Elta GH, Kubiliun NM, Kwon RS, Piraka CR, Scheiman JM, Waljee AK, Hussain HK, Elmunzer BJ. Predicting the likelihood of a persistent bile duct stone in patients with suspected choledocholithiasis: accuracy of existing guidelines and the impact of laboratory trends. *Gastrointest Endosc* 2015; **82**: 88-93 [PMID: 25792387 DOI: 10.1016/j.gie.2014.12.023]
16 **Rubin MI**, Thosani NC, Tanikella R, Wolf DS, Fallon MB, Lukens FJ. Endoscopic retrograde cholangiopancreatography for suspected choledocholithiasis: testing the current guidelines. *Dig Liver Dis* 2013; **45**: 744-749 [PMID: 23540659 DOI: 10.1016/j.dld.2013.02.005]

World Journal of Gastroenterology

Submit a Manuscript: https://www.f6publishing.com

World J Gastroenterol 2022 April 28; 28(16): 1705-1717

DOI: 10.3748/wjg.v28.i16.1705

ISSN 1007-9327 (print) ISSN 2219-2840 (online)

SYSTEMATIC REVIEWS

Risk of venous thromboembolism in children and adolescents with inflammatory bowel disease: A systematic review and meta-analysis

Xin-Yue Zhang, Hai-Cheng Dong, Wen-Fei Wang, Yao Zhang

Specialty type: Gastroenterology and hepatology

Provenance and peer review: Unsolicited article; Externally peer reviewed.

Peer-review model: Single blind

Peer-review report's scientific quality classification

Grade A (Excellent): 0
Grade B (Very good): B, B
Grade C (Good): C
Grade D (Fair): 0
Grade E (Poor): 0

P-Reviewer: Anysz H, Poland; Dabravolski SA, Belarus; Moradi L, Iran

Received: August 19, 2021
Peer-review started: August 19, 2021
First decision: October 16, 2021
Revised: November 1, 2021
Accepted: March 27, 2022
Article in press: March 27, 2022
Published online: April 28, 2022

Xin-Yue Zhang, Hai-Cheng Dong, Wen-Fei Wang, Yao Zhang, Department of Traditional Chinese Medicine, The Children's Hospital, Zhejiang University School of Medicine, National Clinical Research Center for Child Health, Hangzhou 310005, Zhejiang Province, China

Corresponding author: Xin-Yue Zhang, MM, Attending Doctor, Department of Traditional Chinese Medicine, The Children's Hospital, Zhejiang University School of Medicine, National Clinical Research Center for Child Health, No. 57 Zhugan Lane, Xiancheng District, Hangzhou 310005, Zhejiang Province, China. cicelyxyz@zju.edu.cn

Abstract

BACKGROUND

A two- to three-fold increased risk of venous thrombotic events (VTE) has been demonstrated in patients with inflammatory bowel disease (IBD) compared to the general population, but less is known about the risk of VTE in child- and pediatric-onset IBD. In recent years, several studies have reported the rising incidence rate of VTE in juvenile patients with IBD, and the related risk factors have been explored.

AIM

To evaluate the risk of VTE in children and adolescents with IBD.

METHODS

Articles published up to April 2021 were retrieved from PubMed, Embase, Cochrane Library, Web of Science, SinoMed, CNKI, and WANFANG. Data from observational studies and clinical work were extracted. The outcome was the occurrence of VTE according to the type of IBD. The available odds ratio (OR) and the corresponding 95% confidence interval (CI) were extracted to compare the outcomes. Effect size (P), odds ratio (OR), and 95%CI were used to assess the association between VTE risk and IBD disease. Subgroup analyses stratified by subtypes of VTE and IBD were performed.

RESULTS

Twelve studies (7450272 IBD patients) were included in the meta-analysis. Child and adolescent IBD patients showed increased VTE risk (P = 0.02, 95%CI: 0.01-0.03). Subgroup analyses stratified by IBD (ulcerative colitis (UC): P = 0.05, 95%CI: 0.03-0.06; Crohn's disease (CD): P = 0.02, 95%CI: 0.00-0.04) and VTE subtypes (portal vein thrombosis: P = 0.04, 95%CI: 0.02-0.06; deep vein thrombosis: P = 0.03, 95%CI: 0.01-0.05; central venous catheter-related thrombosis: P = 0.23, 95%CI: 0.00-0.46; thromboembolic events: P = 0.02, 95%CI: 0.01-0.03) revealed a sign-

ificant correlation between VTE risk and IBD. Patients with IBD were more susceptible to VTE risk than those without IBD (OR = 2.99, 95%CI: 1.45-6.18). The funnel plot was asymmetric, suggesting the presence of significant publication bias. Pediatric and adolescent IBD patients have an increased VTE risk. UC and CD patients exhibited a high risk of VTE. The risk of VTE subtypes was increased in IBD patients.

CONCLUSION

The current meta-analysis showed that the incidence and risk of VTE are significantly increased in pediatric and adolescent IBD patients. Thus, IBD might be a risk factor for VTE in children and young adults. High-quality prospective cohort studies are necessary to confirm these findings.

Key Words: Thromboembolism; Children; Adolescents; Ulcerative colitis; Crohn's disease; Meta-analysis

©The Author(s) 2022. Published by Baishideng Publishing Group Inc. All rights reserved.

Core Tip: This study suggested that child and adolescent inflammatory bowel disease (IBD) patients showed an increased risk of venous thrombotic events (VTE) (P = 0.02, 95%CI: 0.01-0.03). Subgroup analysis stratified by IBD (ulcerative colitis: P = 0.04, 95%CI: 0.03-0.06; Crohn's disease: P = 0.02, 95%CI: 0.00-0.04) and VTE subtypes (portal vein thrombosis: P = 0.04, 95%CI: 0.02-0.06; deep vein thrombosis: P = 0.03, 95%CI: 0.01-0.05; central venous catheter-related thrombosis: P = 0.13, 95%CI: 0.02-0.23; thromboembolic events: P = 0.02, 95%CI: 0.01-0.03) revealed a significant correlation between VTE incidence and IBD.

Citation: Zhang XY, Dong HC, Wang WF, Zhang Y. Risk of venous thromboembolism in children and adolescents with inflammatory bowel disease: A systematic review and meta-analysis. *World J Gastroenterol* 2022; 28(16): 1705-1717

URL: https://www.wjgnet.com/1007-9327/full/v28/i16/1705.htm

DOI: https://dx.doi.org/10.3748/wjg.v28.i16.1705

INTRODUCTION

Inflammatory bowel disease (IBD) is a digestive system disorder characterized by chronic inflammation of the gastrointestinal (GI) tract[1-5]. The two common manifestations of IBD are ulcerative colitis (UC) and Crohn's disease (CD)[1-5]. The pathogenesis of IBD involves a complex interaction between the host genetics, external environment, gut microbiota, and immune responses[6-8]. The incidence of pediatric and adult IBD is rising steadily worldwide, especially in developed countries[9-11]. Approximately 25% of patients with IBD are diagnosed before the age of 18 years[12,13]. Furthermore, 4% of pediatric IBD occur before the age of 5 years and 18% before the age of 10 years, peaking in adolescence[7].

Venous thromboembolism (VTE) is a potentially severe medical condition with a high recurrence rate [14,15]. IBD is a high-risk factor for the occurrence and development of VTE in adults[16,17]. Routine VTE prophylaxis is recommended for IBD patients during hospitalization[1,18-20]. Pediatric patients with IBD also have an increased predisposition to develop VTE, including deep venous thrombosis (DVT) and pulmonary embolism (PE), although the available evidence is of lower quality[21,22]. The etiology of VTE in IBD is multifactorial and not well defined. It involves the cross-talk between coagulation and inflammation[23,24]. IBD-associated inflammation causes a hypercoagulable state, leading to systemic thrombotic events and local microthrombi in the vessels of the inflamed intestinal mucosa[25,26]. Pediatric IBD patients exhibit various clinical features, including disease location and severity, endoscopic appearance, histology, comorbidities, complications, and response to treatment options[27]. The reported risk factors for VTE in children with IBD include inherent genetics, ethnicity, gender, infection, parenteral nutrition, surgery, specific therapies, disease history, and increased use of central venous catheters (CVCs; the most common factor)[28-30].

Nonetheless, whether the development of VTE complications in IBD treatment is age-dependent is yet to be clarified. The increased risk of VTE in adult patients with IBD is widely recognized[31]. A two- to three-fold increased risk of VTE has been demonstrated in patients with IBD compared to the general population[26]. However, less is known about the risk of VTE in child- and pediatric-onset IBD. In recent years, several studies have reported the rising incidence rate of VTE in juvenile patients with IBD, and the related risk factors have been explored[32-35]. Therefore, this meta-analysis evaluated the association between postoperative VTE risk and IBD in children and adolescent populations.

MATERIALS AND METHODS

According to the Preferred Reporting Items for Systematic Reviews (PRISMA, 2020) guidelines, we conducted a systematic review and meta-analysis. PubMed, Embase, Cochrane Library, Web of Science, SinoMed, CNKI, and WANFANG databases were systematically searched for studies published up to April 2021.

Eligibility criteria

Articles were included if they met the following criteria: (1) Investigating the incidence or risk of VTE in children and adolescents with IBD; (2) IBD and VTE (DVT, pulmonary embolism; CVC-related thrombosis, intracranial venous sinus thrombosis, portal vein thrombosis, thromboembolic events, intra-abdominal thrombus, and cerebrovascular thrombosis) were confirmed medically; (3) language was limited to English or Chinese; and (4) RCT, cohort, or database review design.

Publications were excluded if they were: (1) Letters, review articles, meta-analyses, case-control, case reports, and experimental animal studies; (2) Missing primary data; or (3) Full text unavailable.

Search strategy

PubMed, Embase, Cochrane Library, Web of Science, SinoMed, CNKI, and WANFANG databases were systematically searched for potentially eligible studies published up to April 2021. The MeSH terms used were as follows: "inflammatory bowel disease", "Crohn Disease", "Colitis, Ulcerative" and "Children", "pediatric*" and "Venous Thrombosis Pulmonary", "Embolism vein thrombosis", as well as relevant keywords. The search strategy for PubMed, Embase and Cocharane Central is listed in Supplementary Table 1.

Data extraction and quality assessment

The selection and inclusion of studies were performed by two independent reviewers in two stages, which included the analysis of the titles/abstracts, followed by a full-text assessment. Disagreements were resolved by a third reviewer. Data including the authors' names, publication year, study design, country, sample size, mean age, IBD therapy, patient, VTE type, and male percentage were extracted. The quality assessment was performed in duplicate by two researchers independently (xx and xx). The Newcastle-Ottawa Scale (NOS)[36] was used to assess the methodological quality of eligible observational studies.

Statistical analysis

Statistical analyses were performed using STATA SE 14.0 (StataCorp, College Station, TX, USA). The risk of VTE in IBD was estimated by ES (p) and the corresponding 95% confidence interval (CI). The available odds ratio (OR) and the corresponding 95%CI were extracted to compare the outcomes. In addition, the event incidence was relatively small ($0 < P < 0.2$), and the double arcsine method was also used for data conversion.

Cochran's Q statistic ($P < 0.10$ indicated evidence of heterogeneity) was used to assess heterogeneity among the included studies[37]. When significant heterogeneity ($P < 0.10$) was detected, the random-effects model was applied to combine the effect sizes of the included studies; otherwise, the fixed-effects model was adopted[38]. In addition, sensitivity analyses were performed to identify individual study effects on pooled results and test the reliability of the results.

RESULTS

Literature search and study characteristics

The initial literature database search retrieved 438 studies. The duplicate records and automatically marked ineligible records were filtered out. After screening, 100 reports were assessed for eligibility. Due to insufficient information on participants, exposure, outcomes, and different reports from the same participants, only 12 reports were finally included in this meta-analysis. The study screening flowchart is illustrated in Figure 1.

The characteristics of the 12 eligible studies, including nine cohort studies[21,27,30,32-35,39,40], one RCT[28], and two database reviews[25,41], are listed in Table 1. These studies encompassed 7450272 IBD patients. Eight studies were carried out in the United States, and the others were performed in Canada, Switzerland, Iran, and Korea. The IBD patients had a mean age of < 1-21 years. The proportion of male patients ranged from 42.9% to 71.2%. The IBD subtypes covered UC, CD, indeterminate colitis (IC), and undefined IBD type (IBD-U). Moreover, various VTE subtypes, including intra-abdominal thrombosis (IAT), DVT, venous thromboembolism (VTE), TE, pulmonary thromboembolism (PTE), intracranial venous sinus thrombosis (IVST), PVT, and cerebrovascular thrombosis (CVT), were investigated. In addition, the confounding factors, including age, sex, hypercoagulable status, CVC, parenteral nutrition, cancer, sickle cell anemia, tobacco use, race/ethnicity, payer status, urban/rural status, hospital region,

Table 1 Characteristics of the included studies: ulcerative colitis patients and Crohn's disease patients

Ref.	Country	Study design	Period	Sample size N	Age, years (mean or median)	Male, (%)	Patient	IBD therapy	VTE type
Antiel *et al* [31], 2013	United States	Cohort	1999.1-2011.12	366	≤ 21	No data	UC	Surgery	IAT
Bence *et al* [26], 2020	United States	Cohort	2020.1-2016.6	276	15 (13, 17)	46	CD, UC, IC	Corticosteroids, Biologic therapy, Immunologic therapy	DVT
Cairo *et al* [36], 2017	United States	RCS	2012-2015	410	< 1 (9.8%); 1-5 (15.7%); 6-10 (30%); 11-15 (34.6%); 16-18 (9.9%)	59.5	IBD	No data	VTE
Derderian *et al*[27], 2020	United States	Cohort	2008-2018	49	9.8 ± 4.4	65	UC/IBD-U	Surgery	DVT
Diamond *et al*[32], 2018	United States	Cohort	2015-2017	47	14	46.8	IBD	Systemic steroids; Anti-TNF therapy	CVC-related thrombosis
Diamond *et al*[33], 2010	Canada	Cohort	1999.11.1-2008.2.29	85	14.8 (2.8)	54.1	IBD	Surgery	DVT
Herzog *et al* [34], 2018	Switzerland	Cohort	2006-2017	63	< 17	54	CD; UC or IBD-U	5-ASA Systemic CS; Immunomodulators; Calcineurin inhibitors; TNFα inhibitors, Surgery	TE
Jarchin *et al* [29], 2019	United States	Cohort	2008.1-2017.12	58	0-5 (5%); 6-10 (10%); 11-18 (85%)	66	UC	Anti-TNF only, Vedolizumab only, Anti-TNF+ vedolizumab, Anti-TNF+ vedolizumab+ ustekinumab, Surgery	PVT (within 30 d, > 30 d)
Khosravi *et al*[28], 2020	Iran	Cohort	2019	21	11.12 ± 5.65	42.9	IBD	Surgery	DVT
Lee *et al* [35], 2016	Korea	Cohort	1995.7-2011.6	73	12.49 ± 2.47	71.2	CD	Systemic corticosteroids 5-ASA only, 5-ASA+; azathioprine; 5-ASA only or 5-ASA+ azathioprine	PTE
Nylund *et al*[19], 2013[1]	United States	Database review	1997, 2000, 2003, 2006, and 2009	61076/7318/7379898	15.72 ± 0.02/15.39 ± 0.06/13.57 ± 0.01	49.32/47.55/49.64	CD, UC	No data	TE, PE, DVT, IVST, PVT
Zitomersky *et al*[37], 2013	United States	Database review	2006-2011	532	No data	No data	CD, UC	No data	CVT

[1]Adjusted factors: Age category, sex, hypercoagulable status, central venous catheter, parenteral nutrition, any cancer, sickle cell anemia, tobacco use, race/ethnicity, payer status, urban/rural status, hospital region, and year of inpatient stay.

DVT: Deep venous thrombosis; CD: Crohn's disease; UC: Ulcerative colitis; IC: Indeterminate colitis; VTE: Venous thromboembolism; PE: Pulmonary embolism; RCS: Retrospective comparative study; CVC: Central venous catheter; PTE: Pulmonary thromboembolism; IVST: Intracranial venous sinus thrombosis; PVT: Portal vein thrombosis; TE: Thromboembolic events; IAT: Intra-abdominal thrombosis; CVT: Cerebrovascular thrombosis.

and length of inpatient stay, were adjusted in various studies. According to the NOS evaluation criteria, the methodological quality score was 6 for 10 studies and 8 and 9 for the other two studies, respectively, indicating low-to-moderate bias (Table 2).

Table 2 Quality assessment

Ref.	Representativeness of the exposed cohort	Selection of the non-exposed cohort	Ascertainment of exposure	Demonstration that outcome of interest was not present at start of study	Comparability of cohorts on the basis of the design or analysis	Assessment of outcome	Was follow-up long enough for outcomes to occur	Adequacy of follow-up of cohorts	Total quality scores
Antiel *et al* [31], 2013	1	0	1	1	0	1	1	1	6
Bence *et al* [26], 2020	1	0	1	1	0	1	1	1	6
Cairo *et al* [36], 2017	1	1	1	1	1	1	1	1	8
Derderian *et al*[27], 2020	1	0	1	1	0	1	1	1	6
Diamond *et al*[32], 2018	1	0	1	1	0	1	1	1	6
Diamond *et al*[33], 2010	1	0	1	1	0	1	1	1	6
Herzog *et al*[34], 2018	1	0	1	1	0	1	1	1	6
Jarchin *et al* [29], 2019	1	0	1	1	0	1	1	1	6
Khosravi *et al*[28], 2020	1	0	1	1	0	1	1	1	6
Lee *et al* [35], 2016	1	0	1	1	0	1	1	1	6
Nylund *et al*[19], 2013	1	1	1	1	2	1	1	1	9
Zitomersky *et al*[37], 2013	1	0	1	1	0	1	1	1	6

Association between IBD and VTE risk

The association between IBD and the incidence of VTE was assessed in 12 studies. The pooled results showed that the risk of VTE was significantly increased in IBD patients compared to those without IBD (P = 0.02, 95%CI: 0.01-0.03). Moderate heterogeneity was detected across the included studies (I^2 = 54.7%, $P_{heterogeneity}$ = 0.012, Figure 2). In addition, double arcsine analysis showed similar results (P = 0.03, 95%CI: 0.02-0.04, Supplementary Figure 1).

The subgroup analyses stratified by IBD subtype were performed to evaluate the VTE risk in IBD. Five studies analyzed the UC subtype, and the pooled results suggested significantly increased VTE incidence in UC patients (P = 0.05, 95%CI: 0.03-0.06). No heterogeneity was detected among the studies (I^2 = 0.0%, $p_{heterogeneity}$ = 0.571, Figure 3A). Pooled analysis of four studies established a correlation between VTE risk and CD (P = 0.02, 95%CI: 0.00-0.04), without heterogeneity (I^2 = 0.0%, $p_{heterogeneity}$ = 0.709, Figure 3A). The IBD subtype was not defined in three studies, and a high rate of VTE was also detected in these patients (P = 0.02, 95%CI: 0.01-0.03), without obvious heterogeneity (I^2 = 0.0%, $p_{heterogeneity}$ = 0.702, Figure 3A). Based on one study, the VTE incidence was not increased in IC patients (P = 0.12, 95%CI: -0.04 to 0.27, Figure 3A).

Stratified by VTE subtype, two studies showed significantly increased PVT incidence in IBD patients (P = 0.04, 95%CI: 0.02-0.06; I^2 = 0.0%, $p_{heterogeneity}$ = 0.568, Figure 3B). The pooled analysis of four studies showed a high risk of DVT in IBD patients (P = 0.03, 95%CI: 0.01-0.05) with low heterogeneity (I^2 = 21.8%, $p_{heterogeneity}$ = 0.280, Figure 3B). In addition, one study revealed an increased risk of CVC-related thrombosis in IBD (P = 0.23, 95%CI: 0.00-0.46, Figure 3B). Furthermore, two studies showed a significant association between TE risk and IBD (P = 0.02, 95%CI: 0.01-0.03), without heterogeneity (I^2 = 0.0%, $p_{heterogeneity}$ = 0.862, Figure 3B). No association was found between PTE and IBD disease (P = 0.01, 95%CI: -0.01 to 0.04, Figure 3B) based on one study.

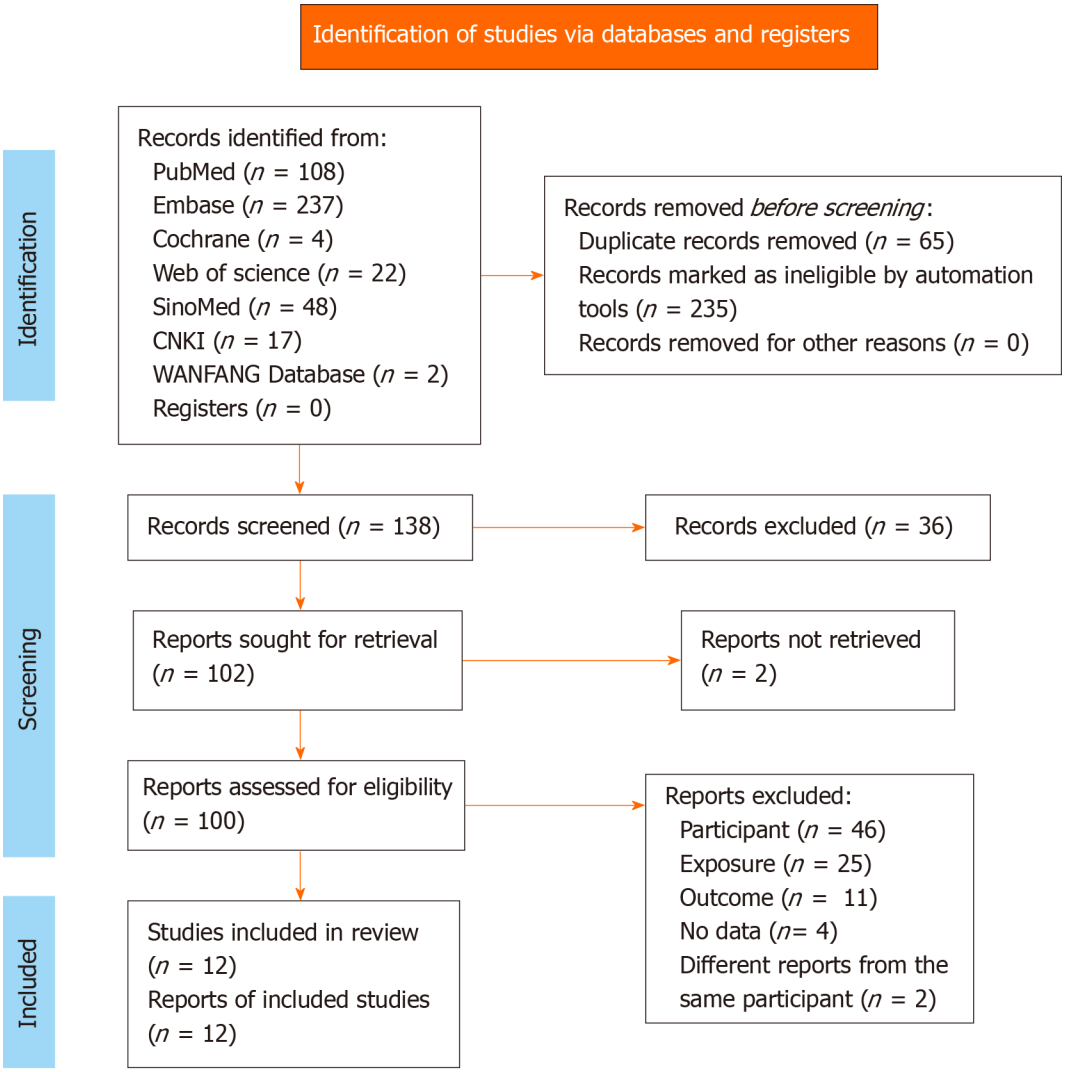

DOI: 10.3748/wjg.v28.i16.1705 **Copyright** ©The Author(s) 2022.

Figure 1 Flowchart of the search process of our study.

Pooled analysis of two studies comparing IBD and non-IBD patients showed a significant correlation between VTE risk and IBD disease (OR = 2.99, 95%CI: 1.45-6.18). Moderate heterogeneity was observed among these studies (I^2 = 58.9%, $p_{heterogeneity}$ = 0.119, Figure 4).

Publication bias

Publication bias was analyzed using a funnel plot. The asymmetrical distribution suggested significant publication bias (Figure 5).

DISCUSSION

The present meta-analysis found that the VTE risk was significantly increased in children and young adults with IBD. A high incidence of VTE was observed in the different subtypes of IBD, including UC, CD, and other undefined IBD diseases. Moreover, multiple VTE signs related to PVT, DVT, TE, and CVC-related thrombosis might be prone to developing during the progression of pediatric and adolescent IBD.

This study suggested that children and young adult IBD patients were susceptible to VTE risk after treatment, despite a low overall incidence. The increased risk of VTE is specific to IBD. Other chronic inflammatory diseases, such as rheumatoid arthritis, or chronic bowel diseases, such as celiac disease, are not found to be accompanied by a high incidence of VTE[26]. The association between VTE risk and IBD has been demonstrated in various IBD patient populations. Currently, there is a lack of systemic reviews on VTE risk in pediatric and adolescent patients. Female pediatric IBD patients were found to be at a high risk of developing VTE[28]. The meta-analysis by Kim *et al*[42] focused on pregnant women with IBD. The findings showed a significantly higher incidence of VTE during pregnancy and

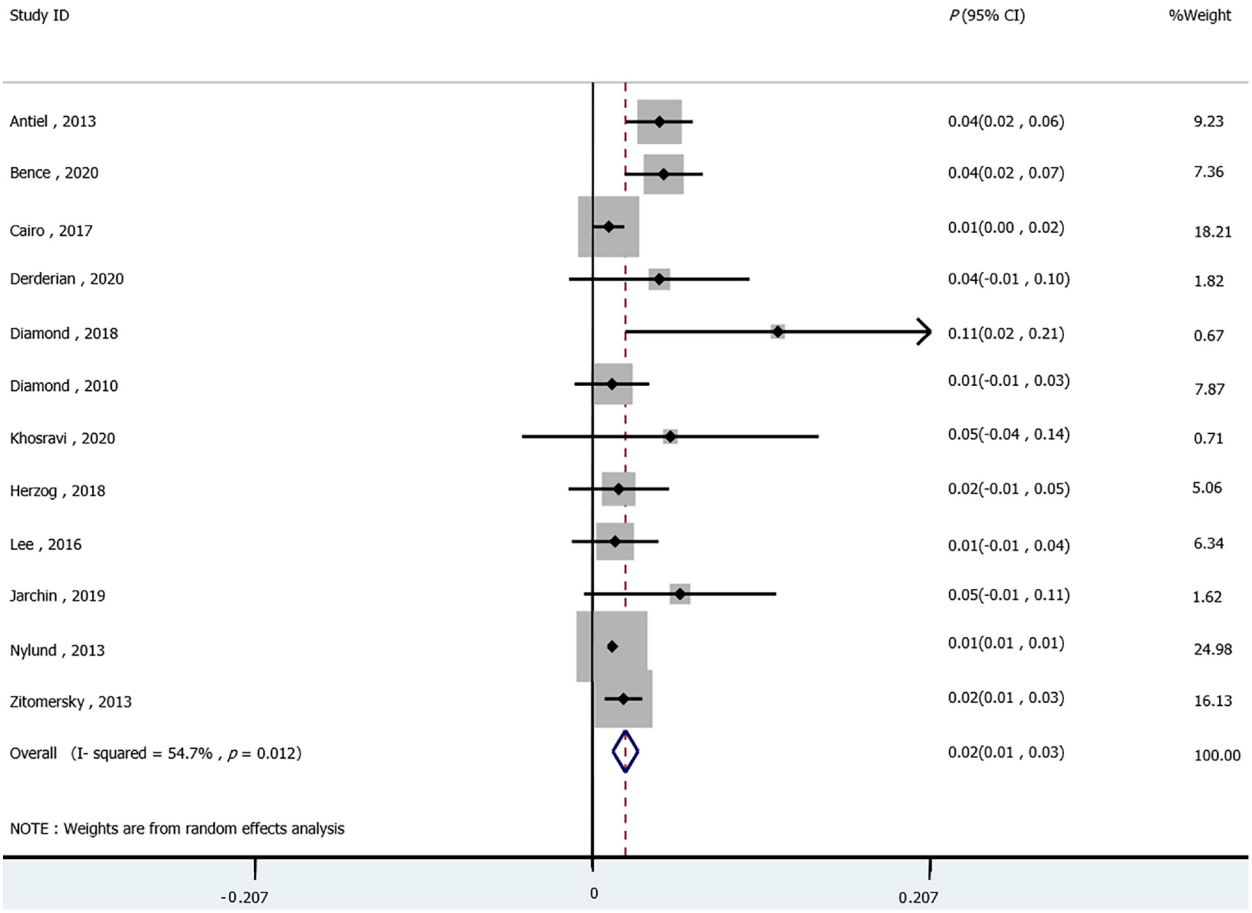

DOI: 10.3748/wjg.v28.i16.1705 **Copyright** ©The Author(s) 2022.

Figure 2 Forest plots of the incidence of venous thromboembolism in inflammatory bowel diseases.

postpartum in female IBD patients. According to the VTE subtype, the risk of DVT increased significantly in pregnant women, whereas the increase in PE was not significant during pregnancy. In the subgroup analysis based on the location of IBD, patients with UC had significantly higher VTE risk during both pregnancy and the postpartum period, while CD patients exhibited increased VTE incidence only during pregnancy. Therefore, elevated VTE risk was found to be more apparent in UC patients than CD patients. A recent study showed a high postsurgical VTE risk in patients with UC but not in those with CD[43]. Similar results were published earlier[44,45]. However, those studies were performed in the postsurgical setting, which is a state known to be associated with an increased risk of VTE[46,47]. Similarly, the current study showed a higher risk of VTE in UC compared to CD in children and young adult IBD patients, and consistently suggested that children with UC might be more susceptible to VTE. The exact causes for this higher VTE risk in UC than CD are unknown, but severe UC is associated with anemia and reactive thrombocytosis, which is conducive to VTE[48,49].

Another meta-analysis by Yuhara *et al*[50] demonstrated that adult patients with IBD (> 20-years-old) were at increased risk for both DVT and PE. The study also showed that confounding factors, such as smoking and body mass index (BMI), did not affect the correlation between IBD and DVT/PE. A large-population database study by Nylund *et al*[25] found that hospitalized children and adolescents with IBD had a high incidence of TE, including DVT and PE. In addition, the study identified older age and abdominal surgery as risk factors for TE in children and young adults with IBD. The Hispanics had a low risk of TE among all children and adolescents. Although tobacco use was a risk factor for TE in adults, it was a protective factor in children with IBD. Interestingly, an increasing trend of TE was observed through the years among children and young adults with IBD, which might be associated with increased hospital admission rates. However, this increasing trend was not clear after multivariable regression analysis. Similarly, the review by Lazzerini *et al*[51] suggested an increased risk of TE in pediatric IBD patients compared to the general population. Our meta-analysis included several updated publications and showed that the risk of PVT, DVT, TE, and CVC-related thrombosis was increased in IBD child and adolescent patients. Moreover, the underlying mechanism of location-related VTE occurrence and development needs further exploration.

Nevertheless, the present study has several limitations. First, moderate heterogeneity was detected in the overall analysis of the correlation between VTE and IBD. On the other hand, low or no heterogeneity was detected after stratifying the studies by subtypes of VTE and IBD. Patients' characteristics,

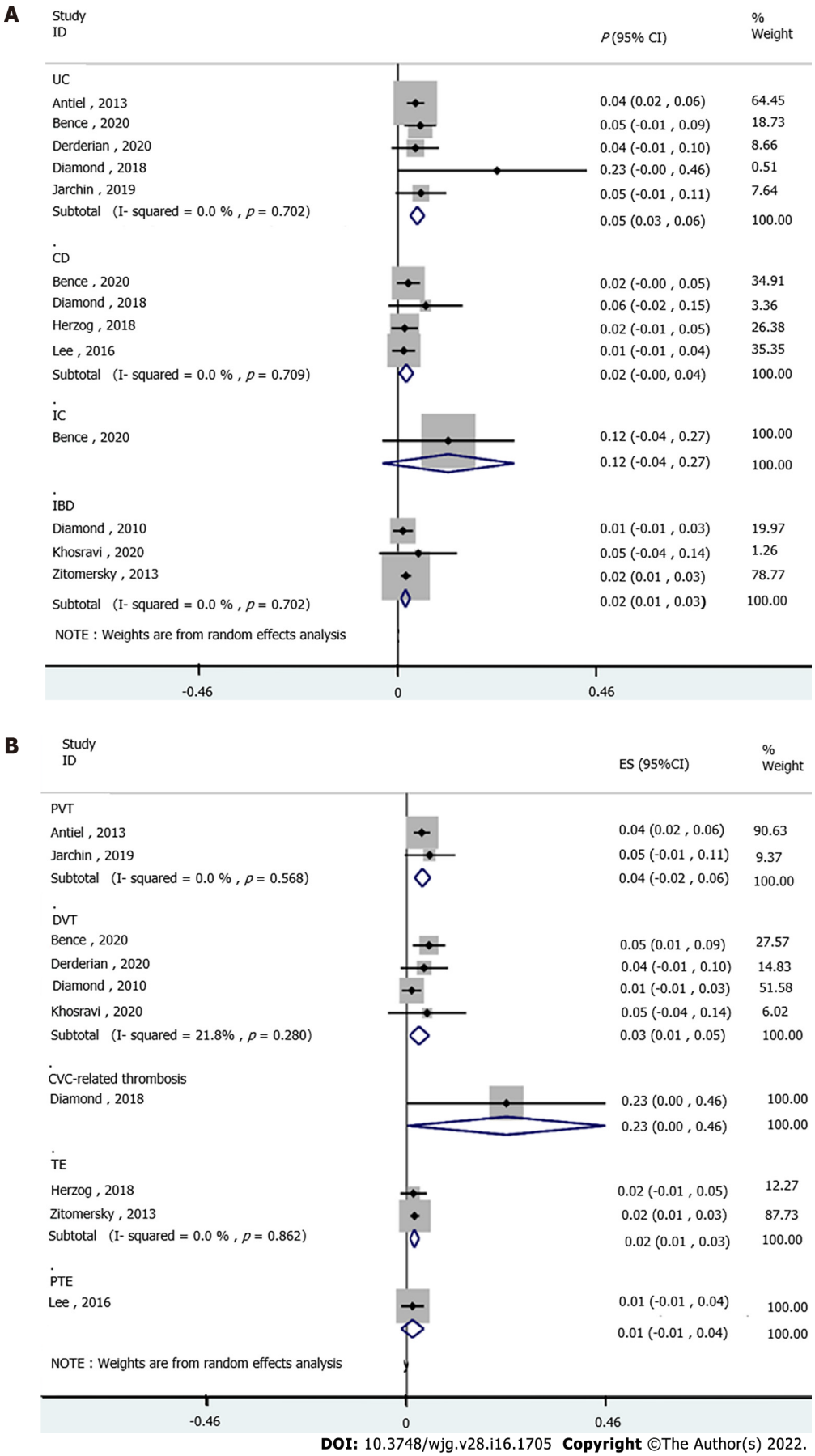

DOI: 10.3748/wjg.v28.i16.1705 **Copyright** ©The Author(s) 2022.

Figure 3 Forest plots. A: Subgroup analysis of the incidence of venous thromboembolism (VTE) in inflammatory bowel diseases (IBD) subtype; B: Subgroup analysis of the incidence of VTE subtype in IBD.

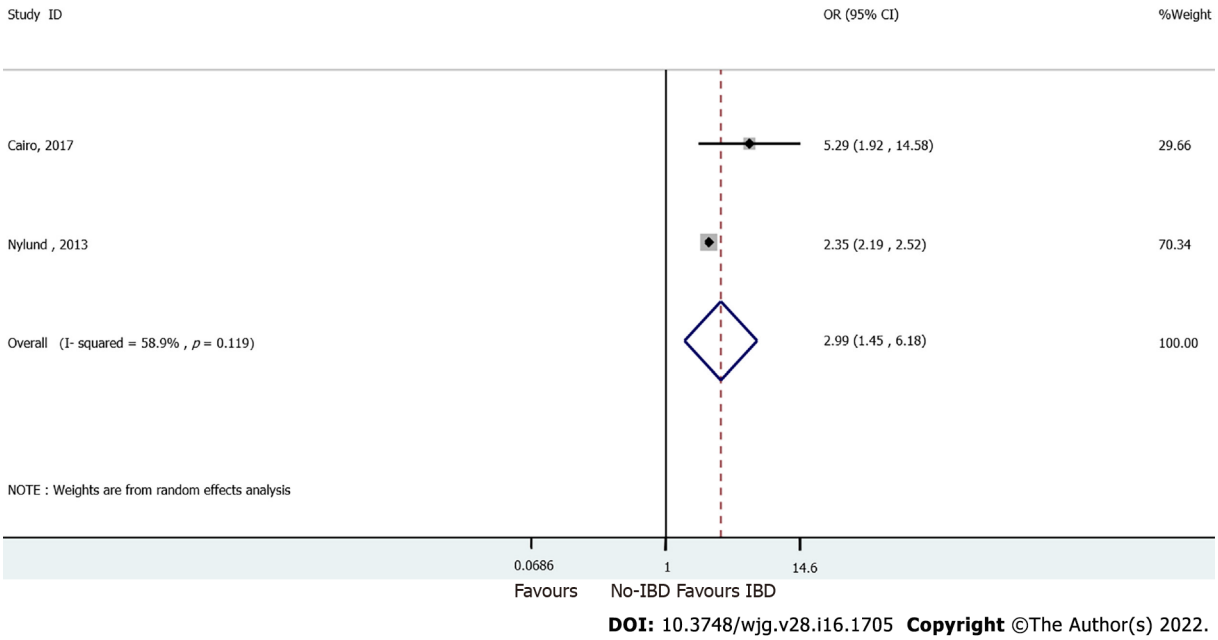

DOI: 10.3748/wjg.v28.i16.1705 **Copyright** ©The Author(s) 2022.

Figure 4 Forest plots of the risk of venous thromboembolism in inflammatory bowel diseases and non-inflammatory bowel diseases.

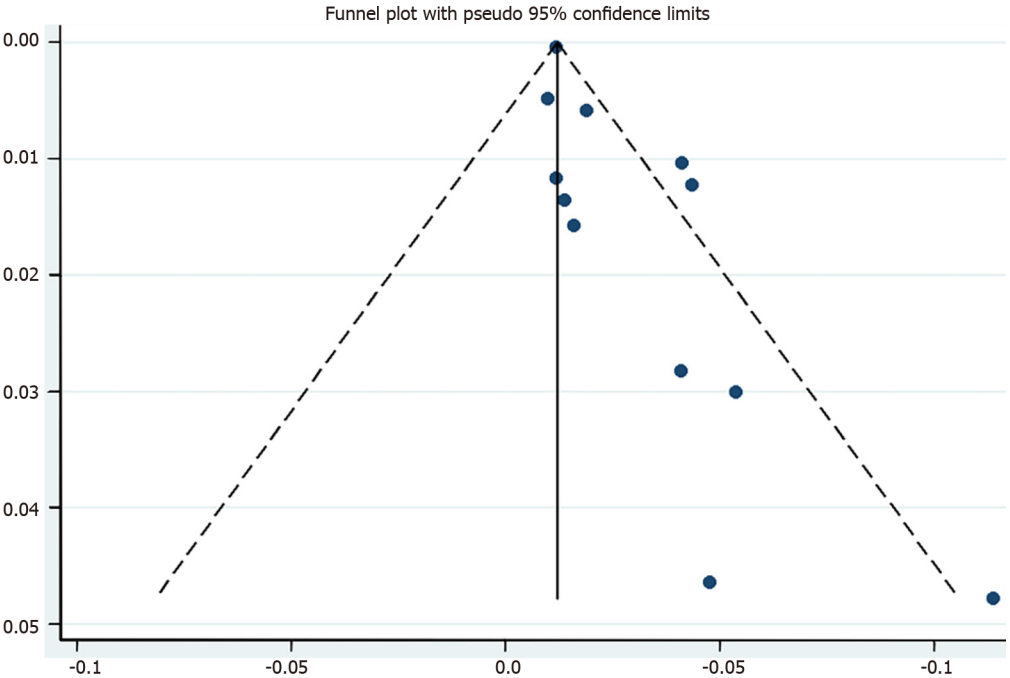

DOI: 10.3748/wjg.v28.i16.1705 **Copyright** ©The Author(s) 2022.

Figure 5 Publication bias; funnel plot of the incidence of venous thromboembolism in inflammatory bowel diseases.

diagnosis of VTE, and intervention therapies might contribute to the variations across the studies and the magnitude of association. Second, certain subgroup analyses only involved a small number of studies and patients, and hence, the findings should be interpreted with caution. Third, the included large-size database review study incorporated registry data of medical records with different populations and settings, which might generate a high selection bias. Fourth, VTE was challenging to diagnose, which might have led to the misclassification of VTE.

CONCLUSION

Pediatric and adolescent IBD patients have an increased risk of VTE. UC and CD patients exhibited a

high risk of VTE. The risk of VTE subtypes was increased in IBD patients.

ARTICLE HIGHLIGHTS

Research background

A two- to three-fold increased risk of venous thrombotic events (VTE) has been demonstrated in patients with inflammatory bowel disease (IBD) compared to the general population, but less is known about the risk of VTE in child- and pediatric-onset IBD. In recent years, several studies have reported the rising incidence rate of VTE in juvenile patients with IBD, and the related risk factors have been explored.

Research motivation

To evaluate the risk of VTE in children and adolescents with IBD.

Research objectives

To evaluate the risk of VTE in children and adolescents with IBD.

Research methods

Articles published up to April 2021 were retrieved from PubMed, Embase, Cochrane Library, Web of Science, SinoMed, CNKI, and WANFANG. Data from observational studies and clinical work were extracted. The outcome was the occurrence of VTE according to the type of IBD. The available odds ratio (OR) and the corresponding 95% confidence interval (CI) were extracted to compare the outcomes. Effect size (P), OR, and 95%CI were used to assess the association between VTE risk and IBD disease. Subgroup analyses stratified by subtypes of VTE and IBD were performed.

Research results

Twelve studies (7450272 IBD patients) were included in the meta-analysis. Child and adolescent IBD patients showed an increased risk of VTE (P = 0.02, 95%CI: 0.01-0.03). Subgroup analyses stratified by IBD (ulcerative colitis (UC): P = 0.05, 95%CI: 0.03-0.06; Crohn's disease (CD): P = 0.02, 95%CI: 0.00-0.04) and VTE subtypes (portal vein thrombosis (PVT): P = 0.04, 95%CI: 0.02-0.06; deep vein thrombosis: P = 0.03, 95%CI: 0.01-0.05; central venous catheter-related thrombosis: P = 0.23, 95%CI: 0.00-0.46; thromboembolic events: P = 0.02, 95%CI: 0.01-0.03) revealed a significant correlation between VTE risk and IBD. Patients with IBD were more susceptible to VTE risk than those without IBD (OR = 2.99, 95%CI: 1.45-6.18). The funnel plot was asymmetric, suggesting the presence of significant publication bias.

Research conclusions

Pediatric and adolescent IBD patients have an increased VTE risk. UC and CD patients exhibited a high risk of VTE. The risk of VTE subtypes was increased in IBD patients.

Research perspectives

Pediatric and adolescent IBD patients have an increased VTE risk. UC and CD patients exhibited a high risk of VTE. The risk of VTE subtypes was increased in IBD patients.

FOOTNOTES

Author contributions: Wang CL, Liang L, Fu JF, Zou CC, Hong F and Wu XM designed the research; Wang CL, Zou CC, Hong F and Wu XM performed the research; Xue JZ and Lu JR contributed new reagents/analytic tools; Wang CL, Liang L and Fu JF analyzed the data; Wang CL, Liang L and Fu JF wrote the paper.

Conflict-of-interest statement: The authors have no conflicts of interest to disclose.

PRISMA 2009 Checklist statement: The authors have read the PRISMA 2009 Checklist, and the manuscript was prepared and revised according to the PRISMA 2009 Checklist.

Open-Access: This article is an open-access article that was selected by an in-house editor and fully peer-reviewed by external reviewers. It is distributed in accordance with the Creative Commons Attribution NonCommercial (CC BY-NC 4.0) license, which permits others to distribute, remix, adapt, build upon this work non-commercially, and license their derivative works on different terms, provided the original work is properly cited and the use is non-commercial. See: http://creativecommons.org/Licenses/by-nc/4.0/

Country/Territory of origin: China

ORCID number: Xin-Yue Zhang 0000-0001-9934-1566; Hai-Cheng Dong 0000-0001-7830-2728; Wen-Fei Wang 0000-0001-7373-234X; Yao Zhang 0000-0003-2855-8690.

S-Editor: Wang LL
L-Editor: Webster JR
P-Editor: Yu HG

REFERENCES

1 **Rubin DT**, Ananthakrishnan AN, Siegel CA, Sauer BG, Long MD. ACG Clinical Guideline: Ulcerative Colitis in Adults. *Am J Gastroenterol* 2019; **114**: 384-413 [PMID: 30840605 DOI: 10.14309/ajg.0000000000000152]
2 **Ko CW**, Singh S, Feuerstein JD, Falck-Ytter C, Falck-Ytter Y, Cross RK; American Gastroenterological Association Institute Clinical Guidelines Committee. AGA Clinical Practice Guidelines on the Management of Mild-to-Moderate Ulcerative Colitis. *Gastroenterology* 2019; **156**: 748-764 [PMID: 30576644 DOI: 10.1053/j.gastro.2018.12.009]
3 **Ungaro R**, Mehandru S, Allen PB, Peyrin-Biroulet L, Colombel JF. Ulcerative colitis. *Lancet* 2017; **389**: 1756-1770 [PMID: 27914657 DOI: 10.1016/S0140-6736(16)32126-2]
4 **Lichtenstein GR**, Loftus EV, Isaacs KL, Regueiro MD, Gerson LB, Sands BE. ACG Clinical Guideline: Management of Crohn's Disease in Adults. *Am J Gastroenterol* 2018; **113**: 481-517 [PMID: 29610508 DOI: 10.1038/ajg.2018.27]
5 **Torres J**, Mehandru S, Colombel JF, Peyrin-Biroulet L. Crohn's disease. *Lancet* 2017; **389**: 1741-1755 [PMID: 27914655 DOI: 10.1016/S0140-6736(16)31711-1]
6 **Zhang YZ**, Li YY. Inflammatory bowel disease: pathogenesis. *World J Gastroenterol* 2014; **20**: 91-99 [PMID: 24415861 DOI: 10.3748/wjg.v20.i1.91]
7 **Rosen MJ**, Dhawan A, Saeed SA. Inflammatory Bowel Disease in Children and Adolescents. *JAMA Pediatr* 2015; **169**: 1053-1060 [PMID: 26414706 DOI: 10.1001/jamapediatrics.2015.1982]
8 **Guan Q**. A Comprehensive Review and Update on the Pathogenesis of Inflammatory Bowel Disease. *J Immunol Res* 2019; **2019**: 7247238 [PMID: 31886308 DOI: 10.1155/2019/7247238]
9 **Kaplan GG**. The global burden of IBD: from 2015 to 2025. *Nat Rev Gastroenterol Hepatol* 2015; **12**: 720-727 [PMID: 26323879 DOI: 10.1038/nrgastro.2015.150]
10 **GBD 2017 Inflammatory Bowel Disease Collaborators**. The global, regional, and national burden of inflammatory bowel disease in 195 countries and territories, 1990-2017: a systematic analysis for the Global Burden of Disease Study 2017. *Lancet Gastroenterol Hepatol* 2020; **5**: 17-30 [PMID: 31648971 DOI: 10.1016/S2468-1253(19)30333-4]
11 **Sýkora J**, Pomahačová R, Kreslová M, Cvalínová D, Štych P, Schwarz J. Current global trends in the incidence of pediatric-onset inflammatory bowel disease. *World J Gastroenterol* 2018; **24**: 2741-2763 [PMID: 29991879 DOI: 10.3748/wjg.v24.i25.2741]
12 **Oliveira SB**, Monteiro IM. Diagnosis and management of inflammatory bowel disease in children. *BMJ* 2017; **357**: j2083 [PMID: 28566467 DOI: 10.1136/bmj.j2083]
13 **Conrad MA**, Rosh JR. Pediatric Inflammatory Bowel Disease. *Pediatr Clin North Am* 2017; **64**: 577-591 [PMID: 28502439 DOI: 10.1016/j.pcl.2017.01.005]
14 **Heit JA**, Spencer FA, White RH. The epidemiology of venous thromboembolism. *J Thromb Thrombolysis* 2016; **41**: 3-14 [PMID: 26780736 DOI: 10.1007/s11239-015-1311-6]
15 **Di Nisio M**, van Es N, Büller HR. Deep vein thrombosis and pulmonary embolism. *Lancet* 2016; **388**: 3060-3073 [PMID: 27375038 DOI: 10.1016/S0140-6736(16)30514-1]
16 **Scoville EA**, Konijeti GG, Nguyen DD, Sauk J, Yajnik V, Ananthakrishnan AN. Venous thromboembolism in patients with inflammatory bowel diseases: a case-control study of risk factors. *Inflamm Bowel Dis* 2014; **20**: 631-636 [PMID: 24552828 DOI: 10.1097/MIB.0000000000000007]
17 **Novacek G**, Weltermann A, Sobala A, Tilg H, Petritsch W, Reinisch W, Mayer A, Haas T, Kaser A, Feichtenschlager T, Fuchssteiner H, Knoflach P, Vogelsang H, Miehsler W, Platzer R, Tillinger W, Jaritz B, Schmid A, Blaha B, Dejaco C, Eichinger S. Inflammatory bowel disease is a risk factor for recurrent venous thromboembolism. *Gastroenterology* 2010; **139**: 779-787, 787.e1 [PMID: 20546736 DOI: 10.1053/j.gastro.2010.05.026]
18 **Bitton A**, Buie D, Enns R, Feagan BG, Jones JL, Marshall JK, Whittaker S, Griffiths AM, Panaccione R; Canadian Association of Gastroenterology Severe Ulcerative Colitis Consensus Group. Treatment of hospitalized adult patients with severe ulcerative colitis: Toronto consensus statements. *Am J Gastroenterol* 2012; **107**: 179-94; author reply 195 [PMID: 22108451 DOI: 10.1038/ajg.2011.386]
19 **Nguyen GC**, Yeo EL. Prophylaxis of venous thromboembolism in IBD. *Lancet* 2010; **375**: 616-617 [PMID: 20149426 DOI: 10.1016/S0140-6736(10)60174-2]
20 **Nguyen GC**, Bernstein CN, Bitton A, Chan AK, Griffiths AM, Leontiadis GI, Geerts W, Bressler B, Butzner JD, Carrier M, Chande N, Marshall JK, Williams C, Kearon C. Consensus statements on the risk, prevention, and treatment of venous thromboembolism in inflammatory bowel disease: Canadian Association of Gastroenterology. *Gastroenterology* 2014; **146**: 835-848.e6 [PMID: 24462530 DOI: 10.1053/j.gastro.2014.01.042]
21 **Antiel RM**, Hashim Y, Moir CR, Rodriguez V, Elraiyah T, Zarroug AE. Intra-abdominal venous thrombosis after colectomy in pediatric patients with chronic ulcerative colitis: incidence, treatment, and outcomes. *J Pediatr Surg* 2014; **49**: 614-617 [PMID: 24726123 DOI: 10.1016/j.jpedsurg.2013.10.004]
22 **McKie K**, McLoughlin RJ, Hirsh MP, Cleary MA, Aidlen JT. Risk Factors for Venous Thromboembolism in Children and Young Adults With Inflammatory Bowel Disease. *J Surg Res* 2019; **243**: 173-179 [PMID: 31181463 DOI: 10.1016/j.jss.2019.04.087]

23 **Branchford BR**, Carpenter SL. The Role of Inflammation in Venous Thromboembolism. *Front Pediatr* 2018; **6**: 142 [PMID: 29876337 DOI: 10.3389/fped.2018.00142]

24 **Vazquez-Garza E**, Jerjes-Sanchez C, Navarrete A, Joya-Harrison J, Rodriguez D. Venous thromboembolism: thrombosis, inflammation, and immunothrombosis for clinicians. *J Thromb Thrombolysis* 2017; **44**: 377-385 [PMID: 28730407 DOI: 10.1007/s11239-017-1528-7]

25 **Nylund CM**, Goudie A, Garza JM, Crouch G, Denson LA. Venous thrombotic events in hospitalized children and adolescents with inflammatory bowel disease. *J Pediatr Gastroenterol Nutr* 2013; **56**: 485-491 [PMID: 23232326 DOI: 10.1097/MPG.0b013e3182801e43]

26 **Coremans L**, Strubbe B, Peeters H. Venous thromboembolism in patients with inflammatory bowel disease: review of literature and practical algorithms. *Acta Gastroenterol Belg* 2021; **84**: 79-85 [PMID: 33639697 DOI: 10.51821/84.1.910]

27 **Herzog D**, Fournier N, Buehr P, Rueger V, Koller R, Heyland K, Nydegger A, Spalinger J, Schibli S, Petit LM, Braegger CP; Swiss IBD Cohort Study Group. Age at disease onset of inflammatory bowel disease is associated with later extraintestinal manifestations and complications. *Eur J Gastroenterol Hepatol* 2018; **30**: 598-607 [PMID: 29360691 DOI: 10.1097/MEG.0000000000001072]

28 **Cairo SB**, Lautz TB, Schaefer BA, Yu G, Naseem HU, Rothstein DH. Risk factors for venous thromboembolic events in pediatric surgical patients: Defining indications for prophylaxis. *J Pediatr Surg* 2018; **53**: 1996-2002 [PMID: 29370891 DOI: 10.1016/j.jpedsurg.2017.12.016]

29 **Lassandro G**, Palmieri VV, Palladino V, Amoruso A, Faienza MF, Giordano P. Venous Thromboembolism in Children: From Diagnosis to Management. *Int J Environ Res Public Health* 2020; **17** [PMID: 32664502 DOI: 10.3390/ijerph17144993]

30 **Diamond CE**, Hennessey C, Meldau J, Guelcher CJ, Guerrera MF, Conklin LS, Sharma KV, Diab YA. Catheter-Related Venous Thrombosis in Hospitalized Pediatric Patients with Inflammatory Bowel Disease: Incidence, Characteristics, and Role of Anticoagulant Thromboprophylaxis with Enoxaparin. *J Pediatr* 2018; **198**: 53-59 [PMID: 29628414 DOI: 10.1016/j.jpeds.2018.02.039]

31 **Zitomersky NL**, Verhave M, Trenor CC 3rd. Thrombosis and inflammatory bowel disease: a call for improved awareness and prevention. *Inflamm Bowel Dis* 2011; **17**: 458-470 [PMID: 20848518 DOI: 10.1002/ibd.21334]

32 **Bence CM**, Traynor MD, Polites SF, Ha D, Muenks P, St. Peter SD, Landman MP, Densmore JC, Potter DD. The incidence of venous thromboembolism in children following colorectal resection for inflammatory bowel disease: A multi-center study. *J Pediatric Surg* 2020

33 **Derderian SC**, Phillips R, Acker SN, Bruny J, Partrick DA. Pediatric ulcerative colitis: three- *vs* two-stage colectomy with ileal pouch-anal anastomosis. *Pediatric Surg International* 2020; **36**: 171-177

34 **Khosravi F**, Ziaeefar P. Early and long-term outcome of surgical intervention in children with inflammatory bowel disease. *Arq Bras Cir Dig* 2020; **33**: e1518 [PMID: 33237162 DOI: 10.1590/0102-672020200002e1518]

35 **Jarchin L**, Spencer EA, Khaitov S, Greenstein A, Jossen J, Lai J, Dunkin D, Pittman N, Benkov K, Dubinsky MC. De Novo Crohn's Disease of the Pouch in Children Undergoing Ileal Pouch-Anal Anastomosis for Ulcerative Colitis. *J Pediatric Gastroenterol Nutr* 2019; **69**: 455-460

36 **Lo CK**, Mertz D, Loeb M. Newcastle-Ottawa Scale: comparing reviewers' to authors' assessments. *BMC Med Res Methodol* 2014; **14**: 45 [PMID: 24690082 DOI: 10.1186/1471-2288-14-45]

37 **Higgins JP**, Thompson SG, Deeks JJ, Altman DG. Measuring inconsistency in meta-analyses. *BMJ* 2003; **327**: 557-560 [PMID: 12958120 DOI: 10.1136/bmj.327.7414.557]

38 **Higgins JPT**, Thomas J, Chandler J, Cumpston M, Li T, Page MJ, Welch VA. Cochrane Handbook for Systematic Reviews of Interventions version 6.1. London: Cochrane Collaboration, 2020

39 **Diamond IR**, Gerstle JT, Kim PCW, Langer JC. Outcomes after laparoscopic surgery in children with inflammatory bowel disease. *Surgical Endoscopy* 2010; **24**: 2796-2802

40 **Lee YA**, Chun P, Hwang EH, Mun SW, Lee YJ, Park JH. Clinical Features and Extraintestinal Manifestations of Crohn Disease in Children. *Pediatr Gastroenterol Hepatol Nutr* 2016; **19**: 236-242 [PMID: 28090468 DOI: 10.5223/pghn.2016.19.4.236]

41 **Zitomersky NL**, Levine AE, Atkinson BJ, Harney KM, Verhave M, Bousvaros A, Lightdale JR, Trenor CC 3rd. Risk factors, morbidity, and treatment of thrombosis in children and young adults with active inflammatory bowel disease. *J Pediatr Gastroenterol Nutr* 2013; **57**: 343-347 [PMID: 23752078 DOI: 10.1097/MPG.0b013e31829ce5cd]

42 **Kim YH**, Pfaller B, Marson A, Yim HW, Huang V, Ito S. The risk of venous thromboembolism in women with inflammatory bowel disease during pregnancy and the postpartum period: A systematic review and meta-analysis. *Medicine (Baltimore)* 2019; **98**: e17309 [PMID: 31568016 DOI: 10.1097/MD.0000000000017309]

43 **McCurdy JD**, Ellen Kuenzig M, Spruin S, Fung OW, Mallik R, Williams L, Murthy SK, Carrier M, Nguyen G, Benchimol EI. Surgery and the Subtype of Inflammatory Bowel Disease Impact the Risk of Venous Thromboembolism After Hospital Discharge. *Dig Dis Sci* 2021 [PMID: 34114153 DOI: 10.1007/s10620-021-07064-5]

44 **Faye AS**, Wen T, Ananthakrishnan AN, Lichtiger S, Kaplan GG, Friedman AM, Lawlor G, Wright JD, Attenello FJ, Mack WJ, Lebwohl B. Acute Venous Thromboembolism Risk Highest Within 60 Days After Discharge From the Hospital in Patients With Inflammatory Bowel Diseases. *Clin Gastroenterol Hepatol* 2020; **18**: 1133-1141.e3 [PMID: 31336196 DOI: 10.1016/j.cgh.2019.07.028]

45 **McKechnie T**, Wang J, Springer JE, Gross PL, Forbes S, Eskicioglu C. Extended thromboprophylaxis following colorectal surgery in patients with inflammatory bowel disease: a comprehensive systematic clinical review. *Colorectal Dis* 2020; **22**: 663-678 [PMID: 31490000 DOI: 10.1111/codi.14853]

46 **Lewis-Lloyd CA**, Pettitt EM, Adiamah A, Crooks CJ, Humes DJ. Risk of Postoperative Venous Thromboembolism After Surgery for Colorectal Malignancy: A Systematic Review and Meta-analysis. *Dis Colon Rectum* 2021; **64**: 484-496 [PMID: 33496485 DOI: 10.1097/DCR.0000000000001946]

47 **Toth S**, Flohr TR, Schubart J, Knehans A, Castello MC, Aziz F. A meta-analysis and systematic review of venous thromboembolism prophylaxis in patients undergoing vascular surgery procedures. *J Vasc Surg Venous Lymphat Disord* 2020; **8**: 869-881.e2 [PMID: 32330639 DOI: 10.1016/j.jvsv.2020.03.017]

48 **Papa A**, Gerardi V, Marzo M, Felice C, Rapaccini GL, Gasbarrini A. Venous thromboembolism in patients with inflammatory bowel disease: focus on prevention and treatment. *World J Gastroenterol* 2014; **20**: 3173-3179 [PMID: 24695669 DOI: 10.3748/wjg.v20.i12.3173]

49 **Yan SL**, Russell J, Harris NR, Senchenkova EY, Yildirim A, Granger DN. Platelet abnormalities during colonic inflammation. *Inflamm Bowel Dis* 2013; **19**: 1245-1253 [PMID: 23518812 DOI: 10.1097/MIB.0b013e318281f3df]

50 **Yuhara H**, Steinmaus C, Corley D, Koike J, Igarashi M, Suzuki T, Mine T. Meta-analysis: the risk of venous thromboembolism in patients with inflammatory bowel disease. *Aliment Pharmacol Ther* 2013; **37**: 953-962 [PMID: 23550660 DOI: 10.1111/apt.12294]

51 **Lazzerini M**, Bramuzzo M, Maschio M, Martelossi S, Ventura A. Thromboembolism in pediatric inflammatory bowel disease: systematic review. *Inflamm Bowel Dis* 2011; **17**: 2174-2183 [PMID: 21910180 DOI: 10.1002/ibd.21563]

World Journal of Gastroenterology

Submit a Manuscript: https://www.f6publishing.com

World J Gastroenterol 2022 April 28; 28(16): 1718-1721

DOI: 10.3748/wjg.v28.i16.1718

ISSN 1007-9327 (print) ISSN 2219-2840 (online)

LETTER TO THE EDITOR

Viral hepatitis: A global burden needs future directions for the management

Henu Kumar Verma, Kiran Prasad, Pramod Kumar, Bhaskar Lvks

Specialty type: Gastroenterology and hepatology

Provenance and peer review: Invited article; Externally peer reviewed.

Peer-review model: Single blind

Peer-review report's scientific quality classification

Grade A (Excellent): 0
Grade B (Very good): 0
Grade C (Good): C, C, C
Grade D (Fair): D
Grade E (Poor): 0

P-Reviewer: Elpek GO, Turkey; Gana JC, Chile; Kumar R, India; Shi Y, China

Received: August 29, 2021
Peer-review started: August 29, 2021
First decision: September 29, 2021
Revised: October 9, 2021
Accepted: March 25, 2022
Article in press: March 25, 2022
Published online: April 28, 2022

Henu Kumar Verma, Department of Immunopathology, Institute of Lungs Biology and Disease, Comprehensive Pneumology Center, Helmholtz Zentrum, Munich 80331, Bayren, Germany

Kiran Prasad, Bhaskar Lvks, Department of Zoology, Guru Ghasidas Vishwavidyalaya, Bilaspur 495001, Chhattisgarh, India

Pramod Kumar, Department of Drug Delivery, Institute of Lung Biology and Disease, Helmholtz Research Center, Munich 80331, Bayren, Germany

Corresponding author: Henu Kumar Verma, PhD, Research Scientist, Senior Researcher, Department of Immunopathology, Institute of Lungs Health and Immunity, Comprehensive Pneumology Center, Helmholtz Zentrum, 85764 Neuherberg, Munich 80331, Bayren, Germany. henu.verma@yahoo.com

Abstract

Viral hepatitis is an acute or chronic liver disease due to the infection from Hepatitis A, B, C, D and E viruses. It can cause severe liver damage such as cirrhosis, liver failure and liver cancer. To avoid such fatal complications, hepatitis patients must be diagnosed, pathologized and treated as soon as possible. Furthermore, these hepatitis viruses infect through different routes, resulting in distinct disease pathologies, severity and even the need for specific treatment strategies to combat the infection.

Key Words: Viral hepatitis; Vaccination; Chronic; Acute; Viral therapy

©The Author(s) 2022. Published by Baishideng Publishing Group Inc. All rights reserved.

Core Tip: Vaccination is the primary strategy for neutralizing several hepatitis viruses and it is highly effective against most hepatitis viruses. However, additional precautions must be taken for patients at a higher risk of infection such as those who take drugs, prisoners, the homeless or homosexuals. From interferon monotherapy and interferon combination therapy with direct-acting antiviral agents to interferon-free regimens which act by viral chain braking are among the measures to control hepatitis. These strategies can play a critical role in achieving World Health Organization's an ambitious but attainable goal of eliminating hepatitis infection by 2030.

Citation: Verma HK, Prasad K, Kumar P, Lvks B. Viral hepatitis: A global burden needs future directions for the management. *World J Gastroenterol* 2022; 28(16): 1718-1721
URL: https://www.wjgnet.com/1007-9327/full/v28/i16/1718.htm
DOI: https://dx.doi.org/10.3748/wjg.v28.i16.1718

TO THE EDITOR

Viral hepatitis, particularly hepatitis B and C, are one of the biggest threats to human health contributing to nearly one-fourth of all deaths among overall infectious disease patients[1]. Despite the substantial evolvement in antiviral therapy and access to effective vaccines, the hepatitis virus elimination goal of the United Nations by the year 2030 is doubtful[2]. To this end, healthcare providers and physician assistants can reduce disease burden through infection prevention, early detection, medical management and collaborative care. At the same time, the development of interferon-based and interferon-free therapeutic approaches may help eradicate the hepatitis viral infection.

We recently read Dr. Persico's group paper entitled "Viral hepatitis: Milestones, unresolved issues and future goals" in your prestigious journal "*World Journal of Gastroenterology*[3]." We sincerely thank the author for providing details about the impact of various hepatitis viruses, current research, the gaps between effective management and currently applicable approaches, and finally, the plans that might effectively manage viral hepatitis.

Viral hepatitis is classified into several types: A, B, C, D, and E. Among these types, B and C are the most common types of viruses that can be transmitted through blood transfusions and are the most lethal due to the induction of chronic illness[4]. In the present review article, the authors mainly focused on the pathologies, clinical manifestations, and various advancements in therapeutic regimes of different hepatitis virus infections.

Furthermore, they elegantly demonstrated progression in hepatitis C virus (HCV) infection treatment regimens from interferon to direct-acting antiviral agents (DAAs) with a relative increase in sustained virological response (SVR) rate. Newer pan-genotypic antiviral therapies, such as sofosbuvir/velpatasvir and glecaprevir/pibrentasvir, have 98%-99% SVR in all genotypes of hepatitis C virus and low drug resistance. It was approved by the FDA in 2016. DAAs are now known to be effective in the treatment of HCV patients who do not have cirrhosis, have compensated cirrhosis or have extrahepatic manifestations and have a lower risk of hepatocellular carcinoma (HCC) recurrence[5]. Besides, various host targeting agents (HTAs) are under clinical studies that target molecules essential for hepatitis C virus entry and replication. Its main advantage is its low mutation rate. The primary targets of HTAs are microRNA-122, Cyclophilin A and HMG-CoA reductase[6].

Current hepatitis B virus (HBV) infection management protocols include the use of nucleoside/nucleotide analogues and interferons both of which reduce HBV replication but do not eradicate the virus. Current therapies' lack of direct impact on virus covalently closed circular DNA (cccDNA) is a major limiting factor for HBV virus elimination[7]. Thus, various gene-editing methods like transcription activator-like effector nucleases, CRISPR/Cas system and zinc finger nuclease are understudies to target cccDNA expression[8].

Several immunomodulatory agents that induce HBV-specific immune responses have recently been developed. Immunomodulatory therapies include agonists, immune checkpoint inhibitors, therapeutic vaccines and engineered HBV-specific T-cell transfer. Agonists activate Toll-like receptors, stimulator of IFN genes, and Retinoic Acid-Inducible Gene-1 to initiate the innate immune response. While immune checkpoint inhibitors such as programmed cell death-1 trigger an adaptive immune response. GS-4774 (vector-based vaccine) trials showed that the vaccine was safe but no significant reduction in HBsAg levels was observed. Other vaccines like INO-1800, TG-1050 and ABX-203 are under clinical investigation[9]. RNAi-based therapies are also evolving against HBV infection which exerts its antiviral activity by post-transcriptional silencing. ARC-520 and ARC-521 (RNAi-based drug) showed a reduction in HBsAg and HBV DNA levels but were discontinued due to rising safety concerns related to drug delivery. Both siRNA-based drug, JNJ-3989, earlier called ARO-HBV and VIR-218 has shown promising results against chronic HBV infection and are under ongoing clinical trials[10].

Hepatitis D virus infection occurs only in HBV-infected people. Pegylated interferon-alpha is the only effective therapy against HDV infection in clinical practice. However, HBV vaccination protects from both HBV and HDV infection. Other therapeutic drugs under clinical trials against HDV infection include Pegylated IFN-lambda, Myrcludex B that blocks hepatitis B and D virus entry in hepatocytes, Lonafarnib that inhibits farnesylation of L-HDAg and its subsequent interaction with HBsAg and REP 2139. Its mechanism is still unclear but it is known to be related to blocking HBsAg release[11].

For hepatitis A, no specific treatment is available. Both improving sanitary conditions and HAV vaccination is the most effective preventive strategy. Vaccination is recommended to high-risk people, patients having chronic liver disease, HIV-positive patients and pregnant women[4].

The authors describe various hepatitis E virus (HEV) genotypes and their transmission routes in detail. HEV1 and HEV2 are the only ones that infect humans and spread *via* the fecal-oral route. There is no effective HEV vaccine available to prevent infection. China developed the HEV-239 vaccine which is safe for pregnant women and provides longer protection. However, it is not permitted in other countries [12].

Other treatment strategies like liver transplantation and management of hepatitis in pregnant women can be included. Liver transplantation is the most effective therapy for HCC and cirrhosis due to HBV and HCV infections. Post-transplantation use of DAA reduces the risk of recurrence and increases the survival rate of patients[13].

Pregnant women are prone to acute and chronic hepatitis infection with a risk of developing fulminant hepatitis and vertical transmission, especially in hepatitis E. Seto *et al*[14] described various management strategies for different subtypes of hepatitis. Ribavirin is known to be teratogenic and thus should be avoided during pregnancy; however, supportive care is preferred. Breastfeeding is encouraged in hepatitis C, D, and A, while in hepatitis E, it is not recommended. HAV vaccination is opted to prevent fetal transmission. DAA treatment during pregnancy is still debatable[14]. Ledipasvir and sofosbuvir use during pregnancy in HCV infection has not been associated with safety concerns[15].

Even with advanced therapies like DAA, there are still challenges to cure and eradicate various subtypes of viral hepatitis. Thus, more investigations are required for multiple drugs under clinical trials to develop better preventive and management strategies. We genuinely appreciate Torre *et al*[3] and colleagues for providing relevant and detailed information on various subtypes of viral hepatitis along with their clinical manifestation and treatment methods.

FOOTNOTES

Author contributions: Verma HK, Prasad K, Kumar P and Lvks B wrote and revised the letter.

Conflict-of-interest statement: The authors declare no conflict of interest.

Open-Access: This article is an open-access article that was selected by an in-house editor and fully peer-reviewed by external reviewers. It is distributed in accordance with the Creative Commons Attribution NonCommercial (CC BY-NC 4.0) license, which permits others to distribute, remix, adapt, build upon this work non-commercially, and license their derivative works on different terms, provided the original work is properly cited and the use is non-commercial. See: http://creativecommons.org/Licenses/by-nc/4.0/

Country/Territory of origin: Germany

ORCID number: Henu Kumar verma 0000-0003-1130-8783; Kiran Prasad 0000-0001-5817-5661; Pramod Kumar 0000-0002-7995-5613; Bhaskar Lvks 0000-0003-2977-6454.

S-Editor: Wang LL
L-Editor: Filipodia
P-Editor: Wang LL

REFERENCES

1 **Thomas DL**. Global Elimination of Chronic Hepatitis. *N Engl J Med* 2019; **380**: 2041-2050 [PMID: 31116920 DOI: 10.1056/NEJMra1810477]
2 **Cox AL**, El-Sayed MH, Kao JH, Lazarus JV, Lemoine M, Lok AS, Zoulim F. Progress towards elimination goals for viral hepatitis. *Nat Rev Gastroenterol Hepatol* 2020; **17**: 533-542 [PMID: 32704164 DOI: 10.1038/s41575-020-0332-6]
3 **Torre P**, Aglitti A, Masarone M, Persico M. Viral hepatitis: Milestones, unresolved issues, and future goals. *World J Gastroenterol* 2021; **27**: 4603-4638 [PMID: 34366625 DOI: 10.3748/wjg.v27.i28.4603]
4 **Castaneda D**, Gonzalez AJ, Alomari M, Tandon K, Zervos XB. From hepatitis A to E: A critical review of viral hepatitis. *World J Gastroenterol* 2021; **27**: 1691-1715 [PMID: 33967551 DOI: 10.3748/wjg.v27.i16.1691]
5 **Horsley-Silva JL**, Vargas HE. New Therapies for Hepatitis C Virus Infection. *Gastroenterol Hepatol (N Y)* 2017; **13**: 22-31 [PMID: 28420944]
6 **Crouchet E**, Wrensch F, Schuster C, Zeisel MB, Baumert TF. Host-targeting therapies for hepatitis C virus infection: current developments and future applications. *Therap Adv Gastroenterol* 2018; **11**: 1756284818759483 [PMID: 29619090 DOI: 10.1177/1756284818759483]
7 **Suk-Fong Lok A**. Hepatitis B Treatment: What We Know Now and What Remains to Be Researched. *Hepatol Commun* 2019; **3**: 8-19 [PMID: 30619990 DOI: 10.1002/hep4.1281]
8 **Zhu A**, Liao X, Li S, Zhao H, Chen L, Xu M, Duan X. HBV cccDNA and Its Potential as a Therapeutic Target. *J Clin Transl Hepatol* 2019; **7**: 258-262 [PMID: 31608218 DOI: 10.14218/JCTH.2018.00054]
9 **Alexopoulou A**, Vasilieva L, Karayiannis P. New Approaches to the Treatment of Chronic Hepatitis B. *J Clin Med* 2020; **9** [PMID: 33019573 DOI: 10.3390/jcm9103187]

10 **van den Berg F**, Limani SW, Mnyandu N, Maepa MB, Ely A, Arbuthnot P. Advances with RNAi-Based Therapy for Hepatitis B Virus Infection. *Viruses* 2020; **12** [PMID: 32759756 DOI: 10.3390/v12080851]

11 **Mentha N**, Clément S, Negro F, Alfaiate D. A review on hepatitis D: From virology to new therapies. *J Adv Res* 2019; **17**: 3-15 [PMID: 31193285 DOI: 10.1016/j.jare.2019.03.009]

12 **Melgaço JG**, Gardinali NR, de Mello VDM, Leal M, Lewis-Ximenez LL, Pinto MA. Hepatitis E: Update on Prevention and Control. *Biomed Res Int* 2018; **2018**: 5769201 [PMID: 29546064 DOI: 10.1155/2018/5769201]

13 **Ferrarese A**, Zanetto A, Gambato M, Bortoluzzi I, Nadal E, Germani G, Senzolo M, Burra P, Russo FP. Liver transplantation for viral hepatitis in 2015. *World J Gastroenterol* 2016; **22**: 1570-1581 [PMID: 26819523 DOI: 10.3748/wjg.v22.i4.1570]

14 **Seto MT**, Cheung KW, Hung IFN. Management of viral hepatitis A, C, D and E in pregnancy. *Best Pract Res Clin Obstet Gynaecol* 2020; **68**: 44-53 [PMID: 32305262 DOI: 10.1016/j.bpobgyn.2020.03.009]

15 **Chappell CA**, Scarsi KK, Kirby BJ, Suri V, Gaggar A, Bogen DL, Macio IS, Meyn LA, Bunge KE, Krans EE, Hillier SL. Ledipasvir plus sofosbuvir in pregnant women with hepatitis C virus infection: a phase 1 pharmacokinetic study. *Lancet Microbe* 2020; **1**: e200-e208 [PMID: 32939459 DOI: 10.1016/S2666-5247(20)30062-8]

World Journal of Gastroenterology

Submit a Manuscript: https://www.f6publishing.com

World J Gastroenterol 2022 April 28; 28(16): 1722-1724

DOI: 10.3748/wjg.v28.i16.1722

ISSN 1007-9327 (print) ISSN 2219-2840 (online)

LETTER TO THE EDITOR

Comment on "Artificial intelligence in gastroenterology: A state-of-the-art review"

Thomas Bjørsum-Meyer, Anastasios Koulaouzidis, Gunnar Baatrup

Specialty type: Gastroenterology and hepatology

Provenance and peer review: Unsolicited article; Externally peer reviewed.

Peer-review model: Single blind

Peer-review report's scientific quality classification

Grade A (Excellent): 0
Grade B (Very good): B
Grade C (Good): C
Grade D (Fair): 0
Grade E (Poor): 0

P-Reviewer: Laskaratos FM, United Kingdom; Oh CK, South Korea

Received: December 1, 2021
Peer-review started: December 1, 2021
First decision: December 26, 2021
Revised: January 7, 2022
Accepted: March 16, 2022
Article in press: March 16, 2022
Published online: April 28, 2022

Thomas Bjørsum-Meyer, Gunnar Baatrup, Department of Surgery, Odense University Hospital, Svendborg 5700, Denmark

Thomas Bjørsum-Meyer, Anastasios Koulaouzidis, Gunnar Baatrup, Department of Clinical Research, University of Southern Denmark, Faculty of Health Science, Odense 5230, Denmark

Corresponding author: Thomas Bjørsum-Meyer, MD, PhD, Associate Professor, Surgeon, Department of Surgery, Odense University Hospital, Baagøes Alle 15, Svendborg 5700, Denmark. thomas.bjoersum-meyer@rsyd.dk

Abstract

Colon capsule endoscopy (CCE) was introduced nearly two decades ago. Initially, it was limited by poor image quality and short battery time, but due to technical improvements, it has become an equal diagnostic alternative to optical colonoscopy (OC). Hastened by the coronavirus disease 2019 pandemic, CCE has been introduced in clinical practice to relieve overburdened endoscopy units and move investigations to out-patient clinics. A wider adoption of CCE would be bolstered by positive patient experience, as it offers a diagnostic investigation that is not inferior to other modalities. The shortcomings of CCE include its inability to differentiate adenomatous polyps from hyperplastic polyps. Solving this issue would improve the stratification of patients for polyp removal. Artificial intelligence (AI) has shown promising results in polyp detection and characterization to minimize incomplete CCEs and avoid needless examinations. Onboard AI appears to be a needed application to enable near-real-time decision-making in order to diminish patient waiting times and avoid superfluous subsequent OCs. With this letter, we discuss the potential and role of AI in CCE as a diagnostic tool for the large bowel.

Key Words: Video capsule endoscopy; Wireless capsule endoscopy; Artificial intelligence; Colonic polyps; Endoscopic surgical procedures; Colon neoplasm

©The Author(s) 2022. Published by Baishideng Publishing Group Inc. All rights reserved.

Core Tip: Colon capsule endoscopy (CCE) generates a vast amount of image material-currently, this material must be assessed manually. Artificial intelligence (AI) as an adjunct to CCE has been reported as having high accuracy for detecting colonic lesions. Future studies need to evaluate AI algorithms for estimating the likelihood of neoplasia and predicting which patients are most likely to benefit from CCE. Onboard capsule intelligence has the potential to generate result reports immediately after completed examinations.

Citation: Bjørsum-Meyer T, Koulaouzidis A, Baatrup G. Comment on "Artificial intelligence in gastroenterology: A state-of-the-art review". *World J Gastroenterol* 2022; 28(16): 1722-1724
URL: https://www.wjgnet.com/1007-9327/full/v28/i16/1722.htm
DOI: https://dx.doi.org/10.3748/wjg.v28.i16.1722

TO THE EDITOR

We read with interest the in-depth review by Kröner *et al*[1]. The authors presented a thorough account of the status and knowledge of artificial intelligence (AI) in everyday practice in gastroenterology[1]. As we apply AI in picture analysis of colon capsule endoscopy (CCE), we feel obliged to offer some relevant insights. The coronavirus disease 2019 (COVID-19) pandemic has accelerated the clinical adoption of CCE as an alternative first-line diagnostic procedure to optical colonoscopy (OC)[2]. CCE is a painless, low-risk procedure that can be performed in the patient's home with minimal contact with healthcare workers and/or other patients, therefore abiding (when possible) by the distancing measures recommended to contain the spread of COVID-19.

Furthermore, CCE is seen as a measure to relieve the pressure on overburdened endoscopy units with long waiting times for OC. The Scottish Capsule Programme has implemented CCE in a large-scale roll-out to patients presenting with lower gastrointestinal symptoms to their general practitioners and found to be eligible for colonic investigation[3]. The programme enables effective upfront screening at the community level to address increasing demand and capacity pressure within the National Health Service.

Until recently, the clinical implementation of CCE has been hampered by low completion rates compared to OC. A significant drawback for CCE is its reliance on extensive orally administered bowel cleansing preparations to gain adequate visualization of the mucosa, as, unlike OC, water wash and suction are not possible. Although research into optimizing and standardizing bowel preparation regimens is ongoing, to date it has failed to meet the minimum standard of 90% for OC[4]. A recent systematic review and meta-analysis of 46 studies including 5000 patients showed that CCE's (pooled) adequate colon cleanliness rate (ACCR) was only 77%[5]. Therefore, further studies aiming to improve CCE's ACCR are mandatory. Another way to achieve more conclusive CCE examinations is to enhance our ability to predict patients at high risk of an insufficient colon cleanliness level. AI algorithms based on demographic data are one possible solution. We are currently running a large randomized trial in Denmark (CFC2015) in which 2015 citizens are allocated to CCE. After the study is completed in Summer 2022, we plan to create algorithms for just such a purpose. The cost-effectiveness of CCE needs to be improved before wider clinical adoption is considered. Hassan *et al*[6] found that improved compliance in the general population is mandatory to make CCE cost-effective compared to OC[6].

CCE produces many images, and reading them is very time-consuming and monotonous, increasing the risk of missing important lesions. Hence, the development of AI-based tools to assist readers is needed. Saraiva *et al*[7], in a recent article, developed a convolutional neural network based on AI. They found that it could detect protruding lesions in the colon with a sensitivity of 90.7% and a specificity of 92.6%[7]. To avoid unnecessary OC after CCE, it is essential to differentiate between hyperplastic polyps (HPs) and adenomatous polyps (APs). By applying flexible spectral imaging colour enhancement, Nakazawa *et al*[8] differentiated HPs from APs with a sensitivity of 91.2% and specificity of 88.2%[8]. Further research is needed to detect sessile serrated lesions using AI-assisted CCE.

The delay between capsule egestion and the completion of video reading and report writing is currently two days. Onboard capsule intelligence has the potential to make near real-time assessments of colonic pathology, creating a report almost immediately after CCE completion. The authors of this letter aspire to the development of onboard integrated AI to make CCE an expeditious diagnostic tool comparable to OC.

FOOTNOTES

Author contributions: Bjørsum-Meyer T conceived of the idea for the manuscript and contributed to the manuscript drafting and critical revision; Koulaouzidis A and Baatrup G contributed to the manuscript drafting and critical

revision.

Conflict-of-interest statement: AK is consultant for Jinshan. He is director of iCERV Ltd and cofounder of AJM Medicaps Ltd. He has received a GivenImaging Ltd-ESGE grant, and material support for clinical research from SynMed/Intromedic. In the last ten years, he has received honoraria & lecture fees from Jinshan, Dr FalkPharma UK and Ferring. He has also received educational travel support from Aquilant, Jinshan, Dr FalkPharma, Almirall, Ferring, and has participated in advisory board meetings for Tillots, Ankon, and Dr FalkPharmaUK.

Open-Access: This article is an open-access article that was selected by an in-house editor and fully peer-reviewed by external reviewers. It is distributed in accordance with the Creative Commons Attribution NonCommercial (CC BY-NC 4.0) license, which permits others to distribute, remix, adapt, build upon this work non-commercially, and license their derivative works on different terms, provided the original work is properly cited and the use is non-commercial. See: https://creativecommons.org/Licenses/by-nc/4.0/

Country/Territory of origin: Denmark

ORCID number: Thomas Bjørsum-Meyer 0000-0001-5253-0802; Anastasios Koulaouzidis 0000-0002-2248-489X; Gunnar Baatrup 0000-0003-0300-5766.

S-Editor: Fan JR
L-Editor: A
P-Editor: Fan JR

REFERENCES

1 **Kröner PT**, Engels MM, Glicksberg BS, Johnson KW, Mzaik O, van Hooft JE, Wallace MB, El-Serag HB, Krittanawong C. Artificial intelligence in gastroenterology: A state-of-the-art review. *World J Gastroenterol* 2021; **27**: 6794-6824 [PMID: 34790008 DOI: 10.3748/wjg.v27.i40.6794]
2 **MacLeod C**, Wilson P, Watson AJM. Colon capsule endoscopy: an innovative method for detecting colorectal pathology during the COVID-19 pandemic? *Colorectal Dis* 2020; **22**: 621-624 [PMID: 32403190 DOI: 10.1111/codi.15134]
3 **ScotCap Clinical Leads Collaboration**. Follow-up of small and diminutive colonic polyps-How to balance the risks in the COVID-19 era. *Colorectal Dis* 2021; **23**: 3061-3064 [PMID: 34510684 DOI: 10.1111/codi.15907]
4 **Hassan C**, East J, Radaelli F, Spada C, Benamouzig R, Bisschops R, Bretthauer M, Dekker E, Dinis-Ribeiro M, Ferlitsch M, Fuccio L, Awadie H, Gralnek I, Jover R, Kaminski MF, Pellisé M, Triantafyllou K, Vanella G, Mangas-Sanjuan C, Frazzoni L, Van Hooft JE, Dumonceau JM. Bowel preparation for colonoscopy: European Society of Gastrointestinal Endoscopy (ESGE) Guideline - Update 2019. *Endoscopy* 2019; **51**: 775-794 [PMID: 31295746 DOI: 10.1055/a-0959-0505]
5 **Bjoersum-Meyer T**, Skonieczna-Zydecka K, Cortegoso Valdivia P, Stenfors I, Lyutakov I, Rondonotti E, Pennazio M, Marlicz W, Baatrup G, Koulaouzidis A, Toth E. Efficacy of bowel preparation regimens for colon capsule endoscopy: a systematic review and meta-analysis. *Endosc Int Open* 2021; **9**: E1658-E1673 [PMID: 34790528 DOI: 10.1055/a-1529-5814]
6 **Hassan C**, Zullo A, Winn S, Morini S. Cost-effectiveness of capsule endoscopy in screening for colorectal cancer. *Endoscopy* 2008; **40**: 414-421 [PMID: 18302080 DOI: 10.1055/s-2007-995565]
7 **Saraiva MM**, Ferreira JPS, Cardoso H, Afonso J, Ribeiro T, Andrade P, Parente MPL, Jorge RN, Macedo G. Artificial intelligence and colon capsule endoscopy: development of an automated diagnostic system of protruding lesions in colon capsule endoscopy. *Tech Coloproctol* 2021; **25**: 1243-1248 [PMID: 34499277 DOI: 10.1007/s10151-021-02517-5]
8 **Nakazawa K**, Nouda S, Kakimoto K, Kinoshita N, Tanaka Y, Tawa H, Koshiba R, Naka Y, Hirata Y, Ota K, Kawakami K, Takeuchi T, Inoue T, Miyazaki T, Sanomura M, Nakamura S, Saito Y, Higuchi K. The Differential Diagnosis of Colorectal Polyps Using Colon Capsule Endoscopy. *Intern Med* 2021; **60**: 1805-1812 [PMID: 33456043 DOI: 10.2169/internalmedicine.6446-20]

Published by **Baishideng Publishing Group Inc**
7041 Koll Center Parkway, Suite 160, Pleasanton, CA 94566, USA
Telephone: +1-925-3991568
E-mail: bpgoffice@wjgnet.com
Help Desk: https://www.f6publishing.com/helpdesk
https://www.wjgnet.com

© 2022 Baishideng Publishing Group Inc. All rights reserved.